Holding the balance; the equilibrium between ERα-activation, epigenetic alterations and chromatin integrity
Flach, K.D.

Citation
Flach, K. D. (2018, September 25). *Holding the balance; the equilibrium between ERα-activation, epigenetic alterations and chromatin integrity*. Retrieved from https://hdl.handle.net/1887/66110

Cover Page

The handle http://hdl.handle.net/1887/66110 holds various files of this Leiden University dissertation.

Author: Flach, K.D.
Title: Holding the balance; the equilibrium between ERα-activation, epigenetic alterations and chromatin integrity
Issue Date: 2018-09-25

Holding the balance;
the equilibrium between ERα-activation, epigenetic alterations and chromatin integrity

Koen Dorus Flach

Holding the balance; the equilibrium between ERα-activation, epigenetic alterations and chromatin integrity

Proefschrift

ter verkrijging van
de graad van Doctor aan de Universiteit Leiden,
op gezag van Rector Magnificus prof.mr. C.J. J.M. Stolker, volgens besluit van het College voor Promoties
te verdedigen op dinsdag 25 september 2018
klokke 13.45 uur

door

Koen Dorus Flach

geboren te Amsterdam

in 1987

Promotor
Prof. Dr. J.J.C. Neefjes

Copromotor
Dr. W.T. Zwart (NKI-AVL)

Promotiecommissie
Prof. dr. V.T.H.B.M. Smit
Prof. dr. H. Ovaa
Prof. dr. B. van de Water
Prof. dr. P.J. van Diest (UMCU)
Prof. dr. J Jonkers (LACDR/ NKI-AVL)
Prof. dr. S.C. Linn (UU/ NKI-AVL)
dr. A.M. Bergman (NKI-AVL)

Table of Content

Thesis outline

Chapter 4   Composition of ERα's transcriptional complex – part 1

Co-regulated gene expression by estrogen receptor-α and liver receptor homolog-1 is a feature of the estrogen response in breast cancer cells. *Chun-Fui Lai, Koen D. Flach, Xanthippi Alexi, Stephen P. Fox, Silvia Ottaviani, Paul T.R. Thiruchelvam, Fiona J. Kyle, Ross S. Thomas, Rosalind Launchbury, Hui Hua, Holly B. Callaghan, Jason S. Carroll, R. Charles Coombes, Wilbert Zwart, Laki Buluwela, and Simak Ali. Nucleic Acids Research, 2013.*

Chapter 5   Composition of ERα's transcriptional complex – part 2

Estrogen Receptor DNA-damage/methylation cycle as drug interface in tamoxifen resistant breast cancer by FEN1 blockade. *Koen Dorus Flach, Manikandan Periyasamy, Ajit Jadhav, Theresa E. Hickey, Mark Opdam, Hetal Patel, Sander Canisius, David M. Wilson III, Dorjbal Dorjsuren, Marja Nieuwland, Roel Kluin, Alexey V. Zakharov, Jelle Wesseling, Lodewyk Frederik Ary Wessels, Sabine Charlotte Linn, Wayne D. Tilley, Anton Simeonov, Simak Ali, Wilbert Zwart. In submission*

Chapter 6   ERα Cofactor phosphorylation

SRC3 phosphorylation at Serine 543 is a positive independent prognostic factor in ER positive breast cancer. *Koen D. Flach*, Wilbert Zwart*, Bharath Rudraraju*, Tarek M.A. Abdel-Fatah, Ondrej Gojis, Sander Canisius, David Moore, Ekaterina Nevedomskaya, Mark Opdam,*

Marjolein Droog, Ingrid Hofland, Steve Chan, Jacqui Shaw, Ian O. Ellis, R. Charles Coombes, Jason S. Carroll, Simak Ali, and Carlo Palmieri. * authors contributed equally. Clinical Cancer Research, 2016.

Holding the balance; the equilibrium between ERα-activation, epigenetic alterations and chromatin integrity

Thesis Outline

General introduction

In this thesis we reflect on the effects differential DNA binding of the estrogen receptor α (ERα) can have on the behavior of breast cancer and which factors can contribute to this. Approximately 70% of all breast tumors are derived from the inner lining of cells in the mammary ducts (also known as luminal tumors) and their proliferation is dependent on the activity of (ERα). During the development and homeostasis of the female reproductive organs ERα plays a key role. In ERα-positive breast tumors however, ERα has a causative role in carcinogenesis (1). ERα can be activated by its natural ligand estradiol (2), a steroidal estrogen, which can induce the formation of an activated ERα-dimer. After a conformational change (3), this dimer "opens up" the co-activator-binding pocket (4) resulting in the recruitment of essential co-factors (5) leading to the assembly of the ERα–transcriptional complex.

One of the mainstay endocrine treatment options for ERα-positive breast cancer patients is tamoxifen (6-8), which is an ERα antagonist and competitively inhibits the interaction of ERα and estrogen, thereby repressing ERα activity (9-11). Alternatively aromatase inhibitors can be used to block the synthesis of estrogen, rendering ERα inactive. Despite these therapeutic options, still a significant proportion of patients develop a recurrence. Although cross-resistance between the different therapeutic options does occur, a proportion of patients that relapse on one type of therapy can still benefit from a different treatment modality. This illustrates the existence of multiple resistance mechanisms which can be treatment selective. A better understanding of ERα-biology and the development of drug resistance, cannot only provide us with novel mechanistic insights, but could also lead the way to the discovery of novel biomarkers and potential drug targets, which can further increase patient survival.

Thesis outline

Chapter 1 provides a general overview of ERα-biology and more specifically the mechanistic insights the genome-wide interrogation of ERα-chromatin binding has brought us. Furthermore we discuss where future developments might take us.

      Chapter 2 describes a well-known mechanism of tamoxifen-resistance; the PKA-induced phosphorylation of ERα at Serine residue 305 (ERαS305-P). We report on the implications this phosphorylation has on the binding repertoire of ERα and describe the discovery of an altered gene expression profile capable of predicting the outcome of patients treated with tamoxifen.

      In **Chapter 3** we provide experimental evidence for a previously unknown ERα-phosphorylation (T594P) and demonstrate how this greatly diminished ERα's binding capacity. Additionally we show that by stabilizing this phosphorylation by administering fusicoccin, ERα-mediated gene transcription was reduced and tumor cell growth was inhibited.

      In **Chapter 4** we report on the fact that ERα-function can also be altered by other nuclear receptors and demonstrate that LRH-1 knockdown led to an altered gene expression profile. Additionally we revealed that there is a large overlap between chromatin binding sites of LRH-1 and ERα, and that at these overlapping regions a synergistic stimulation is present.

      In **Chapter 5** we computationally refined a 111-gene classifier towards a single gene classifier, revealing that FEN1 levels are predictive of outcome in ERα-positive patients treated with tamoxifen. We describe our findings on the complex regulatory interplay between FEN1 and ERα, and postulate three manners by which FEN1 may modulate ERα activity. Additionally we performed a drug screen which led to the discovery of a FEN1-specific and potent inhibitor. We demonstrate a clear sensitivity of ERα-positive breast cancer cell lines to this inhibitor when compared to ERα-negative cell lines, and an even greater sensitivity of tamoxifen-resistant cell lines. The latter suggesting FEN1 inhibition might be a useful novel therapeutic option in the case of tamoxifen resistant breast.

      Chapter 6 contains our findings on the phosphorylation of essential ERα-cofactor SRC3 (SRC3-pS543). This phosphorylation leads to an altered deposition of SRC3 at the chromatin, making it very likely to also alter the gene expression of breast cancer and thereby its phenotype. Furthermore a SRC3-pS543 phospho-specific antibody was capable of identifying patients

with a functional ERα pathway, rendering it a promising novel biomarker for tamoxifen efficacy.

In **Chapter 7** I discuss what the implications of our findings are with regards to a better understanding of ERα-biology and describe the new questions this may invoke. Additionally I discuss how the novel biomarkers described in this thesis could aid in patient stratification and what type of research is still required to successfully implement such a biomarker. With regards to the potential novel drug targets we identified, I describe what the current clinical value of these drug targets would be and what type of evidence still lacks.

References

1.   Hayashi SI, Eguchi H, Tanimoto K, Yoshida T, Omoto Y, Inoue A, et al. The expression and function of estrogen receptor alpha and beta in human breast cancer and its clinical application. Endocr Relat Cancer. 2003;10(2):193-202.

2.   Dahlman-Wright K, Cavailles V, Fuqua SA, Jordan VC, Katzenellenbogen JA, Korach KS, et al. International Union of Pharmacology. LXIV. Estrogen receptors. Pharmacol Rev. 2006;58(4):773-81.

3.   Paige LA, Christensen DJ, Gron H, Norris JD, Gottlin EB, Padilla KM, et al. Estrogen receptor (ER) modulators each induce distinct conformational changes in ER alpha and ER beta. Proc Natl Acad Sci U S A. 1999;96(7):3999-4004.

4.   Shiau AK, Barstad D, Loria PM, Cheng L, Kushner PJ, Agard DA, et al. The structural basis of estrogen receptor/coactivator recognition and the antagonism of this interaction by tamoxifen. Cell. 1998;95(7):927-37.

5.   Glass CK, Rose DW, Rosenfeld MG. Nuclear receptor coactivators. Curr Opin Cell Biol. 1997;9(2):222-32.

6.   Osborne CK, Schiff R. Growth factor receptor cross-talk with estrogen receptor as a mechanism for tamoxifen resistance in breast cancer. Breast. 2003;12(6):362-7.

7.   Tamoxifen for early breast cancer: an overview of the randomised trials. Early Breast Cancer Trialists' Collaborative Group. Lancet. 1998;351(9114):1451-67.

8.   Gradishar WJ. Tamoxifen--what next? Oncologist. 2004;9(4):378-84.

9.   Jordan VC, Murphy CS. Endocrine pharmacology of antiestrogens as antitumor agents. Endocr Rev. 1990;11(4):578-610.

10.   Katzenellenbogen BS, Miller MA, Mullick A, Sheen YY. Antiestrogen action in breast cancer cells: modulation of proliferation and protein synthesis, and interaction with estrogen receptors and additional antiestrogen binding sites. Breast Cancer Res Treat. 1985;5(3):231-43.

11.   Arpino G, De Angelis C, Giuliano M, Giordano A, Falato C, De Laurentiis M, et al. Molecular mechanism and clinical implications of endocrine therapy resistance in breast cancer. Oncology. 2009;77 Suppl 1:23-37.

Chapter 1

Introduction and general discussion

The first decade of Estrogen Receptor cistromics in breast cancer
Koen D Flach and Wilbert Zwart

Division of Molecular Pathology, the Netherlands Cancer Institute,
Amsterdam, the Netherlands

Abstract

The advent of genome-wide transcription factor profiling has revolutionized the field of breast cancer research. Estrogen Receptor alpha (ERα), the major drug target in hormone receptor-positive breast cancer, has been known as a key transcriptional regulator in tumor progression for over 30 years. Even though this function of ERα is heavily exploited and widely accepted as an Achilles heel for hormonal breast cancer, only since the last decade we are beginning to understand how this transcription factor is functioning on a genome-wide scale. Initial ChIP-on-chip analyses have taught us that ERα is an enhancer-associated factor binding to many thousands of sites throughout the human genome, and revealed the identity of a number of directly interacting transcription factors that are essential for ERα action. More recently, with the development of massive parallel sequencing technologies and refinements thereof in sample processing, a genome-wide interrogation of ERα has become feasible and affordable with unprecedented data quality and richness. These studies have revealed numerous additional biological insights in ERα behaviour in cell lines and especially in clinical specimens. So what have we actually learned during this first decade of cistromics in breast cancer and where may future developments in the field take us?

Introduction

Breast cancer is the most prevalent form of cancer in women, with approximately 1.7 million annual new diagnoses (1). Despite the improvement of breast cancer treatment, still over half a million women die of this disease every year (1). Approximately 70% of breast tumors are estrogen receptor α (ERα) positive and tumor cell proliferation is thought to be dependent on the activity of this hormone-mediated transcription factor (2, 3).

The first evidence for a link between estrogens (produced in the ovaries) and breast cancer was reported by George Thomas Beatson in 1896 with a case report describing a premenopausal breast cancer patient with metastatic disease (4). Although not aware of the exact mechanisms of hormonal action in human physiology, Beatson was familiar with a procedure performed in cattle where lactation after giving birth can be extended by removal of the ovaries. Inspired by this phenomenon, Beatson performed a bilateral oophorectomy on his patient, which initially resulted in a complete remission of the disease (4, 5). The protein responsible for this clinical benefit was to be found almost 80 years later, with the seminal discovery of the Estrogen Receptor in 1973 by Elwood Jensen (6). In 1986, a complementary DNA clone of the translated mRNA of the estrogen receptor from MCF-7 human breast cancer cells was sequenced and upon expression gave rise to a functional protein (7). Today, ERα is recognized as the major drug target in hormonal breast cancer. In the adjuvant treatment of ERα-positive disease, receptor-inhibition is achieved by either a direct blockage of ERα-activation through competitive inhibition of estradiol association using tamoxifen (8-10) or by preventing estrogen synthesis using aromatase inhibitors (11). Despite the extensive use of these treatment modalities in adjuvant therapy, a significant number of patients still develop a recurrence (12). Although cross-resistance between the different endocrine therapy options can occur, patients that relapse on one type of endocrine therapy can still benefit from a different treatment modality (13-15), suggesting that multiple resistance mechanisms can exist that may be treatment selective. In order to directly administer the right drug to the right patient, it is vital to increase our knowledge about ERα-functioning as well as its selective responses to prolonged exposure to hormonal agents.

Even though ERα-inhibitors are being used in the clinic since the early 1980's, the direct mode of ERα's genomic action on a genome-wide scale has remained elusive for many years. With the initial development of ChIP-on-chip (chromatin immunoprecipitation coupled with tiling array) technologies, this situation changed dramatically with the interrogation of

ERα action for the first time on a human chromosome-wide scale (16). With the development of massive parallel high-throughput sequencing techniques, a full genome-coverage of ERα became possible (and importantly affordable) through ChIP-seq (17). Now, ten years after the first unbiased and systemic assessment of ERα binding sites in human cell lines, we will discuss what we have learned from the cistromics of ERα and where future developments might take us.

Estrogen Receptor complex formation and its mode-of-action

ERα is activated through the association of its natural ligand estradiol with the receptors' ligand-binding domain, which enables dissociation from chaperone protein Hsp90 (18-20) and facilitates ERα/chromatin interactions (21). Initial ChIP-on-chip experiments have shown ERα to mainly bind enhancer regions (16). Computational DNA sequence motif analyses of ERα binding sites resulted in the identification of a number of upstream transcription factors that facilitate the binding of ERα to the chromatin, including pioneer factor FOXA1 (16, 22) and putative pioneer factors PBX1 (23) and AP-2γ (24) (**Figure 1**). Pioneer factors can associate with compacted chromatin and trigger enhancer competency by de-condensing the chromatin, facilitating the binding of additional chromatin binding factors (25, 26). Additionally, ERα-cooperating transcription factor GATA3 is capable of mediating enhancer accessibility at ERα regulatory regions and has properties similar to FOXA1 (27, 28). Besides binding directly to the DNA, ERα can also associate to the chromatin via other transcription factors, also known as tethering, including RUNX1 (29) and AP-1 (30-32).

After activation, ERα undergoes a conformational change (33), forming a co-activator-binding pocket at the receptors' carboxy-terminus (34). This interaction surface subsequently leads to the recruitment of the members of the p160 co-activator family; SRC1 (NCOA1) (35), SRC2 (NCOA2, TIF2, GRIP1) (36, 37) and SRC3 (NCOA3, p/CIP, AIB1, ACTR) (38-41). The binding of these SRCs to the co-activator-binding pocket of activated ERα has been described to occur both in a competitive manner (exclusive recruitment of one type of SRC) (34, 42, 43) as well as in a joint manner, possibly through hetero-dimerization (44). Reports on the exact stoichiometry within the p160/ERα complex are conflicting, describing a single p160 to associate with an ERα-dimer (43) or two SRCs per active ERα-complex (44, 45), although both situations might occur side-to-side (44). Recently it was shown, for SRC3, that these ERα-interactions occur in a monomeric fashion,
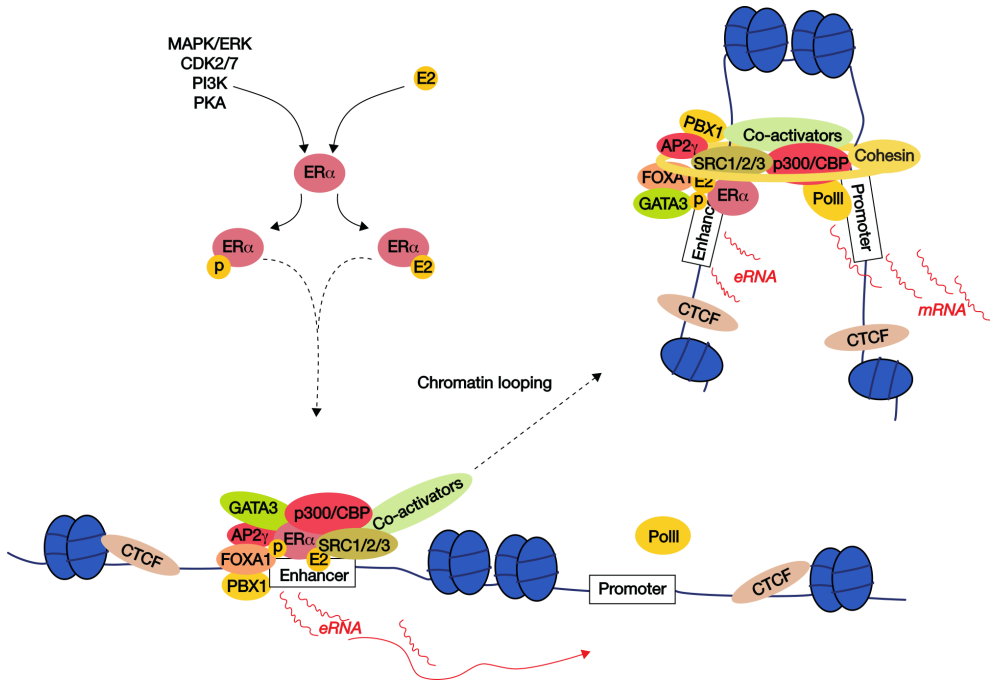
Figure 1: *The Estrogen Receptor α transcriptional complex pathway. When activated by its natural ligand estradiol or by direct phosphorylations, ERα binds to enhancers made accessible by pioneer factors (e.g. FOXA1). A transcriptional complex including p300, CBP, SRCs and other co-activators is assembled and enhancer RNAs are transcribed. After cohesin-stabilized chromatin looping to associated gene promoters, RNA polymerase II (Pol II) is recruited and an active transcriptional complex is formed, capable of transcribing associated genes.*

where two ligand-bound ERα-monomers individually recruit one SRC3 protein, after which an ERα-dimer (binding two SRC3 molecular) associates to single p300 protein (45). The p160 composition of the ERα transcriptional complex influences its genomic binding preferences on a genome-wide scale, consequently resulting in an altered transcriptional repertoire (46) and altered phenotypic behavior (**Figure 2**).

      After ERα binding, p160 proteins can subsequently recruit other essential proteins for transcriptional regulation, including p300 and CBP (47), which can modify chromatin accessibility through their acetyltransferase activity (48). In order to further modify the chromatin towards a transcription favourable landscape, histone modifiers CARM1 (49, 50) and JMJD2B (51, 52) and members of the SWI/SNF chromatin remodelling complex, including

BAF57, are recruited (53) (**Chapter 5**).

      With the recent discovery of estradiol-induced enhancer RNAs (eR-NAs) at a set of ~1200 ERα-bound enhancer elements (54, 55), an additional layer of ERα biology was revealed. This eRNA production is not just limited to ERα-bound enhancers but is for example also apparent for the Androgen Receptor (AR) (56) and p53 (57). DNAse I sensitivity assays demonstrated that eRNAs are capable of regulating genomic access of the transcriptional complex to regulatory regions (58). eRNAs found at ERα binding sites strongly correlated with the enrichment of a number of genomic features associated with enhancers and enhancer looping to target gene promoters (54). The physiological relevance of eRNAs in ERα-biology was further stipulated by the observation that knockdown of a subset of eRNAs (e.g. GREB1 enhancer) reduced the transcription of coding gene transcripts, as well as reducing promoter-enhancer interactions as shown by chromosome conformation capture (3C) (55), although conflicting 3C results have also been described (54). Hah et al. found that inhibition of eRNA production by flavopiridol, a CDK9 inhibitor blocking transcriptional elongation, did not affect other indicators of enhancer activity or estradiol-dependent promoter-enhancer looping (54), leaving the exact role of eRNAs somewhat elusive. These eRNA-associated promoter-enhancer interactions, also known as chromosomal looping structures, have been described to promote ERα-regulated gene transcription and seem to be stabilized by cohesion (55, 59, 60). Recently it was discovered that RNA binding to CBP stimulates its histone acetyl transferase activity, resulting in increased transcription of associated genes (61), providing an additional layer of possible eRNA function. Although these observations hint towards an important role for eRNAs in ERα-regulated transcription, only a subset of eRNAs has yet been investigated thoroughly, with conflicting roles in chromosomal looping, leaving the exact physiological roles for them currently elusive.

      After ERα has recruited its co-factors, an active transcriptional complex can be formed by RNA polymerase II (Pol II) recruitment and transcription of responsive genes can be initiated (62) (**Figure 1**). When treated with tamoxifen, the ligand-binding-domain of ERα adopts an alternative conformation, impairing the docking of p160 proteins to ERα, preventing the correct assembly of the transcriptional complex (34).

      The genome-wide kinetics with which the ERα-complex assembles on the chromatin is not yet fully understood. By using ChIP at three ERα responsive gene-promoters, Shang et al. have reported that ERα and a number
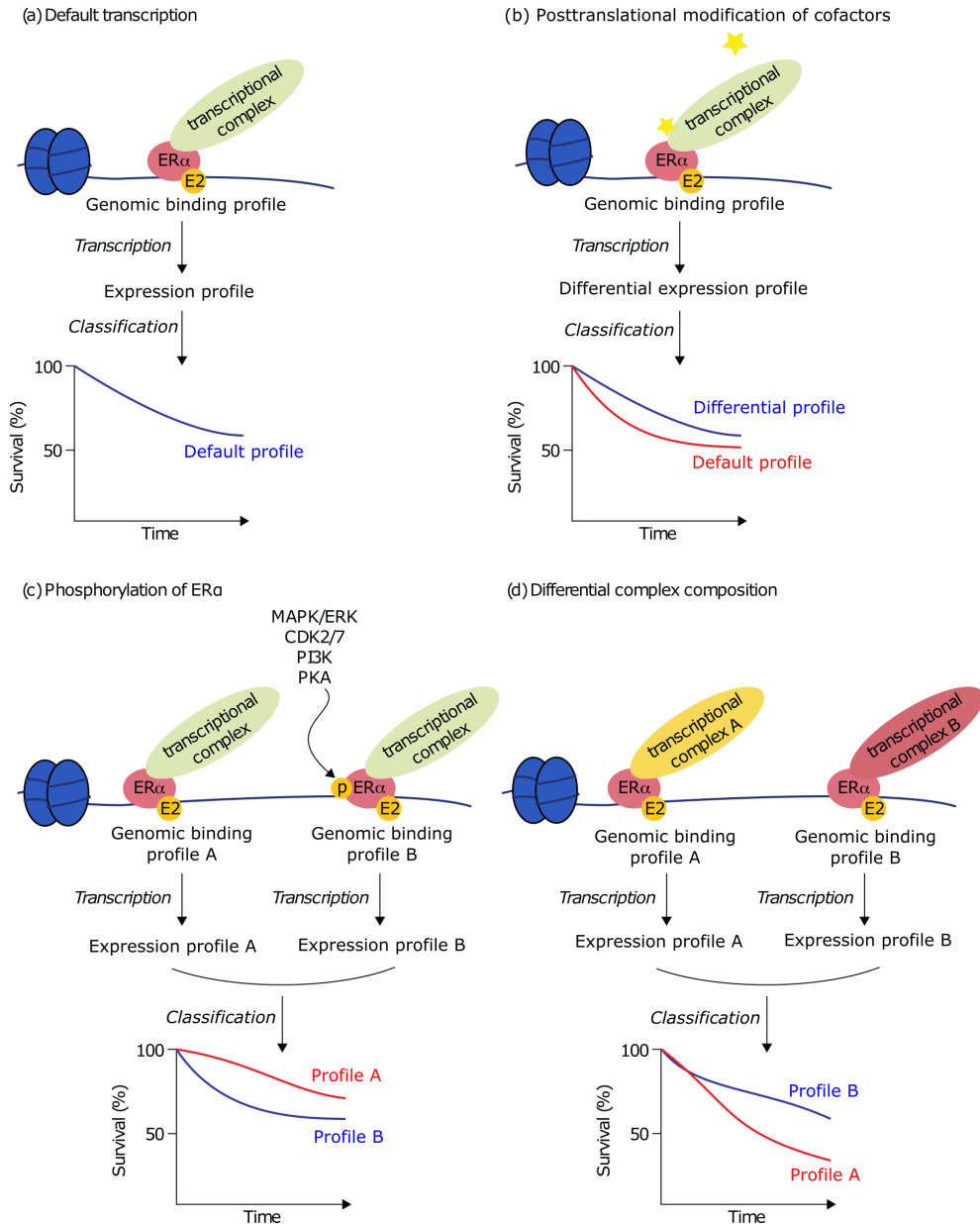
Figure 2: ERα transcriptional complex composition, genomic profile and transcriptional output.

Illustration of ERα-induced transcription, where the genomic binding profile of ERα's transcriptional complex leads to induced transcription and an expression profile on the basis of which a classification profile can be made (a). These genomic, transcriptional and classification profiles can be altered by posttranslational modi-

fications of cofactors (b), phosphorylations on ERα itself (c) and the composition of the transcriptional complex (d).

of its coactivators associate on these estrogen responsive promoters in a cyclic fashion and that these cycles of ERα-complex assembly are followed by transcription (63). This cyclic recruitment of ERα and its coregulators could be confirmed by others, who reported cofactor recruitment to be preceded by histone deacetylases and nucleosome-remodeling complexes at the TFF1 promoter (64). These data imply that transcriptional activation of ERα-responsive genes may require both activating as well as repressive epigenetic processes. Although both papers state that ERα-induced transcriptional activation occurs in a cyclic fashion, both papers only investigated the dynamic nature of ERα on a couple of sites and a comprehensive overview of ERα dynamics on a genome-wide scale is currently lacking. Furthermore, whether this cyclic ERα-complex assembly occurs only on promoters, as studied in both papers, or whether it is also apparent at ERα-bound enhancers remains unclear (**Chapter 5**).

ERα cistromics in breast cancer cell lines

Initially, most reports on ERα chromatin interactions, its dynamics and recruitment of coregulators were centred on single binding site-based analyses, often limited to the TFF1 promoter. With the technological development of tiling arrays, ERα genomic interactions could reliably be assessed on a chromosome-wide scale (16). As technology progressed, this approach was quickly succeeded by massive parallel sequencing technologies, enabling the interrogation of ERα sites on a genome-wide scale, in a cost-effective manner (17). These initial reports resulted in a huge paradigm-shift, completely changing the way we think about ERα genomics. These studies illustrated that even though most pioneering studies on ERα-genomics exclusively interrogated promoters, this genomic behaviour of ERα clearly represents an exception. In fact, only a small proportion of about 5% of ERα binding sites was found at gene promoters; a characteristic feature that has been validated by others (16, 46) and is also apparent for other nuclear receptors, including AR (65) and Glucocorticoid Receptor (GR) (66). Approximately 95% of all ERα binding sites are found at distal cis-regulatory elements (hence designated as 'cistromics' (67)) that were later recognized as enhancer regions. These regions are putative regulatory elements and might not all be functional. Recently a CRISPR-Cas9 screen was used to functionally asses ERα enhancers

elements and their effect on cell proliferation (68). Out of the 99 ERα bindings sites that were targeted, the deletion of only four of them affected cell proliferation, further illustrating that only a subset of ERα bindings sites at cis-regulatory elements might actually be functionally involved in cell proliferation processes.

The discovery of enhancer preference for ERα binding repositioned the classical promoter-centred ERα studies considerably on the level of physiological extrapolation. Chromatin interaction analysis by paired-end tag sequencing (ChIA-PET) analyses, which enables the identification of long-range chromatin interactions, illustrated that the distal enhancer-associated ERα-bindings sites were found to loop to anchor genes through connections with proximal ERα-binding sites, suggesting that ERα functions by bringing genes together for coordinated transcriptional regulation by extensive chromatin looping (59). At the GREB1 and TFF1 locus, this chromatin looping was dependent on ERα expression and was inducible by estradiol stimulation (59, 69). Probing the three-dimensional architecture of the genome by coupling proximity-based ligation with massively parallel sequencing (Hi-C) (70) yielded similar ERα mediated enhancer-promoter interactions (71). These sites of chromatin looping highly correlated with CTCF-binding sites, suggesting CTCF to play a key role defining the boundaries of chromosomal territories and influence gene expression through cross-talk between promoters and regulatory elements (72-74). Besides for ERα, these chromatin loops have also been observed for other nuclear transcription factors, including AR (75) and GR (76).

On the transcriptomic level, the use of global nuclear run-on and sequencing (GRO-seq) (77) analysis increased our understanding of ERα-regulated transcription by identifying primary and immediate estrogen induced effects as opposed to steady-state transcript level analyses (78). GRO-seq demonstrated that estrogen is able to regulate the activity of all three RNA polymerases and led to the discovery of previously undetected estrogen-regulated intergenic transcripts (78). Transcription profiling by GRO-seq could be used for the prediction of de novo enhancers across various cell types (54). In combination with RNA-seq, GRO-seq was able to annotate long noncoding RNAs (lncRNAs) and characterized the lncRNA transcriptome in MCF-7 breast cancer cells, including over 700 previously unannotated lncRNAs (79). Furthermore, GRO-seq analysis at ERα enhancers revealed the existence of estradiol-induced unidirectional and bidirectional eRNAs, that were strongly correlated with enhancer-promoter looping (54). The described role of these

intergenic transcripts in enhancer-promoter looping (55, 59, 60) and the fact that one promoter can be involved in multiple enhancer-associated loops (59, 71), might explain the seemingly large discrepancy between the number of ERα-regulated genes (approximately 2,000 (46)) in relation to the number of ERα-binding sites in the same cell line (>10,000 (17, 22)).

Due to technical limitations in the ChIP-seq protocol, the resolution of DNA binding analyses is typically quite limited with events being mapped with ±300 base pairs. Further refinement of the ChIP-seq procedure has led to the implementation of lambda exonuclease digestion in the protocol (ChIP-exo), enabling high resolution mapping of chromatin binding and identification of unique transcription factor binding sites that could not be identified by ChIP-seq (80-82). The addition of exonucleases also results in the degradation of contaminating DNA, effectively lowering the required depth of sequencing coverage.

Apart from forming the foundations of cis-regulatory gene regulation, chromatin looping and eRNA action, genome-wide profiling analyses of ERα sites can also lead to the identification of additional transcription factor motifs often co-enriched at ERα sites and proximal to estrogen response elements (ERE). These motif analyses revealed the presence of Forkhead binding motifs at roughly 50% of ERα bindings sites (16). This observation led to the discovery that FOXA1 is essential for chromatin accessibility at ERα-sites and crucial for ERα binding and functionality (16, 22). More recently, this same approach was used to identify other pioneer factors for ERα, including PBX1 which can guide ERα to a specific subset of sites (23). When investigating the motifs of ERα-bindings sites identified by ChIA-PET, Tan et al. found that approximately 40% of these binding sites contained the AP-2 motif (24). They next demonstrated that transcription factor AP-2γ can bind to these ERα-bindings sites in a ligand-independent manner and there is a functional interplay between AP-2γ and FOXA1 (24).

Besides the interplay between ERα and its pioneer factors and coregulators, it is becoming increasingly apparent that a complex interplay exists between different steroid hormone receptor family members. The androgen receptor (AR), a transcription factor classically known for its oncogenic role in prostate cancer, is expressed in 84-95% of the ERα-positive breast cancers (83-85) and is usually associated with a favourable outcome (86-88). Exogenous overexpression of AR inhibits ERα-transactivation activity and estrogen induced cell growth (86, 89), which may be explained by a direct competition between ERα and AR at binding the same genomic regions (86). This notion

was further strengthened by ChIP analysis showing AR recruitment to the progesterone receptor promoter in T47D cells (86).

Another steroid hormone receptor family member known for its co-expression and favourable outcome in ERα-positive breast cancer, is the progesterone receptor (PR) (90, 91). Progesterone induces the association of PR with ERα, thereby regulating ERα-chromatin interactions and transcriptional activity, providing mechanistic insights behind the clinical implications of PR-status in ERα-positive tumors (92).

The Glucocorticoid Receptor (GR), in the presence of dexamethasone, is able to associate to similar binding regions as ERα, and GR-stimulation leads to reduced transcription of key ERα-target genes (93, 94). This direct protein-protein interaction between GR and ERα can play an important role in the GR-mediated growth inhibition of ERα positive cells (93). Besides this general inhibitory role of GR, gene specific regulation with both cooperation and antagonism has also been described (95). Apart from direct physical interactions between nuclear receptors, nuclear receptors can also inhibit each other's activity through cross-interference ("squelching"), where direct competition for cofactor recruitment can inhibit nuclear receptor activity without associating to the same genomic regions (96, 97).

Cistromics of ERα coregulators

To date, several studies have compiled an overview of ERα co-regulators and interacting proteins, with numbers varying around 17 (98) to 108 (99). p160 protein family members are reproducibly and consistently identified as part of the ERα complex, for which a level of mutual exclusivity has been described for ERα binding (34, 42, 43). With the recent finding that an activated ERα dimer can bind one p300 protein (45) and p300 and CBP have a substantial overlap of ~70% in binding sites (46), it is not unlikely that a level of mutual exclusivity between p300 and CBP also exists. As a direct consequence thereof, the composition of ERα complexes can differ between different sites on a genome-wide scale, with potentially far-reaching consequences on gene expression profiles (**Chapter 4**). Cistromic analyses of the p160 family members illustrated that even though most genomic sites are shared between SRC1, SRC2 and SRC3, distinct subsets of sites were identified where gene expression was selectively responsive to one specific p160 protein, as part of the ERα-complex (46). Interestingly, the gene-profile under the control of ERα with exclusively SRC3 binding (devoid of SRC1 or SRC2) had prognostic potential, and enabled identification of breast can-

cer patients with a poor outcome after tamoxifen treatment (46). This link between SRC3 gene targets and tamoxifen treatment is in line with previous reports describing increased SRC3 expression, in combination with increased ERBB2 expression, to correlate with a poor tamoxifen response (100-103). Another ERα interacting protein that can affect ERα-complex formation and gene expression, is the transcriptional regulator RIP140 (104). Genes under the specific control of RIP140 (identified by siRNA experiments) could be used to classify tamoxifen-treated patients on clinical outcome (104). Both RIP140 and the p160 family members further stipulate the observation that the composition of the transcriptional complex may differ on a genome-wide scale, which could have direct physiological consequences on the level of transcriptional output and clinical response (**Figure 2**).

ERα phosphorylations and genome-wide effects on ERα action

Besides the composition of the transcriptional complex, phosphorylations on ERα can also regulate the transcriptional activity of the receptor and play a crucial role in endocrine resistance (105, 106) (**Chapter 2, 3**). These phosphorylation-events mainly revolve around serine residues 104/106 (107), 118 (108), 167 (109), 236 (110) and 305 (111) (**Chapter 2**). The kinases involved in phosphorylation on ERα at s104/106 include CDK2 and ERK1/2 (107, 112); for s118 ERK1/2, EGFR and IGF1R (113, 114); for s167 AKT and CK2 (115, 116); for s236 PKA (117) and for s305 PAK1 and PKA (111, 118). The clinical implications of these phosphorylations remain not fully understood, where higher expression of s118 and s167 phosphorylations are generally but not uniformly associated with a favorable outcome in patients on tamoxifen therapy (109, 119-122), whereas the s305 phosphorylation is associated with a poor clinical outcome (122, 123). Furthermore, s118 phosphorylation expression appears to be a predictive biomarker for tamoxifen response (108, 119). Recently, the phosphorylation on the 594 threonine (t594) residue of ERα was found to play a key role in the regulatory interaction of ERα with 14-3-3 proteins (124). This t594 phosphorylation resulted in decreased estradiol-stimulated ERα dimerization, reduced ERα-chromatin interactions and reduced gene expression (124) (**Chapter 3**).

The spectrum of ERα phosphorylation-events appears able to dictate differential transcriptional programs of ERα, as exemplified by the PKA-induced s305 phosphorylation that redirects ERα to differential transcriptional start sites, translating into a 26-gene expression classifier that identified patients with a poor clinical outcome after tamoxifen treatment (105) (**Chapter**

2). Additionally, it was found that stimulation of ERα by the epidermal growth factor (EGF), which induces s118 phosphorylation (125), led to a distinct cistromic landscape and induced a unique set of genes, when compared to estradiol stimulation (126). Stimulation of ERα by AKT, capable of inducing 167 phosphorylation (115), also mediated changes in ERα chromatin binding and altered its transcriptional output (127), further indicating that specific phosphorylations on ERα may yield distinct genomic actions and may target unique locations throughout the genome (**Figure 2**). Although the binding patterns of some of the phosphorylated ERα forms are known, a complete and comparative overview is still lacking. Furthermore, multiple reports have studied ERα cistromics upon activation of a specific cellular signalling cascade, including the previously mentioned AKT or EGF, where it still remains elusive which specific variable is actually responsible for the altered ERα behaviour.

Besides the effect direct ERα phosphorylations can have on ERα's genomic landscape and transcriptional activity, posttranslational modifications of coregulators can also influence ERα action. Where ERα-bound SRC3 binding is predominantly enhancer-bound, phosphorylated SRC3 at Ser543 (pSRC3) was selectively found at promoters of ERα-regulated genes (128) (**Chapter 6**). pSRC3 functioned as an independent prognostic factor as well as a predictive marker for tamoxifen treatment, potentially enabling the identification of patients with a good clinical outcome without receiving adjuvant therapy (128). Additionally, SRC2 can be phosphorylated at Ser736 through the MAPK pathway, increasing SRC2 interactions with p300 and CBP, further facilitating SRC2 recruitment to the ERα complex (129). These posttranslational modifications on coregulators further illustrate the intrinsic complexity and flexibility of ERα transcription complex formation, where multiple cell signaling cascades converge to collaboratively fine-tune ERα action on a genome-wide scale (**Figure 2**).

Cistromic analyses in clinical samples and potential clinical applications

Over recent years, the transition is being made from studying ERα cistromics in cell lines towards genomic interrogation of ERα sites in clinical specimens. Obviously, in contrast to cell lines, clinical samples cannot be readily manipulated and represent heterogeneous populations of multiple cell types. Even with this difference between tumors and cell lines, the cistromic information obtained from both settings yields quite similar conclusions. When looking at ERα, most well-described ERα binding sites found in MCF-

7 cells (16, 17) such as enhancer regions proximal to RARA, GREB1, XBP1 and TFF1, are also observed in tumor specimens (130). Not only for ERα, but also for its coregulators the overlap of chromatin binding in cell lines versus clinical specimens was considerably high. For example, SRC3-pS543 ChIP-seq analyses showed 51% overlap in binding sites between MCF-7 cells and an ER+/PR+ breast tumor, being in the same order of magnitude as found between 2 tumor samples (61% overlap) (128) (**Chapter 6**).

The first analyses of ERα binding patterns in clinical samples directly illustrated the added value of assessing ERα binding in clinical specimens (130), where differential ERα binding sites found between tumors could stratify patients on outcome (130). A more recent study identified ERα chromatin binding patterns in primary breast tumors that enabled patient classification on their response to aromatase inhibition in the metastatic setting (131). This same report analysed profiles for H3K27me3, resulting in a gene classifier that seemed to outperform other prognostic classifiers, including OncotypeDX (132) and PAM50 (133). Since the classification potential of these genes was only partially preserved in a cohort of tamoxifen-treated patients, this suggests some treatment selectivity for patient classification. Both studies demonstrate clear advantages of studying ERα cistromic analyses in clinical specimens, with the potential to facilitate tailored therapy selection and enable patient stratification on outcome.

Although these cistromic classifiers made use of associated gene-profiles, it remains largely unknown which genes in these classifiers are now the driving force behind any prognostic or predictive effect. Fine-tuning these classifiers towards optimized gene sets and further biological investigation of these genes could reveal the biologically most relevant genes for disease progression and might lead to novel biological insights in ERα biology as well as potentially novel drug targets (**Chapter 5**).

Since the main function of ERα is to activate its downstream target genes involved in tumor progression, ERα cistromic analyses may yield novel drug targets. A key example for this line of thought can be found in Myc, representing one of the best-studied ERα responsive genes (134-136) and widely accepted as a potent novel drug target in cancer (137, 138).

Besides targeting ERα-regulated genes to inhibit its stimulatory effect, ERα-cofactors also receive increasing attention as potential drug targets. Small molecule inhibitors against both SRC1 and SRC3 (139, 140) or SRC3 alone (141), as well as a stimulator for SRC3 activity (142) were recently identified and proved successful in inhibiting breast cancer cell proliferation

in vitro as well as in xenograft mouse models. Such novel therapeutic options could revolutionize endocrine therapeutic drug design, not aiming at blocking the receptor itself, but targeting the proteins required for receptor action. Since in case of endocrine therapy resistance ERα can still remain a driver (13-15), such novel inhibitors have the potency to remain effective after progression on currently available endocrine therapies (**Chapter 5**).

Even though promising, at the moment there are no cistromic classifiers being used in the clinic. One of the major practical limitations is the typically low amounts of available tumor tissue. Although initially challenging, continuing technical developments, including single-tube linear DNA amplification method (LindDA) (143) and the combination of a high-sensitivity ChIP-assay with new library preparation procedures (144), have now greatly increased the applicability of ChIP-seq on limited amounts of tissue. Another example of these developments is the incorporation of carrier chromatin that can be removed before library preparation, improving ChIP efficiency while limiting background signal (145). Furthermore, a great promise for the future of ChIP-seq on limited tumor material might be found in the combination of microfluidics, DNA barcoding and sequencing, which recently enabled the generation of ChIP-seq data at a single-cell resolution (146).

Discussion

Within 10 years, ERα genomics has gone from single-locus to genome-wide and towards single-cell. Initial reports on ERα cistromics in breast cancer have revolutionized the way we think about ERα action and ERα-responsive genes. By far, most transcriptional effects found regulated by ERα are represented as eRNAs. With conflicting reports about the role of eRNAs in chromosomal looping, a comprehensive overview of eRNA action, and with this to a certain degree a functional overview of ERα-enhancer action, is currently lacking. Since ERα seems to function mostly through chromatin loops, it is not unlikely that ERα enhancers and a subset of responsive eRNAs are functionally involved in such looping structures.

In ERα-positive breast cancer cell lines and tumors, many thousands of ERα binding sites can be found, of which a large number is shared between them. This could imply a selection pressure throughout human evolution for the maintenance of these ERα sites throughout the human genome. As technological development continues, future studies will further elucidate the functional relevance of all these ERα sites and identify the genomic regions responsible for proliferative potential.

Clearly, our knowledge on ERα genomic regulation in breast cancer has increased exponentially over the last decade. A major factor in this, is the parallel development of novel technologies and computational tools, which not only enable us to generate genomic data with an unprecedented level of data richness and detail, but also with the tools that enable us to process and understand the data. Now, with novel technologies on genome editing (e.g. CRISPR Cas9) and single-cell ChIP-seq analyses, the second decade of cistromics in breast cancer will no doubt unveil another layer of unprecedented complexity in breast cancer and may lead us towards a comprehensive understanding of the disease with its full genomic complexity and diversity.

Disclosure
The authors have no conflict of interest to disclose

References

1.   Ferlay J, Soerjomataram I, Dikshit R, Eser S, Mathers C, Rebelo M, et al. Cancer incidence and mortality worldwide: sources, methods and major patterns in GLOBOCAN 2012. International journal of cancer Journal international du cancer. 2015;136(5):E359-86.

2.   Hayashi SI, Eguchi H, Tanimoto K, Yoshida T, Omoto Y, Inoue A, et al. The expression and function of estrogen receptor alpha and beta in human breast cancer and its clinical application. Endocr Relat Cancer. 2003;10(2):193-202.

3.   Dahlman-Wright K, Cavailles V, Fuqua SA, Jordan VC, Katzenellenbogen JA, Korach KS, et al. International Union of Pharmacology. LXIV. Estrogen receptors. Pharmacol Rev. 2006;58(4):773-81.

4.   Beatson G. On Treatment of Inoperable Cases of Carcinoma of the Mamma: Suggestions for a New Method of Treatment, with Illustrative Cases. Lancet. 1896;2(3802):104-7.

5.   Thomson A. Analysis of Cases in which Oophorectomy was Performed for Inoperable Carcinoma of the Breast. British medical journal. 1902;2(2184):1538-41.

6.   Jensen EV, DeSombre ER. Estrogen-receptor interaction. Science. 1973;182(4108):126-34.

7.   Greene GL, Gilna P, Waterfield M, Baker A, Hort Y, Shine J. Sequence and expression of human estrogen receptor complementary DNA. Science. 1986;231(4742):1150-4.

8.   Jordan VC, Murphy CS. Endocrine pharmacology of antiestrogens as antitumor agents. Endocr Rev. 1990;11(4):578-610.

9.   Katzenellenbogen BS, Miller MA, Mullick A, Sheen YY. Antiestrogen action in breast cancer cells: modulation of proliferation and protein synthesis, and interaction with estrogen receptors and additional antiestrogen binding sites. Breast Cancer Res Treat. 1985;5(3):231-43.

10.   Arpino G, De Angelis C, Giuliano M, Giordano A, Falato C, De Laurentiis M, et al. Molecular mechanism and clinical implications of endocrine therapy resistance in breast cancer. Oncology. 2009;77 Suppl 1:23-37.

11.   Fabian CJ. The what, why and how of aromatase inhibitors: hormonal agents for treatment and prevention of breast cancer. International journal of clinical practice. 2007;61(12):2051-63.

12.   Early Breast Cancer Trialists' Collaborative G, Davies C, Godwin J, Gray R, Clarke M, Cutter D, et al. Relevance of breast cancer hormone receptors and other factors to the efficacy of adjuvant tamoxifen: patient-level meta-analysis of randomised trials. Lancet. 2011;378(9793):771-84.

13.   Vergote I, Amant F, Leunen K, Van Gorp T, Berteloot P, Neven P. Metastatic breast cancer: sequencing hormonal therapy and positioning of fulvestrant. International journal

of gynecological cancer : official journal of the International Gynecological Cancer Society. 2006;16 Suppl 2:524-6.

14.   Wang J, Jain S, Coombes CR, Palmieri C. Fulvestrant in advanced breast cancer following tamoxifen and aromatase inhibition: a single center experience. The breast journal. 2009;15(3):247-53.

15.   Yoo C, Kim SB, Ahn JH, Jung KH, Ahn Y, Gong G, et al. Efficacy of fulvestrant in heavily pretreated postmenopausal women with advanced breast cancer: a preliminary report. Journal of breast cancer. 2011;14(2):135-9.

16.   Carroll JS, Liu XS, Brodsky AS, Li W, Meyer CA, Szary AJ, et al. Chromosome-wide mapping of estrogen receptor binding reveals long-range regulation requiring the forkhead protein FoxA1. Cell. 2005;122(1):33-43.

17.   Welboren WJ, van Driel MA, Janssen-Megens EM, van Heeringen SJ, Sweep FC, Span PN, et al. ChIP-Seq of ERalpha and RNA polymerase II defines genes differentially responding to ligands. The EMBO journal. 2009;28(10):1418-28.

18.   Catelli MG, Binart N, Jung-Testas I, Renoir JM, Baulieu EE, Feramisco JR, et al. The common 90-kd protein component of non-transformed '8S' steroid receptors is a heat-shock protein. The EMBO journal. 1985;4(12):3131-5.

19.   Pratt WB, Toft DO. Steroid receptor interactions with heat shock protein and immunophilin chaperones. Endocr Rev. 1997;18(3):306-60.

20.   Devin-Leclerc J, Meng X, Delahaye F, Leclerc P, Baulieu EE, Catelli MG. Interaction and dissociation by ligands of estrogen receptor and Hsp90: the antiestrogen RU 58668 induces a protein synthesis-dependent clustering of the receptor in the cytoplasm. Molecular endocrinology. 1998;12(6):842-54.

21.   Kumar V, Chambon P. The estrogen receptor binds tightly to its responsive element as a ligand-induced homodimer. Cell. 1988;55(1):145-56.

22.   Hurtado A, Holmes KA, Ross-Innes CS, Schmidt D, Carroll JS. FOXA1 is a key determinant of estrogen receptor function and endocrine response. Nature genetics. 2011;43(1):27-33.

23.   Magnani L, Ballantyne EB, Zhang X, Lupien M. PBX1 genomic pioneer function drives ERalpha signaling underlying progression in breast cancer. PLoS genetics. 2011;7(11):e1002368.

24.   Tan SK, Lin ZH, Chang CW, Varang V, Chng KR, Pan YF, et al. AP-2gamma regulates oestrogen receptor-mediated long-range chromatin interaction and gene transcription. The EMBO journal. 2011;30(13):2569-81.

25.   Zaret KS, Carroll JS. Pioneer transcription factors: establishing competence for gene expression. Genes & development. 2011;25(21):2227-41.

26.   Jozwik KM, Carroll JS. Pioneer factors in hormone-dependent cancers. Nature reviews Cancer. 2012;12(6):381-5.

27. *Theodorou V, Stark R, Menon S, Carroll JS. GATA3 acts upstream of FOXA1 in mediating ESR1 binding by shaping enhancer accessibility. Genome research. 2013;23(1):12-22.*

28. *Kong SL, Li G, Loh SL, Sung WK, Liu ET. Cellular reprogramming by the conjoint action of ERalpha, FOXA1, and GATA3 to a ligand-inducible growth state. Molecular systems biology. 2011;7:526.*

29. *Stender JD, Kim K, Charn TH, Komm B, Chang KC, Kraus WL, et al. Genome-wide analysis of estrogen receptor alpha DNA binding and tethering mechanisms identifies Runx1 as a novel tethering factor in receptor-mediated transcriptional activation. Molecular and cellular biology. 2010;30(16):3943-55.*

30. *Cheung E, Acevedo ML, Cole PA, Kraus WL. Altered pharmacology and distinct coactivator usage for estrogen receptor-dependent transcription through activating protein-1. Proceedings of the National Academy of Sciences of the United States of America. 2005;102(3):559-64.*

31. *Kushner PJ, Agard DA, Greene GL, Scanlan TS, Shiau AK, Uht RM, et al. Estrogen receptor pathways to AP-1. The Journal of steroid biochemistry and molecular biology. 2000;74(5):311-7.*

32. *Umayahara Y, Kawamori R, Watada H, Imano E, Iwama N, Morishima T, et al. Estrogen regulation of the insulin-like growth factor I gene transcription involves an AP-1 enhancer. The Journal of biological chemistry. 1994;269(23):16433-42.*

33. *Paige LA, Christensen DJ, Gron H, Norris JD, Gottlin EB, Padilla KM, et al. Estrogen receptor (ER) modulators each induce distinct conformational changes in ER alpha and ER beta. Proceedings of the National Academy of Sciences of the United States of America. 1999;96(7):3999-4004.*

34. *Shiau AK, Barstad D, Loria PM, Cheng L, Kushner PJ, Agard DA, et al. The structural basis of estrogen receptor/coactivator recognition and the antagonism of this interaction by tamoxifen. Cell. 1998;95(7):927-37.*

35. *Onate SA, Tsai SY, Tsai MJ, O'Malley BW. Sequence and characterization of a coactivator for the steroid hormone receptor superfamily. Science. 1995;270(5240):1354-7.*

36. *Hong H, Kohli K, Garabedian MJ, Stallcup MR. GRIP1, a transcriptional coactivator for the AF-2 transactivation domain of steroid, thyroid, retinoid, and vitamin D receptors. Molecular and cellular biology. 1997;17(5):2735-44.*

37. *Voegel JJ, Heine MJ, Zechel C, Chambon P, Gronemeyer H. TIF2, a 160 kDa transcriptional mediator for the ligand-dependent activation function AF-2 of nuclear receptors. The EMBO journal. 1996;15(14):3667-75.*

38. *Torchia J, Rose DW, Inostroza J, Kamei Y, Westin S, Glass CK, et al. The transcriptional co-activator p/CIP binds CBP and mediates nuclear-receptor function. Nature. 1997;387(6634):677-84.*

39.   Anzick SL, Kononen J, Walker RL, Azorsa DO, Tanner MM, Guan XY, et al. AIB1, a steroid receptor coactivator amplified in breast and ovarian cancer. Science. 1997;277(5328):965-8.

40.   Chen H, Lin RJ, Schiltz RL, Chakravarti D, Nash A, Nagy L, et al. Nuclear receptor coactivator ACTR is a novel histone acetyltransferase and forms a multimeric activation complex with P/CAF and CBP/p300. Cell. 1997;90(3):569-80.

41.   Suen CS, Berrodin TJ, Mastroeni R, Cheskis BJ, Lyttle CR, Frail DE. A transcriptional coactivator, steroid receptor coactivator-3, selectively augments steroid receptor transcriptional activity. The Journal of biological chemistry. 1998;273(42):27645-53.

42.   Carraz M, Zwart W, Phan T, Michalides R, Brunsveld L. Perturbation of estrogen receptor alpha localization with synthetic nona-arginine LXXLL-peptide coactivator binding inhibitors. Chem Biol. 2009;16(7):702-11.

43.   Margeat E, Poujol N, Boulahtouf A, Chen Y, Muller JD, Gratton E, et al. The human estrogen receptor alpha dimer binds a single SRC-1 coactivator molecule with an affinity dictated by agonist structure. J Mol Biol. 2001;306(3):433-42.

44.   Zhang H, Yi X, Sun X, Yin N, Shi B, Wu H, et al. Differential gene regulation by the SRC family of coactivators. Genes & development. 2004;18(14):1753-65.

45.   Yi P, Wang Z, Feng Q, Pintilie GD, Foulds CE, Lanz RB, et al. Structure of a biologically active estrogen receptor-coactivator complex on DNA. Molecular cell. 2015;57(6):1047-58.

46.   Zwart W, Theodorou V, Kok M, Canisius S, Linn S, Carroll JS. Oestrogen receptor-co-factor-chromatin specificity in the transcriptional regulation of breast cancer. The EMBO journal. 2011;30(23):4764-76.

47.   McKenna NJ, Xu J, Nawaz Z, Tsai SY, Tsai MJ, O'Malley BW. Nuclear receptor coactivators: multiple enzymes, multiple complexes, multiple functions. The Journal of steroid biochemistry and molecular biology. 1999;69(1-6):3-12.

48.   Ogryzko VV, Schiltz RL, Russanova V, Howard BH, Nakatani Y. The transcriptional coactivators p300 and CBP are histone acetyltransferases. Cell. 1996;87(5):953-9.

49.   Chen D, Ma H, Hong H, Koh SS, Huang SM, Schurter BT, et al. Regulation of transcription by a protein methyltransferase. Science. 1999;284(5423):2174-7.

50.   Stallcup MR, Chen D, Koh SS, Ma H, Lee YH, Li H, et al. Co-operation between protein-acetylating and protein-methylating co-activators in transcriptional activation. Biochemical Society transactions. 2000;28(4):415-8.

51.   Kawazu M, Saso K, Tong KI, McQuire T, Goto K, Son DO, et al. Histone demethylase JMJD2B functions as a co-factor of estrogen receptor in breast cancer proliferation and mammary gland development. PloS one. 2011;6(3):e17830.

52.   Shi L, Sun L, Li Q, Liang J, Yu W, Yi X, et al. Histone demethylase JMJD2B coordinates H3K4/H3K9 methylation and promotes hormonally responsive breast carcino-

genesis. Proceedings of the National Academy of Sciences of the United States of America. 2011;108(18):7541-6.

53.   Belandia B, Orford RL, Hurst HC, Parker MG. Targeting of SWI/SNF chromatin remodelling complexes to estrogen-responsive genes. The EMBO journal. 2002;21(15):4094-103.

54.   Hah N, Murakami S, Nagari A, Danko CG, Kraus WL. Enhancer transcripts mark active estrogen receptor binding sites. Genome research. 2013;23(8):1210-23.

55.   Li W, Notani D, Ma Q, Tanasa B, Nunez E, Chen AY, et al. Functional roles of enhancer RNAs for oestrogen-dependent transcriptional activation. Nature. 2013;498(7455):516-20.

56.   Wang D, Garcia-Bassets I, Benner C, Li W, Su X, Zhou Y, et al. Reprogramming transcription by distinct classes of enhancers functionally defined by eRNA. Nature. 2011;474(7351):390-4.

57.   Melo CA, Drost J, Wijchers PJ, van de Werken H, de Wit E, Oude Vrielink JA, et al. eRNAs are required for p53-dependent enhancer activity and gene transcription. Molecular cell. 2013;49(3):524-35.

58.   Mousavi K, Zare H, Dell'orso S, Grontved L, Gutierrez-Cruz G, Derfoul A, et al. eRNAs promote transcription by establishing chromatin accessibility at defined genomic loci. Molecular cell. 2013;51(5):606-17.

59.   Fullwood MJ, Liu MH, Pan YF, Liu J, Xu H, Mohamed YB, et al. An oestrogen-receptor-alpha-bound human chromatin interactome. Nature. 2009;462(7269):58-64.

60.   Schmidt D, Schwalie PC, Ross-Innes CS, Hurtado A, Brown GD, Carroll JS, et al. A CTCF-independent role for cohesin in tissue-specific transcription. Genome research. 2010;20(5):578-88.

61.   Bose DA, Donahue G, Reinberg D, Shiekhattar R, Bonasio R, Berger SL. RNA Binding to CBP Stimulates Histone Acetylation and Transcription. Cell. 2017;168(1-2):135-49 e22.

62.   Glass CK, Rose DW, Rosenfeld MG. Nuclear receptor coactivators. Curr Opin Cell Biol. 1997;9(2):222-32.

63.   Shang Y, Hu X, DiRenzo J, Lazar MA, Brown M. Cofactor dynamics and sufficiency in estrogen receptor-regulated transcription. Cell. 2000;103(6):843-52.

64.   Metivier R, Penot G, Hubner MR, Reid G, Brand H, Kos M, et al. Estrogen receptor-alpha directs ordered, cyclical, and combinatorial recruitment of cofactors on a natural target promoter. Cell. 2003;115(6):751-63.

65.   Sharma NL, Massie CE, Ramos-Montoya A, Zecchini V, Scott HE, Lamb AD, et al. The androgen receptor induces a distinct transcriptional program in castration-resistant prostate cancer in man. Cancer cell. 2013;23(1):35-47.

66.   Reddy TE, Pauli F, Sprouse RO, Neff NF, Newberry KM, Garabedian MJ, et al.

Introduction and general discussion

Genomic determination of the glucocorticoid response reveals unexpected mechanisms of gene regulation. Genome research. 2009;19(12):2163-71.

67.   Lupien M, Brown M. Cistromics of hormone-dependent cancer. Endocr Relat Cancer. 2009;16(2):381-9.

68.   Korkmaz G, Lopes R, Ugalde AP, Nevedomskaya E, Han R, Myacheva K, et al. Functional genetic screens for enhancer elements in the human genome using CRISPR-Cas9. Nature biotechnology. 2016;34(2):192-8.

69.   Pan YF, Wansa KD, Liu MH, Zhao B, Hong SZ, Tan PY, et al. Regulation of estrogen receptor-mediated long range transcription via evolutionarily conserved distal response elements. The Journal of biological chemistry. 2008;283(47):32977-88.

70.   Lieberman-Aiden E, van Berkum NL, Williams L, Imakaev M, Ragoczy T, Telling A, et al. Comprehensive mapping of long-range interactions reveals folding principles of the human genome. Science. 2009;326(5950):289-93.

71.   Mourad R, Hsu PY, Juan L, Shen C, Koneru P, Lin H, et al. Estrogen induces global reorganization of chromatin structure in human breast cancer cells. PloS one. 2014;9(12):e113354.

72.   Botta M, Haider S, Leung IX, Lio P, Mozziconacci J. Intra- and inter-chromosomal interactions correlate with CTCF binding genome wide. Molecular systems biology. 2010;6:426.

73.   Handoko L, Xu H, Li G, Ngan CY, Chew E, Schnapp M, et al. CTCF-mediated functional chromatin interactome in pluripotent cells. Nature genetics. 2011;43(7):630-8.

74.   Splinter E, Heath H, Kooren J, Palstra RJ, Klous P, Grosveld F, et al. CTCF mediates long-range chromatin looping and local histone modification in the beta-globin locus. Genes & development. 2006;20(17):2349-54.

75.   Wang Q, Carroll JS, Brown M. Spatial and temporal recruitment of androgen receptor and its coactivators involves chromosomal looping and polymerase tracking. Molecular cell. 2005;19(5):631-42.

76.   Hakim O, John S, Ling JQ, Biddie SC, Hoffman AR, Hager GL. Glucocorticoid receptor activation of the Ciz1-Lcn2 locus by long range interactions. The Journal of biological chemistry. 2009;284(10):6048-52.

77.   Core LJ, Waterfall JJ, Lis JT. Nascent RNA sequencing reveals widespread pausing and divergent initiation at human promoters. Science. 2008;322(5909):1845-8.

78.   Hah N, Danko CG, Core L, Waterfall JJ, Siepel A, Lis JT, et al. A rapid, extensive, and transient transcriptional response to estrogen signaling in breast cancer cells. Cell. 2011;145(4):622-34.

79.   Sun M, Gadad SS, Kim DS, Kraus WL. Discovery, Annotation, and Functional Analysis of Long Noncoding RNAs Controlling Cell-Cycle Gene Expression and Proliferation in Breast Cancer Cells. Molecular cell. 2015;59(4):698-711.

80.   Rhee HS, Pugh BF. Comprehensive genome-wide protein-DNA interactions detected at single-nucleotide resolution. Cell. 2011;147(6):1408-19.

81.   Rhee HS, Pugh BF. ChIP-exo method for identifying genomic location of DNA-binding proteins with near-single-nucleotide accuracy. Current protocols in molecular biology / edited by Frederick M Ausubel [et al]. 2012;Chapter 21:Unit 21 4.

82.   Serandour AA, Brown GD, Cohen JD, Carroll JS. Development of an Illumina-based ChIP-exonuclease method provides insight into FoxA1-DNA binding properties. Genome biology. 2013;14(12):R147.

83.   Niemeier LA, Dabbs DJ, Beriwal S, Striebel JM, Bhargava R. Androgen receptor in breast cancer: expression in estrogen receptor-positive tumors and in estrogen receptor-negative tumors with apocrine differentiation. Modern pathology : an official journal of the United States and Canadian Academy of Pathology, Inc. 2010;23(2):205-12.

84.   Qi JP, Yang YL, Zhu H, Wang J, Jia Y, Liu N, et al. Expression of the androgen receptor and its correlation with molecular subtypes in 980 chinese breast cancer patients. Breast cancer : basic and clinical research. 2012;6:1-8.

85.   Chia K, O'Brien M, Brown M, Lim E. Targeting the androgen receptor in breast cancer. Current oncology reports. 2015;17(2):4.

86.   Peters AA, Buchanan G, Ricciardelli C, Bianco-Miotto T, Centenera MM, Harris JM, et al. Androgen receptor inhibits estrogen receptor-alpha activity and is prognostic in breast cancer. Cancer research. 2009;69(15):6131-40.

87.   Hu R, Dawood S, Holmes MD, Collins LC, Schnitt SJ, Cole K, et al. Androgen receptor expression and breast cancer survival in postmenopausal women. Clinical cancer research : an official journal of the American Association for Cancer Research. 2011;17(7):1867-74.

88.   Castellano I, Allia E, Accortanzo V, Vandone AM, Chiusa L, Arisio R, et al. Androgen receptor expression is a significant prognostic factor in estrogen receptor positive breast cancers. Breast Cancer Res Treat. 2010;124(3):607-17.

89.   Ando S, De Amicis F, Rago V, Carpino A, Maggiolini M, Panno ML, et al. Breast cancer: from estrogen to androgen receptor. Molecular and cellular endocrinology. 2002;193(1-2):121-8.

90.   Blows FM, Driver KE, Schmidt MK, Broeks A, van Leeuwen FE, Wesseling J, et al. Subtyping of breast cancer by immunohistochemistry to investigate a relationship between subtype and short and long term survival: a collaborative analysis of data for 10,159 cases from 12 studies. PLoS medicine. 2010;7(5):e1000279.

91.   Pichon MF, Pallud C, Brunet M, Milgrom E. Relationship of presence of progesterone receptors to prognosis in early breast cancer. Cancer research. 1980;40(9):3357-60.

92.   Mohammed H, Russell IA, Stark R, Rueda OM, Hickey TE, Tarulli GA, et al. Progesterone receptor modulates ERalpha action in breast cancer. Nature. 2015;523(7560):313-7.

93.   Karmakar S, Jin Y, Nagaich AK. Interaction of glucocorticoid receptor (GR) with

estrogen receptor (ER) alpha and activator protein 1 (AP1) in dexamethasone-mediated interference of ERalpha activity. The Journal of biological chemistry. 2013;288(33):24020-34.

94.   Meyer ME, Gronemeyer H, Turcotte B, Bocquel MT, Tasset D, Chambon P. Steroid hormone receptors compete for factors that mediate their enhancer function. Cell. 1989;57(3):433-42.

95.   Bolt MJ, Stossi F, Newberg JY, Orjalo A, Johansson HE, Mancini MA. Coactivators enable glucocorticoid receptor recruitment to fine-tune estrogen receptor transcriptional responses. Nucleic acids research. 2013;41(7):4036-48.

96.   Cahill MA, Ernst WH, Janknecht R, Nordheim A. Regulatory squelching. FEBS letters. 1994;344(2-3):105-8.

97.   Lopez GN, Webb P, Shinsako JH, Baxter JD, Greene GL, Kushner PJ. Titration by estrogen receptor activation function-2 of targets that are downstream from coactivators. Molecular endocrinology. 1999;13(6):897-909.

98.   Foulds CE, Feng Q, Ding C, Bailey S, Hunsaker TL, Malovannaya A, et al. Proteomic analysis of coregulators bound to ERalpha on DNA and nucleosomes reveals coregulator dynamics. Molecular cell. 2013;51(2):185-99.

99.   Mohammed H, D'Santos C, Serandour AA, Ali HR, Brown GD, Atkins A, et al. Endogenous purification reveals GREB1 as a key estrogen receptor regulatory factor. Cell reports. 2013;3(2):342-9.

100.   Osborne CK, Schiff R. Growth factor receptor cross-talk with estrogen receptor as a mechanism for tamoxifen resistance in breast cancer. Breast. 2003;12(6):362-7.

101.   Hurtado A, Holmes KA, Geistlinger TR, Hutcheson IR, Nicholson RI, Brown M, et al. Regulation of ERBB2 by oestrogen receptor-PAX2 determines response to tamoxifen. Nature. 2008;456(7222):663-6.

102.   Shou J, Massarweh S, Osborne CK, Wakeling AE, Ali S, Weiss H, et al. Mechanisms of tamoxifen resistance: increased estrogen receptor-HER2/neu cross-talk in ER/HER2-positive breast cancer. J Natl Cancer Inst. 2004;96(12):926-35.

103.   Zhao W, Zhang Q, Kang X, Jin S, Lou C. AIB1 is required for the acquisition of epithelial growth factor receptor-mediated tamoxifen resistance in breast cancer cells. Biochem Biophys Res Commun. 2009;380(3):699-704.

104.   Rosell M, Nevedomskaya E, Stelloo S, Nautiyal J, Poliandri A, Steel JH, et al. Complex formation and function of estrogen receptor alpha in transcription requires RIP140. Cancer research. 2014;74(19):5469-79.

105.   de Leeuw R, Flach K, Bentin Toaldo C, Alexi X, Canisius S, Neefjes J, et al. PKA phosphorylation redirects ERalpha to promoters of a unique gene set to induce tamoxifen resistance. Oncogene. 2013;32(30):3543-51.

106.   Joel PB, Smith J, Sturgill TW, Fisher TL, Blenis J, Lannigan DA. pp90rsk1 regulates estrogen receptor-mediated transcription through phosphorylation of Ser-167. Molecular

and cellular biology. 1998;18(4):1978-84.

107.   Thomas RS, Sarwar N, Phoenix F, Coombes RC, Ali S. Phosphorylation at serines 104 and 106 by Erk1/2 MAPK is important for estrogen receptor-alpha activity. J Mol Endocrinol. 2008;40(4):173-84.

108.   Kok M, Holm-Wigerup C, Hauptmann M, Michalides R, Stal O, Linn S, et al. Estrogen receptor-alpha phosphorylation at serine-118 and tamoxifen response in breast cancer. J Natl Cancer Inst. 2009;101(24):1725-9.

109.   Yamashita H, Nishio M, Kobayashi S, Ando Y, Sugiura H, Zhang Z, et al. Phosphorylation of estrogen receptor alpha serine 167 is predictive of response to endocrine therapy and increases postrelapse survival in metastatic breast cancer. Breast Cancer Res. 2005;7(5):R753-64.

110.   Atsriku C, Britton DJ, Held JM, Schilling B, Scott GK, Gibson BW, et al. Systematic mapping of posttranslational modifications in human estrogen receptor-alpha with emphasis on novel phosphorylation sites. Molecular & cellular proteomics : MCP. 2009;8(3):467-80.

111.   Michalides R, Griekspoor A, Balkenende A, Verwoerd D, Janssen L, Jalink K, et al. Tamoxifen resistance by a conformational arrest of the estrogen receptor alpha after PKA activation in breast cancer. Cancer cell. 2004;5(6):597-605.

112.   Rogatsky I, Trowbridge JM, Garabedian MJ. Potentiation of human estrogen receptor alpha transcriptional activation through phosphorylation of serines 104 and 106 by the cyclin A-CDK2 complex. The Journal of biological chemistry. 1999;274(32):22296-302.

113.   Park KJ, Krishnan V, O'Malley BW, Yamamoto Y, Gaynor RB. Formation of an IKKalpha-dependent transcription complex is required for estrogen receptor-mediated gene activation. Molecular cell. 2005;18(1):71-82.

114.   Santen RJ, Fan P, Zhang Z, Bao Y, Song RX, Yue W. Estrogen signals via an extra-nuclear pathway involving IGF-1R and EGFR in tamoxifen-sensitive and -resistant breast cancer cells. Steroids. 2009;74(7):586-94.

115.   Campbell RA, Bhat-Nakshatri P, Patel NM, Constantinidou D, Ali S, Nakshatri H. Phosphatidylinositol 3-kinase/AKT-mediated activation of estrogen receptor alpha: a new model for anti-estrogen resistance. The Journal of biological chemistry. 2001;276(13):9817-24.

116.   Arnold SF, Obourn JD, Jaffe H, Notides AC. Serine 167 is the major estradiol-induced phosphorylation site on the human estrogen receptor. Molecular endocrinology. 1994;8(9):1208-14.

117.   Chen D, Pace PE, Coombes RC, Ali S. Phosphorylation of human estrogen receptor alpha by protein kinase A regulates dimerization. Molecular and cellular biology. 1999;19(2):1002-15.

118.   Wang RA, Mazumdar A, Vadlamudi RK, Kumar R. P21-activated kinase-1 phosphorylates and transactivates estrogen receptor-alpha and promotes hyperplasia in mammary

epithelium. The EMBO journal. 2002;21(20):5437-47.

119.   Murphy LC, Niu Y, Snell L, Watson P. Phospho-serine-118 estrogen receptor-alpha expression is associated with better disease outcome in women treated with tamoxifen. Clinical cancer research : an official journal of the American Association for Cancer Research. 2004;10(17):5902-6.

120.   Yamashita H, Nishio M, Toyama T, Sugiura H, Kondo N, Kobayashi S, et al. Low phosphorylation of estrogen receptor alpha (ERalpha) serine 118 and high phosphorylation of ERalpha serine 167 improve survival in ER-positive breast cancer. Endocr Relat Cancer. 2008;15(3):755-63.

121.   Jiang J, Sarwar N, Peston D, Kulinskaya E, Shousha S, Coombes RC, et al. Phosphorylation of estrogen receptor-alpha at Ser167 is indicative of longer disease-free and overall survival in breast cancer patients. Clinical cancer research : an official journal of the American Association for Cancer Research. 2007;13(19):5769-76.

122.   Murphy LC, Seekallu SV, Watson PH. Clinical significance of estrogen receptor phosphorylation. Endocr Relat Cancer. 2011;18(1):R1-14.

123.   Kok M, Zwart W, Holm C, Fles R, Hauptmann M, Van't Veer LJ, et al. PKA-induced phosphorylation of ERalpha at serine 305 and high PAK1 levels is associated with sensitivity to tamoxifen in ER-positive breast cancer. Breast Cancer Res Treat. 2011;125(1):1-12.

124.   De Vries-van Leeuwen IJ, da Costa Pereira D, Flach KD, Piersma SR, Haase C, Bier D, et al. Interaction of 14-3-3 proteins with the estrogen receptor alpha F domain provides a drug target interface. Proceedings of the National Academy of Sciences of the United States of America. 2013;110(22):8894-9.

125.   Bunone G, Briand PA, Miksicek RJ, Picard D. Activation of the unliganded estrogen receptor by EGF involves the MAP kinase pathway and direct phosphorylation. The EMBO journal. 1996;15(9):2174-83.

126.   Lupien M, Meyer CA, Bailey ST, Eeckhoute J, Cook J, Westerling T, et al. Growth factor stimulation induces a distinct ER(alpha) cistrome underlying breast cancer endocrine resistance. Genes & development. 2010;24(19):2219-27.

127.   Bhat-Nakshatri P, Wang G, Appaiah H, Luktuke N, Carroll JS, Geistlinger TR, et al. AKT alters genome-wide estrogen receptor alpha binding and impacts estrogen signaling in breast cancer. Molecular and cellular biology. 2008;28(24):7487-503.

128.   Zwart W, Flach KD, Rudraraju B, Abdel-Fatah TM, Gojis O, Moore D, et al. SRC3 phosphorylation at Serine 543 is a positive independent prognostic factor in ER positive breast cancer. Clinical cancer research : an official journal of the American Association for Cancer Research. 2015.

129.   Lopez GN, Turck CW, Schaufele F, Stallcup MR, Kushner PJ. Growth factors signal to steroid receptors through mitogen-activated protein kinase regulation of p160 coactivator activity. The Journal of biological chemistry. 2001;276(25):22177-82.

130.   Ross-Innes CS, Stark R, Teschendorff AE, Holmes KA, Ali HR, Dunning MJ, et al. *Differential oestrogen receptor binding is associated with clinical outcome in breast cancer. Nature. 2012;481(7381):389-93.*

131.   Jansen MP, Knijnenburg T, Reijm EA, Simon I, Kerkhoven R, Droog M, et al. *Hallmarks of aromatase inhibitor drug resistance revealed by epigenetic profiling in breast cancer. Cancer research. 2013;73(22):6632-41.*

132.   Cobleigh MA, Tabesh B, Bitterman P, Baker J, Cronin M, Liu ML, et al. *Tumor gene expression and prognosis in breast cancer patients with 10 or more positive lymph nodes. Clinical cancer research : an official journal of the American Association for Cancer Research. 2005;11(24 Pt 1):8623-31.*

133.   Parker JS, Mullins M, Cheang MC, Leung S, Voduc D, Vickery T, et al. *Supervised risk predictor of breast cancer based on intrinsic subtypes. Journal of clinical oncology : official journal of the American Society of Clinical Oncology. 2009;27(8):1160-7.*

134.   Dubik D, Dembinski TC, Shiu RP. *Stimulation of c-myc oncogene expression associated with estrogen-induced proliferation of human breast cancer cells. Cancer research. 1987;47(24 Pt 1):6517-21.*

135.   Dubik D, Shiu RP. *Transcriptional regulation of c-myc oncogene expression by estrogen in hormone-responsive human breast cancer cells. The Journal of biological chemistry. 1988;263(25):12705-8.*

136.   Watson PH, Pon RT, Shiu RP. *Inhibition of c-myc expression by phosphorothioate antisense oligonucleotide identifies a critical role for c-myc in the growth of human breast cancer. Cancer research. 1991;51(15):3996-4000.*

137.   Albihn A, Johnsen JI, Henriksson MA. *MYC in oncogenesis and as a target for cancer therapies. Advances in cancer research. 2010;107:163-224.*

138.   Soucek L, Whitfield J, Martins CP, Finch AJ, Murphy DJ, Sodir NM, et al. *Modelling Myc inhibition as a cancer therapy. Nature. 2008;455(7213):679-83.*

139.   Wang Y, Lonard DM, Yu Y, Chow DC, Palzkill TG, O'Malley BW. *Small molecule inhibition of the steroid receptor coactivators, SRC-3 and SRC-1. Molecular endocrinology. 2011;25(12):2041-53.*

140.   Wang Y, Lonard DM, Yu Y, Chow DC, Palzkill TG, Wang J, et al. *Bufalin is a potent small-molecule inhibitor of the steroid receptor coactivators SRC-3 and SRC-1. Cancer research. 2014;74(5):1506-17.*

141.   Yan F, Yu Y, Chow DC, Palzkill T, Madoux F, Hodder P, et al. *Identification of verrucarin a as a potent and selective steroid receptor coactivator-3 small molecule inhibitor. PloS one. 2014;9(4):e95243.*

142.   Wang L, Yu Y, Chow DC, Yan F, Hsu CC, Stossi F, et al. *Characterization of a Steroid Receptor Coactivator Small Molecule Stimulator that Overstimulates Cancer Cells and Leads to Cell Stress and Death. Cancer cell. 2015;28(2):240-52.*

143. *Shankaranarayanan P, Mendoza-Parra MA, Walia M, Wang L, Li N, Trindade LM, et al. Single-tube linear DNA amplification (LinDA) for robust ChIP-seq. Nature methods. 2011;8(7):565-7.*

144. *Adli M, Zhu J, Bernstein BE. Genome-wide chromatin maps derived from limited numbers of hematopoietic progenitors. Nature methods. 2010;7(8):615-8.*

145. *Zwart W, Koornstra R, Wesseling J, Rutgers E, Linn S, Carroll JS. A carrier-assisted ChIP-seq method for estrogen receptor-chromatin interactions from breast cancer core needle biopsy samples. BMC genomics. 2013;14:232.*

146. *Rotem A, Ram O, Shoresh N, Sperling RA, Goren A, Weitz DA, et al. Single-cell ChIP-seq reveals cell subpopulations defined by chromatin state. Nature biotechnology. 2015.*

1

Chapter 2

Posttranslational modification of ERα
-part 1

PKA phosphorylation redirects ERα to promoters of a unique gene set to induce tamoxifen resistance

R de Leeuw[1], KD Flach[2], C Bentin Toaldo[1], X Alexi[2], S Canisius[2,3], J Neefjes[1], R Michalides[1] and W Zwart[2]

[1]Department of Cell Biology, The Netherlands Cancer Institute, Amsterdam, The Netherlands
[2]Department of Molecular Pathology, The Netherlands Cancer Institute, Amsterdam, The Netherlands
[3]Department of Molecular Biology, The Netherlands Cancer Institute, Amsterdam, The Netherlands

Abstract

Protein Kinase A-induced estrogen receptor alpha (ERα) phosphorylation at serine residue 305 (ERαS305-P) can induce tamoxifen resistance in breast cancer. How this phospho-modification affects ERα specificity and translates into tamoxifen resistance is unclear. Here we show that S305-P modification of ERα reprograms the receptor, redirecting it to new transcriptional start sites, thus modulating the transcriptome. By altering the chromatin-binding pattern, Ser305 phosphorylation of ERα translates into a 26-gene expression classifier that identifies breast cancer patients with a poor disease outcome after tamoxifen treatment. MYC-target genes and networks were significantly enriched in this gene classifier that includes a number of selective targets for ERαS305-P. The enhanced expression of MYC increased cell proliferation in the presence of tamoxifen. We demonstrate that activation of the PKA signaling pathway alters the transcriptome by redirecting ERα to new transcriptional start sites, resulting in altered transcription and tamoxifen resistance.

Introduction

Breast cancer is the most frequently diagnosed malignancy among women, with annually around 1.7 million new diagnoses worldwide. Although treatment has strongly improved with the development of adjuvant systemic therapies, still about half a million patients die of the consequences of breast cancer every year (1). The choice of adjuvant treatment is largely based on the pathological subtype of the breast tumor, which can be classified by morphological, molecular and immunohistochemical markers. These subtypes correspond to distinct transcriptional repertoires, which translates in different aggressiveness and metastatic potential (2). 75% of all breast tumors are luminal and proliferation is dependent on the activity the estrogen receptor α (ERα). Inhibition of ERα by endocrine therapy is therefore a major treatment modality for these tumors. Endocrine therapy can be subdivided into two treatment modalities; aromatase inhibitors that block synthesis of the hormone estrogen and anti-estrogens. Anti-estrogens (e.g. tamoxifen) compete with natural estrogens by occupying the hormone-binding site of ERα and either arrest it in the inactive state (3) or inducing degradation of the receptor (4). However, patients can acquire resistance to either type of endocrine therapy. About 25% of the tamoxifen-treated tumors are resistant to this anti-estrogen, even though the tumor continues expressing ERα (5). Consequently, patients unresponsive to tamoxifen may still respond to other anti-estrogens such as fulvestrant or to aromatase inhibitors (4). A major step in treatment success would be achieved when responses to endocrine treatment could be predicted on an individualized basis. Detection of ERαS305-P in patient tissues has enabled the identification of subsets of patients resistant to tamoxifen prior to the onset of treatment (6,5,7). However, not all tamoxifen-resistant patients can be identified by IHC staining, and alternative resistance-inducing mechanisms are likely to play a role in the remaining patient group. Indeed, several causes and contributing factors in tamoxifen resistance have been described in breast cancer patients or cell models, including upregulation of growth factor receptors (like EGFR (8,9), IGFR and HER2 (10,11)), activation of kinases (such as AKT (12), MAPK (13,14), PKA in combination with PAK1 (6,15,16)), and resulting phosphorylation status of ERα (17,18,19,20).

The effects of PKA-induced phosphorylation of ERα at Serine residue 305 (ERαS305-P) in the region between the ligand binding domain and the DNA binding domain are understood in molecular detail. Phosphorylation at Ser305 results in a conformational arrest when exposed to tamoxifen (17), which affects recruitment of coregulators (21). Consequently, tamoxifen acts

as an agonist of ERα instead of an antagonist, now inducing cell growth of breast cancer cell lines (17,22). An antibody detecting ERαS305-P in tumor sections was successful in identifying breast cancer patients with a poor outcome after tamoxifen treatment (6,5,7), translating observations in tissue culture into clinical patient responses.

Since ERα is a nuclear receptor, and its phosphorylation affects recruitment of coregulators, the chromatin binding landscape of ERα and corresponding influence on the transcriptome may change due to this modification. Several kinase pathways including PKA are linked to tamoxifen resistance (22,17,23). Several classical targets for ERα were differentially regulated by PKA, including TFF1 (22). PKA activation does not only phosphorylate ERα, but has many targets, including coregulators of the receptor (24,25,26). The phospho-status of coregulators can also affect ERα function, thereby indirectly affecting the ERα cistrome and transcriptome (26,27). Other PKA targets may even bypass the receptor and change the transcriptome independently. Since kinase activity can alter the chromatin-interaction landscape of ERα (28), deciphering a direct connection between ERαS305-P modification and its targets is essential for understanding tamoxifen resistance. Here, we aim to define the direct target genes of ERαS305-P and test whether this yields predictors for tamoxifen resistance. We determined the resulting transcriptome and performed further bioinformatic analyses to determine a predictive gene signature in patient material. This signature includes unique ERαS305-P induced pathways that explain PKA-related tamoxifen resistance.

Results
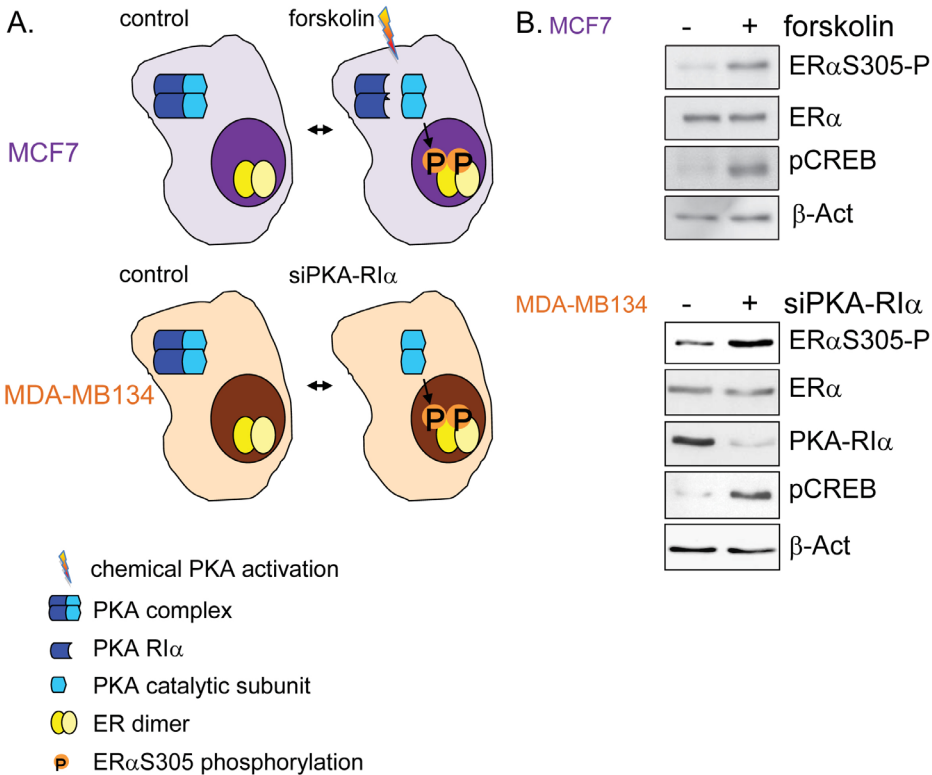
ERαS305 phosphorylation by Protein Kinase A

To study PKA-induced tamoxifen resistance, we used two well-defined and intensely studied breast cancer cell lines MCF7 and MDA-MB134. Both MCF7 and MDA-MB134 express ERα and require estrogens for growth, which is inhibited by tamoxifen (17,29). In MCF7 cells, we activated the PKA pathway by forskolin (30) (**Figure 1A** top) and isolated RNA for microarray and qPCR analyses after 4 hours of tamoxifen exposure to probe early transcriptional responses of ERαS305 phosphorylation. Forskolin treatment induces phosphorylation of ERαS305 as detected by a specific antibody (**Figure 1B** top). While we chemically activated the PKA pathway in MCF7 cells, we decided to confirm results by genetically activating this pathway in MDA-MB134 cells. Here, PKA was activated by silencing the inhibitory

Figure 1

Figure 1: *ERαS305 phosphorylation by Protein Kinase A.*
(A) Experimental setup to activate PKA in MCF7 (top) by forskolin stimulation and in MDA-MB134 (bottom) by PKA-RIα knockdown with lentiviral shRNA. Dissociation (MCF7) or loss (MDA-MB134) of PKA-RIα liberates the active, catalytic subunit of PKA, leading to ERαS305 phosphorylation. (B) Western blot analysis of the model systems. Top: Forskolin treatment of MCF7 cells leads to activated PKA, illustrated by increased p-CREB, and elevated ERαS305 phosphorylation. Bottom: shRNA approach successfully decreases PKA-RIα level in MDA-MB134 cells, leading to increased p-CREB and ERαS305-P.

subunit of PKA, PKA-RIα (**Figure 1A** bottom) (31), which is also observed in tamoxifen-resistant patients (17). When PKA-RIα is silenced, PKA is activated yielding phosphorylation of ERαS305 (17), which was confirmed by Western blot analysis (**Figure 1B** bottom). In addition, increased phosphorylation of PKA substrate CREB confirms that PKA is activated in both cell lines (**Figure 1B**), yielding an elevated ERαS305-P signal. When both methods of

PKA activation were exchanged between the two cell lines, this still resulted in ERαS305 phosphorylation (**Suppl. Figure S1**).

A gene signature for tamoxifen resistance after PKA activation
We analysed the effects of PKA-induced ERαS305 phosphorylation on the transcriptome by expression microarray analysis. Under conditions corresponding to the experiments above (**Figure 1**), cells were deprived of hormones for three days and subsequently treated with tamoxifen, after which the influence of PKA activation was assessed in both cell lines (**Figure 2**). Gene expression distribution is illustrated by the log-ratio, for PKA-activated versus non-activated cells, over intensity (RI) dot plots (**Figure 2A**). In MCF7 cells, we identified 152 upregulated and 108 downregulated genes following PKA activation (260 in total). In MDA-MB134, we found 385 up- and 437 downregulated genes (822 in total) (**Supplementary Table S1 and S2**). In these gene expression profiles, 59 up- and 41 downregulated genes overlapped between MCF7 and MDA-MB134 cells (**Figure 2B and Suppl. Table S3 and S4**). By focusing on the overlap of 100 differentially regulated genes, we eliminated cell line or treatment-specific effects. Among the upregulated hits were two classical ERα gene targets: XBP1 and TFF1, the latter of which was in the top 5 of differentially regulated genes. The top 10 up- and downregulated hits for MCF7 and MDA-MB134 cells are indicated (**Figure 2C**), and a subset was tested and confirmed by qPCR (**Figure 2D**). Next, we tested the 100 differentially regulated genes that are shared between the two cell lines and conditions (59 up, 41 down) as a classifier for outcome in tamoxifen treated breast cancer patients, using a publically available dataset (32). The gene classifier was found to significantly correlate with poor outcome after tamoxifen treatment (p=0.019; hazard ratio=2.5) (**Figure 2E** top). This classifier was validated in an independent patient series (33), again identifying the patients with a poor outcome after tamoxifen treatment (p=0.045; hazard ratio=1.97, **Figure 2E** bottom).
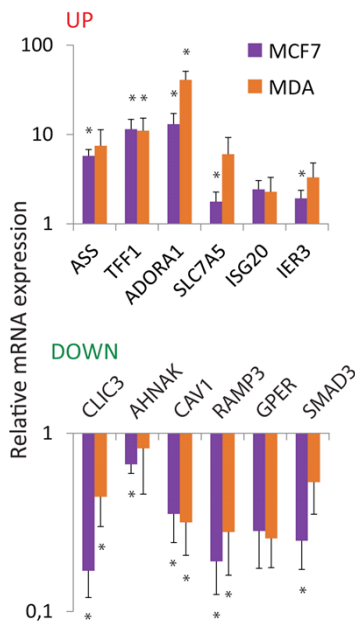
Figure 2

A. RI plots
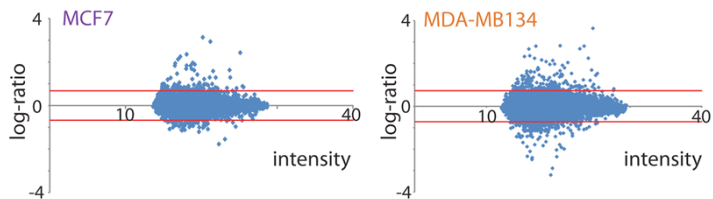
B.
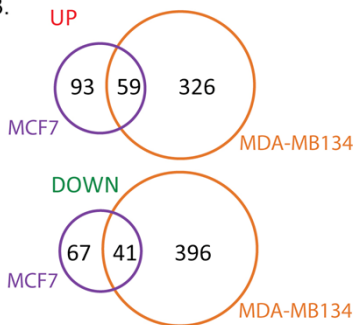
C.

Top 10 hits

MCF7*		MDA-MB134*	
UP	DOWN	UP	DOWN
ASS	CLIC3	CPE	CAV1
TFF1	AHNAK	TFF1	CAV2
MUC5AC	CAV1	ADORA1	SAMD11
ADORA1	TACC1	SLC7A5	KLHL24
SLC7A5	PMP22	PRSS23	CLIC3
ISG20	RAMP3	SLC7A2	CXCR7
CPE	YPEL3	IER3	SCUBE2
PCP4	NRCAM	ASS	SMAD3
SEMA3B	GPER	SEMA3B	TSPAN9
IER3	SMAD3	HS.579631	TACC1

* all hits overlap between MCF7 and MDA134

D. qPCR

E.
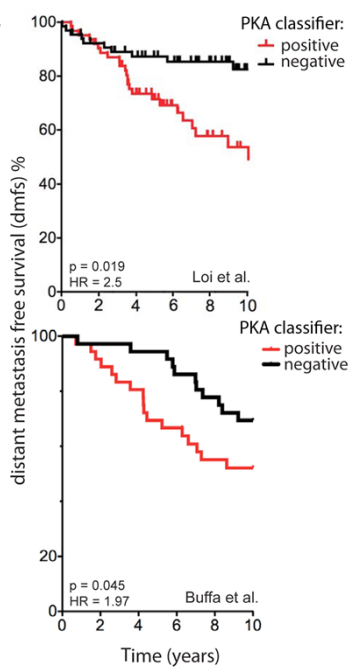
Figure 2: *Gene signature for tamoxifen resistance through PKA activation*
(A) RI-plots of microarray profiles of MCF7 (left) and MDA-MB134 (right). Log-ra-
tio is plotted over intensity. For further analysis, a threshold is used of >1.5x diffe-
rence (log-ratio = 0.585), indicated by the red line, and p<0.05. (B) Venn diagrams
of up- (top) and downregulated (bottom) genes show overlap between MCF7 (pur-
ple) and MDA-MB134 (orange) gene expression signatures.(C) Table of the top 10 of
up- and downregulated genes for MCF7 and MDA-MB134 mRNA expression values.
Genes represented in red (up) or green (down) are tested and confirmed by qPCR.
(D) qPCR validation of a subset of the top hits. mRNA expression is shown as a ratio
tamoxifen/tamoxifen with PKA activation, and internally corrected using β-Actin.
MA = Microarrays values. Error bars represent standard error of the mean (SEM). *
p < 0.05 by Student's t-test. (E) Genes shared between MCF7 and MDA-MB134 are
combined into a 100-gene signature. This signature was applied as a gene classifier
in a disease metastasis free survival analysis. The average gene expression values in
ERα positive, endocrine treated patients selected from Loi et al. (top, (32)) and Buffa
et al. (bottom, (33)) were calculated and ranked for up- and downregulated genes.
Patients were stratified as described in the materials and methods. Patients who
have a positive signature for the classifier show significantly worse disease progres-
sion (Loi data: p=0.019; hazard ratio(HR)=2.5; Buffa data: p=0.045; HR=1.97)

S305P modification of ERα targets the receptor to promoters
PKA activity results in the phosphorylation of many targets, including ERα.
ERα itself has two target sites for PKA, Serine 236 (34) and Serine 305, the
latter of which is predominant and correlates to tamoxifen resistance (17).
To determine the effects of ERαS305 phosphorylation on gene transcription
and chromatin deposition, we analyzed the chromatin-binding landscape of
ERαS305-P by means of ChIP-seq with a specific monoclonal antibody (5). To
this purpose, cells were cross-linked, chromatin fragmented and ERαS305-P
immuno-precipitated. The co-isolated chromatin fragments were ampli-
fied, sequenced and mapped against the human genome reference (**Figure
3A**) (35). MCF7 cells were hormone deprived for three days and stimulat-
ed with forskolin. Since transcriptional alterations were observed four hours
after tamoxifen treatment, the chromatin interaction patterns of ERαS305-P
were studied at an earlier time point as DNA binding precedes transcription.
ERαS305-P binding patterns were compared to chromatin interactions of
total ERα from asynchronously proliferating MCF7 cells (36) to determine
the shared events and unique binding sites for the phosphorylated receptor.
ERαS305-P shows 3327 binding events, of which 912 overlap with total ERα
(**Figure 3C**). The unique subsets of binding patterns were not due to differ-

Figure 3

A.

B.

C. binding events

D. heat map

E. Genomic distribution

F. motif analysis
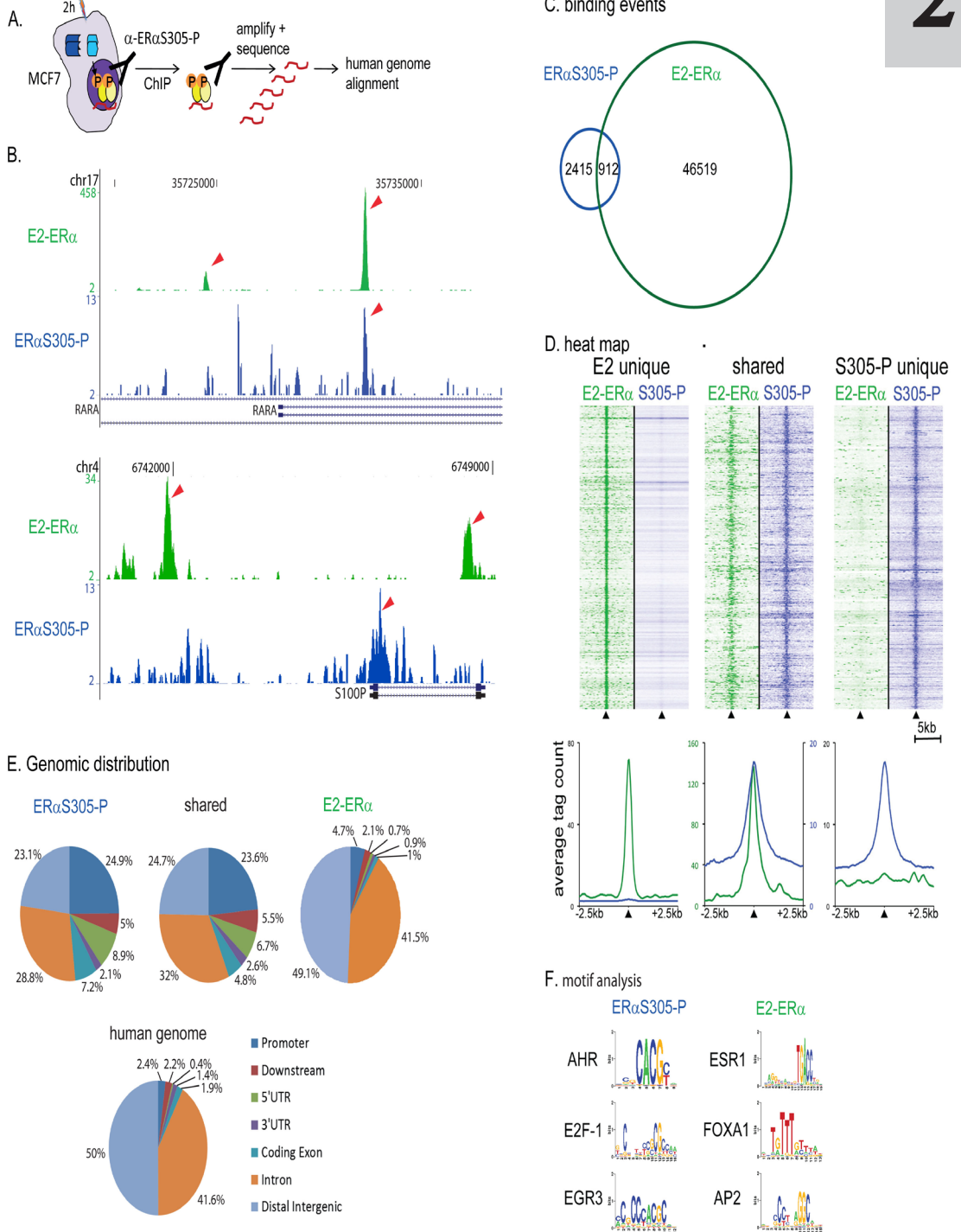
Figure 3*: Distinct chromatin binding patterns of ERαS305-P*
(A) Experimental setup: after 2 hours of forskolin stimulation, ChIPseq is performed using a specific antibody against ERαS305-P. (B) Examples of chromatin interaction to two gene areas for total ERα (green) and S305-phosphorylated ERα (blue). Reti-noic acid receptor alpha (RARA) has an ERα binding site within a 20k nucleotide re-gion of the transcription start, to which ERaS305-P also binds. S100P shows binding for both total and phosphorylated ERα, but ERαS305-P prefers the promoter, whe-reas total ERα binds to a distal enhancer. Arrows denote binding peaks. A 5 kb size marker is indicated. (C) Venn diagram, showing the overlap of ERαS305-P (blue) chromatin binding events versus total ERα (green). Number of shared or unique peaks is indicated. Called peaks were interrogated for overlap and intersected using Galaxy (http://main.g2.bx.psu.edu/). (D) Heat map visualization of the shared and unique peaks for ERαS305-P (blue) and E2-ERα (green). Top: Shown are all peak regions, which were vertically aligned and centered on the binding site (arrowhead) with a 5kb window. Bottom: The signals were quantified and visualized in a 2D line graph, showing the average tag count for ERαS305-P (blue) and total ERα (green) at the shared and unique regions with a 2.5kb window. (E) Genomic distribution of overall ERαS305-P binding (left), total ERα (right) and sites shared between the two (middle). The genomic distributions of binding sites were analyzed using the cis-re-gulatory element annotation system (CEAS) 57. The genes closest to the binding site on both strands were analyzed. If the binding region is within a gene, CEAS software indicates whether it is in a 5'UTR, a 3'UTR, a coding exon, or an intron. Promoter is defined as 1 kb upstream from RefSeq 5' start. If a binding site is >1 kb away from the RefSeq transcription start site, it is considered distal intergenic. ERαS305-P shows preference for promoter sites. (F) Motif analysis of binding sites for ERαS305-P (blue) and total, estradiol-stimulated ERα (green) show a difference in motif prefe-rence. To identify motifs, SeqPos was used 58. SeqPos uses the distances from motif positions to the peak summits (center of the regions) to find the most enriched motifs near peak summits, using TRANSFAC.

ences in peak-calling thresholds, as shown in the raw heat map distributions (**Figure 3D**). These data imply that S305-phosphorylated ERα shares only a subset of the conventional ERα binding sites, but also has its own specific targets sites. Examples of shared and unique sites are shown in **Figure 3B**. Only a subset of the ERαS305-P binding sites as induced by PKA stimulation are shared with EGF-induced ERα chromatin interactions (**Suppl. Figure S2**) (28). These data suggest that distinct ERα-chromatin interaction patterns are induced through different kinase pathways. When the ERαS305-P peaks were

annotated, a striking enrichment for ERαS305-P was observed for promoter regions, 3'UTRs and 5'UTRs, whereas total ERα generally prefers distal enhancers (**Figure 3E**), as described before (37,38). This enrichment on promoter regions is not only observed for the shared interaction sites, but also for unique ERαS305-P peaks. Interestingly, we observed distinct enriched DNA motifs for ERαS305-P as compared to total ERα, implying an active retargeting of the receptor to uncommon sites (**Figure 3F**). The top 3 enriched motifs underlying ERαS305-P binding events were AHR, EGR3 and E2F1. The biological relevance of these transcription factors in tamoxifen resistance was assessed in a cell proliferation assay, which demonstrated that knockdown of AHR, EGR3 and E2F1 can all overcome the growth advantage of PKA-activated MCF7 cells under tamoxifen conditions (**Suppl. Figure S3**). Concluding, modification of ERα at Ser305 not only affects ERα conformation (17), but also chromatin binding sites, transcription and cellular responses.

Interconnection of genes in the classifier
To understand how phosphorylation of ERαS305 drives differential gene expression, resulting in tamoxifen unresponsiveness of breast tumors, we decided to define the functional networks that are differentially (in)activated due to S305-phosphorylation of ERα. An Ingenuity Pathway Analysis (IPA) of the differentially regulated genes in both conditions was performed, which identifies functional connections from a gene list using literature data. Within the top pathways listed in **Figure 4A**, classical ERα targets (TFF1, XBP1, CAV1) as well as interacting partners of ERα for non-classical gene transactivation, such as AP-1 and NFκB (**Suppl. Figure S4**) were found, illustrating expected ERα-mediated gene expression rather than only PKA activation. Nonetheless, a pathway analysis comparison between ERαS305-P and estradiol stimulation of ERα resulted in enrichment of distinct molecular pathways (**Suppl. Table S5 and Figure S5**).

As PKA-activation can induce cell growth in tamoxifen-treated breast cancer cells (22,17), we focused on the third network, which links genes in the classifier to cell growth and proliferation. This network includes MYC as a central player (**Figure 4B**). MYC is not a direct hit in our microarray analysis as it was enriched just below the threshold (1.49x) in MCF7 cells. We validated elevated MYC expression in MCF7 cells following forskolin and tamoxifen stimulation by a more quantitative method: qPCR (**Figure 4C**). PKA activation combined with tamoxifen treatment upregulates MYC expression 1.65-fold, directly coupling ERαS305 phosphorylation to expression

Figure 4

A.	Associated Network Functions	Score
1	Lipid Metabolism, Molecular Transport, Small Molecule Biochemistry	50
2	Cell Signaling, Nucleic Acid Metabolism, Small Molecule Biochemistry	39
3	**Cell Cycle, Cellular Development, Cellular Growth and Proliferation**	32
4	Lipid Metabolism, Small Molecule Biochemistry, Cellular Movement	24
5	Cellular Development, Cellular Growth and Proliferation, Tissue Morphology	13

B.
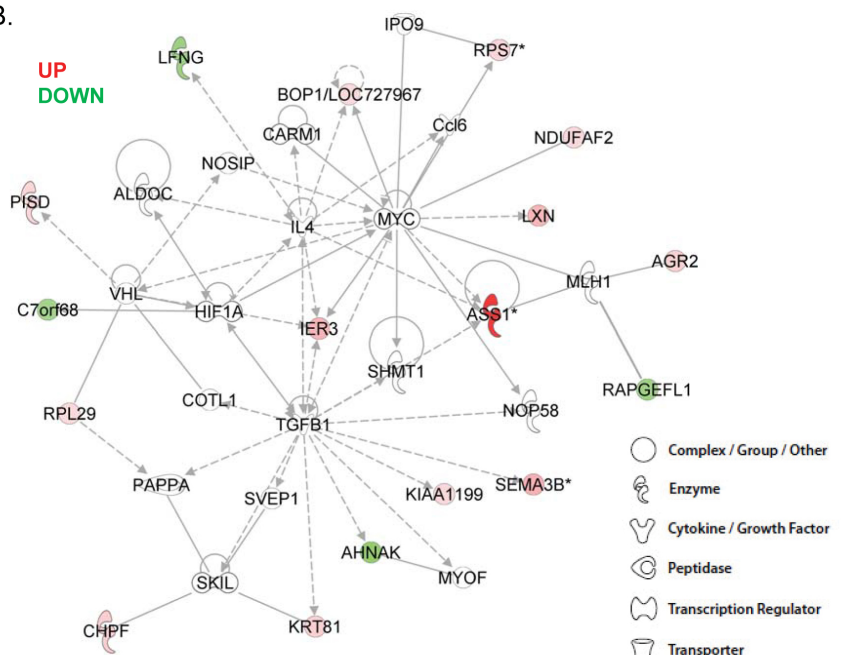
C. qPCR: MYC
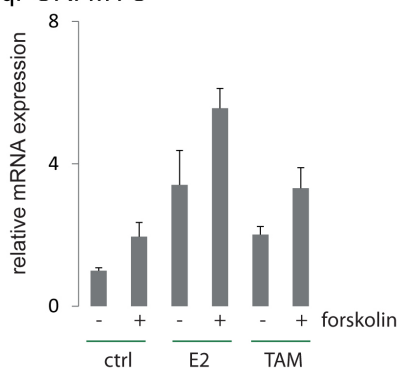
Figure 4: *Interconnection of genes in the classifier*
*(A) Ingenuity pathway analyses reveal direct and indirect links between the genes in our classifier, resulting in the top 5 of significant pathway terms listed in the table and shown in Supplementary Figure S4. Networks are scored based on the number of network eligible genes the list contain contains. Score is a likeliness parameter. (B) Shown is network 3 as shown in bold in Figure 4A. MYC plays a key role, targeting several of the genes from the classifier. Differential expression in the microarray in Figure 2 is illustrated by a red (up) or green (down) color. The nature of the different hits is indicated on the right. (C) MYC qPCR of MCF7 cells after 4 hours of treatment with estradiol (E2), tamoxifen (TAM) or hormone depleted (ctrl) in presence or absence of forskolin to stimulate PKA. Error bars represent SEM. * p < 0.05 by Student's t-test.*

of a well-known oncogene involved in tamoxifen resistance (39,40). Of note, MYC upregulation is already observed after PKA treatment alone, and no additional treatment with tamoxifen is required.

Integration of ERαS305-P chromatin binding with gene expression signatures

Selective ERαS305-P chromatin interactions should translate into transcriptional differences. To assess these, we integrated the ChIP-seq data with the expression data obtained from the microarray studies. This allowed us to extract the direct targets of ERαS305-P from the bulk of genes that are differentially regulated due to overall PKA activation. Among the 100 hits from our classifier, we defined the genes that had a chromatin binding peak for ERαS305-P within a 20k region from the transcription start site, which indicates direct transcriptional regulation by the receptor (41). This identified 26 genes as direct targets of ERαS305-P: 14 of these genes were upregulated and 12 downregulated (**Figure 5A**). Of these direct ERαS305-P targets, nine were distinct from estradiol-stimulated total ERα, implying they are specific for ERαS305-P. Utilized as a classifier in the previously mentioned patient dataset (32), the 26 ERαS305-P targets result in a significant correlation with poor disease outcome (**Figure 5B**. p=0.008 ; HR=2.33). Unfortunately validating the classifier in the *Buffa et al.* (33) dataset was not feasible due to limited patient numbers.

Next, we compared direct ERαS305-P targets with non-phosphorylated ERα with respect to tamoxifen-agonistic response, as measured by qPCR. For non-S305-P target genes, the PKA-stimulatory effects were identical for

Figure 5*: Integration of ERαS305-P chromatin binding and gene expression signatures*

(A) Hierarchical clustering of the 100 genes in the classifier, based on ERαS305-P chromatin binding, estradiol-induced chromatin interactions and gene expression of total ERα. (B) The 26 ERαS305-P hits were applied as a classifier on the patient dataset derived from Loi et al. (32), resulting in a significant correlation with poor disease outcome (p=0.008 ; HR=2.33). Analysis was performed as described in Figure 2D. (C) Scatter plot for qPCR data from genes upregulated by PKA activation, derived from the 100-gene classifier and subdivided into two groups: with (blue

diamonds) or without (red squares) a proximal binding site for ERαS305-P. Ratio for PKA activation over no activation is plotted for presence (Y-axis) or absence (X-axis) of tamoxifen. Diagonal line represents equal ratios irrespective of tamoxifen. (D) Six (representing 23%) of the direct targets are found in the MYC-related Ingenuity network, highlighted in orange. (E) ERαS305-P selectively targets MYC by binding to a distal enhancer and the promoter. Shown are the reads for ERα and ERαS305-P around the MYC gene and the 20kb marker. Arrows indicate the two peaks. (F) MYC overexpression enhances tamoxifen-specific MCF7 cell growth. Absolute cell numbers of triplicates are counted and plotted for YFP-control (ctrl in blue) and MYC (in red). Scale bars represent standard deviations. A student T-test was performed; *: p=0.03. (G) c-MYC protein expression analysis of MYC overexpression, compared to control (ctrl) by western blot. Loading control is β-actin

tamoxifen and vehicle-treated cells implying no tamoxifen-agonism at these genes (**Figure 5C**). However, for the majority of the tested genes with a proximal ERαS305-P binding site, additional transcriptional activity was observed when tamoxifen was combined with PKA treatment, suggesting an agonistic response in addition to PKA stimulation alone (**Figure 5C**).

We then analyzed the new classifier for biological relevance. Seven of the 26 direct targets were functionally connected with MYC, implying that ERαS305-P directly affects the MYC pathway (**Figure 5D**), rather than acting on MYC alone. Since MYC was upregulated in the PKA-activated, tamoxifen-treated MCF7 cells, we explored whether MYC is a direct target of ERαS305-P. To this end, the proximity of the MYC locus was analyzed for ERαS305-P peaks. We observed a chromatin interaction peak at a distal enhancer that has recently been identified (43), and a second peak at the promoter region of MYC (**Figure 5E**, arrows denote the peaks). These and other ERαS305-P/chromatin interaction sites were independently verified by qPCR analysis (**Suppl. Figure S6**). Taken together, we show by ChIP-seq, microarray and qPCR that S305-phosphorylated ERα plays a direct role in MYC transcriptional regulation. MYC upregulation will subsequently affect cell proliferation in response to tamoxifen.

To directly assess the influence of MYC on MCF7 cells proliferation, and the influence of tamoxifen treatment thereon, MYC was transiently overexpressed in MCF7 cells (**Figure 5F**; protein overexpression confirmed in **Figure 5G**). This resulted in a significant increase in cell proliferation both in absence and presence of tamoxifen, linking the enhanced expression of MYC

with cell growth even in presence of this anti-estrogen and thus inducing resistance.

Discussion

Activation of kinase pathways is one of the hallmarks of tumor formation. Most breast cancers are critically dependent on ERα and this nuclear hormone receptor can be modified by a series of kinases, including PKA (12,13,14,15,17). PKA phosphorylates ERα at position 305, inducing a conformational arrest of the receptor upon tamoxifen exposure (17). This eventually results in tamoxifen resistance and cell proliferation in response to tamoxifen exposure (17,22). However, the exact mechanism of tamoxifen resistance remains unknown and is studied here. We show that S305-P modification has a marked effect on the accurate positioning of ERα on transcriptional start sites. This is highly surprising and, in more general terms, suggests that post-translational modifications can have major effects on chromatin binding of transcription factors and thus the transcriptome. In fact, this couples extracellular signalling (in our case by PKA activation) to alterations in transcriptional output by retargeting ERα to alternative binding regions.

The phosphorylated receptor displayed an enrichment for DNA motifs that were distinct from that of total ERα in proliferating cells, suggesting that the phosphorylation directly alters the DNA binding capacities of specificity of the receptor. The top 3 enriched motifs underlying ERαS305-P binding events were AHR, EGR3 and E2F1. These transcription factors are not surprising hits, since each of these has previously been described to play essential roles in ERα biology. EGR3 has been described to be involved in ERα signalling (44) and ERα-mediated invasion, and its expression correlates with poor outcome (45). E2F1 on the other hand was found to be an ERα target that mediates tamoxifen resistance (46) and estradiol-stimulated cell proliferation (47). AHR crosstalks with ER (43) and modulates ERα-mediated gene regulation (48).

The crystal structure data of the full length RXR:PPARγ heterodimer shows an alignment of the hinge region of PPARγ along the DNA (49). This may also occur with the hinge domain of ERα, thereby determining the DNA motif specificity of the receptor. Any modifications in the hinge domain (including S305 phosphorylation) may, as a consequence, alter the DNA-binding preferences of the receptor. The altered binding repertoire of ERαS305-P is surprising, but unlikely to be dictated by this post-translational modification alone. Most likely, the S305-P modification attracts different co-factors that

in assembly alter the chromosome-binding preferences of the receptor. Such effects can be mediated further by phosphorylation of CARM1 (26) or AIB1 (25), but may also be dictated by other factors. ERα binding events are not rigid, but can differ between cell lines (50) and the chromatin-binding pattern can be manipulated by growth factor stimulation (28). To our knowledge, this is the first report describing the direct effect of phosphorylation on the chromatin binding landscape of ERα. The distinct and unique patterns as observed here suggest that phosphorylation events on the receptor not only dictate the transcriptional readout (17), the transcript repertoire (22) and cofactor preferences (21), but also determine to which DNA regions the receptor is able to bind. This yields a complicated view on transcriptional regulation by ERα. As ERα can be modified at different locations by different kinases, different chromatin deposition and thus transcription may be the result. Depending on the activated signalling pathway, a different DNA binding preference of ERα after estrogen activation or tamoxifen exposure may be the result.

Many more ERα/chromatin binding events exist as compared to estradiol-responsive genes (37,51,52). Apparently, the same holds true for ERαS305P binding events. Yet, a clear enrichment of the phosphorylated ERα was found at gene promoters. About 25% of the 3327 binding events was found at a promoter, implying about 830 peaks. Out of the 100 differentially expressed genes that were shared between the MCF7 and MDA-MB134 cell lines, 26 had at least one proximal ERαS305-P binding event, presenting a statistical enrichment over genomic background (Fisher's exact test; p=0.024).

Although we find an enrichment at promoters, not all ERαS305-P bound promoters result in the expression of the corresponding gene in our microarray analyses. This could arise due to the temporal nature of the expression array experiments, suggesting different time points may be needed to pick up differential expression of more of these genes. Nevertheless, our data show that an enrichment of ERαS305-P at promoter sites correlates with expression of the corresponding genes.

We show here for the S305 modification that distinct transcriptional pathways are generated that can explain cell growth of breast cancer cells in response to tamoxifen. Ingenuity pathway analysis illustrated that only limited overlap exists between E2 and ERαS305 associated pathways, even though a high-scoring 'cell proliferation' network was shared between the two conditions (Suppl. Figure S5 and Table S5). What the physiological effects from all non-overlapping pathways would be still needs to be deciphered, and the

additive value of any of these networks in tamoxifen resistance cannot be ruled out. The ERαS305-P distinct gene set has led to the development of a classifier that allows prediction of patient's responses to tamoxifen treatment. Further analyses show that the MYC pathway in particular can be activated, which may explain the more aggressive behavior of such tumors.

Our data illustrate that one single post-translational modification can have a major impact on the chromatin interaction patterns and transcriptome of the estrogen receptor. ERαS305 phosphorylation greatly alters its DNA-binding repetoire, giving rise to distinct responsive gene signature that includes MYC and its related genes. MYC overexpression overcomes tamoxifen action on cell proliferation and hence, a PKA-induced elevation of MYC would induce resistance to tamoxifen. MYC is a well-described gene target of ERα (40) and not solely an ERαS305P dependent gene. However, here we postulate that MYC activation is a means of PKA-induced tamoxifen-resistance, where the typical E2-dependent MYC gene is now activated by a PKA-induced ERαS305P. A link between tamoxifen resistance and MYC has been previously described (40), for which we now present one mechanism by which this can occur.

The plasticity in the chromatin binding patterns of ERα as induced by PKA activation has significant downstream effects that may lie at the very basis of tamoxifen-resistance of breast cancer patients. The genes differentially targeted and transcribed by S305-phosphorylated ERα indeed act as a biologically relevant and understandable classifier for breast cancer patient responses to tamoxifen treatment.

Materials and Methods
Cell culture
MCF7 and MDA-MB134 cells were cultured in DMEM supplemented with 8% FBS and antibiotics (penicillin, streptavidin). To deprive cells of hormones, they were cultured in phenol-red free DMEM with 5% charcoal-treated serum and antibiotics. Cells were stimulated with 10-7 M 4-OH-tamoxifen and/or 10 μM forskolin or vehicle for 4 or 24 hours.

PKA-RIα knockdown
MDA-MB134 cells were infected with lentivirus containing a shRNA (sequence: GGGGATAACTTCTATGTGA) targeting PKA-RIα. Infection was performed in DMEM after 2h incubation with polybrene (5ug/ml). After infection overnight, DMEM with 8% FBS was refreshed. Selection of infected

cells was done with 3ug/ml puromycin.

Biochemical analysis

Western blotting was performed according to standard protocols. Antibodies used were anti-ERα (Santa Cruz Biotechnology), anti-ERαS305-P (Millipore/ Upstate), anti-β-Actin (Millipore/Chemicon), anti-p-Creb (Cell Signaling Technology), anti-PKA-RIα (BD Transduction Laboratories) and anti-c-MYC (Santa Cruz Biotechnology). Signals were detected with a Lumi-light Plus detection kit (Roche).

Microarray experiments

Cells were harvested and homogenized in trizol (Invitrogen). RNA was isolated and hybridized on IlluminaWG-6 expression BeadChip (MDA-MB-134) and Human HT-12 v4 Expression BeadChip (MCF7, performed in triplicate). For data extraction, we used no background correction, applied variance stabilizing transformation and robust spline normalization. Data were log-transformed, ratios of the absolute values were calculated. For the RI plots, the log-ratio was plotted over the intensity, calculated from the absolute intensities as follows: $R = \log$ (PKA-activated / control) and $I = \log$ (PKA-activated x control). P-values absolute-value ratios were calculated with a two-tailed paired t-test. Hits were selected on $p<0.05$ with a ratio threshold of 1.5x.

Bioinformatics patient dataset

We extracted the ERα positive, tamoxifen treated tumors from two published patient datasets (32,33). All the expression data were retrieved for the 100 hits in the classifier. The average expression of all the tested genes was calculated, ranked and divided in two groups. Patients who were stratified in two groups: 1. upregulated genes in the top 50% and the downregulated genes in the bottom 50%. 2. upregulated genes in the bottom 50% and the downregulated genes in the top 50%. Kaplan-Meijer plots were generated using Prism 5 (Graphpad software). P-values were calculated using a log-ranked Gehan-Breslow-Wilcoxon method.

qPCR

Cells were harvested and homogenized in trizol. RNA isolation for qPCR was performed by a phenol-chloroform extraction. cDNA was made with a Superscript III RT kit (Invitrogen) using manufacturer's protocols. qPCR for cDNA and for ChIP-DNA was performed with SYBR Green (Applied Bi-

osystems) on a Chromo4 RT detector (Bio-Rad) using standard protocols. Primers (Invitrogen) were designed with primer3 v0.4.0 and are shown in Supplementary table S6.

ChIP-seq

ChIP experiments were performed as described previously (53). The antibody used was anti-ERαS305-P (Millipore/Upstate). ChIP DNA was amplified as described (35). Sequences were generated by the Illumina GAIIx genome analyzer (using 36-bp reads), processed by the Illumina analysis pipeline version 1.6.1, and aligned to the Human Reference Genome (assembly hg18, NCBI Build36.1, March 2008) using BWA version 0.5.5. Reads were filtered by removing those with a BWA alignment quality score less than 15. A corresponding set of input sequence reads of similar size was obtained by random sampling from the full set of input sequence reads. Enriched regions of the genome were identified by comparing the ChIP samples to input samples using the MACS peak caller (54) version 1.3.7.1 and SICER version 0.0.1 (55), where only peaks shared by both methods were considered.

MYC overexpression and cell proliferation assay

MCF7 cells were cultured in 12-wells plates. After one day of hormone deprivation, MYC was overexpressed by polyethylenimine (PEI, Polysciences (56)) transfection of a RC-CMV c-MYC vector. A pcDNA-YFP empty vector was used as control. Cells were treated in triplicate with estradiol (10-8M), tamoxifen (10-7M), fulvestrant (ICI, 10-7M) or control for 7 days. After trypsinization, cells were counted with a CASYton cell counter (Casy Technology).

Conflict of Interest

The authors declare no conflict of interest.

Acknowledgements

Author contributions

RL, JN, RM and WZ designed all the experiments. RL and KF conducted all the experiments, with help from CBT and XA. RL and SC conducted all

bioinformatics analyses. The paper was written by RL, JN, KF and WZ, with help from all other authors.

References

1   Ferlay J, Soerjomataram I, Dikshit R, Eser S, Mathers C, Rebelo M, Parkin DM, Forman D, Bray F. Cancer incidence and mortality worldwide: sources, methods and major patterns in GLOBOCAN 2012. Int J Cancer. 2015; No. 5.

2   Sorlie T, Perou CM, TibshiraniR, Aas T, Geisler S, Johnsen H et al. Gene expression patterns of breast carcinomas distinguish tumor subclasses with clinical implications. Proc Natl Acad Sci U S A 2001; 98: 10869-10874.

3   Shiau AK, BarstadD, Loria PM, Cheng L, Kushner PJ, Agard DA et al. The structural basis of estrogen receptor/coactivator recognition and the antagonism of this interaction by tamoxifen. Cell 1998; 95: 927-937.

4   Robertson JF. Selective oestrogen receptor modulators/new antioestrogens: a clinical perspective. Cancer Treat Rev 2004; 30: 695-706.

5   Holm C, Kok M, Michalides R, Fles R, Koornstra RH, Wesseling J et al. Phosphorylation of the oestrogen receptor alpha at serine 305 and prediction of tamoxifen resistance in breast cancer. J Pathol 2009; 217: 372-379.

6   Kok M, Zwart W, Holm C, Fles R, Hauptmann M, Van't Veer LJ et al. PKA-induced phosphorylation of ERalpha at serine 305 and high PAK1 levels is associated with sensitivity to tamoxifen in ER-positive breast cancer. Breast Cancer Res Treat 2011; 125: 1-12.

7   Bostner J, Skoog, L, Fornander T, Nordenskjold B, and Stal O. Estrogen receptor-alpha phosphorylation at serine 305, nuclear p21-activated kinase 1 expression, and response to tamoxifen in postmenopausal breast cancer. Clin Cancer Res 2010; 16: 1624-1633.

8   Massarweh S, Osborne CK, Creighton CJ, Qin L, Tsimelzon A, Huang S et al. Tamoxifen resistance in breast tumors is driven by growth factor receptor signaling with repression of classic estrogen receptor genomic function. Cancer Res 2008; 68: 826-833.

9   Fan, P., Wang J, Santen RJ, and Yue W. Long-term treatment with tamoxifen facilitates translocation of estrogen receptor alpha out of the nucleus and enhances its interaction with EGFR in MCF-7 breast cancer cells. Cancer Res 2007; 67: 1352-1360.

10   Shou J, Massarweh S, Osborne CK, Wakeling AE, Ali S, Weiss H et al. Mechanisms of tamoxifen resistance: increased estrogen receptor-HER2/neu cross-talk in ER/HER2-positive breast cancer. J Natl Cancer Inst 2004; 96: 926-935.

11   Riggins RB, Schrecengost RS, Guerrero MS, and Bouton AH. Pathways to tamoxifen resistance. Cancer Lett 2007; 256: 1-24.

12   Kirkegaard T, Witton CJ, McGlynn LM, Tovey SM, Dunne B, Lyon A et al. AKT activation predicts outcome in breast cancer patients treated with tamoxifen. J Pathol 2005; 207: 139-146.

13   Gee JM, Robertson JF, Ellis IO, and Nicholson RI. Phosphorylation of ERK1/2 mitogen-activated protein kinase is associated with poor response to anti-hormonal therapy and decreased patient survival in clinical breast cancer. Int J Cancer 2001; 95: 247-254.

14   Kato S, Endoh H, Masuhiro Y, Kitamoto T, Uchiyama S, Sasaki H et al. Activation of the estrogen receptor through phosphorylation by mitogen-activated protein kinase. Science 1995; 270: 1491-1494.

15   Rayala SK, Molli PR, and Kumar R. Nuclear p21-activated kinase 1 in breast cancer packs off tamoxifen sensitivity. Cancer Res 2006; 66: 5985-5988.

16   Rayala SK, Talukder AH, Balasenthil S, Tharakan R, Barnes CJ, Wang RA et al. P21-activated kinase 1 regulation of estrogen receptor-alpha activation involves serine 305 activation linked with serine 118 phosphorylation. Cancer Res 2006; 66: 1694-1701.

17   Michalides R, Griekspoor A, Balkenende A, Verwoerd D, Janssen L, Jalink K et al. Tamoxifen resistance by a conformational arrest of the estrogen receptor alpha after PKA activation in breast cancer. Cancer Cell 2004; 5: 597-605.

18   de Leeuw R, Neefjes J, and Michalides R. A Role for Estrogen Receptor Phosphorylation in the Resistance to Tamoxifen. Int J Breast Cancer 2011.

19   Skliris GP, Rowan BG, Al Dhaheri M, Williams C, Troup S, Begic S et al. Immunohistochemical validation of multiple phospho-specific epitopes for estrogen receptor alpha (ERalpha) in tissue microarrays of ERalpha positive human breast carcinomas. Breast Cancer Res Treat 2009; 118: 443-453.

20   Skliris GP, Nugent ZJ, Rowan BG, Penner CR, Watson PH, and Murphy LC. A phosphorylation code for oestrogen receptor-alpha predicts clinical outcome to endocrine therapy in breast cancer. Endocr Relat Cancer 2010; 17: 589-597.

21   Zwart, W., Griekspoor A, Berno V, Lakeman K, Jalink K, Mancini M et al. PKA-induced resistance to tamoxifen is associated with an altered orientation of ERalpha towards co-activator SRC-1. EMBO J 2007; 26: 3534-3544.

22   Dudek P and Picard D. Genomics of signaling crosstalk of estrogen receptor alpha in breast cancer cells. PLoS One 2008; 3: e1859-.

23   Miller WR. Regulatory subunits of PKA and breast cancer. Ann N Y Acad Sci 2002; 968: 37-48.

24   Wu RC, Qin J, Yi P, Wong J, Tsai SY, Tsai MJ et al. Selective phosphorylations of the SRC-3/AIB1 coactivator integrate genomic reponses to multiple cellular signaling pathways. Mol Cell 2004; 15: 937-949.

25   Yi P, Feng Q, Amazit L, Lonard DM, Tsai SY, Tsai M et al. Atypical protein kinase C regulates dual pathways for degradation of the oncogenic coactivator SRC-3/AIB1. Mol Cell 2008; 29: 465-476.

26   Carascossa S, Dudek P, Cenni B, Briand PA, and Picard D. CARM1 mediates the ligand-independent and tamoxifen-resistant activation of the estrogen receptor alpha by

cAMP. Genes Dev 2010; 24: 708-719.

27   Lupien M, Eeckhoute J, Meyer CA, Krum SA, Rhodes DR, Liu XS et al. Coactivator function defines the active estrogen receptor alpha cistrome. Mol Cell Biol 2009; 29: 3413-3423.

28   Lupien M, Meyer CA, Bailey ST, Eeckhoute J, Cook J, Westerling T et al. Growth factor stimulation induces a distinct ER(alpha) cistrome underlying breast cancer endocrine resistance. Genes Dev 2010; 24: 2219-2227.

29   Reiner GC and Katzenellenbogen BS. Characterization of estrogen and progesterone receptors and the dissociated regulation of growth and progesterone receptor stimulation by estrogen in MDA-MB-134 human breast cancer cells. Cancer Res 1986; 46: 1124-1131.

30   Al Dhaheri MH and Rowan BG. Protein Kinase A Exhibits Selective Modulation of Estradiol-Dependent Transcription in Breast Cancer Cells that Is Associated with Decreased Ligand Binding, Altered Estrogen Receptor {alpha} Promoter Interaction, and Changes in Receptor Phosphorylation. Mol Endocrinol 2007; 21: 439-456.

31   Bossis I and Stratakis CA. Minireview: PRKAR1A: normal and abnormal functions. Endocrinology 2004; 145: 5452-5458.

32   Loi S, Haibe-Kains B, Desmedt C, Lallemand F, Tutt AM, Gillet C et al. Definition of clinically distinct molecular subtypes in estrogen receptor-positive breast carcinomas through genomic grade. J Clin Oncol 2007; 25: 1239-1246.

33   Buffa FM, Camps C, Winchester L, Snell CE, Gee HE, Sheldon H et al. microRNA-Associated Progression Pathways and Potential Therapeutic Targets Identified by Integrated mRNA and microRNA Expression Profiling in Breast Cancer. Cancer Res 2011; 71: 5635-5645.

34   Chen D, Pace PE, Coombes RC, and Ali S. Phosphorylation of human estrogen receptor alpha by protein kinase A regulates dimerization. Mol Cell Biol 1999; 19: 1002-1015.

35   Schmidt D, Wilson MD, Spyrou C, Brown GD, Hadfield J, and Odom DT. ChIP-seq: using high-throughput sequencing to discover protein-DNA interactions. Methods 2009; 48: 240-248.

36   Robinson JL, Macarthur S, Ross-Innes CS, Tilley WD, Neal DE, Mills IG et al. Androgen receptor driven transcription in molecular apocrine breast cancer is mediated by FoxA1. EMBO J 2011; 30: 3019-3027.

37   Carroll JS, Meyer CA, Song J, Li W, Geistlinger TR, Eeckhoute J et al. Genome-wide analysis of estrogen receptor binding sites. Nat Genet 2006; 38: 1289-1297.

38   Madak-Erdogan Z, Lupien M, Stossi F, Brown M, and Katzenellenbogen BS. Genomic collaboration of estrogen receptor alpha and extracellular signal-regulated kinase 2 in regulating gene and proliferation programs. Mol Cell Biol 2011; 31: 226-236.

39   Miller TW, Balko JM, Ghazoui Z, Dunbier A, Anderson H, Dowsett M et al. A gene expression signature from human breast cancer cells with acquired hormone independence

identifies MYC as a mediator of antiestrogen resistance. Clin Cancer Res 2011; 17: 2024-2034.

40   Musgrove EA, Sergio CM, Loi S, Inman CK, Anderson LR, Alles MC et al. Identification of functional networks of estrogen- and c-Myc-responsive genes and their relationship to response to tamoxifen therapy in breast cancer. PLoS One 2008; 3: e2987-.

41   Louie MC, McClellan A, Siewit C, Kawabata L. Estrogen receptor regulates E2F1 expression to mediate tamoxifen resistance. Mol Cancer Res 2010; 8: 343-352.

42   Fullwood MJ, Liu MH, Pan YF, Liu J, Xu H, Mohamed YB et al. An oestrogen-receptor-alpha-bound human chromatin interactome. Nature 2009; 462: 58-64.

43   Wang C, Mayer JA, Mazumdar A, Fertuck K, Kim H, Brown M et al. Estrogen Induces c-myc Gene Expression via an Upstream Enhancer Activated by the Estrogen Receptor and the AP-1 Transcription Factor. Mol Endocrinol 2011; 25: 1527-1538.

44   Inoue A, Omoto Y, Yamaguchi Y, Kiyama R, Hayashi SI. Transcription factor EGR3 is involved in estrogen-signaling pathway in breast cancer cells. J Mol Endocrinol 2004; 32: 649-661.

45   Suzuki T, Inoue A, Miki Y, Moriya T, Akahira J, Ishida T et al. Early growth responsive gene 3 in human breast carcinoma: a regulator of estrogen-meditated invasion and a potent prognostic factor. Encocr Relat Cancer 2007; 14: 279-292

46   Frietze S, Lupien M, Silver PA, Brown M. CARM1 regulates estrogen-stimulated breast cancer growth through up-regulation of E2F1. Cancer Res 2008; 68: 301-306.

47   Callero MA, Loaiza-Pérez AI. The role of aryl hydrocarbon receptor and crosstalk with estrogen receptor in response of breast cancer cells to the novel antitumor agents benzothiazoles and aminoflavone. Int J Breast Cancer 2011; 923250.

48   Madak-Erdogan Z and Katzenellenbogen BS. Aryl hydrocarbon receptor modulation of estroge receptor a-mediated gene regulation by a multimeric chromatin complex involving the two receptors and the coregulator RIP140. Toxicol Sci 2012; 125: 401-411.

49   Chandra V, Huang P, Hamuro Y, Raghuram S, Wang Y, Burris TP et al. Structure of the intact PPAR-gamma-RXR-alpha nuclear receptor complex on DNA. Nature 2008; 350-356.

50   Krum SA, Miranda-Carboni GA, Lupien M, Eeckhoute J, Carroll JS, and Brown M. Unique ERalpha cistromes control cell type-specific gene regulation. Mol Endocrinol 2008; 22: 2393-2406.

51   Welboren WJ, van Driel MA, Janssen-Megens EM, van Heeringen SJ, Sweep FC, Span PN et al. ChIP-Seq of ERalpha and RNA polymerase II defines genes differentially responding to ligands. EMBO J 2009; 28: 1418-1428.

52   Hurtado A, Holmes KA, Ross-Innes CS, Schmidt D, Carroll JS. FOXA1 is a key determinant of estrogen receptor function and endocrine response. Nat Genet 2009; 43: 27-33.

53   Carroll JS, Liu XS, Brodsky AS, Li W, Meyer CA, Szary AJ et al. Chromosome-wide mapping of estrogen receptor binding reveals long-range regulation requiring the forkhead protein FoxA1. Cell 2005; 15: 33-43.

54   Zhang Y, Liu T, Meyer CA, Eeckhoute J, Johnson DS, Bernstein, B. E. et al. Model-based analysis of ChIP-Seq (MACS). Genome Biol 2008; 9: R137-.

55   Zang C, Schones DE, Zeng C, Cui K, Zhao K, Peng W. A clustering approach for identification of enriched domains from histone modification ChIP-Seq data. Bioinformatics 2009; 25: 1952-8.

56   Boussif O, Lezoualc'h F, Zanta MA, Mergny MD, Scherman D, Demeneix B et al. A versatile vector for gene and oligonucleotide transfer into cells in culture and in vivo: polyethylenimine. Proc Natl Acad Sci U S A 1995; 92: 7297-7301.

57   Ji X, Li W, Song J, Wei L, and Liu XS. CEAS: cis-regulatory element annotation system. Nucleic Acids Res 2006; 34: W551-W554.

58   He HH, Meyer CA, Shin H, Bailey ST, Wei G, Wang Q et al. Nucleosome dynamics define transcriptional enhancers. Nat Genet 2010; 42: 343-347.

Supplementary information

Supplementary Figure S1*: Western blot analysis in MCF7 and MDA-MB134 cells, in which PKA was activation by forskolin and/or PKA-RIγ knockdown. In each condition and cell line, ERαS305 phosphorylation could be induced.*

Supplementary Figure S2*: Venn diagram, showing shared and unique binding events for E2-ERα, EGF-stimulated ERα (green; Lupien et al., Genes Dev 2010 Oct 1;24(19):2219-27.) and ERαS305-P (blue).*

Supplementary Figure S3*: Cell proliferation assay after knockdown of the transcription factors AHR, E2F-1, EGR or ESR1. Cells were seeded in a 384 wells plate and transfected with a smartpool of 4 siRNAs, targeting the corresponding transcription factor using standard protocols (Dharmacon). Cell proliferation was assessed with an Incucyte device (Essen Bioscience) using standard settings. Bars show SD from 4 replicate samples and well confluence at the onset of the experiment was set at 1. Knockdown of these transcription factors can overcome the growth advantage of PKA-activated MCF7 cells under tamoxifen conditions, compared to control.*

Supplementary Figure S4*: Ingenuity pathway analysis (IPA), illustrating the networks 1,2,4 and 5 as described in Figure 3A.*

Supplementary Figure S5*: Venn diagram, corresponding with Ingenuity Pathway analysis presented in Suppl. Table S5. Image shows the number of enriched networks for overlapping and distinct pathways in PKA-induced ERαS305-P versus estradiol-stimulated ERα in MCF7 cells.*

Supplementary Figure S6*: ChIP-qPCR validation. MCF7 were hormone-deprived for 3*

days prior to onset of the experiment. PKA was stimulated using forskolin and ChIP was performed using an ERαS305-P antibody, identical to what was performed for the ChIP-seq. Enrichment of isolated chromatin fragments was assessed by qPCR, which was normalized over control and input.

Supplementary Table 1*: Gene expression profile for PKA-activation in MCF7. Genes are ranked from strongest down- to strongest upregulated gene, indicated by the ratio, or fold-difference, of PKA-activated over non-activated cells in presence of tamoxifen.*

Supplementary Table 2*: Gene expression profile for PKA-activation in MDA-MB134. Genes are ranked from strongest down- to strongest upregulated gene, indicated by the ratio, or fold-difference, of PKA-activated over non-activated cells in presence of tamoxifen.*

Supplementary Table 3*: Upregulated genes shared between MCF7 and MDA-MB134 (1st part of the 100-gene classifier). Upregulated genes from the microarray profiles presented in Suppl. Tables 1 and 2 were compared, resulting in 59 overlapping genes as presented in a Venn diagram (Figure 2B top).*

Supplementary Table 4*: Downregulated genes shared between MCF7 and MDA-MB134 (2nd part of the 100-gene classifier) Downregulated genes from the microarray profiles presented in Suppl. Tables 1 and 2 were compared, resulting in 41 overlapping genes as presented in a Venn diagram (Figure 2B bottom).*

Supplementary Table 5*: Ingenuity Pathway analyses show enriched networks for overlapping genes and distinct gene sets in PKA-induced ERαS305-P and estradiol-stimulated ERα in MCF7 cells.*

Supplementary Table 6*: qPCR primers for hit validation on mRNA (top) and ChIP (bottom) samples, designed with primer3 v0.4.0.*
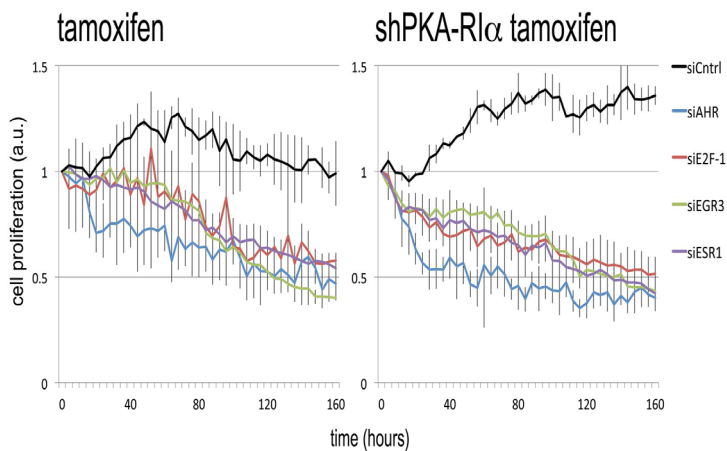
Supplementary Figure S1 – Western blot analysis of PKA activation by forskolin treatment and PKA-RIα knockdown in MCF7 and MDA-MB134 cells
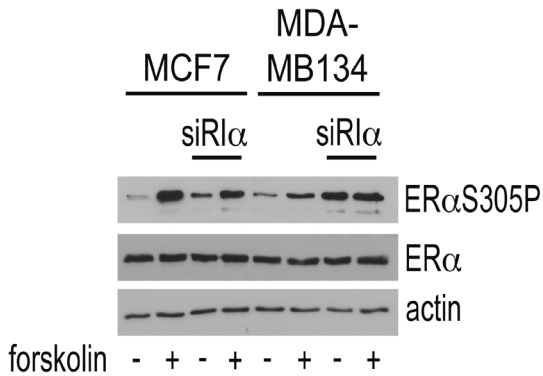
Supplementary Figure S2 – Venn diagram of ERαS305-P ChIPseq data compared with ERα-E2 and ERα-EGF data
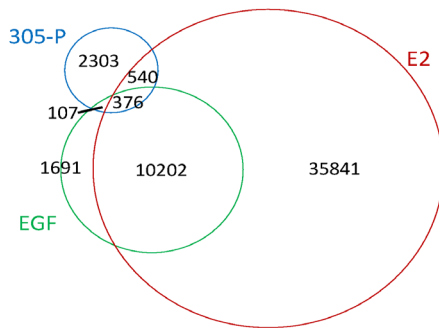
Supplementary Figure S3 – Growth assay after knockdown of AHR, E2F-1, EGR or ESR1

Supplementary figure S4
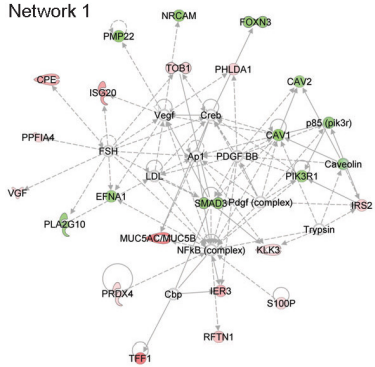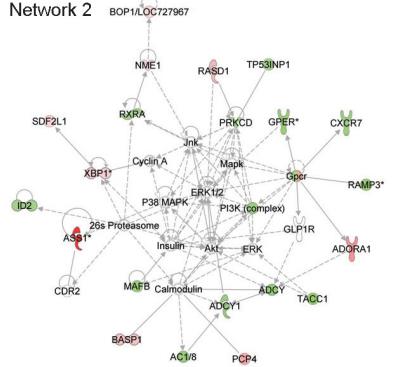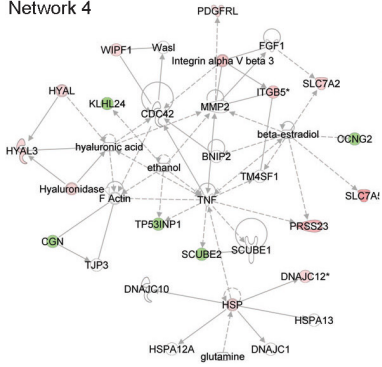
Network 1
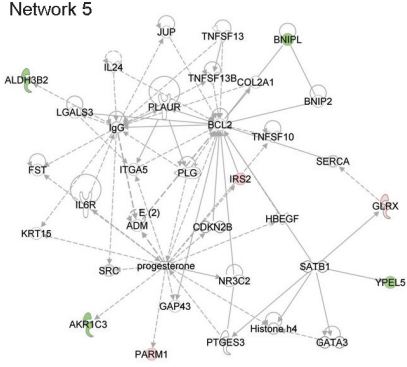
Network 2

legend
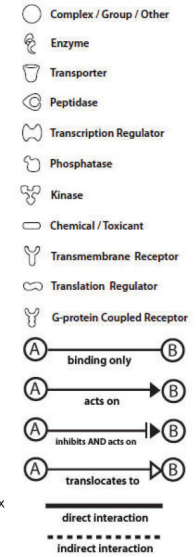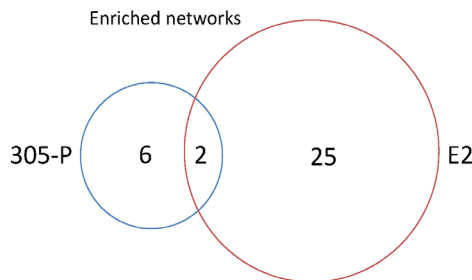
Network 4

Network 5

Supplementary Figure S5 – Venn diagram of Ingenuity Pathway analysis of ERαS305-P only, E2 only and overlapping gene sets (See Suppl. Table 5)

Enriched networks

305-P   6   2   25   E2

Supplementary Figure S6:qPCR validation of ERαS305-P ChIP-seq

primer set	fold enrichment/ control	related to Figure/Table
myc enhancer	273	Fig 5E
myc promoter	23	Fig 5E
S100P promoter	241	Fig 3B
XBP1 enhancer	279	Fig 5A
IER3 promoter	31	Fig 5A
SEMA3B promoter	32	Fig 5A

Supplementary Table 1*: Gene expression profile for PKA-activation in MCF7.*
See online supplemental information
Supplementary Table 2*: Gene expression profile for PKA-activation in MDA-MB134.*
See online supplemental information

Supplementary Table 3*: Upregulated genes shared between MCF7 and MDA-MB134 (1st part of the 100-gene classifier).*

	Symbol	Accession	MCF7	MDA-MB134
1	ASS1|ASS	NM_000050.4|NM_000050.3	8,758	3,471
2	ASS	NM_054012.2	7,646	3,163
3	TFF1	NM_003225.2	5,373	12,485
4	MUC5AC	XM_001134429.1|XM_495860.2	5,106	2,694
5	ADORA1	NM_000674.1	4,362	5,006
6	SLC7A5	NM_003486.5	3,886	4,248
7	ISG20	NM_002201.4	3,703	1,921
8	CPE	NM_001873.1	3,557	16,949
9	PCP4	NM_006198.2	3,542	1,863
10	SEMA3B	NM_001005914.1	3,224	3,122
11	IER3	NM_003897.3|NM_052815.1	3,091	3,769
12	PRSS23	NM_007173.4|NM_007173.3	3,071	4,128
13	LXN	NM_020169.2	2,991	1,710
14	RASD1	NM_016084.3	2,756	1,820
15	BASP1	NM_006317.3	2,441	2,726
16	FAM46A	NM_017633.2|NM_017633.1	2,440	1,907
17	RFTN1|RA	NM_015150.1	2,408	1,690
18	ITGB5	NM_002213.3	2,318	1,659
19	CHPF	NM_024536.4	2,073	1,650
20	SLC7A2	NM_001008539.2|NM_003046.2	1,984	3,880
21	IRS2	NM_003749.2	1,962	1,528
22	ITGB5	NM_002213.3|XM_944693.1	1,953	1,544
23	AGR2	NM_006408.2	1,907	2,017
24	KRT81|KR	NM_002281.2	1,897	2,354
25	XBP1	NM_005080.2	1,847	1,763
26	SEMA3B	NM_001005914.1	1,838	1,806
27	XBP1	NM_001079539.1	1,795	1,674
28	HS.579631	BU536065	1,787	2,898
29	RPS7	NM_001011.3	1,762	1,551
30	PHLDA1	NM_007350.3|NM_007350.2	1,762	2,174
31	MAOA	NM_000240.2	1,761	1,730
32	VGF	NM_003378.2	1,745	1,574
33	TOB1	NM_005749.2	1,740	2,895
34	NME1	NM_000269.2|NM_198175.1	1,735	2,040
35	PISD	NM_014338.3	1,706	2,757
36	SDF2L1	NM_022044.2	1,703	1,803
37	RPS7	NM_001011.3	1,702	1,535
38	DKFZP564	NM_015393.2	1,694	2,685
39	DNAJC12	NM_021800.2	1,694	1,703
40	PPFIA4	NM_015053.1	1,692	1,514
41	NUCB2	NM_005013.2|NM_005013.1	1,681	1,528
42	PDGFRL	NM_006207.1	1,680	1,873
43	DNAJC12	NM_021800.2	1,663	1,574
44	SLC47A1|F	NM_018242.2	1,661	1,525
45	HYAL3	NM_003549.2	1,659	1,512
46	GLRX	NM_002064.1	1,657	2,063
47	KIAA1324	NM_020775.2	1,652	2,827
48	WIPF1	NM_001077269.1	1,635	1,533
49	DNAJC12	NM_201262.1	1,609	1,972
50	KIAA1199	NM_018689.1	1,606	2,496
51	KLK3	NM_001030050.1	1,595	2,449
52	RPL29	NM_000992.2	1,565	1,748
53	S100P	NM_005980.2	1,560	1,839
54	NDUFA12L	NM_174889.3|NM_174889.2	1,558	2,043
55	RGS22	NM_015668.2	1,551	2,565
56	PRDX4	NM_006406.1	1,550	1,952
57	HS.543887	CD640673	1,548	2,079
58	FAM108C1	NM_021214.1|XM_051862.7	1,546	1,936
59	BOP1	NM_015201.3	1,516	1,816

Supplementary Table 4: *Downregulated genes shared between MCF7 and MDA-MB134 (2nd part of the 100-gene classifier).*

	Symbol	Accession	MCF7	MDA-MB134
1	CLIC3	NM_004669.2	0,293	0,455
2	AHNAK	NM_001620.1	0,499	0,643
3	CAV1	NM_001753.3	0,508	0,264
4	TACC1	NM_006283.1	0,514	0,496
5	PMP22	NM_153321.1|NM_153322.1	0,522	0,579
6	RAMP3	NM_005856.2	0,524	0,634
7	YPEL3	NM_031477.4|NM_031477.3	0,531	0,664
8	NRCAM	NM_005010.3	0,546	0,622
9	GPER|GPI	NM_001039966.1|NM_001031682.1	0,551	0,637
10	SMAD3	NM_005902.3	0,554	0,474
11	MAFB	NM_005461.3	0,555	0,517
12	CHES1	NM_005197.2	0,558	0,619
13	AKR1C3	NM_003739.4	0,561	0,520
14	ADCY1	NM_021116.1	0,567	0,651
15	RAMP3	NM_005856.1|NM_005856.2	0,571	0,594
16	CXCR7|CI	NM_020311.2|NM_020311.1	0,578	0,459
17	GPER|GPI	NM_001039966.1	0,579	0,552
18	RAPGEFL	NM_016339.2|NM_016339.1	0,579	0,654
19	LFNG	NM_001040167.1|NM_002304.1	0,579	0,658
20	C6orf141	NM_153344.1	0,584	0,632
21	BNIPL	NM_138278.2|NM_138278.1	0,584	0,613
22	KLHL24	NM_017644.3	0,589	0,453
23	TSPAN9	NM_006675.3	0,594	0,495
24	ALDH3B2	NM_001031615.1|NM_000695.3	0,594	0,538
25	PIK3R1	NM_181523.1|NM_181504.2	0,594	0,646
26	EFNA1	NM_004428.2	0,597	0,601
27	PLA2G10	NM_003561.1	0,601	0,583
28	YPEL2	NM_001005404.3	0,608	0,633
29	LOC64281	XR_018564.1|XM_926703.1	0,616	0,631
30	PRKCD	NM_006254.3|NM_212539.1	0,616	0,557
31	CCNG2	NM_004354.1	0,629	0,661
32	SCUBE2	NM_020974.1	0,632	0,465
33	TP53INP1	NM_033285.2	0,638	0,544
34	CAV2	NM_001233.3	0,638	0,427
35	LMTK3	XM_936372.2|XM_936372.1	0,639	0,531
36	HIG2	NM_013332.3|NM_013332.1	0,640	0,578
37	CGN	NM_020770.1	0,648	0,641
38	ID2	NM_002166.4	0,650	0,593
39	RXRA	NM_002957.3	0,658	0,635
40	YPEL5	NM_016061.1	0,659	0,562
41	SAMD11	NM_152486.2	0,664	0,446

Supplementary Table 5: *Ingenuity Pathway analyses.*
        See online supplemental information
Supplementary Table 6: *qPCR primers for hit validation on mRNA (top) and ChIP (bottom) samples.*
        See online supplemental information

Chapter 3

Posttranslational modification of ERα -part 2

Interaction of 14-3-3 proteins with the estrogen receptor alpha F domain provides a drug target interface

Ingrid J. De Vries-van Leeuwen[a], Daniel da Costa Pereira[a], Koen D. Flach[b], Sander R. Piersma[c], Christian Haase[d], David Bier[e], Zeliha Yalcin[a], Rob Michalides[b], K. Anton Feenstra[f], Connie R. Jiménez[c], Tom F. A. de Greef[g], Luc Brunsveld[d], Christian Ottmann[d,e], Wilbert Zwart[b], and Albertus H. de Boer[a]

[a]Department of Structural Biology, Faculty Earth and Life Sciences, Vrije Universiteit, 1081 HV Amsterdam, The Netherlands
[b]Department of Molecular Pathology, Netherlands Cancer Institute, 1066 CX Amsterdam, The Netherlands
[c]OncoProteomics Laboratory, Department of Medical Oncology, VU University Medical Center, 1081 HV Amsterdam, The Netherlands
[d]Chemical Biology Laboratory, Department of Biomedical Engineering, Eindhoven University of Technology, 5612 AZ, Eindhoven, The Netherlands
[e]Chemical Genomics Centre, Max Planck Institute of Molecular Physiology, 44227 Dortmund, Germany
[f]Center for Integrative Bioinformatics, Vrije Universiteit, 1081 HV Amsterdam, The Netherlands
[g]Institute for Complex Molecular Systems, Eindhoven University of Technology, 5600 MB Eindhoven, The Netherlands

Abstract

Estrogen receptor alpha (ERα) is involved in numerous physiological and pathological processes, including breast cancer. Breast cancer therapy is therefore currently directed at inhibiting the transcriptional potency of ERα, either by blocking estrogen production through aromatase inhibitors or anti-estrogens that compete for hormone binding. Due to resistance, new treatment modalities are needed and as ERα dimerization is essential for its activity, interference with receptor dimerization offers a new opportunity to exploit in drug design. Here we describe a unique mechanism of how ERα dimerization is negatively controlled by interaction with 14-3-3 proteins at the extreme C terminus of the receptor. Moreover, the small-molecule fusicoccin (FC) stabilizes this ERα/14-3-3 interaction. Cocrystallization of the trimeric ERα/14-3-3/FC complex provides the structural basis for this stabilization and shows the importance of phosphorylation of the penultimate Threonine (ERα-T594) for high-affinity interaction. We confirm that T594 is a distinct ERα phosphorylation site in the breast cancer cell line MCF-7 using a phospho-T594–specific antibody and by mass spectrometry. In line with its ERα/14-3-3 interaction stabilizing effect, fusicoccin reduces the estradiol-stimulated ERα dimerization, inhibits ERα/chromatin interactions and downstream gene expression, resulting in decreased cell proliferation. Herewith, a unique functional phosphosite and an alternative regulation mechanism of ERα are provided, together with a small molecule that selectively targets this ERα/14-3-3 interface.

Introduction

The estrogen receptor alpha (ERα) is a ligand-dependent transcription factor and the driving force of cell proliferation in 75% of all breast cancers. Current therapeutic strategies to treat these tumors rely on selective ER modulators (SERMs), like tamoxifen (TAM) (1) or aromatase inhibitors (AIs) that block estradiol synthesis (2). Although the benefits of treating hormone-sensitive breast cancers with SERMs and AIs are evident, resistance to treatment is commonly observed (3, 4). To overcome resistance, selective ERα down-regulators (SERDs) can for instance be applied that inhibit ERα signaling through receptor degradation (5, 6). Approaches that target the ERα/DNA or ERα/co-factor interactions are explored as well (5, 7), but other essential steps in the ERα activation cascade are currently unexploited in drug design, also due to a lack of molecular understanding of the processes at hand.

One such step that is crucial for many aspects of ERα functioning is ligand-driven receptor dimerization (8, 9). 17β-Estradiol (E2) association with the ERα ligand binding domain (LBD) drives large conformational changes (10) resulting in ERα dissociation from chaperones (11, 12), unmasking of domains for receptor dimerization, and DNA binding (13, 14). Whereas the LBD contains the main dimerization domain (15), the extreme C-terminal domain of the receptor (F domain) imposes a restraint on dimerization (15, 16), although the regulation of this remains fully elusive. The F domain is a relatively understudied part of the receptor and due to its flexibility, no structural information has been available until now (16). Analysis of F-domain truncation mutants point to an important role for the last few amino acids in receptor dimerization and transactivation activity (17).

Recently, we reported that the diterpene glucoside fusicoccin (FC), a product of the fungus Phomopsis amygdali (18), induces apoptosis in a number of cancer cell lines, in synergy with the cytokine IFN alpha (IFNα) (19). In plants, the molecular mechanism of FC's action is highly specific through a unique stabilization of the interaction of 14-3-3 proteins and the C terminus of plasma membrane proton ATPases, with a key role for the penultimate (phosphorylated) Thr of the ATPase (20–22). 14-3-3 Proteins are a family of adapter proteins conserved in all eukaryotic organisms, with key positions in vital cellular processes as well as pathogenesis, like neurodegeneration and tumor development (23, 24). The sequence homology of the extreme C terminus of the plant ATPase and human ERα and the observed effect of FC on the growth of ERα positive breast tumor cells led us to explore the effect of FC on ERα function in these cells.

We show here that ERα interacts with 14-3-3 proteins, with a key role for the penultimate Threonine of ERα (T594). Mutation of T594 strongly enhances the estradiol-dependent ERα dimerization and transactivation. As shown by cocrystallization, binding of the T594 phosphorylated ERα C terminus in the 14-3-3 binding groove leaves a cavity that can be filled by the FC molecule. We confirm that T594 is a distinct ERα phosphorylation site in the breast cancer cell line MCF-7 using a phospho-T594–specific antibody and by mass spectrometry. Furthermore, FC has a negative effect on ERα/chromatin interactions, E2-dependent gene transcription, and cell growth. With this, we provide an alternative ERα regulating mechanism, involving the ERα F domain and provide a unique druggable interface between ERα and 14-3-3 proteins, together with a small molecule (FC) that functions as a proof of principle, which highlights the potential druggability of this protein/protein interaction surface for alternative therapeutics design in breast cancer.

Results

ERα F Domain Interacts with 14-3-3 Proteins.

Sequence alignment of the ERα F domain from a wide range of animals, from human to frog, shows a high degree of variation in amino acid composition, with the exception of the last two amino acids, which are invariably Thr,Val or Thr,Ile (TV or TI) (**Fig. 1A**). This conservation of the ERα C terminus points to a conserved function of the tip and in view of the analogy with the plant ATPase C-terminal tip (Fig. S1A), which is involved in 14-3-3 interactions (22, 25), we performed a yeast-two hybrid (Y2H) assay with the C-terminal half of ERα (ERα-LBD302–595) against all seven human 14-3-3 isoforms. Yeast growth is observed with all 14-3-3 isoforms on triple drop-out plates (**Fig. 1B**), providing evidence for direct physical interaction between these proteins. The penultimate T594 of ERα is essential for 14-3-3 interaction because cells transformed with ERαT594A did not grow (**Fig. 1B**). Helix 12, which is directly N terminal to the F domain, undergoes dramatic conformational changes upon ligand binding (26) and this will most likely change the position of the F domain as well. To test whether ligand binding renders the F domain more accessible for interaction with 14-3-3 proteins, a yeast two-hybrid (β-galactosidase, β-gal) assay was performed to quantitatively assess the ERα/14-3-3 interaction. Both E2 and 4-hydroxytamoxifen (4OH-TAM) strongly enhance the ERα-LBD/14-3-3θ interaction and again ERα-LBDT594A does not interact with 14-3-3θ (**Fig. 1C**). Similar results
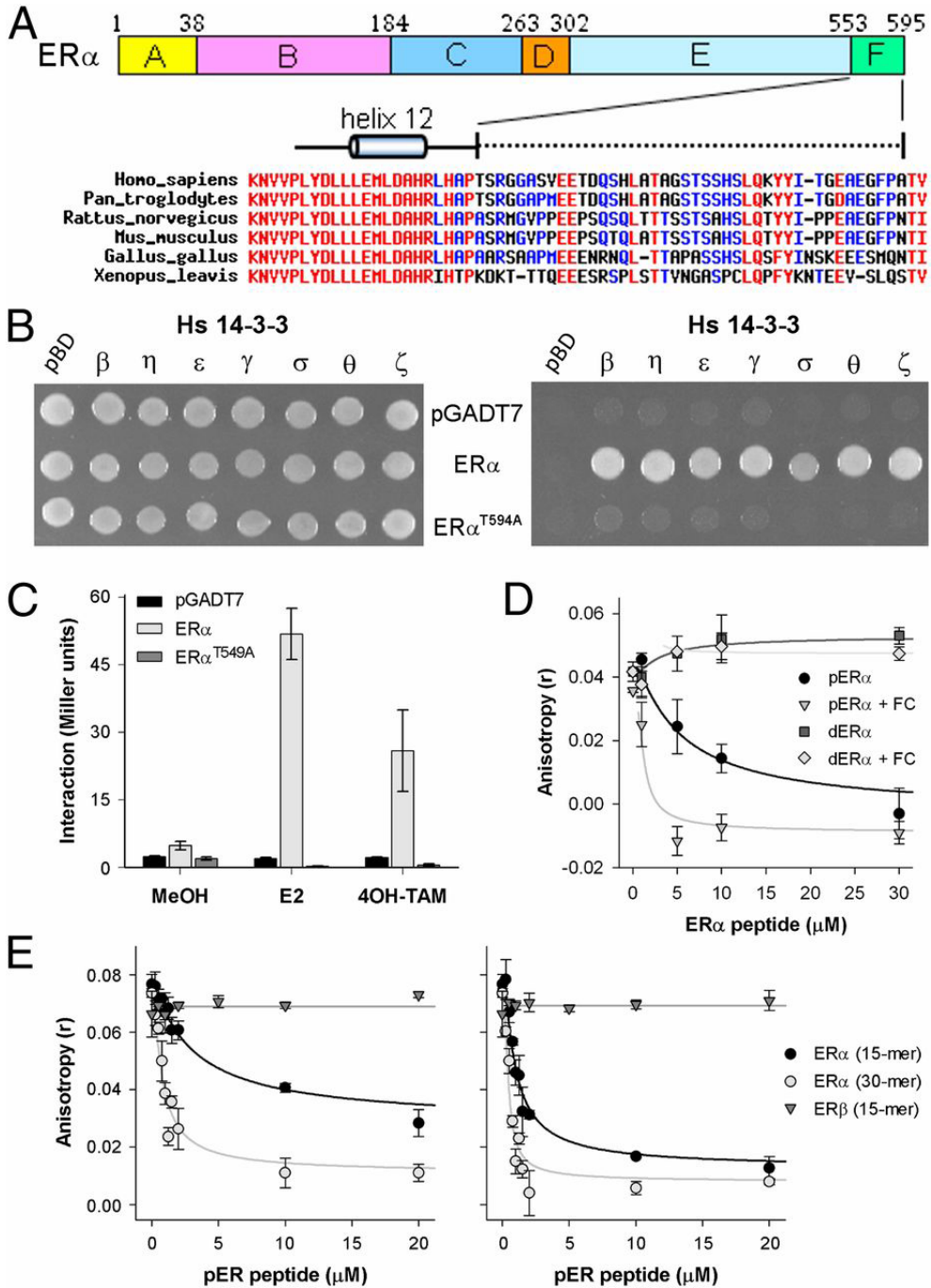
**Figure 1***: Interaction of ERα and 14-3-3 depends on T594 phosphorylation and is enhanced by FC.*
(A) Overview of ERα, with the F domain highlighted and the alignment of the ERα/F domain from various species. (B) ERα-LBD and ERα-LBDT594A interaction with all seven human 14-3-3 isoforms in yeast, tested for colony growth (Left; DDO) and for interaction (Right; TDO). ERα-LBD interacts with all seven human 14-3-3 isoforms, whereas no interaction is observed for ERα-LBDT594A. (C) The 14-3-3θ interactions with ERα-LBD and ERα-LBDT594A with ERα ligands (n = 3, ± SD) (Fig. S1 B and C). (D) Interaction between 14-3-3θ and the C-terminal (de)-phospho-ERα peptide, as measured by fluorescence anisotropy, with (open symbols) or without (closed symbols) FC (n = 2, ±SD) (Fig. S1D and Table S1). (E) Comparison of the interaction of 14-3-3ζ with a short (15 aa) or long (30 aa) C-terminal pERα peptide as well as a short (15 aa) C-terminal pERβ peptide with (Right) or without (Left) FC (n = 2, ±SD).

have been obtained with other 14-3-3 isoforms as well as full-length ERα (Fig. S1 B and C), which shows that (ant)agonist binding to the receptor increases the accessibility of the F domain for 14-3-3 interaction. Using a competitive fluorescence anisotropy 14–3-3 assay, we tested if T594 phosphorylation and FC influence the affinity of the ERα F domain for 14-3-3 proteins (27). The ERα F-domain peptide, last 15 amino acids, revealed two aspects of interaction: phosphorylation of T594 is essential for interaction (in support of the Y2H results) and the presence of FC increases the apparent affinity of the peptide 5- to 16-fold, depending on the 14-3-3 isoform used (**Fig. 1D** and Fig. S1D and Table S1). Although the ERβ protein contains a penultimate serine residue that can be phosphorylated, no interaction with 14-3-3 protein is observed for the phosphorylated ERβ F-domain peptide with or without FC, indicating ER isoform specificity (**Fig. 1E**). Furthermore, a longer ERα F domain phosphopeptide (30 amino acids) is still responsive to FC, while having a higher affinity for 14-3-3 proteins, which suggests that the F domain has multiple points of contact with the 14-3-3 protein (**Fig. 1E**).

Crystal Structure of the Trimeric Complex.
The structural basis for the effects described above was elucidated by co-crystallization of the 15-aa F-domain phosphopeptide (pERα), 14-3-3σ and FC. First, the peptide was crystallized with the 14-3-3 protein. Crystals were obtained within 5–7 d and could directly be flash cooled and diffracted to 2.02 Å. The 14-3-3 protein displayed the typical, W-like shaped dimer with both
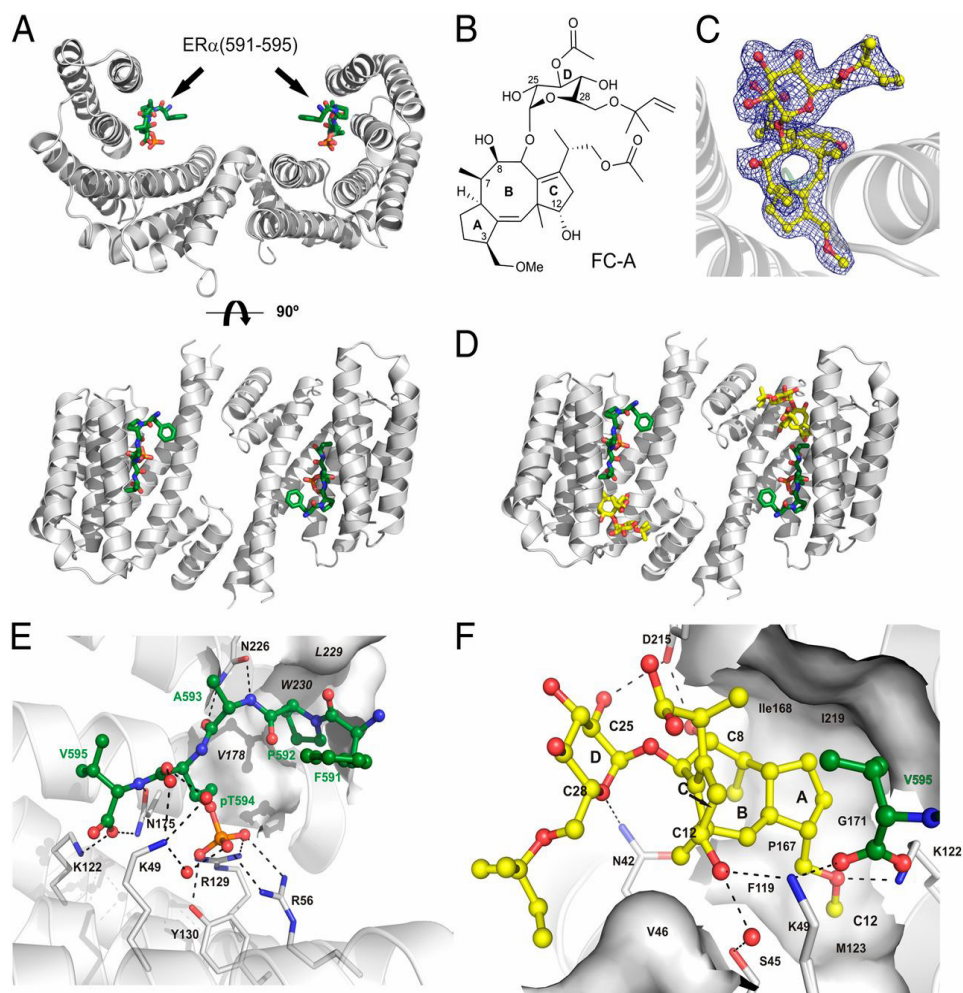
Figure 2*: Cocrystallization of 14-3-3, the phosho-ERα peptide, and fusicoccin. (A) Overview of 14-3-3σ dimer (gray) complexed with phosho-ERα peptide (green). (B)Structure of fusicoccin A (FC). (C) Electron density map (2Fo-Fc, contoured at 1 σ) of fusicoccin (yellow) bound to 14-3-3/pERα complex. (D) Overview of 14-3-3 dimer (gray) complexed with phospho-ERα peptide (green) and FC (yellow). (E) pERα (green) interaction with 14-3-3σ (gray). (F) Fusicoccin (yellow) interaction with 14-3-3σ (gray) and pERα peptide (green). Polar interactions: dashed lines, 14-3-3 residues for interaction, black; hydrophobic 14-3-3 interaction surfaces, white; and water molecules conferring polar interactions, red.*

monomers accommodating one ERα peptide (**Fig. 2A** and Fig. S2A). The peptide shows an elongated conformation and is mainly bound by polar contacts with coordination of the phosphate moiety of pT594 by 14-3-3's K49, R56, R129 and Y130. To determine how FC (**Fig. 2B**) acts on this protein complex, we soaked binary 14-3-3σ/pERα crystals with FC. Clear additional electron density for the FC molecule could be determined (**Fig. 2C**), allowing the unambiguous spatial determination of the binding mode. One FC molecule is coordinated by each 14-3-3 monomer sitting right next to the C terminus of the pERα peptide (**Fig. 2D** and Fig. S2B). Here, FC is contacting both protein partners thereby filling a gap in the interface of 14-3-3 and pERα (**Fig. 2 E and F** and Fig. S2C). Binding of FC to the binary 14-3-3σ/pERα complex seems to be mainly driven by entropic effects and shape complementarity. FC covers 147.1 Å2 of solvent-exposed surface in the complex and dislocates at least 19 water molecules. Because the free, protein-unbound form of FC (28) is very similar to the structure of FC observed in our ternary complex, also the entropy penalty upon binding of FC is expected to be rather low (see also Table S2).

ERα C Terminus Controls Receptor Dimerization.
To examine the capacity of FC to bind endogenous 14-3-3 and ERα, an affinity pull-down with FC beads (FC was coupled covalently to magnetic hydrazide beads after changing the vinyl group into a reactive aldehyde) was performed in a lysate prepared from MCF-7 cells. The FC beads were first functionally tested (Fig. S3 A and B). Subsequently, a pull-down with MCF-7 cell lysate was performed and this shows that both endogenous 14-3-3 and ERα bind specifically to the FC beads (**Fig. 3A**). In a reverse pull-down experiment with recombinant ERα-LBD as bait, FC also enhanced the binding of 14-3-3 proteins to ERα (**Fig. 3B**). Next, we addressed the question how 14-3-3 protein interaction affects ERα function. In view of the reported function of the F domain in receptor dimerization (16), we tested whether 14-3-3 binding and FC interfere with receptor dimerization. A Y2H β-gal assay with ERα-LBD or ERα-LBDT594A confirmed that the F-domain C terminus controls receptor dimerization (**Fig. 3C**), as reported before (17). Strikingly, the T594A mutation, which annihilates the 14-3-3 interaction (**Fig. 1 B and C**), strongly enhances (ant)agonist-driven receptor dimerization. Similar results have been obtained with full-length ERα or ERαT594A (Fig. S3C). To test whether FC affects ERα dimerization in human cells as well, two N-terminally tagged ERα constructs, HA-ERα and GFP-ERα, were expressed in
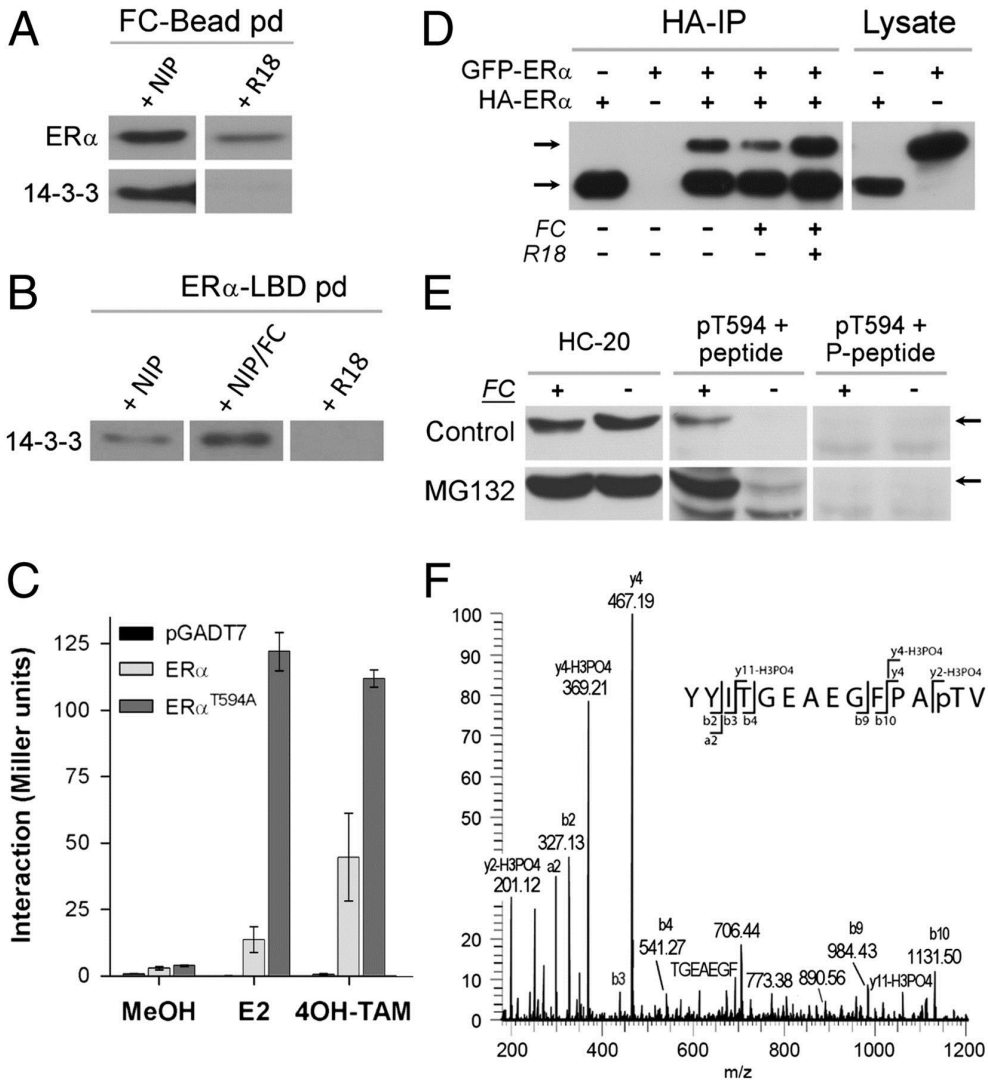
Fig. 3: *14-3-3 Interaction with ERα affects ERα dimerization and T594 is phosphorylated in MCF-7 cells.*

(A) Pull-down with FC-coated beads isolates endogenous ERα and 14-3-3 (Western blot) from MCF-7 cell lysate; NIP, noninteracting peptide; R18, 14-3-3 blocking peptide (see also Fig. S3 A and B). (B) Endogenous 14-3-3 binding to recombinant ERα-LBD in the presence of NIP, NIP+FC, and R18. (C) Yeast two-hybrid assay with ERα-LBD/ERα-LBD, and ERα-LBDT594A/ERα-LBDT594A showing enhanced dimerization of the ERα mutant (E2, 17β-estradiol; 4OH-TAM, tamoxifen (n

= 3, ±SD) (Fig. S3C). (D) Western blot analysis (HC-20 antibody) of HA-ERα IP from HEK293 cells expressing HA-ERα and GFP-ERα; cells treated with FC (10 μM) show reduced dimerization, whereas R18 added to the cell lysate enhances the dimerization. (E) Western blot analysis with the HC-20 and pT594 antibodies of cell lysate from MCF-7 cells treated with combinations of the proteasome inhibitor MG132 (5 μM) and/or FC (30 μM). The pT594 antibody was used in the presence of the nonphosphorylated (Center) and the T594 phosphorylated ERα peptide (Right).(F) Mass-spectrometry analysis of the C-terminal ERα peptide purified from a trypsin digested MCF-7 cells lysate with the pT594 antibody. Shown is the tandem MS (MS2) spectrum of the C-terminal ERα tryptic peptide showing modification by phosphorylation at threonine 594 (Fig. S5).

HEK293 cells. Immunoprecipitation (IP) of HA-ERα shows receptor dimerization: besides HA-ERα also GFP-ERα is present in the IP (**Fig. 3D**, lane 3). Cells treated with FC show less GFP-ERα in the IP, whereas inclusion of the 14-3-3 competing R18 peptide in the cell lysate during the IP strongly enhances dimerization. These results are in line with the Y2H results and suggest that interaction of 14-3-3 proteins at the ERα C terminus has a negative effect on receptor dimerization.

T594 Is a Distinct ERα Phosphosite.
Thus far, experimental evidence for ERα-T594 phosphorylation has not been described in the literature. However, all evidence shown above indicates that T594 phosphorylation is essential for creating a high-affinity 14-3-3 binding site at the ERα C terminus. To demonstrate endogenous ERα-T594 phosphorylation, we generated an antibody that specifically recognizes the phosphorylated T594 residue. Specificity of the pT594 antibody is demonstrated with a dot blot (Fig. S4A) and Western blotting of cell lysate of HEK293 cells expressing ERα, ERα-T594A, and ERα-Δ4 (Fig. S4B). Next, we did Western blots using the ERα common antibody (HC-20) and the pT594 antibody on cell lysate from MCF-7 cells that were treated without or with FC for 24 h (**Fig. 3E**). Whereas control cells do not show a band recognized by the pT594 antibody, cells treated with FC clearly show a band, which disappears when the antibody is blocked with its antigen, the pT594 peptide. When cells are also treated with the proteasome inhibitor MG132, phosphorylated ERα is already detectable without FC treatment (**Fig. 3E**) and with FC the effect on T594 phosphorylation is even more prominent. To confirm that T594 is a genuine phosphoresidue, we digested the FC/MG132 MCF-7 cell lysate

with trypsin and used the pT594 antibody to IP the C-terminal ERα phospho-peptide. Mass-spectrometry analysis of this fraction identified the C-terminal ERα peptide (14 aa) with T594 phosphorylated (**Fig. 3F** and Fig. S5). We conclude that T594 is a phosphorylated residue in MCF-7 cells and that FC "protects" the T594 phosphosite resulting in increased phosphorylation.

FC Reduces Genome-Wide Chromatin Interactions of ERα.
Because ERα interacts with DNA as a dimer, we expected that an FC/14-3-3-induced reduction of receptor dimerization would prevent ERα/DNA inter-actions. Chromatin immunoprecipitation (ChIP) was performed for ERα, and the receptor/chromatin interaction for two well-described ERα binding events [nuclear receptor-interacting protein 1 (NRIP1) and X-box binding protein 1 (XBP1)] (29) was studied. For both ERα binding sites, FC significantly re-duced the chromatin interaction of ERα as well as its coactivator amplified in breast cancer 1 (AIB1) (**Fig. 4A**). To assess the effect of FC on ERα/chroma-tin associations on a genome-wide scale, ChIP was followed by high-through-put sequencing (ChIP-seq). Again, FC decreased ERα/chromatin interactions, and peak intensities were decreased by FC treatment (**Fig. 4B**). Under con-trol conditions, 26,987 ERα binding events were found on a genome-wide scale (**Fig. 4C**). This number of binding events was greatly diminished by FC treatment, where 16,829 ERα sites were found. The sites shared under both control and FC conditions ("shared regions") were the strongest ERα binding events, which were significantly lowered in intensity by FC treatment (**Fig. 4D** and quantified in **Fig. 4E**). The less strong ERα binding sites were unique for the control conditions ("control unique") and lost due to an FC-induced decrease of peak intensity beyond the detection threshold of the peak-call-ing algorithm. Consequently, the number of ERα peaks decreased upon FC treatment (**Fig. 4C**). No selectivity was observed for the type of ERα interac-tion that was lost (monomer versus dimer) based on DNA motif analysis or whether they were mediated by direct ERα/DNA binding or through specific-ity protein 1 (SP1) or complexes of the transcription factors Fos and Jun (Fos/Jun) (Fig. S6). These results show that FC-mediated loss of ERα/chromatin interaction is highly effective, nonselective for the mode of ERα chromatin interactions as based on DNA motif analysis, and occurs genome-wide.

Fusicoccin Reduces ERα Transactivation and Cell Growth.
Next, the biological consequences of FC-induced ERα/14-3-3 stabilization and reduced ERα/chromatin interactions were investigated. First, the influ-
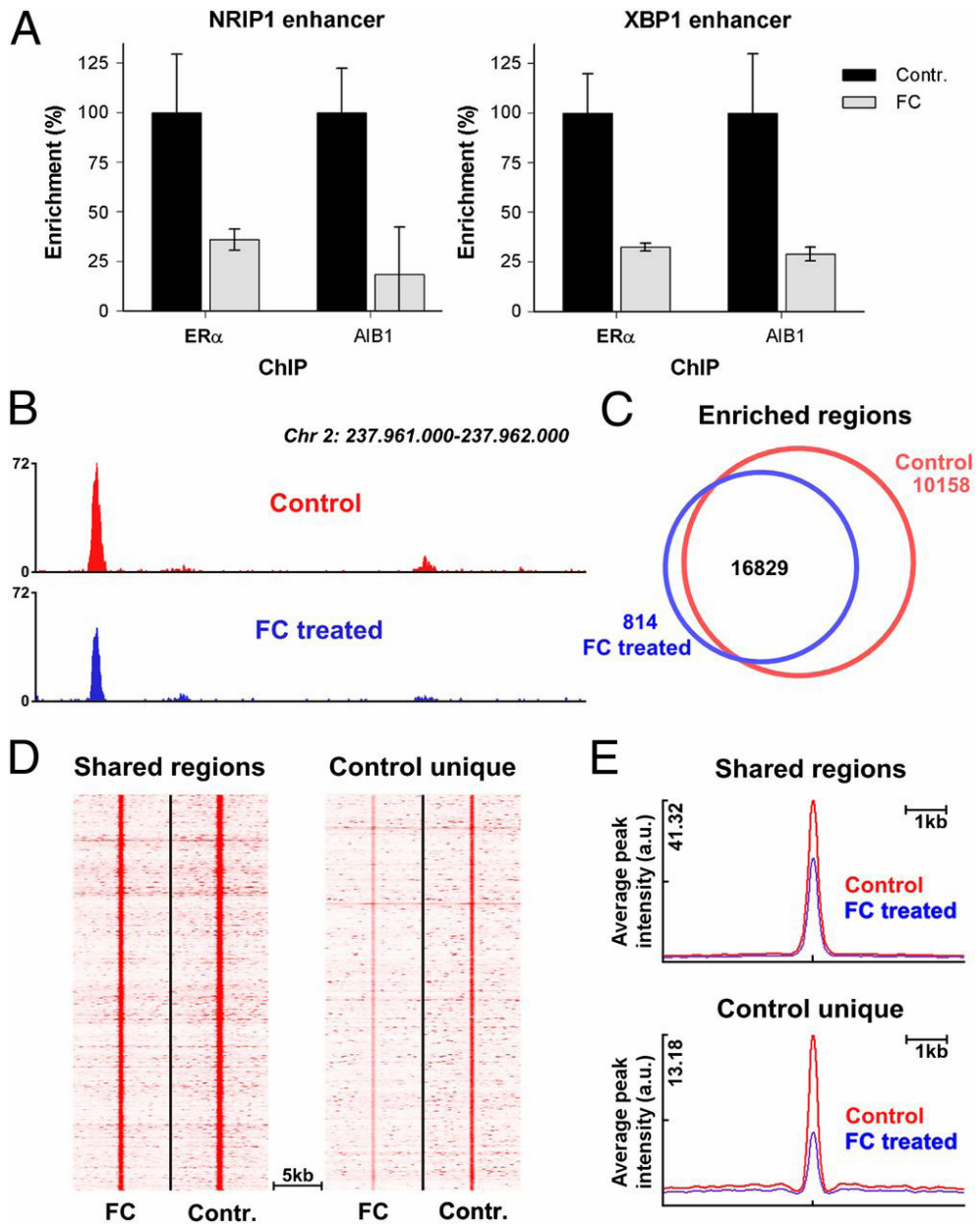
Fig. 4: *FC reduces genome-wide chromatin/ERα interactions.*
(A) qPCR of NRIP1 and XBP1 enhancer elements after ChIP for ERα and AIB1 in the absence or presence of 10 μM FC (n = 3, ±SD). (B) Genome browser snapshot, illustrating decrease of ERα/chromatin interaction after FC treatment. Genomic

coordinates and tag count are indicated. (C) Venn diagram showing ERα binding events in absence (red) and presence (blue) of FC. (D) Heatmap visualizing intensity of ERα binding events in FC and control-treated cells at regions found under both conditions (shared; Left) and sites that are lost after FC treatment (control unique; Right) (E) Average peak intensity of ERα binding sites as visualized in D.

ence of FC on ERα transcriptional activity was tested, as well as the role of the F-domain C-terminal tip therein. To rule out any influence of endogenous receptor, we made use of ERα-negative human osteosarcoma cell line U2OS, a well-annotated model system for ERα action (30). ERα-mediated estrogen response element-luciferase reporter (ERE-luc) expression was measured in U2OS cells cotransfected with ERα wild type (ERα-WT) and two C-terminal mutants: ERα-T594A and ERα-Δ4, a construct lacking the last four amino acids. ERα-T594A may still exhibit partial FC sensitivity, because studies on the FC target in plants (the H+-ATPase) have shown that interaction of the nonphosphorylated H+-ATPase and 14-3-3 proteins do occur, provided that FC is present (31, 32). ERα-Δ4 should be FC insensitive because the amino acids that line the 14-3-3 groove and contact the FC molecule (**Fig. 2**) are missing. As shown in **Fig. 5A**, FC significantly reduces the ERα-WT transcriptional activity in a dose-dependent manner, with an inhibition of more than 60% at 1 nM E2. The transcriptional activity of ERα-Δ4 is indeed unaffected by FC and is much higher than that of ERα-WT (note that the scale of the y axis is different). Cells transfected with ERα-T594A also show enhanced transcriptional activity compared with ERα-WT in the absence of FC and, as expected, the transcriptional activity shows some FC sensitivity, albeit less than that of ERα-WT. These experiments illustrate that the ERα C terminus is essential for regulating ERα activity and for the inhibitory effect of FC thereon. Furthermore, FC does not affect the transcriptional activity of ERβ (**Fig. 5B**), indicating that the 14-3-3/FC interaction is indeed isoform specific (see also Fig. 1E).

To further determine the effect of FC on endogenous ERα-mediated gene transcription, we analyzed transcript levels of a number of E2-dependent genes in the absence and presence of FC. As shown in **Fig. 5C**, FC treatment significantly reduced E2-mediated transcription of these genes. In line with these data, FC treatment significantly inhibited E2-induced cell proliferation in a dose-dependent manner (), and this effect on proliferation was not apoptosis related (Fig. S7).

Cumulatively, we have shown a unique mode of ERα inhibition in-
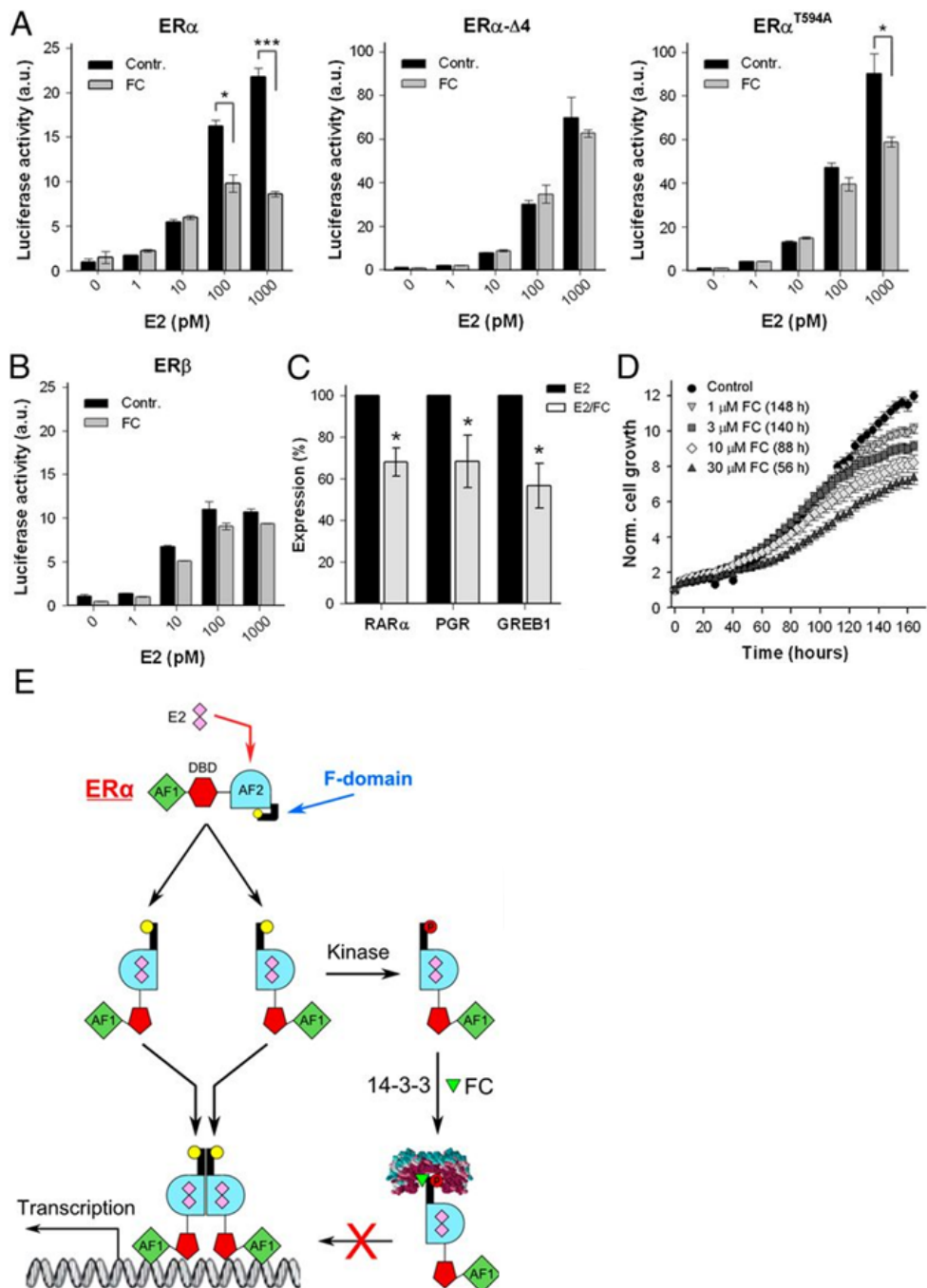
Fig. 5*: Effect of fusicoccin on ERα gene activation and cell growth.*
(A) Normalized transactivation activity (ERE-luciferase assay) of ERα, ERαΔ4 (lacking the last four amino acids), and ERαT594A, for various E2 concentrations in the presence and absence of 10 µM FC (n = 3, ±SD *P < 0.05; ***P < 0.001). (B) Same as A, now analyzing the normalized ERβ transactivation (n = 2, ±SD). (C) qPCR expression analysis of ERα regulated genes [progesterone receptor (PGR), retinoid acid receptor alpha (RARα), and gene regulated by estrogen in breast cancer 1 (GREB1)] in hormone-deprived MCF-7 cells treated with E2 (10 nM) or E2/ FC (10 µM) (n = 7, ±SEM, *P < 0.05). (D) E2-induced MCF-7 cell proliferation is inhibited by FC. Time to reach significant (P < 0.05) inhibition is indicated in parentheses (n = 12, ±SEM) (Fig. S6). (E) Model showing ERα activation, the function of 14-3-3, and FC on the F domain and receptor activation. Ligand binding (E2) drives conformational changes that displace the F domain, which enables receptor dimerization and transcriptional activation. Displacement of the F domain also renders the C-terminal tip (yellow) accessible for phosphorylation of T594 (red). Subsequent 14-3-3 binding, and stabilization by FC, keeps the receptor in a monomeric state, thereby reducing DNA interaction, gene transcription, and cell growth.

volving the newly identified phosphorylated T594 residue, which operates through the interaction of the ERα F-domain tip with 14-3-3 proteins. Stabilizing this ERα/14-3-3 interaction through small molecule inhibitors like FC suffices in functionally reducing ERα/DNA interactions, gene transcription, and cell proliferation.

Discussion

Blocking ERα functioning is the major treatment modality in luminal breast cancer (33–35). Most efforts to modulate the ERα activity have focused on a single pocket buried in the ERα protein, where agonists, antagonists, and selective modulators interact with ERα: the ligand-binding pocket. Because treatment resistance is commonly observed, focus is shifting toward the identification of small-molecule inhibitors that target sites outside this ligand-binding pocket, like the coactivator-binding groove, allosteric sites in the LBD, and the interface for DNA contact (34, 36). Receptor dimerization is an essential step in the cascade of events through which ERα modulates gene expression and therefore any changes that alter ERα dimerization will have profound effects on ERα function. After binding of ligand, ERα monomers undergo dramatic conformational changes exposing sequences required for dimerization and evidence has been presented that the carboxy terminal

F domain imparts internal restraint on ER dimerization (17, 37). Notably, mutations in the last few amino acids of the F domain somehow relieve the restraint on dimerization imposed by the F domain and enhance transcriptional activity (17). Understanding the molecular mechanism that gives the F-domain C terminus control over ERα dimerization will provide new tools to interfere with the ligand-driven dimerization process and thus ligand-dependent ERα activation in ERα-positive tumor cells.

In this report we demonstrate that the ERα F-domain C terminus contains a mode-III binding motif for 14-3-3 proteins (38) and moreover, that the ERα/14-3-3 interface can be targeted by the small-molecule FC. The effect of FC described here is unique among all known small molecules that modulate the ERα activity, as it targets a unique protein–protein interaction interface and stabilizes rather than disturbs an ERα/macromolecule interaction. This mode of FC action, which can be described as a "molecular glue," has been well documented for the plant ATPase/14-3-3 interaction (21, 22) and this study shows that the compound/substrate interactions, as well as their functional consequences, are conserved across species.

At the molecular level, the Y2H, fluorescence anisotropy and cocrystallization studies all point to an alternative mechanism of ERα regulation, where 14-3-3 proteins interact with the very C terminus of the ERα F domain, with a key role for phosphorylation of the penultimate T594. We uniquely demonstrate that T594 is an in vivo phosphosite in the breast cancer cell line MCF-7. Because phosphorylated ERα accumulates in cells where proteosomal degradation is inhibited, we hypothesize that the T594 phosphorylated ERα is a short-lived intermediate in the cycle of receptor activation/degradation. This may be the reason why phosphorylation of T594 has gone unnoticed thus far. FC clearly enhances the level of T594 phosphorylation, probably because the phosphosite is shielded from phosphatase activity by an increase in affinity for 14-3-3 proteins, a well-known effect described for the FC target in plants, the H+-ATPase (39, 40). This mode-III 14-3-3 interaction provides the framework for a model where the ERα C terminus negatively affects receptor dimerization, consistent with previously published work (17), through interaction with 14-3-3 proteins, as shown here. At the cellular level, the (FC stabilized) interaction between ERα and 14-3-3s negatively affects receptor/DNA interactions, the transactivation activity and ERα-dependent cell growth. Furthermore, this interaction can be targeted by small molecules, like FC, and FC is receptor specific as it only targets ERα without affecting ERβ, which is a positive feature in view of the antiproliferative role described

for ERβ (41, 42).

Taken together, our results establish an alternative and selective mode of ERα regulation (Fig. 5E), where the receptor's F domain becomes amenable for interaction with 14-3-3 proteins after ligand binding. FC is a small molecule ligand that specifically modulates the interaction surface between ERα and its regulatory 14-3-3 protein, albeit at a relatively low affinity. Therefore, this small molecule and related fusicoccanes (43) may provide the very basis for the development of an entirely unique class of antiestrogenic compounds in the treatment of breast cancer.

Materials and Methods

Human ERα (WT or T594A point mutant) and/or 14-3-3 proteins were transfected in yeast cells, using the lithium acetate method (44), to analyze their interaction or study ERα dimerization in a Y2H assay. Double dropout plates (DDOs) were used to check for colony viability and triple dropout plates (TDOs) to test for interaction. The interaction in the presence of various ligands was quantified with a yeast two-hybrid β-galactosidase assay as described before (44).

Competitive anisotropy measurements were performed with ERα peptides consisting of the last 15 (short) or 30 (long) amino acids of ERα, with T594 being phosphorylated (pERα) or dephosphorylated (dERα). In this, the peptides need to compete with the carboxyfluorescein labeled SWpTY peptide (FAM-SWpTY, where pT indicates phosphorylated Threonine) for 14-3-3 binding as described before (27).

In pull-down assays, with GST-ERα-LBD or FC-coated beads, MCF-7 lysate was mixed with a noninteracting peptide (NIP) or the 14-3-3 interacting R18 peptide. The associated endogenous ERα and/or 14-3-3 proteins were subsequently visualized by Western blotting.

ERα activity was measured with an ERE-Luc assay in transfected U2OS cells, using the Dual-Luciferase Reporter Assay (Promega). MCF-7 cell growth and apoptosis induction, treated with FC or methanol and E2, was measured on the IncuCyte FLR (Essen BioScience), using a CellPlayer 96-Well Kinetic Caspase-3/7 apoptosis assay kit. Cell confluence and apoptosis was determined by analyses of phase-contrast/fluorescent images using an algorithm from Confluence v1.5 in combination with IncuCyte software.

For the identification of the phosphorylated C-terminal ERα peptide, cell lysate from MG132/FC-treated MCF-7 cells was trypsin digested and the pT594 antibody was used to IP the phosphopeptide. MS/MS spectra of the

eluted peptides were acquired with a Q Exactive mass spectrometer (ThermoScientific).

ChIPs were performed as described previously (29). Sequences were generated on the Illumina HiSeq. 2000 and aligned to the human reference genome. Tools used for enriched region analyses, motif analyses, data snapshots, and heatmap generation are described in SI Materials and Methods. For gene expression analyses equal amounts of cDNA from (un)treated MCF-7 cells were analyzed with SYBR Green (Applied Biosystems) and an MJ Opticon Monitor (BioRad). Data were analyzed with qgene96.

The complex of 14-3-3σΔc (amino acids 1–231) and the short pERα peptide was crystallized using the hanging-drop method. The structure was solved by molecular replacement using Protein Data Bank (PDB) ID: 3P1N as template. The ternary complex was produced by soaking fusicoccin into the binary crystals. Details are described in SI Materials and Methods. The structures of the 14-3-3σΔc/pERα (4JC3) and the 14-3-3σΔc/pERα/FC (4JDD) complexes have been deposited in the PDB.

Author contributions: I.J.D.V.-v.L., K.D.F., R.M., C.O., W.Z., and A.H.d.B. designed research; I.J.D.V.-v.L., D.d.C.P., K.D.F., S.R.P., C.H., D.B., Z.Y., K.A.F., and A.H.d.B. performed research; C.H., R.M., and L.B. contributed new reagents/analytic tools; I.J.D.V.-v.L., D.d.C.P., K.D.F., S.R.P., D.B., Z.Y., K.A.F., C.R.J., T.F.A.d.G., C.O., W.Z., and A.H.d.B. analyzed data; and I.J.D.V.-v.L., T.F.A.d.G., L.B., C.O., W.Z., and A.H.d.B. wrote the paper.

The authors declare no conflict of interest.

References

1.   Ariazi EA, Ariazi JL, Cordera F, Jordan VC (2006) Estrogen receptors as therapeutic targets in breast cancer. Curr Top Med Chem 6(3):181–202.

2.   Asselin-Labat M-L, et al. (2010) Control of mammary stem cell function by steroid

hormone signalling. Nature 465(7299):798–802.

3.   Bergamaschi A, Katzenellenbogen BS (2012) *Tamoxifen downregulation of miR-451 increases 14-3-3ζ and promotes breast cancer cell survival and endocrine resistance. Oncogene 31(1):39–47.*

4.   Zwart W, et al. (2007) *PKA-induced resistance to tamoxifen is associated with an altered orientation of ERalpha towards co-activator SRC-1. EMBO J 26(15):3534–3544.*

5.   Shanle EK, Xu W (2010) *Selectively targeting estrogen receptors for cancer treatment. Adv Drug Deliv Rev 62(13):1265–1276.*

6.   Wardell SE, Marks JR, McDonnell DP (2011) *The turnover of estrogen receptor α by the selective estrogen receptor degrader (SERD) fulvestrant is a saturable process that is not required for antagonist efficacy. Biochem Pharmacol 82(2):122–130.*

7. Carraz M, Zwart W, Phan T, Michalides R, Brunsveld L (2009) *Perturbation of estrogen receptor alpha localization with synthetic nona-arginine LXXLL-peptide coactivator binding inhibitors. Chem Biol 16(7):702–711.*

8.   Powell E, Wang Y, Shapiro DJ, Xu W (2010) *Differential requirements of Hsp90 and DNA for the formation of estrogen receptor homodimers and heterodimers. J Biol Chem 285(21):16125–16134.*

9.   Zhang YH, Li ZG, Sacks DB, Ames JB (2012) *Structural basis for Ca2+-induced activation and dimerization of estrogen receptor α by calmodulin. J Biol Chem 287(12):9336–9344.*

10.   Brzozowski AM, et al. (1997) *Molecular basis of agonism and antagonism in the oestrogen receptor. Nature 389(6652):753–758.*

11.   Mahalingam D, et al. (2009) *Targeting HSP90 for cancer therapy. Br J Cancer 100(10):1523–1529.*

12.   Fliss AE, Benzeno S, Rao J, Caplan AJ (2000) *Control of estrogen receptor ligand binding by Hsp90. J Steroid Biochem Mol Biol 72(5):223–230.*

13.   Helsen C, et al. (2012) *Structural basis for nuclear hormone receptor DNA binding. Mol Cell Endocrinol 348(2):411–417.*

14.   Powell E, Xu W (2008) *Intermolecular interactions identify ligand-selective activity of estrogen receptor alpha/beta dimers. Proc Natl Acad Sci USA 105(48):19012–19017.*

15.   Peters GA, Khan SA (1999) *Estrogen receptor domains E and F: Role in dimerization and interaction with coactivator RIP-140. Mol Endocrinol 13(2):286–296.*

16.   Skafar DF, Zhao CQ (2008) *The multifunctional estrogen receptor-alpha F domain. Endocrine 33(1):1–8.*

17.   Yang J, Singleton DW, Shaughnessy EA, Khan SA (2008) *The F-domain of estrogen receptor alpha inhibits ligand induced receptor dimerization. Mol Cell Endocrinol 295(1-2):94–100.*

18.   Ballio A, et al. (1964) *Fusicoccin: A New Wilting Toxin produced by Fusicoccum*

amygdali Del. Nature 203(4942):297.

19.   *de Vries-van Leeuwen IJ, et al. (2010) Fusicoccin-A selectively induces apoptosis in tumor cells after interferon-alpha priming. Cancer Lett 293(2):198–206.*

20.   *Korthout HA, de Boer AH (1994) A fusicoccin binding protein belongs to the family of 14-3-3 brain protein homologs. Plant Cell 6(11):1681–1692.*

21.   *Würtele M, Jelich-Ottmann C, Wittinghofer A, Oecking C (2003) Structural view of a fungal toxin acting on a 14-3-3 regulatory complex. EMBO J 22(5):987–994.*

22.   *Ottmann C, et al. (2007) Structure of a 14-3-3 coordinated hexamer of the plant plasma membrane H+ -ATPase by combining X-ray crystallography and electron cryomicroscopy. Mol Cell 25(3):427–440.*

23.   *Morrison DK (2009) The 14-3-3 proteins: Integrators of diverse signaling cues that impact cell fate and cancer development. Trends Cell Biol 19(1):16–23.*

24.   *Steinacker P, Aitken A, Otto M (2011) 14-3-3 proteins in neurodegeneration. Semin Cell Dev Biol 22(7):696–704.*

25.   *Jahn T, et al. (1997) The 14-3-3 protein interacts directly with the C-terminal region of the plant plasma membrane H(+)-ATPase. Plant Cell 9(10):1805–1814.*

26.   *Tanenbaum DM, Wang Y, Williams SP, Sigler PB (1998) Crystallographic comparison of the estrogen and progesterone receptor's ligand binding domains. Proc Natl Acad Sci USA 95(11):5998–6003.*

27.   *Wu M, et al. (2006) SWTY—a general peptide probe for homogeneous solution binding assay of 14-3-3 proteins. Anal Biochem 349(2):186–196.*

28.   *Ballio A, et al. (1991) H-1-NMR conformational study of Fusicoccin and related compounds - molecular conformation and biological activity. Phytochemistry 30(1):137–146.*

29.   *Zwart W, et al. (2011) Oestrogen receptor-co-factor-chromatin specificity in the transcriptional regulation of breast cancer. EMBO J 30(23):4764–4776.*

30.   *Kallio A, et al. (2008) Estrogen and the selective estrogen receptor modulator (SERM) protection against cell death in estrogen receptor alpha and beta expressing U2OS cells. Mol Cell Endocrinol 289(1-2):38–48.*

31.   *Fuglsang AT, et al. (2003) The binding site for regulatory 14-3-3 protein in plant plasma membrane H+-ATPase: involvement of a region promoting phosphorylation independent interaction in addition to the phosphorylation-dependent C-terminal end. J Biol Chem 278(43):42266–42272.*

32.   *Jelich-Ottmann C, Weiler EW, Oecking C (2001) Binding of regulatory 14-3-3 proteins to the C terminus of the plant plasma membrane H+ -ATPpase involves part of its autoinhibitory region. J Biol Chem 276(43):39852–39857.*

33.   *Zwart W, Theodorou V, Carroll JS (2011) Estrogen receptor-positive breast cancer: A multidisciplinary challenge. Wiley Interdiscip Rev Syst Biol Med 3(2):216–230.*

34.   Shapiro DJ, Mao C, Cherian MT (2011) *Small molecule inhibitors as probes for estrogen and androgen receptor action. J Biol Chem 286(6):4043–4048.*

35.   Nilsson S, Koehler KF, Gustafsson JA (2011) *Development of subtype-selective oestrogen receptor-based therapeutics. Nat Rev Drug Discov 10(10):778–792.*

36.   Moore TW, Mayne CG, Katzenellenbogen JA (2010) *Minireview: Not picking pockets: Nuclear receptor alternate-site modulators (NRAMs). Mol Endocrinol 24(4):683–695.*

37.   Koide A, et al. (2007) *Identification of regions within the F domain of the human estrogen receptor alpha that are important for modulating transactivation and protein-protein interactions. Mol Endocrinol 21(4):829–842.*

38.   de Boer AH, van Kleeff PJ, Gao J (2013) *Plant 14-3-3 proteins as spiders in a web of phosphorylation. Protoplasma 250(2):425–440.*

39.   Olsson A, Svennelid F, Ek B, Sommarin M, Larsson C (1998) *A phosphothreonine residue at the C-terminal end of the plasma membrane H+-ATPase is protected by fusicoccin-induced 14-3-3 binding. Plant Physiol 118(2):551–555.*

40.   Kinoshita T, Shimazaki K (2001) *Analysis of the phosphorylation level in guard-cell plasma membrane H+-ATPase in response to fusicoccin. Plant Cell Physiol 42(4):424–432.*

41.   Bartella V, et al. (2012) *Estrogen receptor beta binds Sp1 and recruits a corepressor complex to the estrogen receptor alpha gene promoter. Breast Cancer Res Treat 134(2):569–581.*

42.   Fox EM, Davis RJ, Shupnik MA (2008) *ERbeta in breast cancer—onlooker, passive player, or active protector? Steroids 73(11):1039–1051.*

43.   de Boer AH, de Vries-van Leeuwen IJ (2012) *Fusicoccanes: Diterpenes with surprising biological functions. Trends Plant Sci 17(6):360–368.*

44.   Schoonheim PJ, et al. (2007) *14-3-3 adaptor proteins are intermediates in ABA signal transduction during barley seed germination. Plant J 49(2):289–301.*

Supplementary information

Fig. S1. *C-terminal ERα F domain tip interacts with 14-3-3 proteins.*

(A) Alignment of the last 52 amino acids of human ERα and the H+-ATPase of Nicotiana plumbaginifolia (PMA2) and Arabidopsis thaliana (AHA2). The three amino acids most important for the FC/14-3-3/receptor complex formation are indicated (↓). (B) Yeast two-hybrid assay; ligands stimulate the interaction of various 14-3-3 isoforms with WT ERα-LBD, but not ERα-LBDT594A. (C) Quantification of the interaction of 14-3-3θ with full-length WT ERα and ERαT594A, in the presence of ERα ligands. (D) Analysis of the interaction between the short (15 aa) phosphorylated C-terminal ERα peptide (pERa) and all human 14-3-3 isoforms and 14-3-3σ-ΔC. Curves are fitted as described in SI Material and Methods.

Fig. S2. *Cocrystallization of 14-3-3 and the pERα peptide and soaked fusicoccin.*

(A) Stereoview of the pERα peptide (green) in the 2Fo-Fc density map (contoured at 1σ) occupying half of the amphipathic 14-3-3 binding groove (white surface). (B) Stereoview of the pERα peptide (green) and fusicoccin (yellow) in the 2Fo-Fc density map (contoured at 1σ) occupying the amphipathic full binding groove of a 14-3-3σ monomer (white). (C) Detailed view of the interaction of ERα (green) and fusicoccin (yellow) with 14-3-3σ (white). Polar interactions are indicated by dashed lines and 14-3-3 residues implicated in these interactions are labeled in black. Hydrophobic 14-3-3 interaction surface is depicted as white solid surface. Red spheres are water molecules conferring polar interactions.

Fig. S3. *Functional test on FC beads and 14-3-3 interaction with full-length ERα affects dimerization.*
(A) Specifically bound endogenous 14-3-3 proteins can only be eluted from FC-coupled beads (FC beads) with the 14-3-3 interacting R18 peptide, when bound in the presence of a C-terminal peptide derived from the plant H+-ATPase (YpTV) and not with a noninteracting peptide (NIP). (B) 14-3-3 Western blot on the pull-down samples of A confirms the specificity of the 14-3-3 interaction to the FC-coupled beads. (C) Yeast two-hybrid assay for ERα dimerization: The full-length-ERα/ERα-LBD and full length-ERαT594A/ERα-LBDT594A dimerize in the presence of ERα ligands.

Fig. S4. *The pT594-antibody is specific for the T594-phosphorylated ERα C-terminal epitope.*
(A) Dot blot with different amounts of nonphosphorylated (peptide: KYYITGEAEGFPATV) and phosphorylated peptide (P-peptide: KYYITGEAEGFPATP V) spotted. The blot was probed with the pT594-ERα antibody. (B) Western blot with HC-20 antibody and pT594-ERα antibody on cell lysate of HEK293 cells expressing wild-type ERα, ERα-T594A, and ERα-Δ4; cells were grown with FC (10 μM) for 24 h. Whereas the HC-20 antibody shows that ERα is expressed in all three transfected cells, the pT594-ERα antibody only recognizes a band in wild-type ERα transfected cells. This demonstrates that the pT594-ERα antibody is specific for the T594 phosphorylated ERα protein.

Fig. S5. *Mass-spectrometry analysis of the C-terminal ERα peptide shows phosphorylation of the penultimate threonine, T594.*
(A) Extracted ion chromatogram of synthetic ERα C-terminal tryptic phosphopeptide YYITGEAEGFPApTV phosphorylated at T594. The extraction window is m/z 799.31–38. (B) The corresponding peptide from MCF-7 digest, after IP is shown. In A and B coelution at 89–90 min is observed. (C) Accurate intact mass of the peptide, corresponding to the [M+2H]2+ monoisotopic peak at m/z 799.3447, for the synthetic and MCF7-derived phosphopeptide, respectively. (D) See C. (E) MS/MS spectrum of synthetic YYITGEAEGFPApTV. The absence of basic residues (protein C terminus) and presence of acidic residues, as well as a phosphate

group, result in a poor MS/MS spectrum. However, the y2-H3PO4 (m/z 201.1234), y4 (m/z 467.1901), and y4-H3PO4 (m/z 369.2132) ions conclusively localize the phosphate group to T594. (F) Corresponding MS/MS spectrum for the MCF-7–derived phosphopeptide. The fragment ions b2, a2, y2-H3PO4, y4-H3PO4, and y4 ions are detected in similar intensity ratios as observed for the synthetic phosphopeptide identifying the MCF-7–derived phospho-peptide and localizing the site of phosphorylation to T594.

Fig. S6. *ERα/DNA binding mode is not selectively altered by FC treatment.*
(A) Top three motifs for the shared (Left) and control unique (Right) ERα binding events. (B) Average peak intensity of shared (Left) and control unique (Right) ERα binding events mediated directly by ERα or through specificity protein 1 (SP1) and complexes of the transcription factors Fos and Jun (Fos/Jun) as identified through motif scanning of ERα-binding sites, in the absence (red) or presence (blue) of FC.

Fig. S7. *Fusicoccin does not induce apoptosis in E2-treated MCF-7 cells.*
E2-induced MCF-7 apoptosis was assessed over time in the presence of various FC concentrations (30 μM FC shown here), by analyzing the CellPlayer 96-Well Kinetic Caspase-3/7 Apoptosis assay kit. For all FC concentrations, no significant apoptosis induction was observed.

Fig. S1

Fig. S2

Fig. S3

Fig. S4

A
peptide

1 ng   10 ng   25 ng

P-peptide

B

WT *T⁵⁹⁴A* *Δ4*

pT594

HC-20

Fig. S5

E

YYLTGEAEGFPATV

F
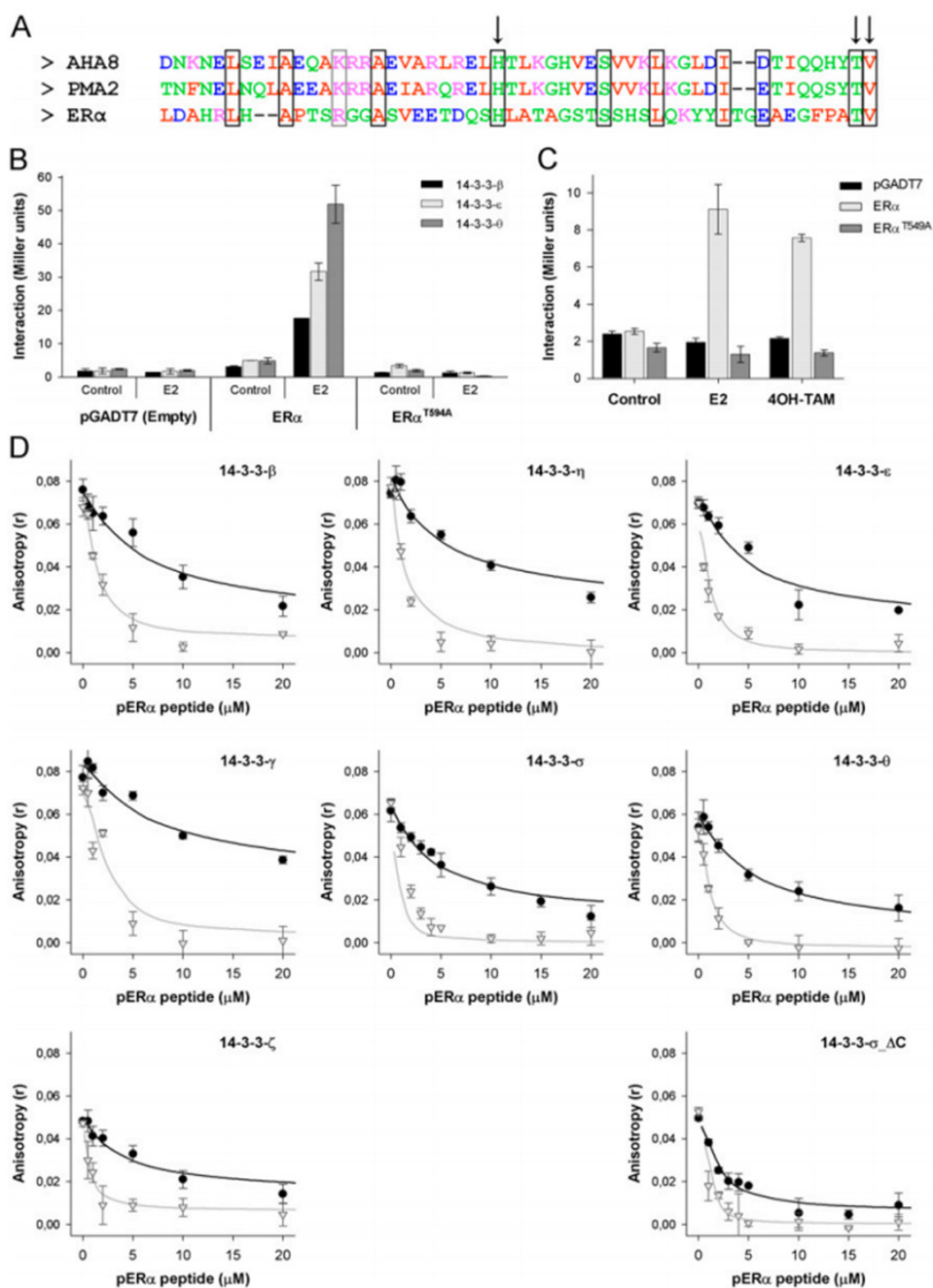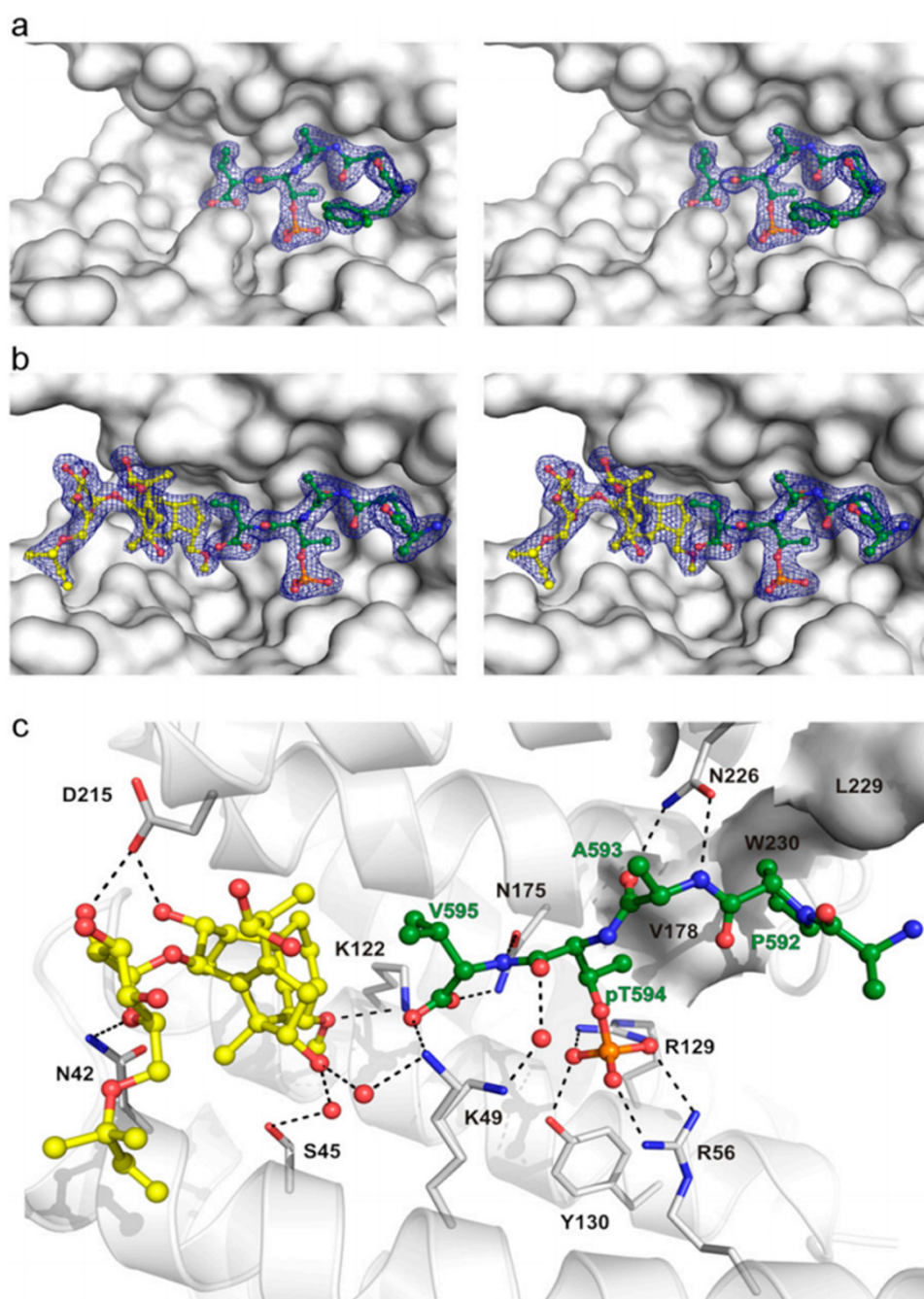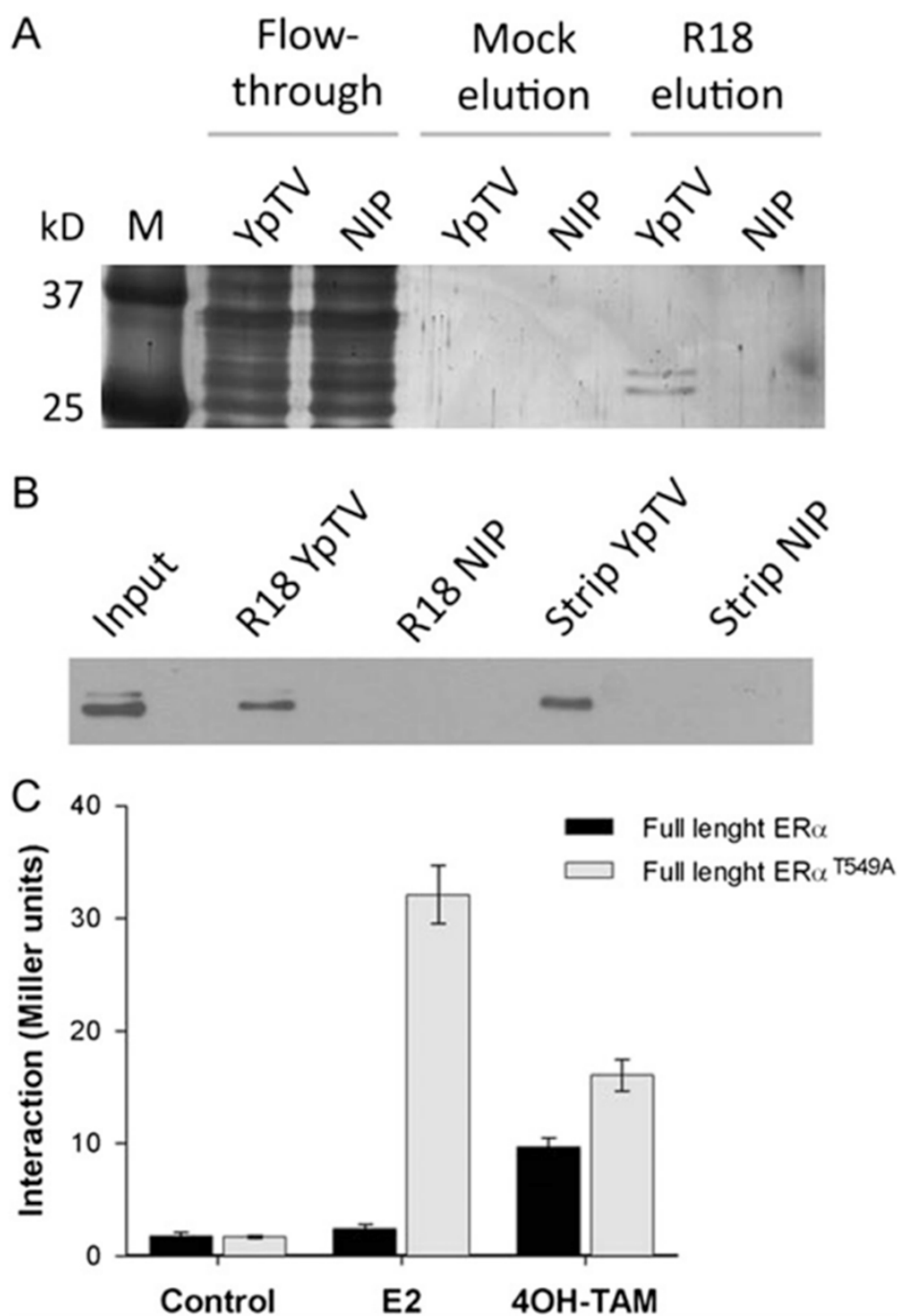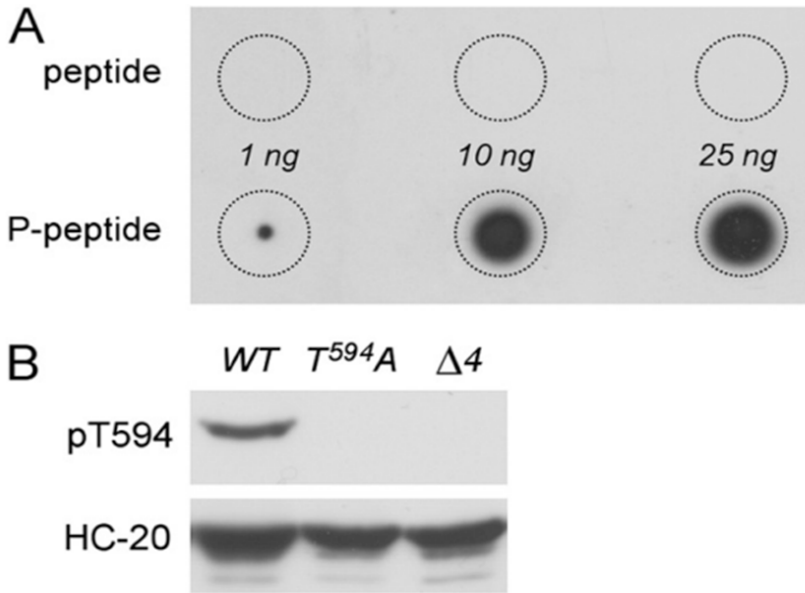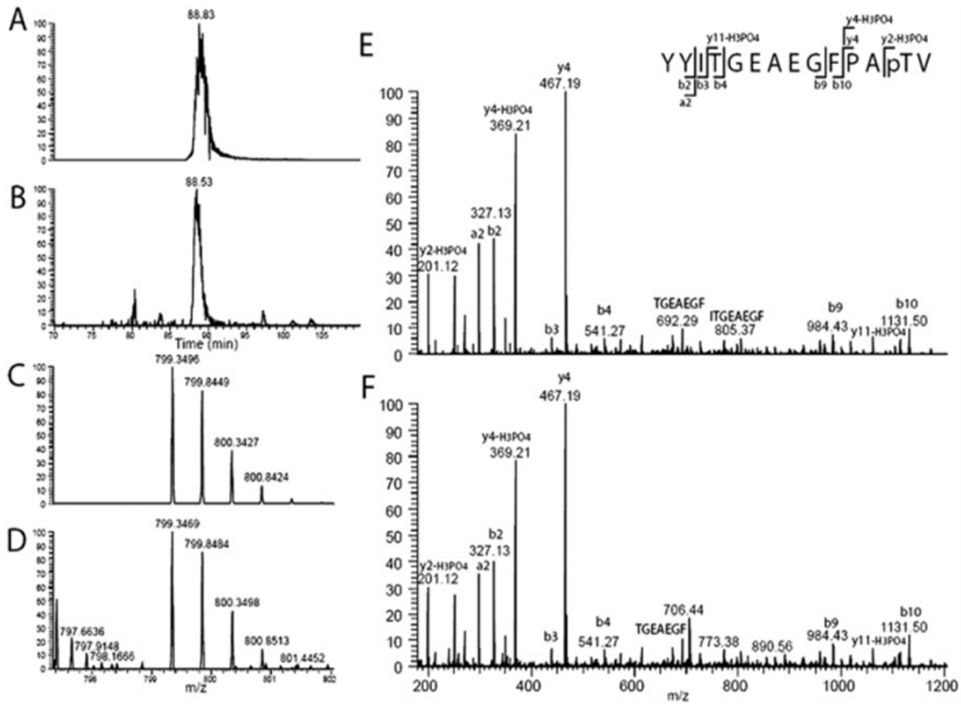
Fig. S6

Fig. S7

Table S1. FC enhances the affinity of the short pERα peptide for all 14-3-3 isoforms

K_d, μM, ±SEM	Control	10 μM FC	Affinity increase
β	0.99 (0.29)	0.11 (0.03)	9.1
η	0.94 (0.32)	0.19 (0.06)	4.9
ε	0.69 (0.21)	0.07 (0.04)	10.4
γ	1.09 (0.36)	0.15 (0.11)	7.1
σ	1.61 (0.32)	0.10 (0.03)	16.4
θ	0.90 (0.20)	0.06 (0.01)	15.1
ζ	0.57 (0.18)	0.05 (0.02)	10.9
σ-ΔC	0.33 (0.07)	0.07 (0.05)	5

Interaction affinity (K_d) of the short pERα peptide for all 14-3-3 isoforms, as calculated from the curves in Fig. S1D. Values in parenthesis are +/− SEM.

Table S2. Data collection and refinement statistics for 4JC3 and 4JDD

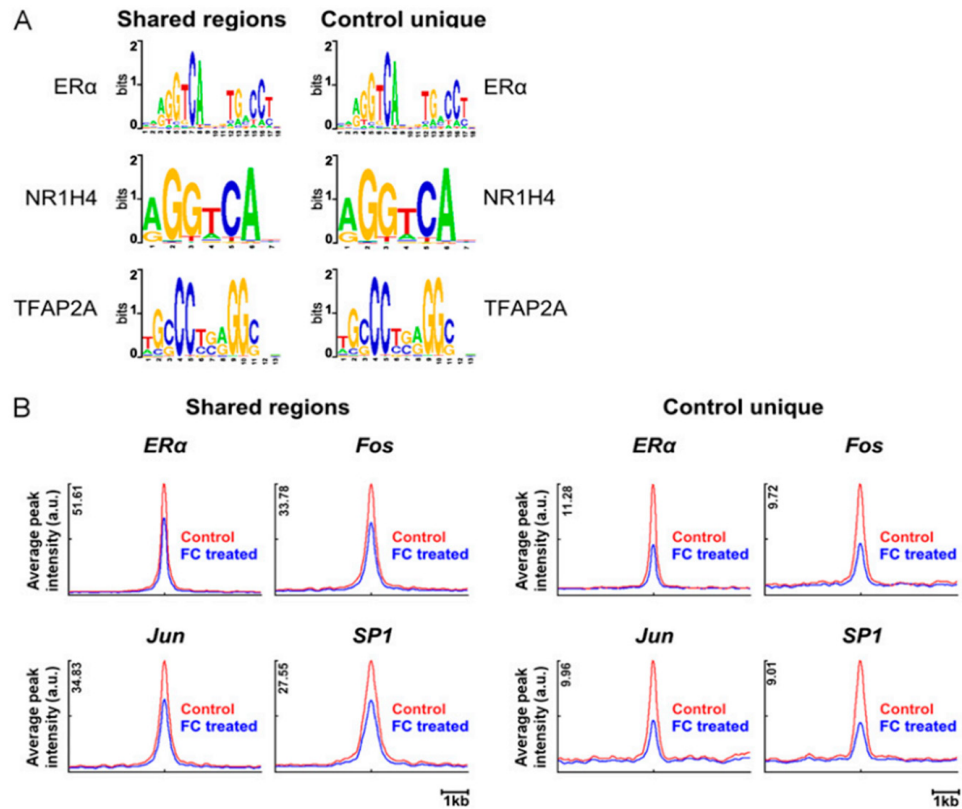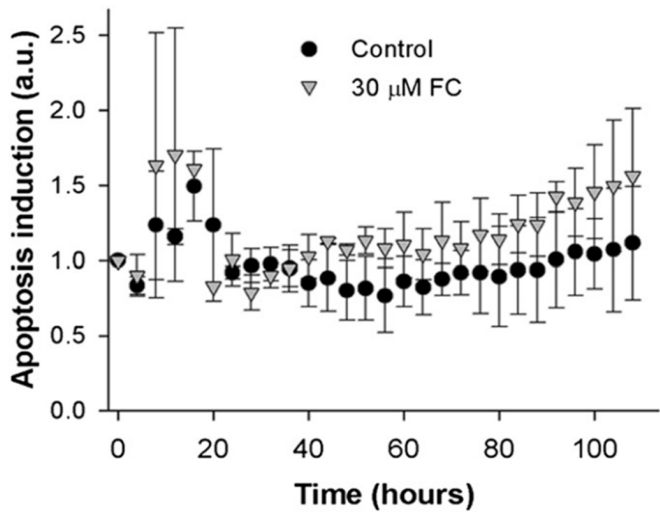|	4JC3	4JDD
Data collection		
Space group	C222$_1$	C222$_1$
Cell dimensions		
A, b, c, Å	82.2, 112.49, 62.45	82.49, 111.43, 62.24
A, β, γ, °	90, 90, 90	90, 90, 90
Resolution, Å	19.52–2.05 (2.1–2.05)	19.80–2.1 (2.15–2.0)
R_{meas}, %	8.4 (34.9)	12.0 (51.0)
I/σI	24.16 (6.85)	17.79 (4.77)
Completeness, %	99.3	100.0
Redundancy	14.94 (14.7)	15.1 (14.9)
Refinement		
Resolution, Å	19.5–2.05 (2.1–2.05)	19.80–2.1 (2.15–2.0)
No. reflections	141777	135424
Unique reflections	18518	17090
R_{work}/R_{free}	0.1778/0.235	0.1924/0.2316
No. atoms		
Protein	1850	1847
Ligand	42	42
		(FUSICOCCIN 48)
Solvent	177	101
B factors, Å$_2$		
Protein	14.3	19.70
Ligand	23.7	26.78
		(FUSICOCCIN 23.14)
Water	19.01	21.0
R.m.s. deviations		
Bond lengths, Å	0.019	0.020
Bond angles, °	1.767	1.992
Ramachandran plot		
Favored, %	98.7	97.9
Allowed, %	1.7	2.1
Generously allowed, %	0	0
Disallowed, %	0	0

Values in parenthesis are for the highest resolution shell.

Chapter 4

Composition of ERα's transcriptional complex – part 1

Co-regulated gene expression by estrogen receptor-α and liver receptor homolog-1 is a feature of the estrogen response in breast cancer cells
Chun-Fui Lai[1], Koen D. Flach[2], Xanthippi Alexi[2], Stephen P. Fox[1], Silvia Ottaviani[1], Paul T.R. Thiruchelvam[1], Fiona J. Kyle[1], Ross S. Thomas[1], Rosalind Launchbury[3], Hui Hua[1], Holly B. Callaghan[1], Jason S. Carroll[3], R. Charles Coombes[1], Wilbert Zwart[2], Laki Buluwela[1] and Simak Ali[1]

[1]Department of Surgery and Cancer, Imperial College London, London W120NN, UK
[2]Department of Molecular Pathology, The Netherlands Cancer Institute, 1066 CX Amsterdam, Netherlands
[3]Cancer Research UK, Cambridge Research Institute, Li Ka Shing Centre, Cambridge CB2 0RE, UK

Abstract

Oestrogen receptor α (ERα) is a nuclear receptor that is the driving transcription factor expressed in the majority of breast cancers. Recent studies have demonstrated that the liver receptor homolog-1 (LRH-1), another nuclear receptor, regulates breast cancer cell proliferation and promotes motility and invasion. To determine the mechanisms of LRH-1 action in breast cancer, we performed gene expression microarray analysis following RNA interference for LRH-1. Interestingly, gene ontology (GO) category enrichment analysis of LRH-1–regulated genes identified oestrogen-responsive genes as the most highly enriched GO categories. Remarkably, chromatin immunoprecipitation coupled to massively parallel sequencing (ChIP-seq) to identify genomic targets of LRH-1 showed LRH-1 binding at many ERα binding sites. Analysis of select binding sites confirmed regulation of ERα−regulated genes by LRH-1 through binding to oestrogen response elements, as exemplified by the TFF1/pS2 gene. Finally, LRH-1 overexpression stimulated ERα recruitment, while LRH-1 knockdown reduced ERα recruitment to ERα binding sites. Taken together, our findings establish a key role for LRH-1 in the regulation of ERα target genes in breast cancer cells and identify a mechanism in which co-operative binding of LRH-1 and ERα at oestrogen response elements controls the expression of oestrogen-responsive genes.

Introduction

Oestrogens play diverse roles in the body, most notably in the development and maintenance of female and male reproductive systems and secondary sexual characteristics (1). Oestrogens are also implicated in the physiology of the brain, bone and the cardiovascular system, as evidenced by the increased risk of cardiovascular disease and osteoporosis following the decline in oestrogen levels during menopause (1–3). Oestrogens also play a central role in promoting breast cancer growth (4), as well as being implicated in uterine and ovarian cancers (5,6). Two closely related members of the nuclear receptor (NR) superfamily of transcription factors, oestrogen receptor α (ERα) and ß (ERß) mediate oestrogen actions (7,8). The majority (70–80%) of breast cancers express ERα, and this transcription factor is believed to drive cancer cell proliferation. Therefore, ERα activity is inhibited in breast cancer patients with endocrine therapies using anti-oestrogens, such as tamoxifen and fulvestrant or by inhibiting oestrogen biosynthesis either by using aromatase inhibitors in postmenopausal women or with lutenising hormone releasing hormone (LHRH) agonists in premenopausal women. These therapies are well-tolerated and have been a major factor in the improvement in patient survival seen in recent years. However, up to 50% of patients with ERα-positive disease that would require endocrine therapies do not respond, while many responders eventually relapse, with few treatment options being available following the development of resistance (4,9). Hence, a better understanding of the mechanisms of ERα action would aid patient stratification and identify new therapeutic targets.

Ligand binding to ERα promotes recruitment to cis-regulatory regions by direct binding to DNA at oestrogen response elements (EREs) in target genes, or indirectly through interaction with other transcription factors such as AP1 and Sp1 (10,11) and consequent activation or repression of gene expression. Chromatin immunoprecipitation (ChIP) studies have shown that oestrogen addition initiates cycles of ERα association and dissociation from EREs, with concomitant cycles of transcriptional co-regulator recruitment leading to chromatin remodelling and histone modification and cyclical recruitment of the RNA polymerase II (PolII) machinery and subsequent transcription initiation (12–15). These cycles of co-regulator and PolII recruitment are accompanied by cycles of reversal and re-establishment of many, although not all, induced chromatin modifications.

While it is incontrovertible that ERα drives the growth response in the majority of breast tumours, there is mounting evidence that ERα does

not act on its own and that other transcription factors are essential for ERα action in breast cancer. Gene expression profiling and genomic approaches for genome-wide identification of ERα binding regions, such as ChIP-chip and ChIP-seq, have allowed the identification of direct ERα targets in breast cancer cells (16–19) and in tumours (20). These studies have also highlighted the importance of other transcription factors in the ERα response, such as FoxA1 (also known as HNF3α). FoxA1 expression is associated with ERα positivity in breast cancer and FoxA1 is one of the minimal set of genes that define ERα-positive luminal cancer (21). FoxA1, which has been proposed to facilitate binding of other transcription factors to DNA through its action in promoting chromatin accessibility (22), is frequently present at regions of ERα binding in the absence of oestrogen and appears to be a key determinant of ERα binding following oestrogen addition (16,23,24). GATA proteins also act as 'pioneer factors', promoting transcription factor recruitment (22), and GATA3 guides ERα chromatin interactions and its expression is strongly associated with ERα-positive luminal A breast cancer subtype (25). Thus, FoxA1, GATA3, as well as the transcription factors AP-2γ, TLE1 and PBX1, act as pioneer factors for ERα DNA binding by promoting chromatin accessibility and long-range chromatin interactions (26,27). Interestingly, some of these pioneer factors are themselves ERα-regulated genes, indicating a feed-forward mechanism that can act to reinforce oestrogenic signals in breast cancer cells.

A role in ERα signalling for other NRs has recently been highlighted by the finding that retinoic acid receptor-α, an oestrogen-regulated gene in breast cancer (28,29), localizes to ERα binding sites to modulate the expression of oestrogen-regulated genes (30,31), providing crosstalk between oestrogen and retinoid signalling in breast cancer cells. Moreover, androgen receptor (AR) expression is strongly associated with ERα positivity and AR inhibits expression of oestrogen-responsive genes in ERα-positive breast cancer cells (32). Indeed, a small subset of breast tumours, termed the 'molecular apocrine' subtype, which are ERα-negative but express AR (33), typically express genes normally expressed in ERα-positive breast cancer (34). Recent expression microarray and AR ChIP-seq data generated for a cell line characteristic of molecular apocrine breast cancer, MDA-MB-453 (ERα-/PR-/AR+), showed that AR activates transcription of many typical ERα target genes through AR recruitment to sites that are normally bound by ERα in luminal MCF-7 cells (35). These findings indicate another mode of crosstalk between ERα and other NRs mediated by co-operative and/or antagonistic

interactions.

Liver receptor homolog-1 (LRH-1) (NR5A2) is expressed in developing and adult tissues of endodermal origin, including liver, pancreas, intestine and the ovary (36,37). Functionally, LRH-1 has been implicated in the regulation of bile acid and cholesterol homeostasis (36,37) and the regulation of inflammatory responses in the liver and gut (38). LRH-1 is also important for steroid hormone biosynthesis in the ovary (39), but also extra-ovarian tissues, including preadipocytes, where LRH-1 regulates aromatase expression (40,41). LRH-1 is also critical in development. Disruption of the LRH-1 gene in mice is embryonic lethal at day E6.5–7.5 (42), and LRH-1 regulates expression of the key pluripotency factor Oct4 in the developing embryo epiblast (43). Indeed, LRH-1 can replace Oct4 in the reprogramming of mouse somatic cells to induced pluripotent stem cells and induces expression of Nanog, a transcription factor important for maintaining pluripotency in undifferentiated embryonic stem cells (44,45).

LRH-1 has also been implicated in cancer. Mice heterozygous for an adenomatosis polyposis coli (APC) mutation and an LRH-1 inactivating mutation developed fewer intestinal tumours than mice harbouring the APC mutation only, and LRH-1 heterozygous mice developed fewer azoxymethane-induced aberrant crypt foci (46). LRH-1 expression is elevated in pancreatic cancer and promotes pancreatic cancer cell growth through stimulation of cyclin D1, cyclin E1 and c-Myc (47), while genome-wide association studies implicate mutations in the LRH-1 gene in pancreatic ductal adenocarcinoma (48). Aromatase is an LRH-1 target gene, which catalyses the conversion of androgens (primarily androstenedione and testosterone) to oestrogens. Aromatase expression and activity is low in breast cancer cells; rather there is an increase in aromatase expression/activity in tumour-bearing breast stroma compared with normal breast stroma, leading to the proposal that LRH-1 may aid breast cancer progression in postmenopausal women by promoting local oestrogen biosynthesis (40,41,49).

Although the real importance of local oestrogen production for breast cancer remains unclear (50,51), recent work demonstrates that LRH-1 is also expressed in breast cancer cells where its expression is ERα-regulated (52,53). In breast carcinoma, LRH-1 expression is associated with ERα positivity (54). Functional studies have shown that LRH-1 plays a direct role in regulating breast cancer cell proliferation and promotes breast cancer cell motility and invasion (52,53,55). Based on these findings, we have identified LRH-1–regulated genes using gene expression microarray profiling and

ChIP-seq to map LRH-1 binding events in proliferating breast cancer cells. We show that LRH-1 is an important regulator of oestrogen-responsive gene expression that shares many binding sites with ERα. Importantly, at shared sites, LRH-1 promotes ERα recruitment and vice versa, ERα stimulates LRH-1 recruitment, thus providing evidence for a novel mode of NR co-operativity in breast cancer cells.

Results

LRH-1 regulates the expression of oestrogen-responsive genes in breast cancer cells

Recent studies have shown that LRH-1 regulates breast cancer cell proliferation and motility (52,53,55). To identify genes that mediate LRH-1 action in breast cancer cells, global gene expression profiling was performed following LRH-1 silencing using siRNAs. RNA was prepared from MCF-7 cells transfected with two independent LRH-1 siRNAs that gave >90% LRH-1 knockdown (**Figure 1A and B**). Hierarchical cluster analysis identified 222 genes the expression of which was significantly altered (P < 0.01, fold change >1.5) with both siRNAs, when compared with the control siRNA (siControl) (**Figure 1C**). GO analysis showed that the most highly enriched GO terms for these genes were 'response to oestrogen stimulus' and 'response to hormone stimulus' (**Figure 1D**), implicating LRH-1 in the regulation of oestrogen-regulated genes in breast cancer cells.

To determine if LRH-1 directly regulates the expression of oestrogen-responsive genes, ChIP-seq in MCF-7 cells was carried out using antibodies for LRH-1. However, none of the antibodies commercially available provided sufficient enrichment for peak calling to identify LRH-1 binding regions (data not shown). A recent study utilized ectopic expression of epitope-tagged LRH-1 to identify LRH-1–regulated genes in mouse embryonic stem cells (44). Using a similar strategy, we performed ChIP-seq following transfection of MCF-7 cells with HA-tagged LRH-1 (as exemplified in **Figure 2A**). Aligned reads were acquired and following stringent cut-offs using two independent replicates, peak calling identified 4876 LRH-1 binding sites, of which 1723 (35%) were shared with ERα (**Figure 2B**). The shared and unique binding patterns were not dictated by different thresholds in peak calling algorithms, as shown by heatmap analyses (**Figure 2C** and Supplementary Figure S1). Previous publications have demonstrated that the vast majority of ERα binding events map to enhancers and introns, with few sites mapping to
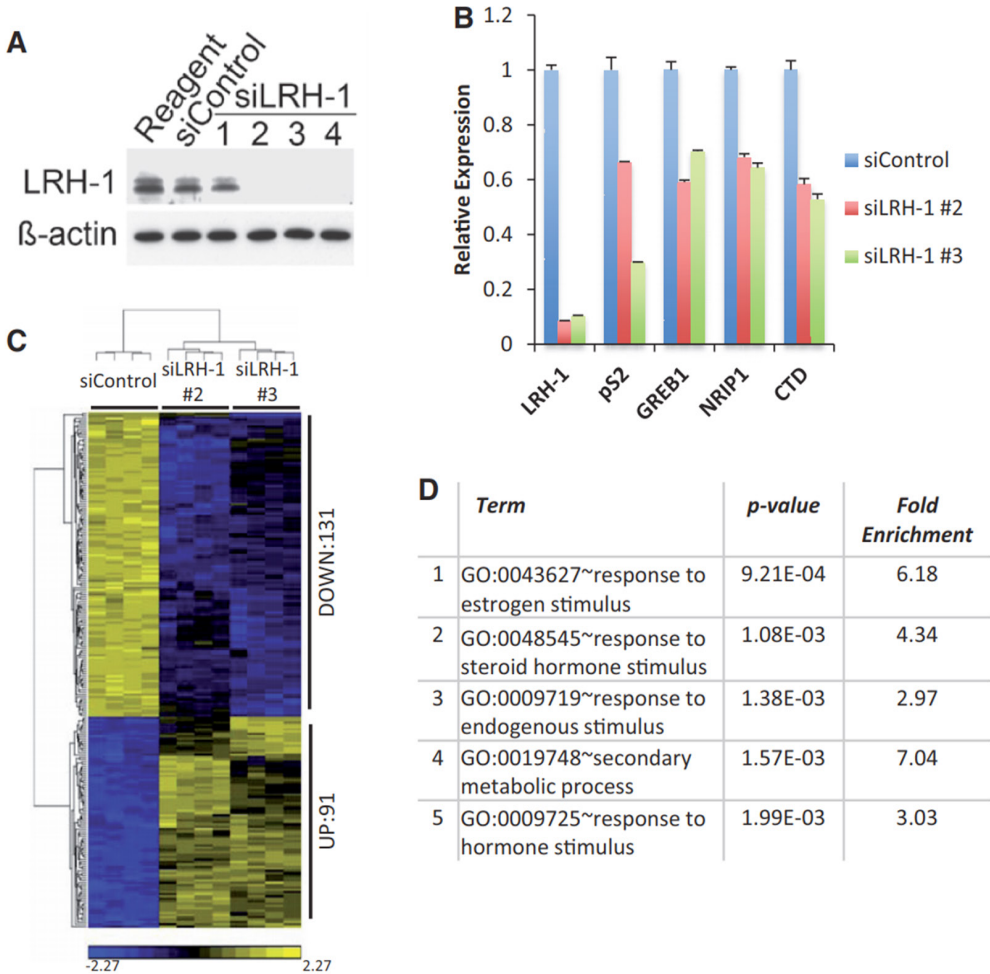
Figure 1: *Expression profiling shows that LRH-1 regulates the expression of oestrogen-regulated genes.*
(A) Western blot analysis of MCF-7 cell extracts prepared following transfection with control siRNA or four independent siRNAs for LRH-1. (B) Quantitative RT-PCR analysis was performed using three independent RNA preparations made from siControl– or siLRH-1–transfected MCF-7 cells. Error bars represent standard errors of the mean (SEM). (C) Gene expression profiling was carried out using four independent replicates of MCF-7 cells transfected with siControl, siLRH-1 #2 or siLRH-1 #3. Shown are significant differentially expressed genes at P < 0.01 corrected for false discovery rate (FDR), together with a fold change >1.5 and <−1.5. (D) GO category enrichments of the genes differentially regulated by siLRH-1 are shown.

promoter proximal regions. The majority of LRH-1 and ERα binding events, both unique and shared, were similarly located within introns and regions distal to gene promoters (**Figure 2D**).

The majority of NRs bind as dimers to sequence motifs arranged as two copies of a hexameric motif, 5′-AGGYCR-3′, organized as direct or inverted repeats, as exemplified by ERα and the ERE (7). A C-terminal extension to the canonical zinc binding motifs in NR DNA binding domains mediates binding of several NRs to DNA response elements 3 bp longer than the standard hexameric sequences. SF1 and LRH-1 bind as monomers to a sequence having the consensus 5′-YCAAGGYCR-3′, where YCA is the 5′ extension to the AGGYCR sequence to which most NR bind (36,69). Analysis of the LRH-1 binding sites for enriched DNA sequences identified a motif similar to this consensus LRH-1 binding element, with the sequence 5′-SYCARGGYCA-3′ (**Figure 2E** and Supplementary Figure S2). A motif consistent with the ERE consensus site was the top hit in the ERα unique sites, while the shared LRH-1/ERα sites were enriched in the LRH-1 motif. Motif analyses using a candidate scanning approach identified NR binding motifs, with the top hits for the LRH-1 unique sites being the SF1 and LRH-1 binding motifs. For the shared events, SF1/LRH-1 and ESR1 sites were enriched, while the ESR1 site was the top hit for the ERα unique sites. This analysis also highlighted enrichment for TFAP2C (AP2γ), FOXA1, GATA3 and AP-1 (Fos, Jun) sites in the analysis of the ERα unique sites (Supplementary Figure S3). This enrichment is consistent with previous global binding site studies for ERα (26,70). TFAP2C and FOS/JUN sites were also enriched in the LRH-1 unique and LRH-1/ERα shared sites (Supplementary Figures S4 and S5). Interestingly, FOXA1 and GATA3, being essential components of the ERα transcription complex and its activity (24,25), were found present at the LRH-1/ERα shared and ERα unique sites. Both FOXA1 and GATA3 were absent from the regions only bound by LRH-1, suggesting that these factors may not be important for LRH-1 binding, at least in the case of the LRH-1 unique sites.

LRH-1 binds to EREs in regulatory regions of a subset of oestrogen-regulated genes

To explore the potential link between LRH-1 and ERα in regulation of common target genes, we focused on the archetypal ERα target gene, pS2, for mechanistic investigations (Supplementary Figure S6A). LRH-1 recruitment to the ERα binding region was confirmed by ChIP (**Figure 3A**). EMSA
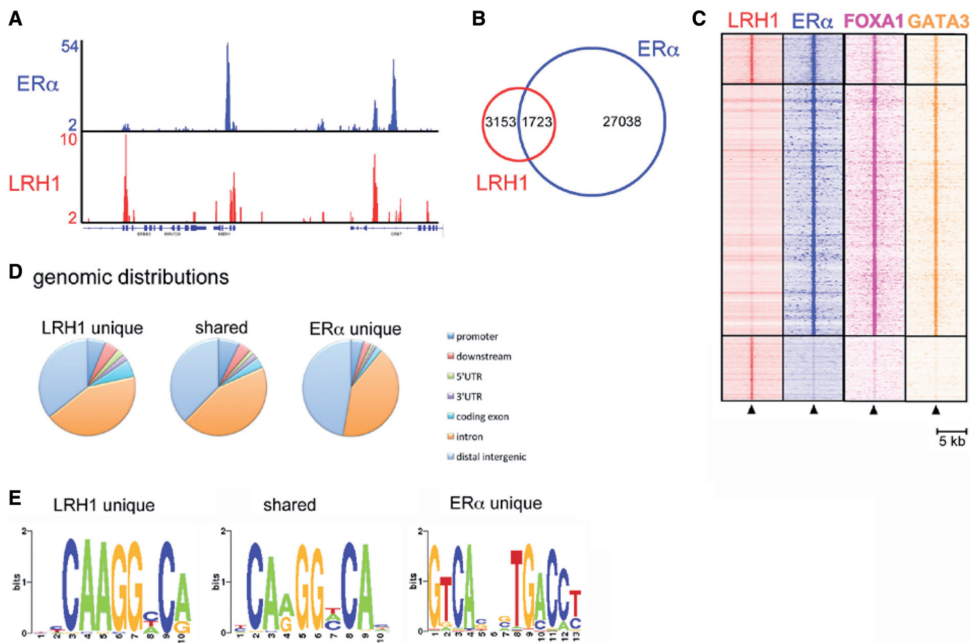
Figure 2*: LRH-1 associates with ERα binding regions in chromatin.*
(A) ChIP-seq was carried out using HA and ERα antibodies for HA-LRH-1–trans-fected MCF-7 cells. Genome browser snapshot of ChIP-seq samples for ERα and HA-LRH-1 on proliferating cells. Y bar shows tag count. (B) Venn diagram of LRH-1 and ERα binding events. (C) Shown is a heatmap, with a window of 5 kb around the binding sites, depicting all shared and unique binding events for LRH-1 and ERα vertically aligned. Additionally, the binding events of the FOXA1 (24) and GATA3 (25) ChIP-sequencing data sets are shown. (D) The genomic distribution of shared and unique binding events. (E) De novo motif analysis of the shared and unique ERα and LRH-1 binding events.

demonstrated LRH-1 binding to the pS2 ERE and confirmed the expected sequence requirements for LRH-1 binding (**Figure 3B, C and E**). Mutation within the 5′-AGGTCA motif prevented LRH-1 and ERα binding, whereas mutation in the 3′ motif prevented ERα binding, but did not influence LRH-1 binding. Similar results were obtained for the ERE motif within the shared LRH-1 and ERα binding region in the NRIP1 gene, another well-studied ERα-regulated gene (**Figure 3D** and Supplementary Figure S6A). The importance of the 5′ sequences for LRH-1 binding was shown by mutation of the chicken vitellogenin gene ERE to introduce the 5′ extension. These mutations
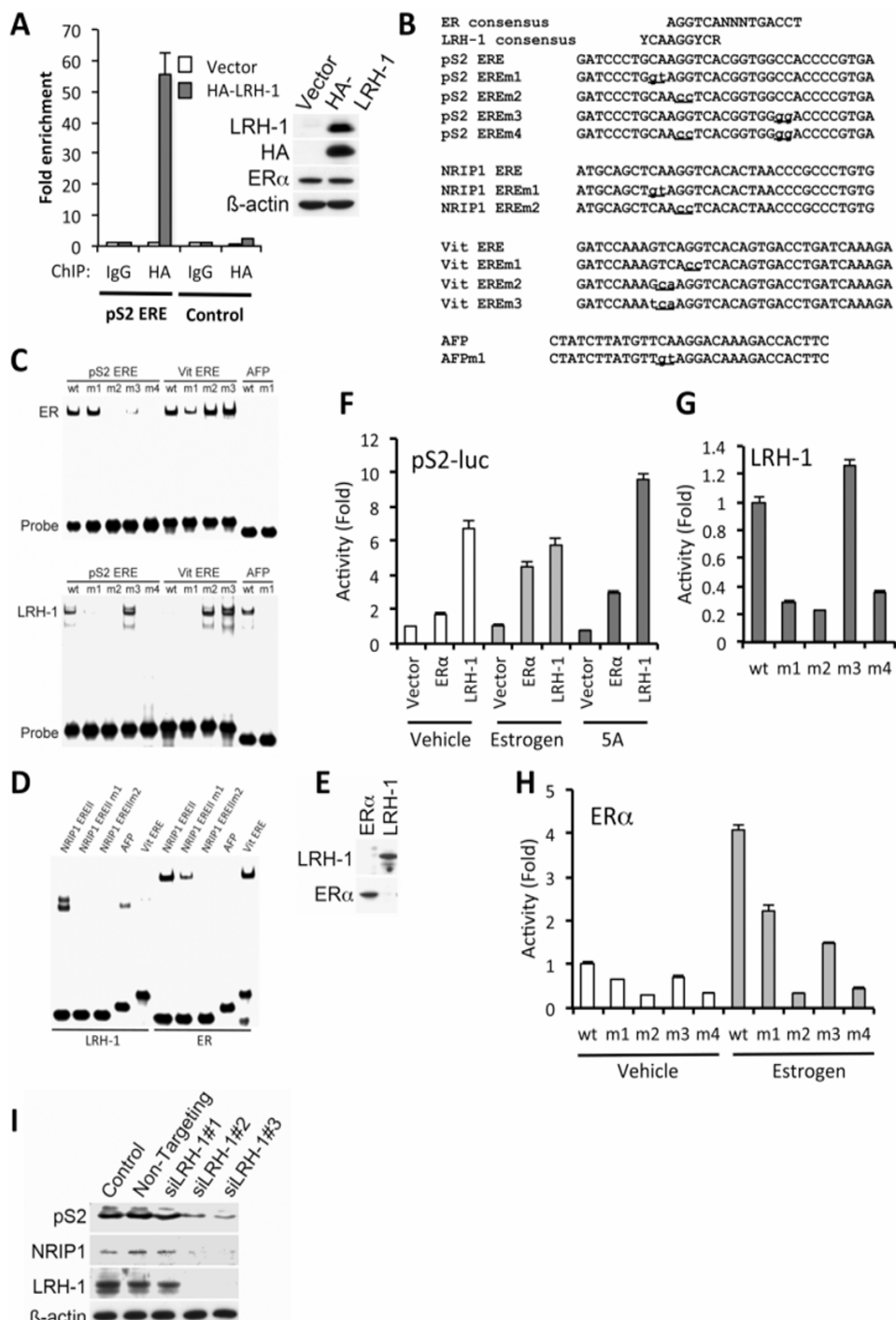
Figure 3*: LRH-1 regulates pS2 gene expression through binding to the pS2 ERE. (A)ChIP was carried out using IgG (control) or HA antibodies, following transfection of MCF-7 cells with empty vector or HA-LRH-1, followed by real-time PCR using primers for the pS2 ERE region, or with primers amplifying a region upstream of the pS2 ERE (control), as described (14). For each PCR, enrichment is shown relative to the vector control, as mean values for three replicates; error bars represent SEM. Western blotting of HA-LRH-1–transfected MCF-7 cell extracts is also shown. (B)Sequences for consensus ERα and LRH-1 binding sites are shown above the sequence of the pS2 ERE. The NRIP1 intronic ERE, chicken vitellogenin ERE and the LRH-1 binding sites in the mouse AFP gene. Mutations generated in these sequences are shown in lower case and are underlined. (C) EMSA was carried out using oligonucleotides having the sequences shown in (B). LRH-1 and ERα were produced using coupled in vitro transcription/translation (IVTT). (D) See C (E) Western blotting of IVTT products for LRH-1 and ERα are shown. (F) COS-1 cells were transfected with pS2-luc, together with ERα and LRH-1, as shown. Reporter gene activities were corrected for transfection efficiency by normalizing to Renilla luciferase activity and are shown relative to reporter gene activity for the vehicle-treated vector control. Shown are the mean pS2-luc activities from three independent transfections; errors bars = SEM. (G) COS-1 cells were transfected with LRH-1, together with pS2-luc or mutant reporters, as shown. Following normalization for the transfection control (renilla), activities are shown relative to the activities obtained for pS2-luc.(H) As in G but now cells were transfected with ERα.*

allowed LRH-1 binding to the vitellogenin ERE.

LRH-1 stimulated a reporter gene encoding 1006 bp of the pS2 gene promoter, containing the ERE (59). This ERE sequence is required for activation of pS2 expression by LRH-1 because deletion of the ERE sequence (pS2ΔERE-luc) largely abrogated reporter gene activation by LRH-1 (**Figure 3F** and Supplementary Figure S6B). Substitutions in the 5′ extension, the 5′ hexameric sequence, but not in the 3′ hexameric motif, prevented LRH-1 activation of the pS2 reporter gene (**Figure 3G**). Together, these findings demonstrate that LRH-1 can bind to the pS2 gene promoter proximal ERE, to stimulate pS2 gene expression.

LRH-1 knockdown in MCF-7 cells resulted in a reduction in pS2 and NRIP1 expression for two independent siRNAs (**Figures 1B and and 3I**). The expression of AGR3, PDZK1 and RET, genes to which LRH-1 is recruited at ERα binding regions (Supplementary Figure S7), was similarly reduced on LRH-1 knockdown (Supplementary Figure S8). Together, these results

show that LRH-1 can be recruited to ERα binding regions, and that binding to select EREs allows LRH-1 regulation of ERα target genes.

Synergistic recruitment between LRH-1 and ERα to EREs at ERα binding regions

As shown above, LRH-1 knockdown gave a marked reduction in expression of pS2, NRIP1 and other genes for which LRH-1 binding to ERα binding regions was observed by ChIP-seq, demonstrating that LRH-1, like ERα, promotes expression of these genes. This raises the possibility that ERα and LRH-1 co-operatively regulate expression of ERα target genes. Indeed, ectopic expression of LRH-1 in MCF-7 cells stimulated ERα recruitment to the pS2 promoter (**Figure 4A**). Conversely, siLRH-1 treatment reduced ERα recruitment to the pS2 promoter (**Figure 4B**). To extend this finding, ChIP-seq for ERα following siLRH-1 treatment was carried out to determine the importance of LRH-1 for ERα binding to ERα binding sites. LRH-1 knock-down resulted in a reduction by ~50% in the intensity of ERα binding events (**Figure 4C** and Supplementary Figure S9A). The reduction in ERα binding exemplified for pS2 (TFF1), PDZK1, RET and AGR3 (**Figure 4D**) was confirmed by ChIP-QPCR (Supplementary Figure S9B–E). Moreover, ectopic expression of LRH-1 stimulated ERα binding at these regions (**Figure 4A and E**; Supplementary Figure S10). The ELOVL2 gene serves as an example of an ERα binding site to which LRH-1 is not recruited (Supplementary Figure S10). In this case, LRH-1 silencing did not influence ERα recruitment (Supplementary Figure S9F).

To determine if LRH-1 functions to promote or maintain cofactor recruitment, we performed ChIP for p300 and CREB Binding Protein (CBP), well-known ERα co-activators (12) following LRH-1 silencing. There was a significant decrease in p300 and CBP binding at all loci (**Figure 5A and B**). Binding of the AIB1 co-activator was also decreased in the absence of LRH-1 (**Figure 5C**). These data illustrate that the LRH-1 and ERα shared sites are also occupied by typical ERα co-activators. Mining publically available data sets for SRC1, SRC2, SRC3 (AIB1), p300 and CBP (71) illustrated that this was indeed the case, and cofactor recruitment was found enriched at LRH-1/ERα sites on a genome-wide level. There was, however, no appreciable difference in p300 binding. This suggests that co-operativity between LRH-1 and ERα promotes co-activator recruitment at co-regulated genes. The changes in cofactor binding were reflected in changes in chromatin structure following LRH-1 silencing, as demonstrated by reduction in levels of histone
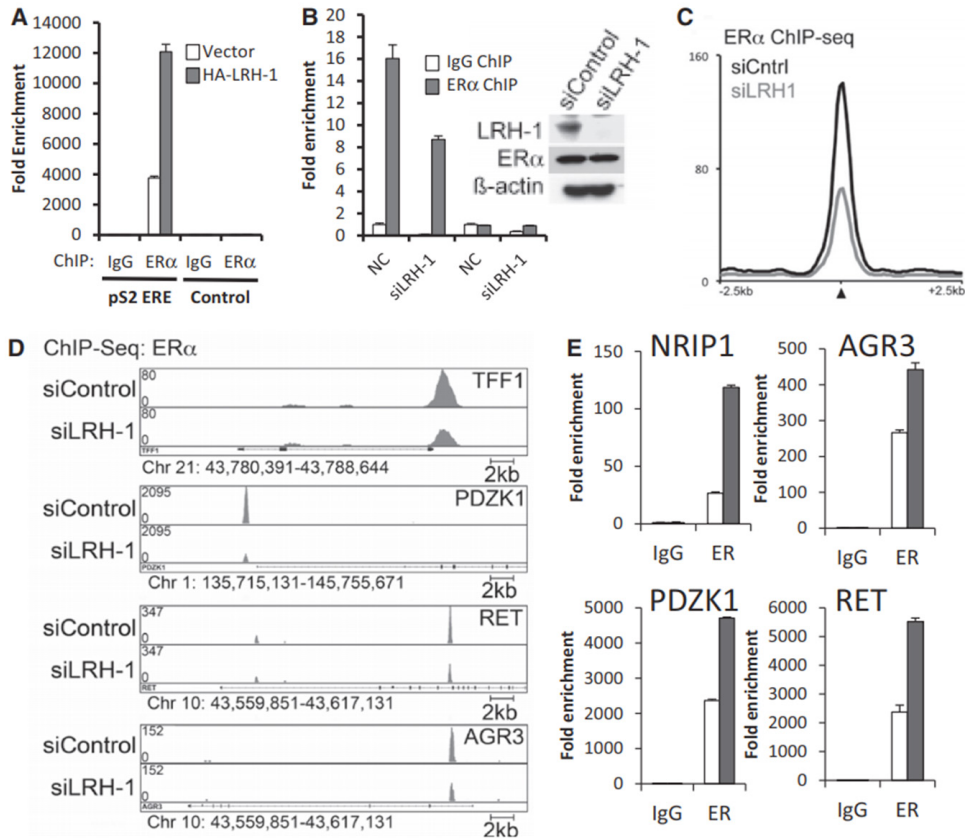
Figure 4: *LRH-1 promotes ERα binding to the ERα binding sites.*
(A) ERα ChIP was carried out using chromatin prepared for the ChIP shown in Figure 3A. Enrichment is shown relative to the IgG control as mean values for three replicates. (B) ERα ChIP was performed following MCF-7 treatment with siControl (NC) or siLRH-1 (n = 3). Western blotting for LRH-1 and ERα is also shown. (C) Average signal intensity of ERα binding events is shown for MCF-7 cells treated with siControl or siLRH-1. (D) Genome browser snapshots of ChIP-seq samples for ERα from siControl– or siLRH-1–treated MCF-7 cells are shown. Y bar shows tag count. (E) ERα ChIP for ERα binding regions is shown for vector (clear bars) and LRH-1– transfected (grey bars) MCF-7 cells (n = 3, error bars = SEM).

marks associated with gene expression, namely acetylation of histone H3 (**Figure 5E–G**). Also reduced on LRH-1 silencing were levels of H3 lysine 4 trimethylation (H3K4Me3), a marker of transcriptional activity (72) at the pS2 promoter (**Figure 5F**), as well as PolII recruitment (**Figure 5H**). These
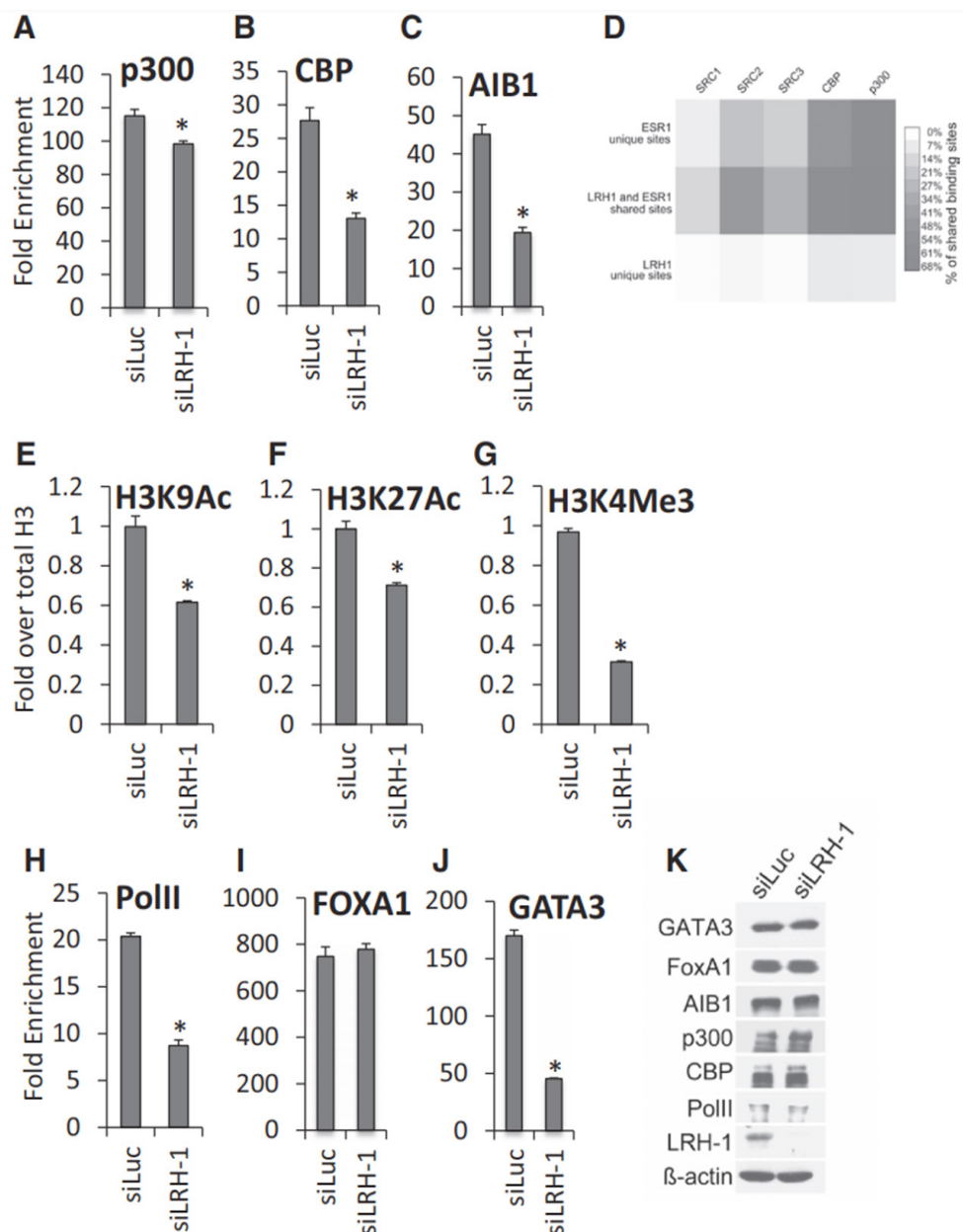
Figure 5: LRH-1 is required for co-activator loading and histone modification. MCF-7 cells were transfected with LRH-1 siRNA. ChIP was performed using antibodies for ERα cofactors (A–C, I and J), histone H3 acetylation and methylation marks (E–G) or PolII (H), followed by real-time PCR of the pS2 ERE, as shown.

Enrichment is shown relative to the IgG control (n = 3). The acetylated and methylated H3 ChIP was first normalized to total H3, then to the IgG control. Errors bars = SEM, *P < 0.05.

Heatmap of ERα co-activator binding [data from (71)], showing the percentage of overlapping SRC1, SRC2, SRC3, CBP and p300 binding events at LRH-1 and ERα unique and shared sites. (K) Western blotting of the lysates in parts (A–C, E–J), is shown.

findings, together with the reduction in mRNA levels of these genes (Supplementary Figure S8), are further indicative of a requirement for LRH-1 for the transcription of these oestrogen-responsive genes. Note that there was no change in levels of these proteins with LRH-1 knockdown (**Figure 5K**).

Interestingly, LRH-1 knockdown did not affect FOXA1 binding to ERα binding regions (**Figure 5I**). This may be a reflection of the described presence of FOXA1 before ERα recruitment and its requirement for ERα recruitment to chromatin (16,23,24). The importance of FOXA1 has also been demonstrated for other NRs, e.g. AR (35), and it might also be required for LRH-1 recruitment. However, binding of GATA3, which is also critical for ERα recruitment, was significantly reduced following LRH-1 silencing (**Figure 5J**), identifying another mechanism by which LRH-1 regulates ERα recruitment. There was no reduction in FOXA1 or GATA3 protein levels on LRH-1 knockdown (**Figure 5K**).

The above results demonstrate a requirement for LRH-1 for the transcription of oestrogen-responsive genes in breast cancer cells. However, treatment of MCF-7 cells with oestrogen stimulated LRH-1 binding to these sites (**Figure 6A–C** and Supplementary Figure S11). Moreover, treatment of MCF-7 cells with ICI182 780, an anti-oestrogen that results in ERα degradation, reduced LRH-1 binding (**Figure 6D–F** and Supplementary Figure S12). Note that levels of ectopically expressed LRH-1 are unaffected by oestrogen or ICI182 780 treatment. Together, these results demonstrate that as LRH-1 stimulates ERα binding, ERα reciprocally promotes LRH-1 recruitment.

Discussion

LRH-1 is a NR transcription factor that plays important roles in development, reproduction and metabolism. Its role in reverse cholesterol transport and bile acid homeostasis has been especially well studied, and it has been shown that LRH-1 acts as a potentiation factor for the LXR oxysterol receptors through binding to sites proximal to LXR binding sites to induce expression of key
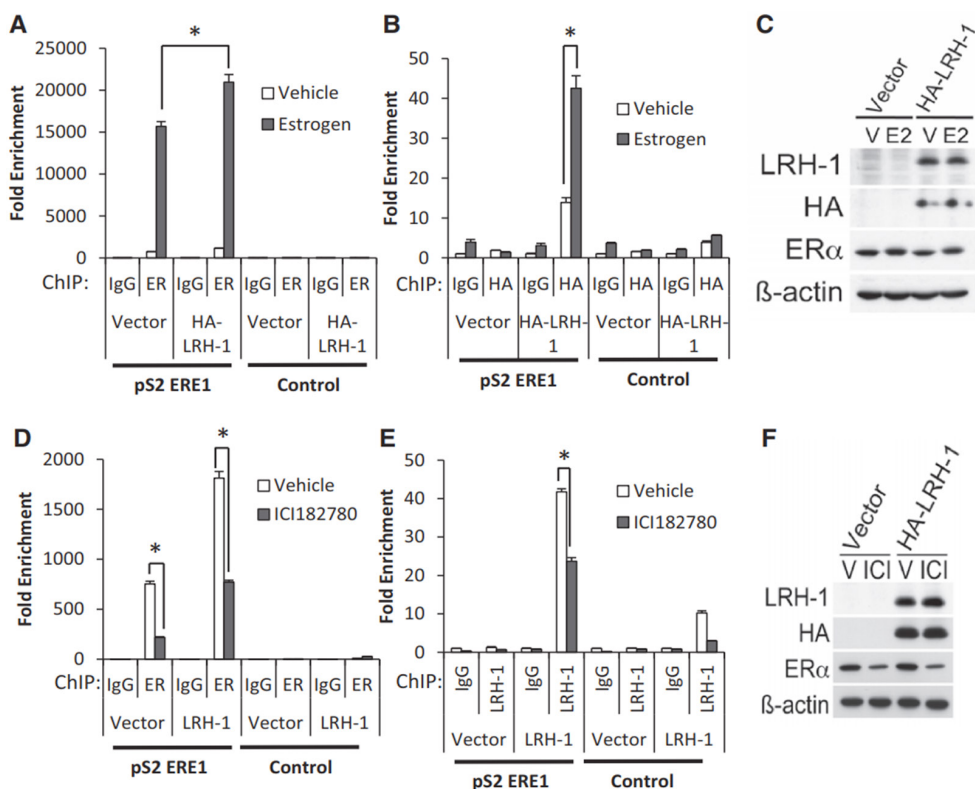
Figure 6: *Modulation of ERα activity regulates LRH-1 recruitment to ERα binding regions.*
MCF-7 cells transfected with HA-LRH-1 were treated with oestrogen for 45 min (A–C) or with ICI182 780 for 24 h (D–F). ChIP for ERα (A and D) or LRH-1 (B and E) was performed. The mean enrichment relative to the IgG control for three independent experiments is shown. Errors bars = SEM, *P < 0.05. (C and F) Western blotting of the lysates is shown.

genes involved in these processes, including CYP7A1, CYP8B1, CETP, SREB-1c and FAS (36,73–77). The bile acid receptor FXR is also implicated in crosstalk with LRH-1 and ChIP-seq for FXR and LRH-1 reveals that almost a quarter of hepatic LRH-1 binding sites are located in close proximity to FXR binding sites, suggesting that co-operativity between LRH-1 and FXR is important for the regulation of metabolic genes in the liver (78,79).

LRH-1 is a direct ERα target gene (52,53), its expression correlates with ERα in breast tumours (54) and it promotes breast cancer proliferation and invasion (55). We now show that LRH-1 is an important regulator of

ERα target genes because LRH-1 siRNA resulted in reduced expression of oestrogen-responsive genes. Moreover, LRH-1 ChIP-seq analysis shows that a substantial proportion of LRH-1 binding sites map to ERα binding sites, with enrichment of the LRH-1 binding motif being evident at these sites. This indicates that LRH-1 functions in breast cancer cells not only by mediating oestrogen action at non-ERα target genes following stimulation of its expression by ERα (which may be viewed as a classic mechanism by which a signal transduction pathway response may be amplified) but also by potentiating ERα action at many genes that are direct targets of ERα. The co-operativity between LRH-1 and ERα was further illustrated by the substantial overlap in binding sites between the ERα unique binding sites and ERα/LRH-1 shared sites with FOXA1 and GATA3, both well-established parts of the ERα transcription complex.

Of particular note was our observation of overlapping LRH-1 and ERα binding sites, to which binding of both factors was confirmed. This is in contrast to the metabolic genes regulated by LRH-1/LXR and LRH-1/FXR, where binding at proximal but non-overlapping sites has been described (73–79). Analysis of one of these overlapping binding sites, at the pS2 promoter ERE shows that LRH-1 binds to the 5′ hexamer of this ERE, the sequence around this hexamer being consistent with the extended sequence to which LRH-1 binds. This finding is consistent with a previous report that showed LRH-1 binding to the pS2 and GREB1 EREs (80). We further show here that LRH-1 stimulated pS2 expression and LRH-1 knockdown showed that it is required for pS2 expression. Interestingly, LRH-1 overexpression promoted ERα recruitment, while LRH-1 knockdown by siRNA inhibited ERα binding to the pS2 ERE, indicative of a requirement of LRH-1 for ERα binding. Similar promotion of ERα recruitment by LRH-1 was observed for the NRIP1 intronic ERE, as well as ERα binding regions associated with other oestrogen-responsive genes. ERα ChIP-seq following LRH-1 silencing also demonstrated a reduction in ERα binding, consistent with an important role for LRH-1 in promoting ERα binding. Further investigation of the LRH-1 ChIP-seq data also showed detectable LRH-1 signal at additional ERα binding sites, excluded by the peak call algorithm, due to threshold stringency (Supplementary Figure S13). This suggests that LRH-1 is recruited, albeit weakly, to a considerable proportion of ERα binding sites, further highlighting the importance of LRH-1 for ERα action in breast cancer cells.

Our data are indicative of co-occupancy of the two receptors at a proportion of ERα binding sites. However, we failed to reChIP ERα follow-

ing ChIP for LRH-1, or vice versa. Nor were we able to obtain evidence for co-binding of ERα and LRH-1 in EMSA, using the pS2 ERE oligonucleotides. Immunoprecipitation of ERα did not co-immunoprecipitate LRH-1 in MCF-7 cells, nor did we detect an interaction in co-immunoprecipitation experiments in COS-1 cells following LRH-1 and ERα overexpression (data not shown). Together, these results indicate that the co-operativity between LRH-1 and ERα does not involve co-occupancy of binding sites by these receptors. This raises the possibility that these receptors bind the pS2 ERE through a sequential recruitment mode of action, so-called 'assisted loading', recently described for binding of the glucocorticoid receptor (GR) and a mutant oestrogen receptor that can bind to a GR response element (81). This study demonstrated that binding of one NR does not reduce steady state binding of another NR; rather binding of one NR can facilitate subsequent binding of a second NR by promoting chromatin accessibility, leading to steady state levels of several NRs at the same response element. In agreement with this possibility, LRH-1 silencing reduced levels of GATA3 and co-activator recruitment, histone modifications associated with active chromatin as well as PolII binding. These results suggest that LRH-1 promotes cofactor recruitment and chromatin changes that facilitate ERα recruitment. Additionally, ChIP following the addition of oestrogen promoted LRH-1 recruitment, while ERα downregulation with ICI182 780 treatment inhibited LRH-1 binding, suggestive of a mechanism involving cyclical binding of ERα and LRH-1 to the regulatory regions of oestrogen-responsive genes. These findings show that ERα and LRH-1 co-regulate many oestrogen target genes and highlight LRH-1 as an important mediator of the oestrogen response in breast cancer cells.

The importance of LRH-1 for the expression of oestrogen-responsive genes described here identifies it as a putative drug target in breast cancer. Given that AR has been shown to regulate the expression of ERα target genes in ERα-negative breast cancer (35), it will be interesting to determine the potential importance of LRH-1 in the regulation of ERα target genes in endocrine resistant breast cancer and/or in ERα-negative breast cancer and consequently its therapeutic potential in breast cancer subtypes currently lacking targeted therapies.

Material and Methods

Cell culture
MCF-7 and COS-1 cells, obtained from American Type Culture Collection (LGC Standards, UK), were routinely cultured in Dulbecco's modified Eagle's medium (DMEM) containing 10% foetal calf serum (FCS). For oestrogen depletion experiments, the cells were transferred to DMEM lacking phenol red and containing 5% dextran-coated charcoal-stripped FCS (DSS) for 72 h. 17ß-estradiol (oestrogen) was added to a final concentration of 10 nM, and ICI182 780 (fulvestrant) was added to a final concentration of 100 nM. The synthetic LRH-1 agonist, compound 5A was added to a final concentration of 30 µM (53,56).

Plasmids
The Renilla luciferase reporter gene was RLTK (Promega, UK). The LRH-1 expression plasmid pCI-LRH-1 and the LRH-1 firefly luciferase reporter gene SF-1-luc were gifts from Dr Donald McDonnell (57). HA-tagged LRH-1 (pCI-HA3-LRH-1) was generated by insertion of 3xHA coding sequence from pMXB-3HA-mNR5A2 (44) into pCI-LRH-1 to generate HA-tagged human LRH-1 variant 4 (53). The ERα expression plasmid has been described previously (58). The pS2-luc and pS2-ΔERE-luc reporter genes were kindly provided by Dr Vincent Giguere (59). pS2-luc mutants were generated by site-directed mutagenesis using the Quickchange kit from Stratagene, UK.

Reporter gene assays
For transient transfection, COS-1 cells were seeded in 24-well plates in DMEM lacking phenol red and supplemented with 5% DSS. Following seeding for 24 h, cells were transfected using FuGENE HD (Promega, UK), with 100 ng of luciferase reporter genes, 10 ng of ERα and 50 ng of LRH-1. Oestrogen (10 nM) or compound 5A (30 µM) were added as indicated. Luciferase activities were determined after a further 24 h, using the Dual-Glo Luciferase Assay kit (Promega, UK). RLTK was transfected to control for transfection efficiency, so firefly luciferase activities were calculated relative to the Renilla luciferase (RLTK) activities.

siRNA transfections
Cells were transfected with double-stranded RNA oligonucleotides using the Lipofectamine RNAiMax reverse transfection method (Invitrogen, UK),

according to manufacturer's protocols. ON-TARGETplus SMARTpool for LRH-1 (LU-003430, Thermofisher), or individual siRNAs from the SMART-pool, were used as indicated in figure legends. siLuc control (D-002050; Thermofisher) or Control siRNA (1027251; Qiagen) were transfected as negative controls. All siRNA experiments used the double-stranded RNA oligonucleotides at a final concentration of 80 nM.

Western blotting
Cells were cultured and whole-cell lysates were prepared as described previously (60). Antibodies used for western blotting are detailed in Supplementary Materials.

Quantitative reverse transcriptase-polymerase chain reaction
Total RNA was collected and real-time reverse transcriptase-polymerase chain reaction (RT-PCR) was performed as previously described (61). Real-time RT-PCR was carried out using Taqman Gene Expression Assays (Applied Biosystems, UK). Assay details can be found in the Supplementary Materials.

Electrophoretic mobility shift assay
HA-LRH-1 and ERα proteins, made using the TNT coupled transcription/ translation system (Promega), were used for electrophoretic mobility shift assay (EMSA), as described previously (62), with the exception that the oligonucleotides were labelled at the 5′ end with DY782, allowing detection of complexes using a LiCoR Odyssey Infrared imaging system.

Chromatin Immunoprecipitations
ChIPs were performed as described previously (63). For each ChIP, 10 μg of antibody (detailed in Supplementary Information) and 100 μl of Dynalbeads Protein A (10002D; Invitrogen) were used. Primers for real-time PCR are also provided in Supplementary Materials.

ChIPs and Solexa sequencing
ChIP DNA was amplified as described (63). Sequences were generated by the Illumina Hiseq 2000 genome analyser (using 50 bp reads), and aligned to the Human Reference Genome (assembly hg19, February 2009). Enriched regions of the genome were identified by comparing the ChIP samples with an input sample using the MACS peak caller (64) version 1.3.7.1. All ChIP-seq analyses were performed in duplicate, where only the peaks shared by both

replicates were considered. The numbers of reads obtained, the percentage of reads aligned and the number of peaks called are detailed in Supplementary Figure S1.

Motif analysis, heatmaps and genomic distributions of binding events
ChIP-seq data snapshots were generated using the Integrative Genome Viewer IGV 2.2 (www.broadinstitute.org/igv/) and the UCSC genome browser (http://genome.ucsc.edu). Motif analyses were performed through the Cistrome (cistrome.org), applying the SeqPos motif tool (65). The genomic distributions of binding sites were analysed using the cis-regulatory element annotation system (CEAS) (66). The genes closest to the binding site on both strands were analysed. If the binding region is within a gene, CEAS software indicates whether it is in a 5′ untranslated region (5′ UTR), a 3′ untranslated region (3′ UTR), a coding exon or an intron. Promoter is defined as 3 kb upstream from RefSeq 5′ start. If a binding site is >3 kb away from the RefSeq transcription start site, it is considered distal intergenic. For integration with gene expression data, binding events were considered proximal when identified in a gene body or within 20 kb upstream of the transcription start site. Heatmaps were generated using Seqminer, using default settings (67).

Gene expression microarray analysis
MCF-7 cells were transfected with LRH-1 siRNA #2, #3 or with a non-targeting siRNA (siControl; D-001210-10, Thermofisher). RNA was extracted 72 h later using the QIAGEN RNeasy Kit (Qiagen Ltd., UK). Following assessment of RNA integrity, four independent biological replicates for each siRNA treatment were used for microarray analysis. The analysis was performed using HumanHT-12 v 3.0 Expression BeadChiP (Illumina). The BeadChiP image data were preprocessed using GenomeStudio (Illumina). The expression data were then log2 transformed and quantile-normalized using Partek Genomics Suite. Gene ontology (GO) analyses were performed using the database for annotation, visualization and integrated discovery (DAVID) (http://david.abcc.ncifcrf.gov) (68). The microarray data have been deposited with the NCBI Gene Expression Omnibus (GEO) (http://ncbi.nlm.nih.gov/geo/) under accession number GSE47803. The ChIP-seq data are available under accession number GSE49390.

Conflict of Interest
The authors declare no conflict of interest.

References

1. Hewitt,S.C., Harrell,J.C. and Korach,K.S. (2005) Lessons in estrogen biology from knockout and transgenic animals. *Annu. Rev. Physiol.*, 67, 285–308.
2. Deroo,B.J. and Korach,K.S. (2006) Estrogen receptors and human disease. *J. Clin. Invest.*, 116, 561–570.
3. Ali,S., Buluwela,L. and Coombes,R.C. (2011) Antiestrogens and their therapeutic applications in breast cancer and other diseases. *Annu. Rev. Med.*, 62, 217–232.
4. Ali,S. and Coombes,R.C. (2002) Endocrine-responsive breast cancer and strategies for combating resistance. *Nat. Rev. Cancer*, 2, 101–112.
5. O'Donnell,A.J., Macleod,K.G., Burns,D.J., Smyth,J.F. and Langdon,S.P. (2005) Estrogen receptor-alpha mediates gene expression changes and growth response in ovarian cancer cells exposed to estrogen. *Endocr. Relat. Cancer*, 12, 851–866.
6. Shang,Y. (2006) Molecular mechanisms of oestrogen and SERMs in endometrial carcinogenesis. *Nat. Rev. Cancer*, 6, 360–368.
7. Mangelsdorf,D.J., Thummel,C., Beato,M., Herrlich,P., Schutz,G., Umesono,K., Blumberg,B., Kastner,P., Mark,M., Chambon,P. et al. (1995) The nuclear receptor superfamily: the second decade. *Cell*, 83, 835–839.
8. Dahlman-Wright,K., Cavailles,V., Fuqua,S.A., Jordan,V.C., Katzenellenbogen,-J.A., Korach,K.S., Maggi,A., Muramatsu,M., Parker,M.G. and Gustafsson,J.A. (2006) International union of pharmacology. LXIV. Estrogen receptors. *Pharmacol. Rev.*, 58, 773–781.
9. Osborne,C.K. and Schiff,R. (2011) Mechanisms of endocrine resistance in breast cancer. *Annu. Rev. Med.*, 62, 233–247.

10. Bjornstrom,L. and Sjoberg,M. (2005) Mechanisms of estrogen receptor signaling: convergence of genomic and nongenomic actions on target genes. Mol. Endocrinol., 19, 833–842.

11. Safe,S. and Kim,K. (2008) Non-classical genomic estrogen receptor (ER)/specificity protein and ER/activating protein-1 signaling pathways. J. Mol. Endocrinol., 41, 263–275.

12. Shang,Y., Hu,X., DiRenzo,J., Lazar,M.A. and Brown,M. (2000) Cofactor dynamics and sufficiency in estrogen receptor-regulated transcription. Cell, 103, 843–852.

13. Metivier,R., Penot,G., Hubner,M.R., Reid,G., Brand,H., Kos,M. and Gannon,F. (2003) Estrogen receptor-alpha directs ordered, cyclical, and combinatorial recruitment of cofactors on a natural target promoter. Cell, 115, 751–763.

14. Reid,G., Hubner,M.R., Metivier,R., Brand,H., Denger,S., Manu,D., Beaudouin,J., Ellenberg,J. and Gannon,F. (2003) Cyclic, proteasome-mediated turnover of unliganded and liganded ERalpha on responsive promoters is an integral feature of estrogen signaling. Mol. Cell, 11, 695–707.

15. Metivier,R., Reid,G. and Gannon,F. (2006) Transcription in four dimensions: nuclear receptor-directed initiation of gene expression. EMBO Rep., 7, 161–167.

16. Carroll,J.S., Liu,X.S., Brodsky,A.S., Li,W., Meyer,C.A., Szary,A.J., Eeckhoute,J., Shao,W., Hestermann,E.V., Geistlinger,T.R. et al. (2005) Chromosome-wide mapping of estrogen receptor binding reveals long-range regulation requiring the forkhead protein FoxA1. Cell, 122, 33–43.

17. Lin,C.Y., Vega,V.B., Thomsen,J.S., Zhang,T., Kong,S.L., Xie,M., Chiu,K.P., Lipovich,L., Barnett,D.H., Stossi,F. et al. (2007) Whole-genome cartography of estrogen receptor alpha binding sites. PLoS Genet., 3, e87.

18. Fullwood,M.J., Liu,M.H., Pan,Y.F., Liu,J., Xu,H., Mohamed,Y.B., Orlov,Y.L., Velkov,S., Ho,A., Mei,P.H. et al (2009) An oestrogen-receptor-alpha-bound human chromatin interactome. Nature, 462, 58–64.

19. Welboren,W.J., van Driel,M.A., Janssen-Megens,E.M., van Heeringen,S.J., Sweep,F.C., Span,P.N. and Stunnenberg,H.G. (2009) ChIP-Seq of ERalpha and RNA polymerase II defines genes differentially responding to ligands. EMBO J., 28, 1418–1428.

20. Ross-Innes,C.S., Stark,R., Teschendorff,A.E., Holmes,K.A., Ali,H.R., Dunning,M.J., Brown,G.D., Gojis,O., Ellis,I.O., Green,A.R. et al. (2012) Differential oestrogen receptor binding is associated with clinical outcome in breast cancer. Nature, 481, 389–393.

21. Lacroix,M. and Leclercq,G. (2004) About GATA3, HNF3A, and XBP1, three genes co-expressed with the oestrogen receptor-alpha gene (ESR1) in breast cancer. Mol. Cell. Endocrinol., 219, 1–7.

22. Cirillo,L.A., Lin,F.R., Cuesta,I., Friedman,D., Jarnik,M. and Zaret,K.S. (2002) Opening of compacted chromatin by early developmental transcription factors HNF3 (FoxA) and GATA-4. Mol. Cell, 9, 279–289.

23. Laganiere,J., Deblois,G., Lefebvre,C., Bataille,A.R., Robert,F. and Giguere,V. (2005) Location analysis of estrogen receptor alpha target promoters reveals that FOXA1 defines a domain of the estrogen response. Proc. Natl Acad. Sci. USA, 102, 11651–11656.

24. Hurtado,A., Holmes,K.A., Ross-Innes,C.S., Schmidt,D. and Carroll,J.S. (2011) FOXA1 is a key determinant of estrogen receptor function and endocrine response. Nat. Genet., 43, 27–33.

25. Theodorou,V., Stark,R., Menon,S. and Carroll,J.S. (2013) GATA3 acts upstream of FOXA1 in mediating ESR1 binding by shaping enhancer accessibility. Genome Res., 23, 12–22.

26. Tan,S.K., Lin,Z.H., Chang,C.W., Varang,V., Chng,K.R., Pan,Y.F., Yong,E.L., Sung,W.K. and Cheung,E. (2011) AP-2gamma regulates oestrogen receptor-mediated long-range chromatin interaction and gene transcription. EMBO J., 30, 2569–2581.

27. Magnani,L., Eeckhoute,J. and Lupien,M. (2011) Pioneer factors: directing transcriptional regulators within the chromatin environment. Trends Genet., 27, 465–474.

28. Roman,S.D., Ormandy,C.J., Manning,D.L., Blamey,R.W., Nicholson,R.I., Sutherland,R.L. and Clarke,C.L. (1993) Estradiol induction of retinoic acid receptors in human breast cancer cells. Cancer Res., 53, 5940–5945.

29. Rishi,A.K., Shao,Z.M., Baumann,R.G., Li,X.S., Sheikh,M.S., Kimura,S., Bashirelahi,N. and Fontana,J.A. (1995) Estradiol regulation of the human retinoic acid receptor alpha gene in human breast carcinoma cells is mediated via an imperfect half-palindromic estrogen response element and Sp1 motifs. Cancer Res., 55, 4999–5006.

30. Hua,S., Kittler,R. and White,K.P. (2009) Genomic antagonism between retinoic acid and estrogen signaling in breast cancer. Cell, 137, 1259–1271.

31. Ross-Innes,C.S., Stark,R., Holmes,K.A., Schmidt,D., Spyrou,C., Russell,R., Massie,C.E., Vowler,S.L., Eldridge,M. and Carroll,J.S. (2010) Cooperative interaction between retinoic acid receptoralpha and estrogen receptor in breast cancer. Genes Dev., 24, 171–182.

32. Peters,A.A., Buchanan,G., Ricciardelli,C., Bianco-Miotto,T., Centenera,M.M., Harris,J.M., Jindal,S., Segara,D., Jia,L., Moore,N.L. et al. (2009) Androgen receptor inhibits estrogen receptor-alpha activity and is prognostic in breast cancer. Cancer Res., 69, 6131–6140.

33. Farmer,P., Bonnefoi,H., Becette,V., Tubiana-Hulin,M., Fumoleau,P., Larsimont,D., Macgrogan,G., Bergh,J., Cameron,D., Goldstein,D. et al. (2005) Identification of molecular apocrine breast tumours by microarray analysis. Oncogene, 24, 4660–4671.

34. Doane,A.S., Danso,M., Lal,P., Donaton,M., Zhang,L., Hudis,C. and Gerald,W.L. (2006) An estrogen receptor-negative breast cancer subset characterized by a hormonally regulated transcriptional program and response to androgen. Oncogene, 25, 3994–4008.

35. Robinson,J.L., Macarthur,S., Ross-Innes,C.S., Tilley,W.D., Neal,D.E., Mills,I.G. and Carroll,J.S. (2011) Androgen receptor driven transcription in molecular apocrine breast cancer is mediated by FoxA1. EMBO J., 30, 3019–3027.

36. Fayard,E., Auwerx,J. and Schoonjans,K. (2004) LRH-1: an orphan nuclear receptor involved in development, metabolism and steroidogenesis. Trends Cell Biol., 14, 250–260.

37. Fernandez-Marcos,P.J., Auwerx,J. and Schoonjans,K. (2011) Emerging actions of the nuclear receptor LRH-1 in the gut. Biochim. Biophys. Acta, 1812, 947–955.

38. Venteclef,N., Jakobsson,T., Ehrlund,A., Damdimopoulos,A., Mikkonen,L., Ellis,E., Nilsson,L.M., Parini,P., Janne,O.A., Gustafsson,J.A. et al. (2010) GPS2-dependent corepressor/SUMO pathways govern anti-inflammatory actions of LRH-1 and LXRbeta in the hepatic acute phase response. Genes Dev., 24, 381–395.

39. Duggavathi,R., Volle,D.H., Mataki,C., Antal,M.C., Messaddeq,N., Auwerx,J., Murphy,B.D. and Schoonjans,K. (2008) Liver receptor homolog 1 is essential for ovulation. Genes Dev., 22, 1871–1876.

40. Clyne,C.D., Kovacic,A., Speed,C.J., Zhou,J., Pezzi,V. and Simpson,E.R. (2004) Regulation of aromatase expression by the nuclear receptor LRH-1 in adipose tissue. Mol. Cell. Endocrinol., 215, 39–44.

41. Clyne,C.D., Speed,C.J., Zhou,J. and Simpson,E.R. (2002) Liver receptor homologue-1 (LRH-1) regulates expression of aromatase in preadipocytes. J. Biol. Chem., 277, 20591–20597.

42. Pare,J.F., Malenfant,D., Courtemanche,C., Jacob-Wagner,M., Roy,S., Allard,D. and Belanger,L. (2004) The fetoprotein transcription factor (FTF) gene is essential to embryogenesis and cholesterol homeostasis and is regulated by a DR4 element. J. Biol. Chem., 279, 21206–21216.

43. Gu,P., Goodwin,B., Chung,A.C., Xu,X., Wheeler,D.A., Price,R.R., Galardi,C., Peng,L., Latour,A.M., Koller,B.H. et al. (2005) Orphan nuclear receptor LRH-1 is required to maintain Oct4 expression at the epiblast stage of embryonic development. Mol. Cell. Biol., 25, 3492–3505.

44. Heng,J.C., Feng,B., Han,J., Jiang,J., Kraus,P., Ng,J.H., Orlov,Y.L., Huss,M.,

Yang,L., Lufkin,T. et al. (2010) The nuclear receptor Nr5a2 can replace Oct4 in the reprogramming of murine somatic cells to pluripotent cells. Cell Stem Cell, 6, 167–174.

45. Wang,W., Yang,J., Liu,H., Lu,D., Chen,X., Zenonos,Z., Campos,L.S., Rad,R., Guo,G., Zhang,S. et al. (2011) Rapid and efficient reprogramming of somatic cells to induced pluripotent stem cells by retinoic acid receptor gamma and liver receptor homolog 1. Proc. Natl Acad. Sci. USA, 108, 18283–18288.

46. Schoonjans,K., Dubuquoy,L., Mebis,J., Fayard,E., Wendling,O., Haby,C., Geboes,K. and Auwerx,J. (2005) Liver receptor homolog 1 contributes to intestinal tumor formation through effects on cell cycle and inflammation. Proc. Natl Acad. Sci. USA, 102, 2058–2062.

47. Benod,C., Vinogradova,M.V., Jouravel,N., Kim,G.E., Fletterick,R.J. and Sablin,E.P. (2011) Nuclear receptor liver receptor homologue 1 (LRH-1) regulates pancreatic cancer cell growth and proliferation. Proc. Natl Acad. Sci. USA, 108, 16927–16931.

48. Petersen,G.M., Amundadottir,L., Fuchs,C.S., Kraft,P., Stolzenberg-Solomon,R.Z., Jacobs,K.B., Arslan,A.A., Bueno-deMesquita,H.B., Gallinger,S., Gross,M. et al. (2010) A genomewide association study identifies pancreatic cancer susceptibility loci on chromosomes 13q22.1, 1q32.1 and 5p15.33. Nat. Genet., 42, 224–228.

49. Lazarus,K.A., Wijayakumara,D., Chand,A.L., Simpson,E.R. and Clyne,C.D. (2012) Therapeutic potential of Liver Receptor Homolog-1 modulators. J. Steroid Biochem. Mol. Biol., 130, 138–146.

50. Dunbier,A.K., Anderson,H., Ghazoui,Z., Folkerd,E.J., A'Hern,R., Crowder,R.J., Hoog,J., Smith,I.E., Osin,P., Nerurkar,A. et al. (2010) Relationship between plasma estradiol levels and estrogenresponsive gene expression in estrogen receptor-positive breast cancer in postmenopausal women. J. Clin. Oncol., 28, 1161–1167.

51. Lonning,P.E., Haynes,B.P., Straume,A.H., Dunbier,A., Helle,H., Knappskog,S. and Dowsett,M. (2011) Recent data on intratumor estrogens in breast cancer. Steroids, 76, 786–791.

52. Annicotte,J.S., Chavey,C., Servant,N., Teyssier,J., Bardin,A., Licznar,A., Badia,E., Pujol,P., Vignon,F., Maudelonde,T. et al. Nucleic Acids Research, 2013, Vol. 41, No. 22 10239 (2005) The nuclear receptor liver receptor homolog-1 is an estrogen receptor target gene. Oncogene, 24, 8167–8175.

53. Thiruchelvam,P.T., Lai,C.F., Hua,H., Thomas,R.S., Hurtado,A., Hudson,W., Bayly,A.R., Kyle,F.J., Periyasamy,M., Photiou,A. et al. (2011) The liver receptor homolog-1 regulates estrogen receptor expression in breast cancer cells. Breast Cancer Res. Treat., 127, 385–396.

54. Miki,Y., Clyne,C.D., Suzuki,T., Moriya,T., Shibuya,R., Nakamura,Y., Ishida,T.,

Yabuki,N., Kitada,K., Hayashi,S. et al. (2006) Immunolocalization of liver receptor homologue-1 (LRH-1) in human breast carcinoma: possible regulator of insitu steroidogenesis. Cancer Lett., 244, 24–33.

55. *Chand,A.L., Herridge,K.A., Thompson,E.W. and Clyne,C.D. (2010) The orphan nuclear receptor LRH-1 promotes breast cancer motility and invasion. Endocr. Relat. Cancer, 17, 965–975.*

56. *Whitby,R.J., Dixon,S., Maloney,P.R., Delerive,P., Goodwin,B.J., Parks,D.J. and Willson,T.M. (2006) Identification of small molecule agonists of the orphan nuclear receptors liver receptor homolog-1 and steroidogenic factor-1. J. Med. Chem., 49, 6652–6655.*

57. *Wang,W., Zhang,C., Marimuthu,A., Krupka,H.I., Tabrizizad,M., Shelloe,R., Mehra,U., Eng,K., Nguyen,H., Settachatgul,C. et al. (2005) The crystal structures of human steroidogenic factor-1 and liver receptor homologue-1. Proc. Natl Acad. Sci. USA, 102, 7505–7510.*

58. *Tora,L., Mullick,A., Metzger,D., Ponglikitmongkol,M., Park,I. and Chambon,P. (1989) The cloned human oestrogen receptor contains a mutation which alters its hormone binding properties. EMBO J., 8, 1981–1986.*

59. *Lu,D., Kiriyama,Y., Lee,K.Y. and Giguere,V. (2001) Transcriptional regulation of the estrogen-inducible pS2 breast cancer marker gene by the ERR family of orphan nuclear receptors. Cancer Res., 61, 6755–6761.*

60. *Lucey,M.J., Chen,D., Lopez-Garcia,J., Hart,S.M., Phoenix,F., Al-Jehani,R., Alao,J.P., White,R., Kindle,K.B., Losson,R. et al. (2005) T:G mismatch-specific thymine-DNA glycosylase (TDG) as a coregulator of transcription interacts with SRC1 family members through a novel tyrosine repeat motif. Nucleic Acids Res., 33, 6393–6404.*

61. *Lopez-Garcia,J., Periyasamy,M., Thomas,R.S., Christian,M., Leao,M., Jat,P., Kindle,K.B., Heery,D.M., Parker,M.G., Buluwela,L. et al. (2006) ZNF366 is an estrogen receptor corepressor that acts through CtBP and histone deacetylases. Nucleic Acids Res., 34, 6126–6136.*

62. *Metzger,D., Berry,M., Ali,S. and Chambon,P. (1995) Effect of antagonists on DNA binding properties of the human estrogen receptor in vitro and in vivo. Mol. Endocrinol., 9, 579–591.*

63. *Schmidt,D., Wilson,M.D., Spyrou,C., Brown,G.D., Hadfield,J. and Odom,D.T. (2009) ChIP-seq: using high-throughput sequencing to discover protein-DNA interactions. Methods, 48, 240–248.*

64. *Zhang,Y., Liu,T., Meyer,C.A., Eeckhoute,J., Johnson,D.S., Bernstein,B.E., Nusbaum,C., Myers,R.M., Brown,M., Li,W. et al. (2008) Model-based analysis of ChIP-Seq (MACS). Genome Biol., 9, R137.*

65. He,H.H., Meyer,C.A., Shin,H., Bailey,S.T., Wei,G., Wang,Q., Zhang,Y., Xu,K., Ni,M., Lupien,M. et al. (2010) Nucleosome dynamics define transcriptional enhancers. *Nat. Genet.*, 42, 343–347.

66. Ji,X., Li,W., Song,J., Wei,L. and Liu,X.S. (2006) CEAS: cisregulatory element annotation system. *Nucleic Acids Res.*, 34, W551–W554.

67. Ye,T., Krebs,A.R., Choukrallah,M.A., Keime,C., Plewniak,F., Davidson,I. and Tora,L. (2011) seqMINER: an integrated ChIPseq data interpretation platform. *Nucleic Acids Res.*, 39, e35.

68. Huang da,W., Sherman,B.T. and Lempicki,R.A. (2009) Systematic and integrative analysis of large gene lists using DAVID bioinformatics resources. *Nat. Protoc.*, 4, 44–57.

69. Solomon,I.H., Hager,J.M., Safi,R., McDonnell,D.P., Redinbo,M.R. and Ortlund,E.A. (2005) Crystal structure of the human LRH-1 DBD-DNA complex reveals Ftz-F1 domain positioning is required for receptor activity. *J. Mol. Biol.*, 354, 1091–1102.

70. Carroll,J.S., Meyer,C.A., Song,J., Li,W., Geistlinger,T.R., Eeckhoute,J., Brodsky,A.S., Keeton,E.K., Fertuck,K.C., Hall,G.F. et al. (2006) Genome-wide analysis of estrogen receptor binding sites. *Nat. Genet.*, 38, 1289–1297.

71. Zwart,W., Theodorou,V., Kok,M., Canisius,S., Linn,S. and Carroll,J.S. (2011) Oestrogen receptor-co-factor-chromatin specificity in the transcriptional regulation of breast cancer. *EMBO J.*, 30, 4764–4776.

72. Ruthenburg,A.J., Allis,C.D. and Wysocka,J. (2007) Methylation of lysine 4 on histone H3: intricacy of writing and reading a single epigenetic mark. *Mol. Cell*, 25, 15–30.

73. Goodwin,B., Jones,S.A., Price,R.R., Watson,M.A., McKee,D.D., Moore,L.B., Galardi,C., Wilson,J.G., Lewis,M.C., Roth,M.E. et al. (2000) A regulatory cascade of the nuclear receptors FXR, SHP-1, and LRH-1 represses bile acid biosynthesis. *Mol. Cell*, 6, 517–526.

74. Lu,T.T., Makishima,M., Repa,J.J., Schoonjans,K., Kerr,T.A., Auwerx,J. and Mangelsdorf,D.J. (2000) Molecular basis for feedback regulation of bile acid synthesis by nuclear receptors. *Mol. Cell*, 6, 507–515.

75. Luo,Y., Liang,C.P. and Tall,A.R. (2001) The orphan nuclear receptor LRH-1 potentiates the sterol-mediated induction of the human CETP gene by liver X receptor. *J. Biol. Chem.*, 276, 24767–24773.

76. Watanabe,M., Houten,S.M., Wang,L., Moschetta,A., Mangelsdorf,D.J., Heyman,R.A., Moore,D.D. and Auwerx,J. (2004) Bile acids lower triglyceride levels via a pathway involving FXR, SHP, and SREBP-1c. *J. Clin. Invest.*, 113, 1408–1418.

77. Matsukuma,K.E., Wang,L., Bennett,M.K. and Osborne,T.F. (2007) A key role for

orphan nuclear receptor liver receptor homologue-1 in activation of fatty acid synthase promoter by liver X receptor. J. Biol. Chem., 282, 20164–20171.

78. Chong,H.K., Biesinger,J., Seo,Y.K., Xie,X. and Osborne,T.F. (2012) Genome-wide analysis of hepatic LRH-1 reveals a promoter binding preference and suggests a role in regulating genes of lipid metabolism in concert with FXR. BMC Genomics, 13, 51.

79. Chong,H.K., Infante,A.M., Seo,Y.K., Jeon,T.I., Zhang,Y., Edwards,P.A., Xie,X. and Osborne,T.F. (2010) Genome-wide interrogation of hepatic FXR reveals an asymmetric IR-1 motif and synergy with LRH-1. Nucleic Acids Res., 38, 6007–6017.

80. Chand,A.L., Wijayakumara,D.D., Knower,K.C., Herridge,K.A., Howard,T.L., Lazarus,K.A. and Clyne,C.D. (2012) The orphan nuclear receptor LRH-1 and ERalpha activate GREB1 expression to induce breast cancer cell proliferation. PLoS One, 7, e31593.

81. Voss,T.C., Schiltz,R.L., Sung,M.H., Yen,P.M., Stamatoyannopoulos,J.A., Biddie,S.C., Johnson,T.A., Miranda,T.B., John,S. and Hager,G.L. (2011) Dynamic exchange at regulatory elements during chromatin remodeling underlies assisted loading mechanism. Cell, 146, 544–554.

Supplementary information

Supplementary Figure1-13
See online supplemental information

Chapter 5

Composition of ERα's transcriptional complex – part 2

Estrogen Receptor DNA-damage/methylation cycle as drug interface in tamoxifen resistant breast cancer by FEN1 blockade

Koen Dorus Flach[1], Manikandan Periyasamy[2], Ajit Jadhav[3], Theresa E. Hickey[4], Mark Opdam[5], Hetal Patel[2], Sander Canisius[6], David M. Wilson III[7], Dorjbal Dorjsuren[3], Marja Nieuwland[8], Roel Kluin[8], Alexey V. Zakharov[3], Jelle Wesseling[5], Lodewyk Frederik Ary Wessels[6], Sabine Charlotte Linn[5], Wayne D. Tilley[4], Anton Simeonov[3], Simak Ali[2], Wilbert Zwart[1]

[1]Department of Oncogenomics, [5]Department of Molecular Pathology, [6]Department of Molecular Carcinogenesis, [8]Genomics core facility, The Netherlands Cancer Institute, 1066 CX Amsterdam, The Netherlands. [2]Department of Surgery and Cancer, Imperial College London, Hammersmith Hospital Campus, Du Cane Road, London W12 0NN, UK. [3]National Center for Advancing Translational Sciences, National Institutes of Health, 9800 Medical Center Drive, MSC 3370, MD 20892, US. [4]Dame Roma Mitchell Cancer Research Laboratories, Adelaide Medical School, Faculty of Health Sciences, DX Number 650 801, University of Adelaide, Adelaide, South Australia 5005, Australia. [7]Laboratory of Molecular Gerontology, Intramural Research Program, National Institute on Aging, National Institutes of Health, Bayview Blvd 251, Baltimore, MD 21224, US.

In submission

Abstract

Estrogen receptor α (ERα) is a key transcriptional regulator in the majority of breast cancers. ERα-positive patients are frequently treated with tamoxifen, but resistance is common. Herein, a 111-gene outcome prediction-classifier was refined, revealing FEN1 as strongest determining factor in ERα-positive prognostication. We demonstrate FEN1 levels are predictive of outcome in tamoxifen-treated patients, and show FEN1 is required and sufficient for tamoxifen-resistance in ERα-positive cell lines. We show FEN1 dictates the transcriptional-activity of ERα by facilitating the formation and repair of hormone-induced DNA damage, ultimately resulting in DNA methylation changes. FEN1 blockade induced proteasome-mediated degradation of activated ERα, resulting in loss of ERα-driven gene expression and eradicated tumor cell proliferation. Finally, a high-throughput 460.000 compound screen identified a novel FEN1 inhibitor, which effectively blocks ERα-function and inhibits proliferation of tamoxifen-resistant cell lines as well as ex-vivo cultured ERα-positive breast tumors, providing therapeutic proof-of-principle for FEN1 blockade in tamoxifen-resistant breast cancer.

Introduction

Approximately 70% of all breast tumors are of the luminal subtype and their proliferation often depends on the activity of estrogen receptor α (ERα). Following estradiol (E2)-binding, a transcriptional complex is formed, initiated by Steroid Receptor Co-activator (SRC) p160 recruitment, which drives ERα-mediated transcription and cell proliferation programs (1).

Tamoxifen is often used in ERα–positive breast cancer patients, where it competitively blocks E2-binding, preventing co-activator-binding pocket formation and inhibiting cell proliferation (2). P160 member SRC3 (NCOA3, AIB1) is frequently amplified in breast tumors and correlates with a poor outcome after tamoxifen treatment (3).

Previously, we assessed the genome-wide chromatin binding landscape of all three p160 coactivators in MCF-7 breast cancer cells (4). Unique chromatin binding sites for each of the p160 family members were found, where genomic regions preferentially bound by SRC3 were uncovered proximal to 111 E2-responsive genes. Based on these genes, a prognostic classifier for outcome after tamoxifen treatment was developed. Which individual genes in the original classifier are critically involved in the observed clinical outcome remains elusive.

Besides recruitment of classic coregulators such as p160 proteins, DNA-modulating and DNA repair factors can also be recruited by ERα (5), as recently shown for APOBEC3B (6). APOBEC3B induces C-to-U deamination at ERα binding regions, leading to uracil DNA glycosylase (UNG) recruitment and ultimately to phosphorylation of H2AX at Serine 139 (γH2AX) (6). While in theory the resulting UNG-mediated region of DNA that contains neither a purine nor a pyrimidine (abasic site), can be repaired by the Base Excision Repair (BER) pathway (7), however the exact interplay of BER proteins with ERα function remains unclear.

FEN1 is a member of the RAD2 nuclease family and cleaves overhanging flaps structures that arise during lagging-strand DNA synthesis (e.g. Okazaki fragments) (8) or long-patch BER, yielding a single-stranded DNA nick which can be ligated by DNA-ligase 1 (LIG1) (7). FEN1 deficiency predisposes to tumor development and FEN1 is upregulated in numerous tumor types, including breast cancer (9). Although endogenous ERα/FEN1 interactions have not been reported, incubation of immobilized FLAG-tagged ERα with MCF-7 nuclear extracts did identify FEN1 as an ERα-associating protein (10). Even though FEN1 was described as recruited to the TFF1 promoter and FEN1 knockdown resulted in reduced TFF1 mRNA expression, it remains

unknown whether FEN1 regulates estrogen responsiveness in a genome wide manner or by which mechanism. Additionally, FEN1 levels correlate negatively with overall survival in breast cancer (11), but whether ERα-status is the driving force behind this clinical observation remains unclear.

Here, we demonstrate that FEN1 dictates the transcriptional activity of ERα by facilitating the formation and BER of hormone-induced DNA damage, ultimately resulting in DNA methylation changes. The induction and processing of DNA damage by FEN1 is essential for ERα-activity, regulating responsive gene expression and ERα-induced cell proliferation. We demonstrate that FEN1 alters ERα's activity by stabilizing chromatin interactions after activation. We show that FEN1 is a predictive marker of tamoxifen response in ERα-positive breast cancer patients, being both sufficient and essential for ERα-positive cell proliferation in the presence of tamoxifen. A novel small molecule inhibitor of FEN1 blocked tamoxifen resistant cell proliferation and primary ERα-positive tumor explants, yielding a novel therapeutic lead in the management of tamoxifen therapy resistance. Cumulatively, we present a pioneering proof-of-concept that spans from gene classifier and causal gene identification, to molecular mechanism, novel drug development and validation in ERα-positive breast cancer.

Results

FEN1 levels correlate with breast cancer patient survival after tamoxifen treatment

In a previous report, we identified 111 genes that predict outcome in tamoxifen-treated ERα-positive breast cancer patients (4). To reveal drivers causally involved in the observed patient outcome, we refined the gene signature to identify a minimal set of genes without losing predictive capacity (**Figure 1A**). Computationally minimizing the 111-gene classifier by Prediction Analysis for Microarrays (PAM) (12) and Lasso-penalized logistic regression (13) in two independent cohorts of tamoxifen-treated patients (14, 15) illustrated that the classifier could be reduced to four genes before losing its stratification potential: FEN1, MCM2, STARD13 and HBP1 (**Figure 1A**). Validation of the four genes in the METABRIC dataset (16) demonstrated that only FEN1 was significant by multivariate analysis in ERα-positive, but not ERα-negative cases (Sup Fig S1A), suggesting ERα-specific predictive potential of FEN1.

To assess the clinical impact of FEN1 as a single-gene classifier on
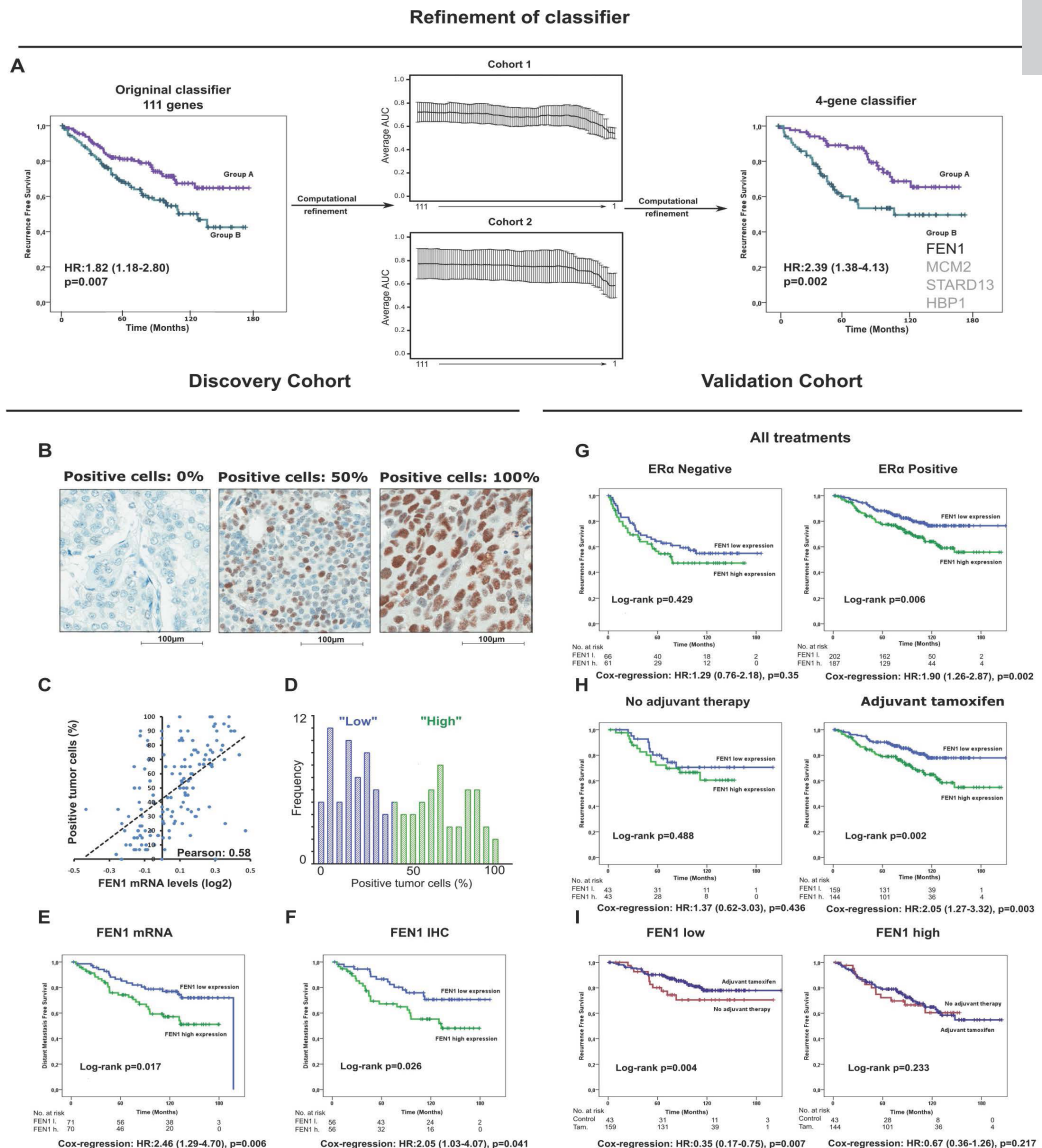
Figure 1. *FEN1 levels as predictive marker for tamoxifen response of breast cancer patients.*
(A) Computational refinement of 111-gene classifier towards 4-gene classifier of FEN1, MCM2, HBP1 and STARD13. PAM and Lasso-penalized logistic regression was performed to determine the minimum number of genes without affecting performance. (Left) Recurrence-Free Survival (RFS) of patients categorized according to

111-gene classifier. Cox regression is shown. (Middle) Step-wise minimization of the 111-genes with corresponding average area under the curve (AUC) in two cohorts. (Right) RFS of patients categorized according to 4-gene classifier. Cox regression is shown. See also Sup Fig S1A (B) Three representative IHC tumor cores, staining negative (0%), intermediate (50%) or entirely positive (100%) for FEN1. Scale bar is 100 μm. (C) Scatterplot showing FEN1 mRNA levels (X-axis) related to FEN1 protein expression (% tumor cells, Y-axis), from the same tumor samples. Dotted line indicates trend line. Pearson correlation coefficient = 0.58. (D) Bar graph showing the individual IHC-scores for all tumor samples. Tumors were stratified in "Low" (IHC-score ≤ 36%) or "High" (IHC-score > 36%) FEN1. (E) Distant Metasta-sis-Free Survival (DMFS) of tamoxifen-treated patients categorized according to FEN1 mRNA levels. Log-rank and Cox regression is shown. See also Sup table S1. (F) As in E, but now patients were categorized according to FEN1 IHC-score. (G) Randomized clinical trial: RFS of patients stratified by ERα-status and categorized according to FEN1 IHC-score. Log-rank and Cox regression is shown. See also Sup table S1 and Sup Fig S1B. (H) As in G, but now patients were stratified for adjuvant therapy (none or tamoxifen) and categorized according to FEN1 IHC-score. See also Sup table S1. (I) As in G, but now patients were stratified for FEN1 IHC-score and categorized according to adjuvant therapy (none or tamoxifen). See also Sup table S1.

survival, we first used samples of ERα-positive cases that received adju-vant tamoxifen (Discovery-cohort) (17), using microarray-based ("mRNA") and immunohistochemistry-based ("IHC") FEN1 expression ranging from 0-100% positive tumor cells (**Figure 1B**), which correlated with FEN1 mRNA levels (Pearson correlation coefficient=0.58) (**Figure 1C**). For both mRNA and IHC, the median was used to stratify patients into "Low" and "High" FEN1 groups (**Figure 1D**). FEN1 mRNA (HR: 2.46, p=0.006) (**Figure 1E**) (Sup table S1) and protein (HR: 2.05, p=0.041) (**Figure 1F**) (Sup table S1) expression were associated with Distant Metastasis-Free Survival (DMFS), with high FEN1 levels correlating with a poor survival. These re-sults were validated in an independent cohort, randomized between tamox-ifen or no adjuvant endocrine therapy (Validation cohort) (18). This cohort contains a matched non-tamoxifen treated group, making it extremely useful to directly assess FEN1's tamoxifen specific predictive potential, providing an extra level of evidence not available from other tamoxifen cohorts that lack a non-treated control group (19).

In this cohort, FEN1 was associated with Recurrence-Free Survival

(RFS) in ERα-positive patients (n=389) (HR=1.90, p=0.002) (**Figure 1G**), also after multivariate correction for age, tumor grade, tumor stage, HER2, PgR and lymph node status (adjusted HR=1.58, p=0.047) (Sup Table S1), and confirmed in the METABRIC dataset (Sup Fig S1A,B). No association was found between FEN1 levels and RFS in ERα-negative breast cancer patients (n=127) (HR=1.29, p=0.35) (**Figure 1G** and Sup Fig S1B). Furthermore, high FEN1 significantly correlated with poor outcome in tamoxifen-treated patients (HR=2.05, p=0.003), but not for patients not receiving endocrine therapy (HR=1.37, p=0.436) (**Figure 1H**) (Sup table S1).

To further investigate whether FEN1 associates with disease progression (prognostic classifier) or whether its levels are informative for treatment response (predictive classifier), patients were stratified according to FEN1 levels and categorized by tamoxifen treatment (**Figure 1I**). Patients with high FEN1 did not benefit from tamoxifen (HR=0.67, p=0.217), while tamoxifen-treated patients with low FEN1 had a better survival (HR=0.35, p=0.007), also after multivariate correction (high FEN1 adjusted HR=0.67, p=0.213; low FEN1 adjusted HR=0.39, p=0.015) (Sup table S1).

As the standard regimens of hormonal treatment for ERα-positive breast cancer have changed since the time of our validation cohort, we tested how FEN1 levels would perform in a cohort using more contemporary hormonal therapies (METABRIC). In patients treated with hormonal therapy, high FEN1 was associated poor disease-specific survival (HR=2.09, p<0.001), also after multivariate correction (adjusted HR=1.83, p<0.001) (Sup Figure S1C). The predictive potential of FEN1 levels was further illustrated by the interaction test between FEN1 levels and hormonal therapy status (HR=2.19, p<0.001; adjusted HR=1.86, p<0.001) (Sup Figure S1C). Additionally, we assessed whether the menopausal status of a patient would influence the performance of FEN1 as predictive biomarker, as in the clinical setting tamoxifen is predominately used in pre-menopausal women. Both in premenopausal (HR=5.29, p<0.001) and postmenopausal patients (HR=1.79, p<0.001), FEN1 levels were significantly associated with patient outcome, also after multivariate correction (premenopausal adjusted HR=5.57, p<0.001; postmenopausal adjusted HR=1.62, p<0.001) (Sup Figure S1D).

In summary, FEN1 levels are not predictive of outcome in ERα-negative breast cancers, nor in ERα-positive disease in the absence of adjuvant endocrine therapy. Only in ERα-positive patients who were treated with tamoxifen FEN1 levels were negatively associated with outcome, rendering FEN1 a predictive marker for tamoxifen treatment response.

FEN1 is essential for ERα-chromatin interactions and complex formation

FEN1 functions as a predictive marker for tamoxifen resistance in ERα–positive breast cancer. To determine whether FEN1 directly affects ERα activity, we tested if FEN1 is recruited to the ERα genomic complex. Based on co-immunoprecipitations, endogenous ERα and FEN1 interact in MCF7 cells, which is enhanced by E2 (**Figure 2A**). Knockdown of FEN1, as validated by western blot (Sup Fig 2A,B), abrogated ERα-chromatin interactions, which coincided with a loss of p300 binding (**Figure 2B,C,D** and Sup Fig S2C) and RNA Polymerase II (Sup Fig S2C) at these sites. FOXA1 chromatin binding (**Figure 2B,C,D**) and chromatin accessibility (**Figure 2E**) did not decrease by siFEN1, implicating FEN1 as a regulator of ERα-chromatin interactions downstream of FOXA1.

The main mode of action of FEN1 is 5' flap excision through its endonuclease activity (20), which is abrogated by the FEN1-D181A mutation (21). Overexpression of wild type FEN1 (FEN1-WT) enhanced ERα-chromatin interactions, while overexpression of FEN1-D181A (FEN1-dead) did not (**Figure 2F** and Sup Fig S2B), demonstrating that the nuclease activity of FEN1 is critical in regulating ERα-chromatin interactions.
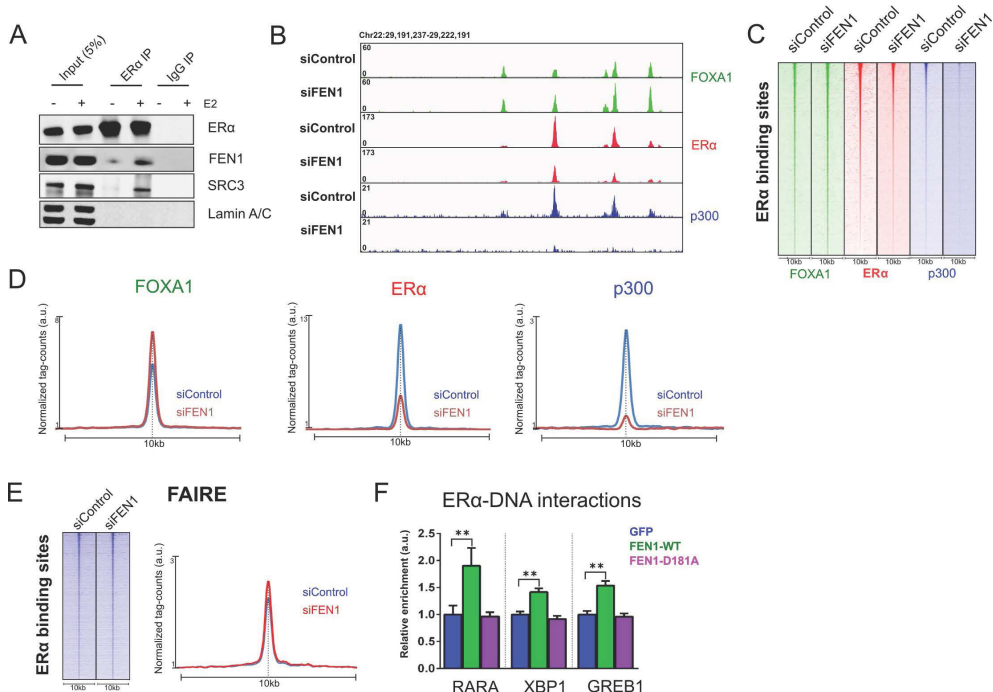
Figure 2. *FEN interacts with ERα and dictates ERα-chromatin interactions and complex formation.*

(A) Co-immunoprecipitation analyses demonstrate E2-induced ERα/FEN1 interactions. Protein levels were determined for ERα, FEN1, SRC3 and negative control Lamin A/C. Cells were treated with (+) or without (-) E2 before immunoprecipitation of ERα or IgG. Shown is an example of two biological replicates. (B) Genome browser snapshot at the XBP1 locus, illustrating FOXA1 (green), ERα (red) and p300 (blue) binding events for siFEN1 and control. Genomic coordinates and tag count are indicated. See also Sup Fig S2B,C. (C) Heatmap visualizing binding events of FOXA1 (green), ERα (red) and p300 (blue) at ERα binding sites after FEN1 knockdown. All binding events are vertically aligned and centered on the ERα peak, with a 10 kb window. Peaks were sorted on ERα intensity. See also Sup Fig S2B,C. (D) Normalized tag counts of FOXA1, ERα and p300 are plotted, showing average signal intensity within a 10kb window. (E) (Left) As in C but now binding events of Formaldehyde-Assisted Isolation of Regulatory Elements sequencing (FAIRE-seq) are visualized. Shown is an example of two biological replicates. (Right) As in D but now normalized tag counts of FAIRE are plotted. (F) ChIP-qPCR of ERα after overexpression of FEN1-WT (green), FEN1-D181A (purple) or control GFP (blue). ERα-bindings sites at enhancers proximal to XBP1, RARA and GREB1 were assessed. Signals are normalized over control genomics regions, after which siControl (blue) is set as 1. Shown is an example of three biological replicates. N=4 with mean ± SD. Henceforth asterisks: *=p-value<0.05, **=p-value<0.01 and ***=p-value<0.001 Students T-test. See also Sup Fig S2B,C.

FEN1 controls ERα-mediated transcription and cell proliferation

The above results demonstrate that FEN1 modulates ERα-chromatin interactions and complex formation. Next, we assessed whether FEN1 can regulate ERα-mediated transcription and cell proliferation. Knockdown of FEN1 reduced ERα-regulated gene activation of known target genes TFF1, XBP1 and RARA (**Figure 3A**), while FEN1 overexpression had the opposite effect (**Figure 3B**), in line with increased ERα-chromatin binding (**Figure 2**).

FEN1 knockdown in MCF-7 cells decreased ERα-mediated cell growth under DMSO, tamoxifen and E2 conditions (**Figure 3C**; siRNA deconvolution in Sup Fig S3A), while FEN1 overexpression increased cell proliferation under these conditions (**Figure 3D**). The observed decrease in cell proliferation after siFEN1 was validated in ERα-positive T47D cells (Sup Fig S3B). Neither manipulating FEN1 levels in fulvestrant (a selective estrogen receptor down-regulator) treated cells, nor FEN1 knockdown in ERα-nega-

tive MDA-MB-231 and CAL120 cells (**Figure 3E**), affected cell proliferation, implicating that the observed effects are mediated through ERα and not broadly related to the role of FEN1 in DNA replication (20). Cumulatively, we demonstrate that FEN1 regulates ERα-mediated transcription and cell proliferation, and that FEN1 is both required and sufficient to dictate ERα-driven cell proliferation in the presence of tamoxifen.

FEN1 is required for the induction and BER of ERα-initiated DNA damage

Given FEN1's key role in modulating ERα-activity, we hypothesized a FEN1 inhibitor used specifically in an ERα-positive setting could have great therapeutic potential. Since FEN1 inhibitors have been developed before on a small scale (22, 23) but were not effective in breast cancer cell lines on their own (24), we performed a small-molecule compound screen of over 460,000 compounds to identify novel inhibitors of FEN1's flap-cleaving activity. A previously reported non-radioactive FEN1 activity assay was used (25) in which a small DNA product containing fluorophore donor 6-TAMRA (6-Carboxytetramethylrhodamine) is cleaved and released by FEN1 from a DNA flap structure labeled with a fluorescent quencher (Black Hole Quencher 2), resulting in measurable fluorescence (**Figure 4A**). A quantitative high throughput robotics screen (26) was performed on 465,195 compounds (27), identifying 2,485 active FEN1 inhibitors (**Figure 4B** and Sup Fig S4A). As part of the NIH Molecular Libraries Program (https://commonfund.nih.gov/molecularlibraries), these compounds have been profiled for their effect in >150 biochemical and cell-based assays including DNA-repair and related screens (e.g. APE1, POLB, POLK, POLH, POLI, PCNA, DNA binding). Furthermore, cheminformatics filters have been applied to annotate compounds for their reactivity (28). The selectivity profiling data and filters for reactive functional groups were used to triage the 2,485 active FEN1 inhibitors, and a set of 22 inhibitors was selected for further biological validation.

After testing the 22 hits on MCF-7 cell proliferation, we continued with the three most potent hits for further validation (Sup Fig S4B). In line with the ERα-specific effect of FEN1 knockdown (**Figure 3**), we selected FENi#2 (MLS002701801) as most potent and promising hit, as this was the only compound to efficiently inhibit ERα-positive cells at 100 nM, but not ERα-negative MDA-MB-231 and CAL120 cells (**Figure 4B** and Sup Fig S4C) (Sup Table S2).

Since ERα-cofactor APOBEC3B can induce C-to-U modifications and

mRNA expression
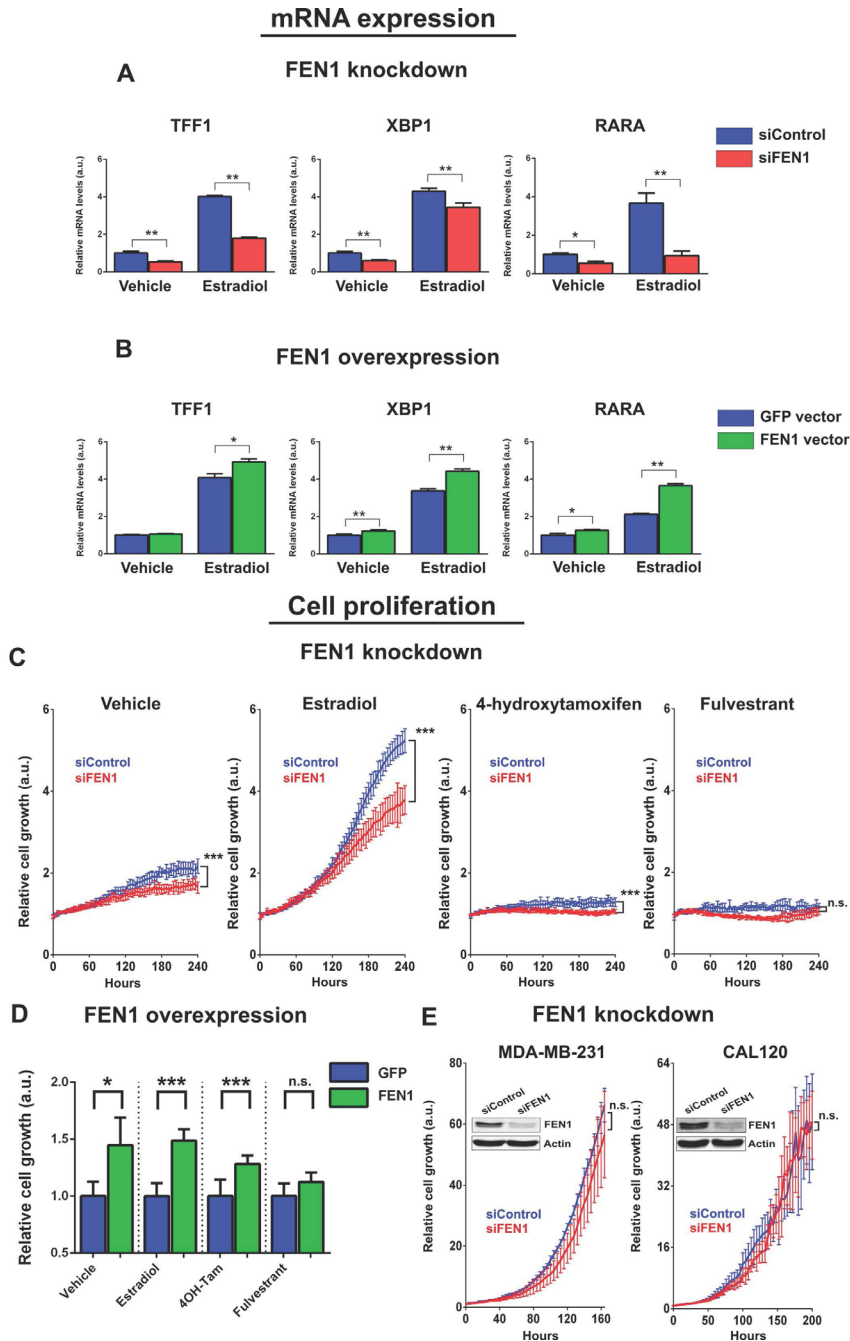
Figure 3. *FEN1 regulates ERα-mediated transcription and proliferation.*
(A) Relative mRNA levels of TFF1, XBP1 or RARA with or without E2. TBP and

UNG recruitment at ERα binding sites, which is essential for ERα-mediated transcriptional activity (6), we hypothesized that FEN1 might be functionally involved in a long-patch BER response following the formation of abasic sites, thereby regulating ERα-activity. In agreement with a BER response near ERα-binding sites, we observed BER-members XRCC1 and PARP1 (7), to bind these genomic regions (**Figure 4C** and Sup Fig S4D), with PARP1 being previously described as co-regulator of ERα (29). The targeted C-to-U events can ultimately give rise to γH2AX formation at ERα sites (6), as assessed by ChIP-seq (**Figure 4D**). This γH2AX-induction was validated by immunofluorescence, where E2 stimulation induced γH2AX foci (**Figure 4E,F**). FEN1 inhibition through 100 nM FENi#2 blocked this E2-induced γH2AX-formation (**Figure 4E,F** and Sup Fig S4E).

As γH2AX is indicative of DNA damage, and BER of C-to-U sites would induce single stranded DNA nicks, we assessed whether FEN1 inhibition would affect E2-induced DNA damage. For this, we used biotin-16-deoxyuridine triphosphate (dUTP) labeling of DNA-breaks with terminal deoxynucleotide transferase (TdT) (30) followed by biotin ChIP-qPCR to directly assess DNA nicks. Consistent with previous reports (6, 30), biotin incorporation was increased 15 minutes after E2 stimulation, returning to basal levels at 30 minutes (**Figure 4G**). This induction was not seen at a non-ERα-binding region or with E2 stimulation in the absence of biotin-labeled dUTP. FEN1
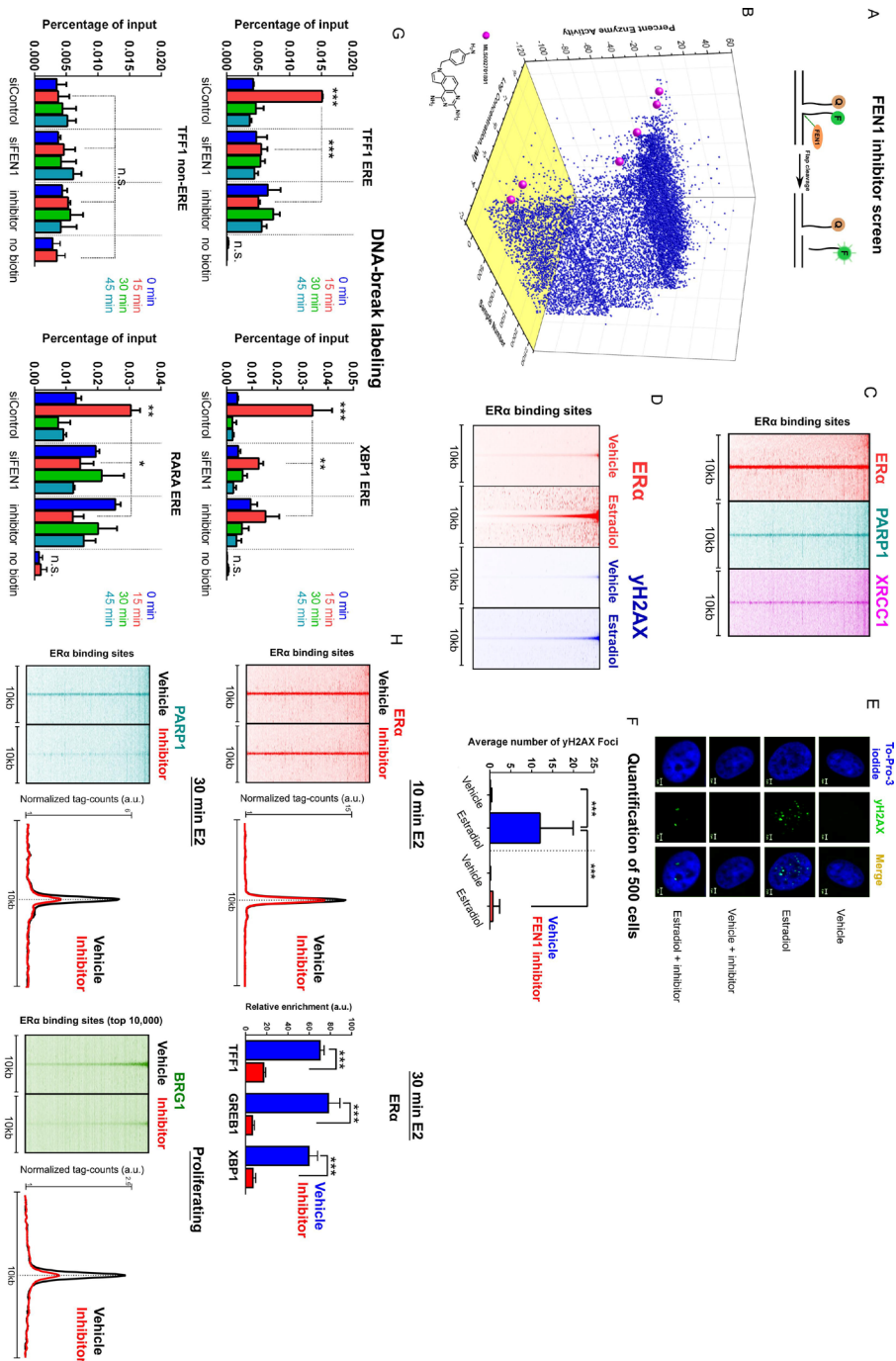
Figure 4. *FEN1 inhibitor screen and the role of FEN1 in ERα-induced γH2AX signaling and DNA damage.*

Composition of ERα's transcriptional complex – part 2

(A) Fluorescence based assay used to assess flap-cleaving by FEN1. A double-strand-ed DNA flap substrate containing two tags, a fluorophore-donor (6-TAMRA) and a fluorophore-quencher (BHQ2), is exposed to FEN1 protein in the presence or absence of small-molecule compounds. Upon flap-cleavage the DNA product con-taining the fluorophore is released, resulting in measurable fluorescence signal. (B) Concentration response profile of the 2,485 compounds found active as FEN1 in-hibitors, identifying MLS002701801 (FENi#2) (purple dot) as our top hit. For each compound the concentration (log) and the percentage of altered FEN1 enzyme ac-tivity is depicted. See also Sup Table S2 and Sup Fig S4A,B,C. (C) Heatmap visual-izing ranked binding events of ERα (red), PARP1 (dark cyan) and XRCC1 (purple) at ERα binding sites. Hormone-deprived cells where treated with E2 for 10 (ERα and XRCC1) or 30 minutes (PARP1). All binding events at ERα bound regions after 10 minutes of E2 were analyzed, vertically aligned and centered at the center of the peak, with a 10kb window. See also Sup Fig S4D. (D) As in C but now binding events of ERα (red) and γH2AX (blue) at ERα binding sites, under vehicle or E2 conditions are visualized. Peaks were sorted on ERα intensity. (E) Induction of γH2AX-foci by E2 stimulation as visualized through immunofluorescence. Hormone-deprived cells where treated with ethanol or E2 for 15 minutes, with or without FEN1 inhibitor. Shown is a representative cell stained for γH2AX (green). To-Pro-3-iodide was used to visualize the nucleus (blue). Scale bar indicates 2μm. (F) The average number of γH2AX-foci per cell as quantified in 500 cells. Shown is a representative exper-iment of two biological replicates. N=500 with mean ± SD. See also Sup Fig S4E. (G) DNA-break labeling assay. Cells were transfected with siControl or siFEN1 or pretreated with a FEN1 inhibitor. Hormone-deprived cells were treated for 0, 15, 30 and 45 minutes of E2. Three ERα-binding sites and one non-ERα-binding site were investigated. No biotin was included as negative control. Shown is a representa-tive experiment of two biological replicates. N=3 with mean ± SD. (H) (Upper left) Heatmap visualizing ranked binding events of ERα (red) at ERα sites. Hormone-de-prived cells where pretreated with a vehicle or FEN1 inhibitor and subsequently stimulated with E2 for 10 minutes. All binding events at ERα sites after 10 minutes of E2 were analyzed, vertically aligned and centered at the center of the peak, with a 10kb window. Normalized tag counts are plotted, showing average signal intensity. (Upper right) ChIP-qPCR analyses of ERα for enhancers proximal to TFF1, GREB1 and XBP1. Hormone-deprived cells where pretreated with a vehicle (blue) or FEN1 inhibitor (red) and stimulated with E2 for 30 minutes. Signal was normalized over control genomics regions. Shown is an example of three biological replicates. N=4 with mean ± SD. (Bottom left) As in Upper left but now PARP1 binding sites were analyzed for cells stimulated with E2 for 30 minutes. (Bottom right) As in Upper left

inhibition or siFEN1 blocked E2-mediated DNA damage induction (**Figure 4G**), suggesting FEN1 regulates ERα-activity through formation or processing of ERα-induced DNA damage. Reduced damage could not be explained by lower ERα-chromatin interactions at time points preceding DNA damage (10 minutes after E2 stimulation) (**Figure 4H** and Sup Fig S4F). However, after the point of damage induction (30 minutes of E2 stimulation), FEN1 inhibition did decrease ERα and PARP1 binding (**Figure 4H** and Sup Fig S4F), implicating the importance of BER-mediated DNA nicks in modulation of ERα-activity.

In line with the known role of γH2AX in promoting chromatin remodeling (31), FEN1 inhibition decreased both γH2AX formation and recruitment of BRG1; the catalytic subunit of the SWI/SNF chromatin remodeling complex (31) (**Figure 4H** and Sup Fig S4F), which chromatin interactions overlapped ERα-bindings sites.

FEN1 inhibition also enhanced E2-induced ERα-degradation (Sup Fig S4G), mediated by proteasomal activity (32). Pretreatment with proteasome inhibitor MG132 prevented FENi#2-induced reduction of ERα-chromatin interactions (Sup Fig S4G), suggesting that improper induction and processing of ERα-induced DNA damage through FEN1 blockade targets ERα for degradation. Since ERα-chromatin interactions are not affected by FEN1 inhibition until the point of damage induction (**Figure 4H** and Sup Fig S4F), this favors a model wherein FEN1 alters ERα's activity by regulating the stability of its chromatin binding after activation by E2.

Cumulatively, we identified FENi#2 as a potent and specific FEN1 inhibitor, and demonstrate that FEN1 regulates ERα-activity through functional formation of E2-induced DNA damage. FEN1 inhibition reduced BRG1 recruitment and ultimately stimulated proteasome-mediated degradation of ERα.

FEN1 inhibition perturbs ERα mediated changes in DNA methylation

Methylation status of ERα binding sites is tightly coupled with ERα activity (33), in which ERα activity was reported to induce TFF1 promoter demethylation (34), but whether this happens on a more genome-wide scale remains elusive. Since APOBEC3B-mediated C-to-U modifications at ERα-bound enhancers (6) appear to be repaired by the BER-pathway, and BER promotes DNA demethylation (35), we hypothesized that FEN1 is functionally involved

in genome-wide ERα DNA demethylation upon activation.

To investigate whether ERα activation triggers genome-wide DNA methylation changes through FEN1 action, we made use of Reduced Representation Bisulfite Sequencing (RRBS) (36) to map differentially methylated DNA regions after 45 minutes of E2 stimulation in the presence or absence of FEN1 inhibitor. RRBS allows for enrichment of genomic areas with a high CpG content, therefore including the majority of (potentially ERα-regulated) promoters.

Differential binding analyses identified 11,353 altered regions upon E2 stimulation, from which 418 high-confidence regions were selected by applying a stringent cutoff (minimum of ten methylation-informative bases and total methylation difference of at least ±20%). E2 stimulation triggered DNA methylation changes, ranging from ~82% of hyper to ~73% of hypomethylation, which was strongly reduced upon FEN1 inhibition (**Figure 5A,B quantified in C**). These regions were on average 203 bps, contained an average of 16 methylation-informative bases and were mainly located near gene promoters (**Figure 5D**). Of these 418 differentially methylated regions, ~53% was <20kb of an ERα site (**Figure 5D,E**). These ERα-associated regions contained 4570 methylation-informative bases, where altered methylation status upon E2 treatment ranged from ~48% of hyper to ~47% of hypomethylation (**Figure 5E**), which was fully abolished by FEN1 inhibition (**Figure 5F**). Cumulatively, we find that ERα activation induces changes in DNA methylation which are abrogated upon FEN1 inhibition.

FEN1 inhibition as novel drug option in tamoxifen resistant breast cancer

Since tamoxifen-resistant cell lines (37) and tumors (38) still require ERα function, an alternative mode of blocking ERα action through FEN1 inhibition would have strong clinical potential.

First, the optimal time point of ERα-chromatin interactions after E2 treatment was determined, with 30 minutes of E2 stimulation resulting in maximum ERα-chromatin interactions (**Figure 6A** and Sup Fig S5A), consistent with previous TFF1 promoter-based studies (39). Overnight pretreatment with 100 nM FEN1 inhibitor significantly inhibited E2-induced ERα-chromatin interactions and ERα-driven gene transcription (**Figure 6B**) in MCF-7 cells, analogous to siFEN1 (**Figure 2, 3**). In the absence of E2, ERα protein levels were unaffected by the FEN1 inhibitor (Sup Fig S5B), indicating decreased ERα-chromatin interactions and gene transcription were not due to

5
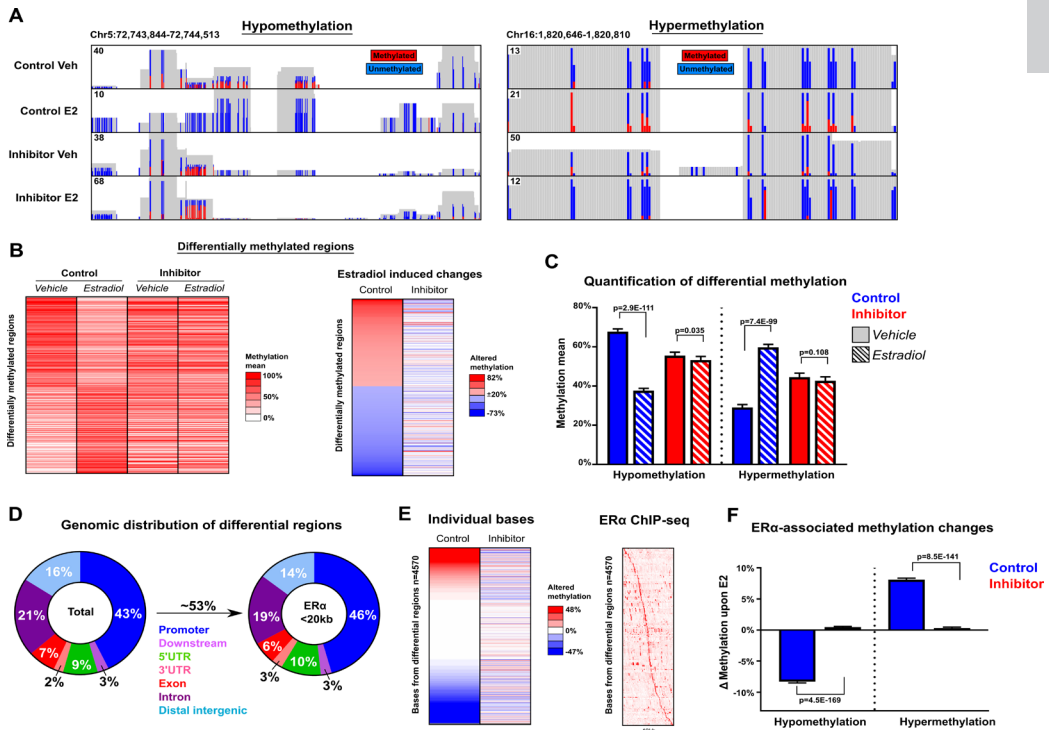
Figure 5. *FEN1 inhibition perturbs E2-stimulated differential DNA methylation. (A) Genome browser snapshot of RRBS at two loci, illustrating E2 induced hypo- (Left) and hypermethylation (Right). Colored bars indicate methylation-informative bases with corresponding methylated (red) and unmethylated (blue) reads. Genomic coordinates and tag count are indicated. Shown is one of two biological replicates. (B) (Left) Heatmap visualizing ranked differentially methylated regions upon E2 stimulation. The average methylation mean of two biological replicates is shown. (Right) As in Left but now percentage of altered methylation upon E2 stimulation is shown in the absence (control) or presence of FEN1 inhibitor (inhibitor). (C) Quantification of the average methylation mean at the differential regions upon E2 stimulation in a control or inhibitor setting. Differential regions are split into hypo and hypermethylation. (D) Genomic distribution of all differentially methylated regions (Left) and regions <20kb of an ERα site (Right). (E) (Left) As in B but now altered methylation of individual methylation-informative bases from ERα-associated regions are shown. Shown is one of two biological replicates. (Right) Heatmap visualizing binding events of ERα at methylation-informative bases. All binding events are vertically aligned and centered on the individual bases, with a 20 kb window. Peaks were sorted on distance of ERα to individual bases. (F) Quantification of the average*

change in methylation of individual methylation-informative bases from E. Changes are split into hypo and hypermethylation.

reduced initial amounts of ERα protein.

Colony formation assays were performed for a panel of human breast cancer cell lines; (a) MCF-7 and T47D (ERα+), (b) MCF7-T and TAMR (tamoxifen resistant MCF-7 derivatives (40, 41)) and (c) BT-20 and CAL-120 (ERα-). Cells were treated with increasing concentrations of FEN1 inhibitor in the presence or absence of tamoxifen (**Figure 6C,D**), confirming tamoxifen responsiveness of the sensitive cell lines (**Figure 6C,D**). Proliferation of MCF-7 and T47D cells was inhibited in a dose-dependent manner with IC50 values of 69 and 78 nM of the inhibitor, respectively (Sup table S3). In contrast, sensitivity to FEN1 inhibition for ERα-negative cell lines BT-20 and CAL120 was limited, with an IC50 of 314 nM in BT20, while not reaching 50% inhibition in CAL120 cells. Interestingly, tamoxifen resistant MCF-7 derivatives showed enhanced sensitivity to FEN1 inhibition in relation to the parental cells (IC50= 29 nM for both tamoxifen resistant cell lines).

To validate the efficacy of FEN1 inhibition in ERα-positive breast cancer, we used ex vivo primary ERα-positive tumor cultures (i.e. explants) (42, 43) in the presence or absence of compound FENi#2. Tumors were cut into small pieces and randomized between vehicle, FEN1 inhibitor or tamoxifen treatments and cultured for 3-6 days on gelatin sponges, allowing sustained tissue architecture and viability (43). Explants were stained for cell proliferation marker Ki67 and scored by a pathologist. Upon FEN1 inhibition, all four tumor explants demonstrated reduced proliferation (Ki67) (**Figure 6E,F**). For 3 of 4 explants, sufficient material was available for a tamoxifen group, demonstrating comparable reductions in Ki67 (Sup Fig S5C).

Taken together, we show that pharmacological inhibition of FEN1 efficiently blocks ERα-driven tumor cell proliferation, with enhanced potency in tamoxifen-resistant cells. As FEN1 perturbation inhibits primary tumor tissue growth, we demonstrate therapeutic potential of our FEN1 inhibitor in the treatment of ERα-positive cancer.

Discussion

Several multi-gene prognostic classifiers have been reported that stratify breast cancer patients based on outcome (44). Most of these classifiers lack biological insights regarding the drivers of tumor progression. Here, we refined a 111-gene classifier to a single gene predictor of disease outcome, re-
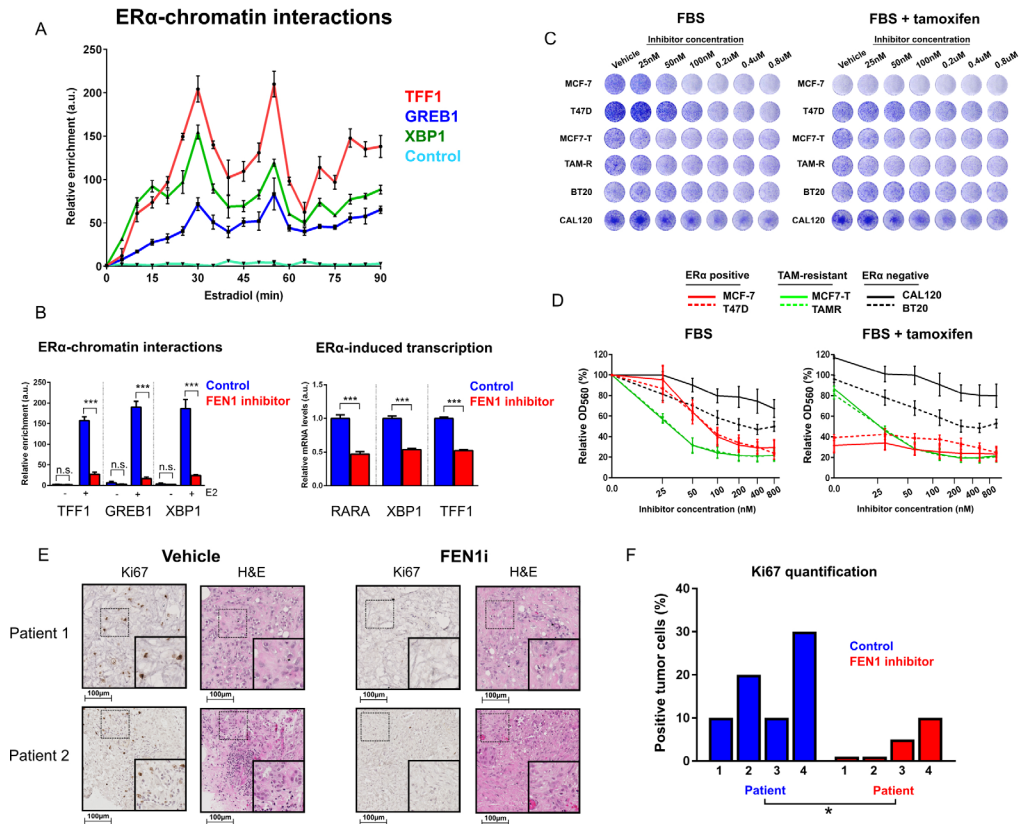
Figure 6. *Small molecule-mediated inhibition of FEN1 blocks ERα action and prevents cell proliferation.*

(A) ERα ChIP-qPCR analyses of hormone-deprived cells treated for 90 minutes with E2 using 5 minute intervals. Three positive regions for ERα-binding were assessed (TFF1, GREB1 and XBP1) and one known negative region (Neg control). Data are normalized over t=0. N=4 with mean ± SD. See also Sup Fig S5A. (B) (left) As in A but now hormone-deprived cells were pretreated with vehicle or FEN1 inhibitor prior to 30 minutes E2 treatment. Signals are normalized over control genomics regions. Shown is a representative experiment of two biological replicates. N=4 with mean ± SD. (right) Relative mRNA levels of RARA, XBP1 and TFF1 with or without FEN1 inhibitor. TBP and UBC were used as control. Shown is a representative experiment of two biological replicates. N=4 with mean ± SD. (C) Colony formation analyses for breast cancer cell lines; MCF-7 and T47D (ERα+), MCF7-T and TAMR (tamoxifen resistant MCF-7 derivatives) and BT-20 and CAL-120 (ERα-). Cells were treated with increasing concentrations of FEN1 inhibitor in the presence or absence

of tamoxifen. Representative experiment is shown of at least 4 biological replicates. (D) Relative quantified crystal violet staining (OD560) of colony formation assay depicted in (C). Shown are mean values of at least 4 biological experiments where all OD560 data were normalized to vehicle treated FBS. Error bars indicate SEM. See also Sup table S3. (E) Ex vivo primary human ERα-positive tumor cultures in the presence or absence of 200 nM FEN1 inhibitor. Explants were fixed and stained for Ki67 and H&E. Shown are representative tumor regions for two patients with digital zoom in the lower right corner. (F) Indication of the percentage of Ki67 positive tumor cells in tumor explants cultured in the presence or absence of FEN1 inhibitor. Paired Students T-test was used to assess the difference between treatment groups. See also Sup Fig S5C.

vealing a drug target with clinical potential in the treatment of tamoxifen resistant breast tumors. We identified FEN1 as a predictive marker for tamoxifen resistance in clinical specimens, with potential for outcome-prediction exclusive in ERα-positive breast cancers.

FEN1 overexpression is found in multiple tumor types, including breast cancer (9), in which it was reported to have prognostic potential (11). Our novel observation that FEN1 exclusively has prognostic potential in ERα-positive cases is in line with our cell proliferation analyses, where perturbation of FEN1 was only effective in ERα-positive cell lines, while yielding no detectable effects in ERα-negative cells. FEN1/ERα interactions were hormone-regulated and coincided with γH2AX signaling at the same sites. At these genomic regions, the transcriptional activity of ERα appeared closely linked with the DNA damage response; a process in which FEN1's nuclease activity is required. The seemingly contradictory role of DNA damage repair protein FEN1 in the induction of DNA damage might be explained by it being part of a fail-safe mechanism, only allowing the induction of relevant damage intermediates when FEN1 is part of the ERα complex. A similar observation has been reported for DNA-dependent protein kinase (DNA-PK), where DNA-PK inhibition by NU7441 also resulted in the absence of γH2AX formation upon ERα-activation (6). Consequently, this favors a model wherein FEN1 blockade reduces ERα-responsive gene expression and ERα-driven cell proliferation by deregulating ERα-chromatin interactions after activation by E2, most likely due to improper induction and processing of DNA damage.

Accumulating evidence repositions DNA repair factors as coactivators of transcription, facilitating chromatin remodeling (5). This chromatin remodeling at ERα-binding regions can be initiated by BRG1 (45), the recruit-

ment of which is promoted by γH2AX (31). Failure to induce DNA damage at ERα regions diminished BRG1 recruitment (6), implicating ERα-induced damage as facilitator of chromatin remodeling. FEN1 is critically involved in ERα-mediated γH2AX-formation, dictating BRG1 recruitment (**Figure 4H**) to regulate transcription. Additionally, chromatin-bound ERα can promote 8-oxoguanine modifications and thereby 8-oxoguanine-DNA glycosylase 1 recruitment and BER, triggering chromatin conformational changes essential for ERα-induced transcription (46). Together with APOBEC3B-mediated C-to-U modification at ERα-bound regions (6) and the fact that BER can promote DNA demethylation (35), we now show that BER upon ERα-stimulation induces active promoter demethylation; a process in which FEN1 is essential (**Figure 5**). Besides these regions of hypomethylation, we also find E2 stimulation yields regions of hypermethylation. As DNA methyltransferases have been reported to co-occupy ERα-interacting regions near the TFF1 and FOXA1 promoter (34, 47), the balance between methylating (e.g. DNMT's) and demethylating (e.g. FEN1's role in BER) proteins at ERα-binding sites may drive the directionality of DNA methylation alterations at these sites. Although not short-term E2 driven, differential hypermethylation between hormone-sensitive and endocrine resistant MCF-7 derivatives has been observed and proposed as possible mechanism for endocrine resistance and did result in differential ERα-binding capacities (48), further illustrating DNA methylation changes can regulate ERα-activity.

The role of FEN1 in ERα-induced transcription might be further explained by the fact that DNA nicks could resolve topological strain generated by transcription-induced DNA supercoiling, which, if unresolved, is able to affect transcription (49). Additionally, the known role of DNA damage repair proteins in the regulation of RNA-DNA hybrid structures (R-loops) (50) and their generation during ERα-induced transcription (51), is suggestive of a role for FEN1 in regulating ERα-induced transcriptional activity, DNA structures and genome instability.

Small molecule–mediated inhibition of FEN1 functionally abrogated ERα-activity and ultimately human tumor explant proliferation. With an inhibitor effective in the nM-range, we illustrate that FEN1 inhibition might yield a promising novel therapy for ERα-positive breast cancer. While FEN1 inhibition has been described before, it has mainly been linked to chemo-sensitization (52, 53) or as a part of synthetic lethal interactions (22, 54), but not as an effective therapy strategy on its own (24). Here we report the first effective single-agent application of FEN1 inhibition by specifically targeting

ERα-positive breast cancer. Most importantly, tamoxifen resistant cell lines showed an increased sensitivity for FEN1 blockade; a feature that could possibly be exploited in the treatment of advanced breast cancer, thereby providing a novel targeted therapy in case of tamoxifen resistance.

Materials and Methods

Colony formation
For the colony formation assay 2500 cells/well were plated in 48-well format in appropriate culture medium. After attachment of cells to the bottom of the well, the FEN1 inhibitor was administered and when appropriate 100 nM 4OH-tamoxifen was added. After 7 days cells were fixed with 100% of methanol and cells were stained with 0.2% crystal violet. For quantification the crystal violet was dissolved in 10% acetic acid and the optical density was measured at 560 nm.

Cell culture
MCF-7, T47D, MDA-MB-231, CAL120 cells were cultured in DMEM medium in the presence of 10% FBS and antibiotics (penicillin, streptavidin). TAMR and MCF7-T cells were cultured in phenol-red-free DMEM containing 5% charcoal-treated serum (CTS; HyClone), 2 mmol/L of L-glutamine, antibiotics and 100 nM 4OH-tamoxifen. BT20 cells were cultured in MEM in the presence of 10% FBS and antibiotics. For hormone deficient conditions, cells were deprived of hormone for 72 hours, by culturing in phenol-red-free DMEM containing 5% charcoal-treated serum, antibiotics and supplemented with L-glutamine, prior to hormone treatment. Hormone treatments consisted of solvent Dimethylsulfoxide (DMSO), 10 nM of estradiol, 100 nM of 4OH-tamoxifen or 100 nM of fulvestrant. All cell lines were tested for mycoplasma and were genotyped for authenticity.

siRNA and plasmid
For knockdown experiments 25 nM of single or pooled duplexes of siRNA against FEN1 (Dharmacon MU-010344-01) or a non-targeting control pool (Dharmacon, D-001206-14-20) were transfected with Dharmafect according to manufactures protocol. The expression plasmids pShuttle-FEN1hWT (wild type FEN1) and pShuttle-FEN1DA (D181A point mutant) were kindly provided by Sheila Stewart (Addgene plasmid #35027 and #35028) (21) and cells were transfected with Polyethylenimine (PEI). When appropriate cells

were hormone-deprived for 24 hours prior to siRNA transfection or overexpression and further hormone-deprived for 48-72 hours.

Chromatin Immunoprecipitation (ChIP) and Formaldehyde-assisted isolation of regulatory elements (FAIRE)
ChIP experiments were performed as described previously (4) with the following modifications. Three to ten micrograms of antibody was prebound overnight to protein A Dynabeads magnetic beads (Invitrogen). The magnetic bead-chromatin complexes were harvested and washed 10 times with RIPA buffer (50 mM HEPES [pH 7.6], 1 mM EDTA, 0.7% Na deoxycholate, 1% NP-40, 0.5 M LiCl). Antibodies used were anti-ERα (sc-543), anti-p300 (sc-585), anti-FOXA1 (sc-6554), anti-BRG1 (sc-10768), anti-PARP1 (sc-1561) from Santa Cruz Biotechnologies and anti-RNA polymerase II (ab5408), anti-XRCC1 (ab9147) from Abcam. In figure 4, publically available ChIP-seq data was used; ERα (37) and γH2AX (GSE57426) (6). Formaldehyde-assisted isolation of regulatory elements (FAIRE) was performed as described previously (55).

Solexa ChIP and FAIRE sequencing and enrichment analysis
ChIP DNA was amplified as described (56). Sequences were generated by the Illumina Hiseq 2000 genome analyser (using 51 or 65 bp reads), and aligned to the Human Reference Genome (assembly hg19, February 2009). Peak calling over input was performed using MACS peak caller (57) version 1.3.7.1 and DFilter (58), only considering peaks shared by both peak callers. For Figure 2B and Figure 4C all ERα binding regions after 45 minutes of estradiol as published before (37) were used. Details on the number of reads obtained and the percentage of reads aligned can be found below. ChIP-seq and FAIRE-seq data can be found on GEO: GSE95302

Sequencing snapshots and Heatmaps
ChIP-seq and RRBS data snapshots were generated using the Integrative Genome Viewer IGV 2.2 (www.broadinstitute.org/igv/). Heatmaps were generated using Seqminer, with default settings (59).

Characteristics of ERα and γH2AX ChIP-Seq data
ChIP   Published
ERα vehicle   E-MTAB-223 (Hurtado et al., 2011)
ERα estradiol E-MTAB-223 (Hurtado et al., 2011)

γH2AX vehicle   GSE57426 (Periyasamy et al., 2015)
γH2AX estradiol   GSE57426 (Periyasamy et al., 2015)

Characteristics of ChIP-Seq and FAIRE-seq samples

ChIP	Total tag count	# tags after filtering	% of tags after filtering
ERα siControl	7781308	7438883	95.6
ERα siFEN1	14756460	13972667	94.7
P300 siControl	7175975	6987295	97.4
P300 siFEN1	12257252	11672856	95.2
FOXA1 siControl	19374850	15196594	78.4
FOXA1 siFEN1	14684955	13312265	90.7
FAIRE siControl	20840022	18945798	90.9
FAIRE siFEN1	19089826	17367171	90.9
ERα 10 min E2 vehicle	27769120	26639560	95.9
ERα 10 min E2 FEN1 inhibitor	26580604	25540190	96.0
XRCC1 10 min E2	25039992	23979349	95.7
PARP1 30 min E2 vehicle	24826707	22424144	90.3
PARP1 30 min E2 FEN1 inhibitor	25045100	23528730	93.9
BRG1 control	21291086	20282090	95.3
BRG1 fen1 inhibitor	21350779	19952407	93.5

mRNA expression and ChIP-qPCR

For mRNA expression; after hormone deprivation cells were treated for 6 hours with DMSO or 10 nM estradiol, after which total RNA was collected by phenol-chloroform extraction. cDNA was made with a Superscript III RT kit (Invitrogen) using manufacturer's protocols after which qPCR was performed. TBP and UBC were used as housekeeping genes. For ChIP: DNA-protein interactions were harvested with ChIP and obtained DNA regions were used after immunoprecipitation. qPCR was performed with SYBR Green (Applied Biosystems) on a Roche LightCycler® 480 Real-Time PCR System using standard protocols. A negative region near the cyclin D1 (CCND1) promoter was used as a negative control. When appropriate an additional negative control primer (Neg 2) was taken along. Primers are described below.

Primers cDNA

Gene	Sequence	
Homo sapiens trefoil factor 1 **(TFF1)**	ATCGACGTCCCTCCAGAAGA	(FWD)
	TGGGACTAATCACCGTGCTG (REV)	
X-box binding protein 1 **(XBP1)**	GGGAAGGGCATTTGAAGAAC	(FWD)
	ATGGATTCTGGCGGTATTGA (REV)	
retinoic acid receptor alpha **(RARA)**	GACCAGATCACCCTCCTCAA	(FWD)
	GTCCGAGAAGGTCATGGTGT (REV)	
TATA box binding protein **(TBP)**	GTTCTGGGAAAATGGTGTGC	(FWD)
	GCTGGAAAACCCAACTTCTG (REV)	
ubiquitin C **(UBC)**	ATTTGGGTCGCAGTTCTTG	(FWD)
	TGCCTTGACATTCTCGATGGT (REV)	

Primers ChIP

Gene	Sequence	
cyclin D1 **(CCND1) (Neg 1)**	TGCCACACACCAGTGACTTT	(FWD),
	ACAGCCAGAAGCTCCAAAAA (REV)	
Homo sapiens trefoil factor 1 **(TFF1)**	TGGTCAAGCTACATGGAAGG	(FWD)
	CCATGGGAAAGAGGGACTTT (REV)	
growth regulation by estrogen in breast cancer 1 **(GREB1)**	CACTTTGAGCAAAAGCCACA	(FWD)
	GCTGCGGCAATCAGAAGTAT (REV)	
X-box binding protein 1 **(XBP1)**	GGTCACAGGCTGCCAAGTAT	(FWD)
	AGCCCCAGTTATGGCGTAAT (REV)	
retinoic acid receptor alpha **(RARA)**	CTCAGGACAGGGCAAGAGTG	(FWD)
	AAGCCACTCCAAGGTAGGTG (REV)	
Negative control 2 **(Neg 2)**	TGGCCCTTGATACTGGAGTC	(FWD)
	GACATCCAAGGCAAGATGGT (REV)	
PDZ Domain Containing 1 **(PDZK1)**	AGGCCCAGCAAAGACAAATG (FWD)	
	AAACCACAGGCTGAGGACTG (REV)	

Co-Immunoprecipitation

Immunoprecipitations were performed as described previously (60). MCF-7 cells were lysed in RIPA whole cell lysate buffer containing protease inhibitors. Lysates were pre-cleared by incubating with pre-clearing beads (Immunocruz, Santacruz) at 4oC for 2 hours. 5µg of ERα antibody (ER HC20) was incubated with agarose beads (Immunocruz, Santacruz) for 2 hours at 4oC. Agarose beads conjugated with ERα antibody were washed three times with ice-cold PBS and re-suspended in PBS and transferred to the pre-cleared lysates for overnight incubation. Following incubation, beads were washed six times in ice-cold PBS and re-suspended in 2X sample buffer (Sigma, 0.125 M Tris-HCL at pH 6.8, 4% SDS, 20% Glycerol, 10% β-mercaptoethanol and 0.004% bromophenol blue) and heated at 95oC for 10 minutes, and then analyzed by western blot. Antibodies used for IP; anti-ERα (sc-543) from Santacruz, and for WB; anti-ERα (6F11) from Leica Biosystems, anti-AIB1 (BD

bioscience, cat no; 611105) and anti-Lamin A/C (sc-7292) and anti-FEN1 (sc-28355) from Santacruz.

Western blot

Cells were lysed with 2x laemmli buffer (containing 1:500 Na3VO4, 1:10 NaF, 1:13 β-Glutamate, 1:100 Protease inhibitors, 1:100 Phosphatase inhibitors). Western blot samples contained 10% DTT and 4% bromophenol blue and were incubated for 5 minutes at 95 °C. Samples were run on 10% SDS-Page gel and transferred to nitrocellulose membranes. Used primary antibodies: anti-p300 (sc-585), anti-FOXA1 (sc-6554), anti-ERα (sc-543) and anti-FEN1 (sc-13051) from Santa Cruz Biotechnologies, anti-RNA polymerase II (ab5408) from Abcam and 1:10.000 actin from Millipore (MAB1501R). Used secondary antibodies: 1:10.000 Licor Odyssey IRDue. Membranes were scanned and analysed with Odyssey V3.0.

Patient cohorts

The discovery-cohort has previously been used and described (17). In short; ERα-positive patients that received tamoxifen in the adjuvant setting, but did not receive adjuvant chemotherapy, were selected from The Netherlands Cancer Institute–Antoni van Leeuwenhoek Hospital (NKI–AVL). Distant metastases were regarded as failure to treatment and used as events. RNA was hybridized on 44 K oligomicroarrays, as described previously (61). The median IHC-score and mRNA expression value was chosen as the cutoff-point.

The validation-cohort has been described before (IKA trial, 1982-1994) (18). In short: ERα-positive patients (no adjuvant chemotherapy) were randomized between 1 year tamoxifen versus no adjuvant therapy. After 1 year a second randomization was performed; 2 additional years of tamoxifen or to stop further treatment. Further patient characteristics and clinical outcome of the original study group (1662 patients) have been described before (62). For 739 patients sufficient tumor material for IHC was available (62). The median IHC-score value was chosen as the cutoff-point.

Immunohistochemistry

Tissue microarrays (TMAs) were constructed using formalin-fixed paraffin embedded (FFPE) tumor blocks. A total of three (0.6 mm) cores per tumor were embedded in the TMA. TMAs were stained for FEN1 and hematoxylin-eosin (HE) with the ULTRA BenchMark IHC/ISH Staining Module of the NKI. Antibody used was anti-FEN1 (sc-13051) from Santa Cruz Biotechnol-

ogies. The percentage of FEN1-positive invasive tumor cells were scored. One TMA was scored independently in a blinded manner by a second observer to calculate inter-observer variability (κ=0.708). The inter-observer variability was analyzed using the (weighted) Cohen's kappa coefficient.

For ex-vivo tumor cultures, tissue sections were incubated with a Ki67 primary antibody (MIB1 1:400; DAKO M7240 Glostrup, Denmark) at 4C overnight followed by detection using a biotinylated anti-mouse secondary antibody at 1:400 dilution (DAKO E0433, Glostrup, Denmark) for 30 min followed by incubation with horseradish peroxidase-conjugated streptavidin (DAKO P0397, Glostrup, Denmark). Visualization of immunostaining was performed using 3,3-diaminobenzidine (Sigma D9015).

Statistics
PAM (12) was performed to determine the minimum number of genes required to attain accurate separation of good and poor survival. Here, good and poor survival was defined based on whether or not a distant metastasis occurred within five years. The number of genes was selected such that the area under the ROC curve (AUC) was optimized in a 10-fold cross validation. Subsequently, Lasso-penalized logistic regression (13) was used to obtain a robust selection of the best performing genes across two cohorts (14, 15). To this end, 1,000 cross-validation analyses were performed for each cohort to select gene subsets optimizing the AUC. Genes were then ranked according to how many times they were part of the optimal gene set in either of the two cohorts. Finally, the previously determined optimal number of genes were selected starting from the highest ranked gene.

Pearson's correlation coefficient was used to assess the correlation between relative FEN1 mRNA levels and FEN1 IHC scores. Survival curves were constructed using the Kaplan-Meier method and compared using log-rank test. Unadjusted and adjusted Cox proportional hazard regression analyses were performed; for the discovery-cohort the covariates age (<60 versus ≥60), diameter of the tumor (≤20 mm versus 20-50 mm versus >50 mm), tumor grade (grade 1 versus grade 2 versus grade 3) and the number of affected lymph nodes (Negative versus 1-3 versus ≥4); and for the validation-cohort the covariates age (< 65 versus ≥ 65), grade (grade 1-2 versus grade 3), tumor stage (T1-T2 versus T3-4), HER2 status (negative versus positive), PgR status (negative versus positive). In the validation-cohort all analyses were stratified for nodal status (negative versus positive) because lymph node positive patients, after 1989, skipped the first randomization and all received 1

year of tamoxifen. A p-value <0.05 was considered as a significant result and FEN1 levels were used a binary factor to assess the interaction with adjuvant treatment. A two-tailed Student's t-test was performed when appropriate.

Biotin labeling of DNA strand breaks
Biotin labelling of DNA strand breaks was performed as described (6, 30). MCF-7 cells were hormone deprived for 3 days before the addition of 10 nM estradiol (0, 15, 30 or 45 minutes treatment). Additionally cells were transfected with siRNA against FEN1 or pretreated with 100 nM of FEN1 inhibitor as appropriate. Real-Time PCR System using standard protocols. Primers are described below.

Gene	Sequence
Homo sapiens trefoil factor 1 **(TFF1)**	CCCGTGAGCCACTGTTGT (FWD) ATGGGAGTCTCCTCCAACCT (REV)
Non ERE control near TFF1	TTAAGTGATCCGCCTGCTTT (FWD) ATGGGAGTCTCCTCCAACCT (REV)
X-box binding protein 1 **(XBP1)**	GGTCACAGGCTGCCAAGTAT (FWD) AGCCCCAGTTATGGCGTAAT (REV)
retinoic acid receptor alpha **(RARA)**	CTCAGGACAGGGCAAGAGTG (FWD) AAGCCACTCCAAGGTAGGTG (REV)

Immunofluorescence
Immunofluorescence analysis was performed as described previously (6). Briefly, hormone-deprived MCF-7 cells were cultured on glass coverslips before the addition of 10 nM E2. Additionally cells were pretreated with 100 nM of FEN1 inhibitor as appropriate. Cells were fixed with 4% paraformaldehyde for 10 minutes and permeabilized with 0.2% Triton X-100. Used primary antibody was γH2AX (05-636, Millipore) and for secondary Alexa fluor 488 (Invitrogen) was used. ToPro (Invitrogen) nuclear dye was used to visualize nuclei. Images were acquired using a Carl Zeiss confocal microscope using LSM 510 image browser. Images were analyzed using Fuji Image J (NIH, USA) and Cell Profiler (Broad Institute, USA) to quantify number of foci per cell.

FEN1 inhibitor Screen
The previously reported non-radioactive FEN1 activity assay (25) was combined with a quantitative high throughput screen (qHTS) (26) and implemented on a fully integrated robotic system (63), utilizing a large scale chemical library arrayed in qHTS-formatted 1536-well based plates (27). A total of 465,195 compounds were tested. Automated large-scale curve fitting and

classification of curve types were determined (26). Using this classification, 3,543 compounds were considered inconclusive or weak inhibitors due to either lower quality curves or moderate inhibition. Another 1,123 compounds demonstrated a dose dependent increase of fluorescent signal, but were regarded as likely inactive due to suspected auto-fluorescence, which was observed in the initial background read. A total of 2,485 compounds were categorized as active FEN1 inhibitors and as part of the NIH Molecular Libraries Program (https://commonfund.nih.gov/molecularlibraries) profiled for their effect in over 150 biochemical and cell-based assays. Furthermore, cheminformatics filters were applied to the chemical library to annotate compounds for their reactivity (28). See also PubChem AID: 488816, 588795 and 720498.

Reduced Representation Bisulfite Sequencing and analyses
The methylation landscape MCF-7 cells was determined using Reduced Representation Bisulfite Sequencing (RRBS). Bisulfite treated DNA was prepared using the Premium RRBS Kit from Diagenode (C02030032). Sequences were generated with an Illumina HiSeq 2500 (using 65 bp reads) and aligned to a bisulfite-converted Human Reference Genome Hg19 with Bismark v0.14.6 (64), using bowtie 2-2.2.5 (65) and samtools-1.3 (66). The Bismark methylation extractor was run to obtain methylation scores per cytosine. Methylation scores were processed using the bsseq package to determine differentially methylated regions between E2 and control. Regions containing <10 methylation sites or a mean difference <0.2 were omitted from further analyses. Differentially methylated regions in the near vicinity of ERα chromatin interactions (<20kb) were analysed as ERα-associated regions. The genomic distribution of RRBS regions were analysed using the cis-regulatory element annotation system (CEAS) (67). RRBS data can be found on GEO: GSE95302. Characteristics of paired RRBS samples.

Sample	Total tag count	# tags after filtering	% of tags after filtering
Control vehicle repl1	22988934	19945060	86,8
Control estradiol repl1	18942001	16422184	86,7
Inhibitor vehicle repl1	22757385	19751457	86,8
Inhibitor estradiol repl1	38067207	32952601	86,6
Control vehicle repl2	30460112	26387978	86,6
Inhibitor vehicle repl2	19841342	17211823	86,7
Inhibitor estradiol repl2	31047474	26898577	86,6

Primary ex-vivo tumor cultures

Breast tumor samples and relevant clinical data were obtained from women undergoing surgery at the Burnside Private Hospital, Adelaide, South Australia, with informed, written consent. This study was approved by the University of Adelaide Human Research Ethics Committee (approval numbers: H-065-2005; H-169-2011). Following surgery, excised tissue samples were cultured ex vivo as described previously previously (42, 43). Briefly, tumor pieces were cultured on gelatin sponges in full medium containing a vehicle, FEN1 inhibitor (200 nM) or, when enough material was present, tamoxifen (2 uM). After 3 to 6 days, tissue was fixed in 4% formalin in phosphate-buffered saline (PBS) at 4 °C overnight and subsequently processed into paraffin blocks. Slices (2 μm) were stained with haematoxylin and eosin or Ki67 and examined by a pathologist to confirm the presence/proportion of tumor cells. Tumor slides were scored by a pathologist for the percentage of Ki67 positive tumor cells.

Author contributions

Conceptualization, K.D.F and W.Z.; Methodology, K.D.F, M.P., S.A., D.D., A.J., D.M.WIII., A.S., T.E.H., W.D.T. and W.Z.; Validation, A.J. and J.W.; Formal Analysis, K.D.F., A.J. and S.C.; Inhibitor Screening and Analysis, D.D., A.J., A.V.Z., D.M.WIII.; Investigation, K.D.F, M.P., H.P., A.J., T.E.H. and M.O.; Resources, A.S. and S.C.L.; Writing Final Draft, K.D.F. and W.Z., with help of all authors; Visualization, K.D.F. and W.Z.; Supervision, S.A., A.S., L.F.A.W., W.D.T. and W.Z.; Funding Acquisition, W.D.T. , D.M.WIII., A.S., S.A. and W.Z.

References

1.   *Glass CK, Rose DW, Rosenfeld MG. Nuclear receptor coactivators. Curr Opin Cell Biol. 1997;9(2):222-32.*

2.   *Jordan VC, Murphy CS. Endocrine pharmacology of antiestrogens as antitumor agents. Endocrine reviews. 1990;11(4):578-610.*

3.   *Shou J, Massarweh S, Osborne CK, Wakeling AE, Ali S, Weiss H, et al. Mechanisms of tamoxifen resistance: increased estrogen receptor-HER2/neu crosstalk in ER/HER2-positive breast cancer. J Natl Cancer Inst. 2004;96(12):926-35.*

4.   *Zwart W, Theodorou V, Kok M, Canisius S, Linn S, Carroll JS. Oestrogen receptor-co-factor-chromatin specificity in the transcriptional regulation of breast cancer. EMBO J. 2011;30(23):4764-76.*

5.   *Fong YW, Cattoglio C, Tjian R. The intertwined roles of transcription and repair proteins. Molecular cell. 2013;52(3):291-302.*

6.   *Periyasamy M, Patel H, Lai CF, Nguyen VT, Nevedomskaya E, Harrod A, et al. APOBEC3B-Mediated Cytidine Deamination Is Required for Estrogen Receptor Action in Breast Cancer. Cell Rep. 2015;13(1):108-21.*

7.   *Krokan HE, Bjoras M. Base excision repair. Cold Spring Harbor perspectives in biology. 2013;5(4):a012583.*

8.   *Zheng L, Shen B. Okazaki fragment maturation: nucleases take centre stage. Journal of molecular cell biology. 2011;3(1):23-30.*

9.   *Singh P, Yang M, Dai H, Yu D, Huang Q, Tan W, et al. Overexpression and hypomethylation of flap endonuclease 1 gene in breast and other cancers. Molecular cancer research : MCR. 2008;6(11):1710-7.*

10.   *Schultz-Norton JR, Walt KA, Ziegler YS, McLeod IX, Yates JR, Raetzman LT, et al. The deoxyribonucleic acid repair protein flap endonuclease-1 modulates estrogen-responsive gene expression. Molecular endocrinology. 2007;21(7):1569-80.*

11.   *Abdel-Fatah TM, Russell R, Albarakati N, Maloney DJ, Dorjsuren D, Rueda OM, et al. Genomic and protein expression analysis reveals flap endonuclease 1 (FEN1) as a key biomarker in breast and ovarian cancer. Mol Oncol. 2014.*

12.   *Tibshirani R, Hastie T, Narasimhan B, Chu G. Diagnosis of multiple cancer types by shrunken centroids of gene expression. Proc Natl Acad Sci U S A. 2002;99(10):6567-72.*

13.   *Friedman J, Hastie T, Tibshirani R. Regularization Paths for Generalized Linear Models via Coordinate Descent. Journal of statistical software. 2010;33(1):1-22.*

14.   *Loi S, Haibe-Kains B, Desmedt C, Lallemand F, Tutt AM, Gillet C, et al. Definition of clinically distinct molecular subtypes in estrogen receptor-positive breast carcinomas through genomic grade. J Clin Oncol. 2007;25(10):1239-46.*

15.   *Buffa FM, Camps C, Winchester L, Snell CE, Gee HE, Sheldon H, et al. microRNA-associated progression pathways and potential therapeutic targets identified by integrated mRNA and microRNA expression profiling in breast cancer. Cancer Res. 2011;71(17):5635-45.*

16.   *Curtis C, Shah SP, Chin SF, Turashvili G, Rueda OM, Dunning MJ, et al. The genomic and transcriptomic architecture of 2,000 breast tumours reveals novel subgroups. Nature. 2012;486(7403):346-52.*

17.   *Kok M, Koornstra RH, Margarido TC, Fles R, Armstrong NJ, Linn SC, et al. Mammosphere-derived gene set predicts outcome in patients with ER-positive breast cancer. J Pathol. 2009;218(3):316-26.*

18.   *Michalides R, van Tinteren H, Balkenende A, Vermorken JB, Benraadt J, Huldij J, et al. Cyclin A is a prognostic indicator in early stage breast cancer with and without tamoxifen treatment. Br J Cancer. 2002;86(3):402-8.*

19.   *Beelen K, Zwart W, Linn SC. Can predictive biomarkers in breast cancer guide adjuvant endocrine therapy? Nat Rev Clin Oncol. 2012;9(9):529-41.*

20.   *Zheng L, Jia J, Finger LD, Guo Z, Zer C, Shen B. Functional regulation of FEN1 nuclease and its link to cancer. Nucleic acids research. 2011;39(3):781-94.*

21.   *Saharia A, Teasley DC, Duxin JP, Dao B, Chiappinelli KB, Stewart SA. FEN1 ensures telomere stability by facilitating replication fork re-initiation. The Journal of biological chemistry. 2010;285(35):27057-66.*

22.   *van Pel DM, Barrett IJ, Shimizu Y, Sajesh BV, Guppy BJ, Pfeifer T, et al. An evolutionarily conserved synthetic lethal interaction network identifies FEN1 as a broad-spectrum target for anticancer therapeutic development. PLoS genetics. 2013;9(1):e1003254.*

23.   *Tumey LN, Bom D, Huck B, Gleason E, Wang J, Silver D, et al. The identification and optimization of a N-hydroxy urea series of flap endonuclease 1 inhibitors. Bioorg Med Chem Lett. 2005;15(2):277-81.*

24.   *Exell JC, Thompson MJ, Finger LD, Shaw SJ, Debreczeni J, Ward TA, et al. Cellularly active N-hydroxyurea FEN1 inhibitors block substrate entry to the active*

site. Nature chemical biology. 2016;12(10):815-21.

25.   *Dorjsuren D, Kim D, Maloney DJ, Wilson DM, 3rd, Simeonov A. Complementary non-radioactive assays for investigation of human flap endonuclease 1 activity. Nucleic acids research. 2011;39(2):e11.*

26.   *Inglese J, Auld DS, Jadhav A, Johnson RL, Simeonov A, Yasgar A, et al. Quantitative high-throughput screening: a titration-based approach that efficiently identifies biological activities in large chemical libraries. Proc Natl Acad Sci U S A. 2006;103(31):11473-8.*

27.   *Yasgar A, Shinn P, Jadhav A, Auld D, Michael S, Zheng W, et al. Compound Management for Quantitative High-Throughput Screening. Jala. 2008;13(2):79-89.*

28.   *Jadhav A, Ferreira RS, Klumpp C, Mott BT, Austin CP, Inglese J, et al. Quantitative analyses of aggregation, autofluorescence, and reactivity artifacts in a screen for inhibitors of a thiol protease. Journal of medicinal chemistry. 2010;53(1):37-51.*

29.   *Zhang F, Wang Y, Wang L, Luo X, Huang K, Wang C, et al. Poly(ADP-ribose) polymerase 1 is a key regulator of estrogen receptor alpha-dependent gene transcription. The Journal of biological chemistry. 2013;288(16):11348-57.*

30.   *Ju BG, Lunyak VV, Perissi V, Garcia-Bassets I, Rose DW, Glass CK, et al. A topoisomerase IIbeta-mediated dsDNA break required for regulated transcription. Science. 2006;312(5781):1798-802.*

31.   *Lee HS, Park JH, Kim SJ, Kwon SJ, Kwon J. A cooperative activation loop among SWI/SNF, gamma-H2AX and H3 acetylation for DNA double-strand break repair. EMBO J. 2010;29(8):1434-45.*

32.   *Nawaz Z, Lonard DM, Dennis AP, Smith CL, O'Malley BW. Proteasome-dependent degradation of the human estrogen receptor. Proc Natl Acad Sci U S A. 1999;96(5):1858-62.*

33.   *Ung M, Ma X, Johnson KC, Christensen BC, Cheng C. Effect of estrogen receptor alpha binding on functional DNA methylation in breast cancer. Epigenetics. 2014;9(4):523-32.*

34.   *Kangaspeska S, Stride B, Metivier R, Polycarpou-Schwarz M, Ibberson D, Carmouche RP, et al. Transient cyclical methylation of promoter DNA. Nature. 2008;452(7183):112-5.*

35.   *Bhutani N, Burns DM, Blau HM. DNA demethylation dynamics. Cell. 2011;146(6):866-72.*

36.   *Meissner A, Gnirke A, Bell GW, Ramsahoye B, Lander ES, Jaenisch R. Reduced representation bisulfite sequencing for comparative high-resolution DNA methylation analysis. Nucleic acids research. 2005;33(18):5868-77.*

37.   *Hurtado A, Holmes KA, Ross-Innes CS, Schmidt D, Carroll JS. FOXA1 is a key determinant of estrogen receptor function and endocrine response. Nature genet-*

ics. 2011;43(1):27-33.

38.   *Robinson DR, Wu YM, Vats P, Su F, Lonigro RJ, Cao X, et al. Activating ESR1 mutations in hormone-resistant metastatic breast cancer. Nature genetics. 2013;45(12):1446-51.*

39.   *Jeong KW, Kim K, Situ AJ, Ulmer TS, An W, Stallcup MR. Recognition of enhancer element-specific histone methylation by TIP60 in transcriptional activation. Nature structural & molecular biology. 2011;18(12):1358-65.*

40.   *Fan M, Yan PS, Hartman-Frey C, Chen L, Paik H, Oyer SL, et al. Diverse gene expression and DNA methylation profiles correlate with differential adaptation of breast cancer cells to the antiestrogens tamoxifen and fulvestrant. Cancer Res. 2006;66(24):11954-66.*

41.   *Knowlden JM, Hutcheson IR, Jones HE, Madden T, Gee JM, Harper ME, et al. Elevated levels of epidermal growth factor receptor/c-erbB2 heterodimers mediate an autocrine growth regulatory pathway in tamoxifen-resistant MCF-7 cells. Endocrinology. 2003;144(3):1032-44.*

42.   *Dean JL, McClendon AK, Hickey TE, Butler LM, Tilley WD, Witkiewicz AK, et al. Therapeutic response to CDK4/6 inhibition in breast cancer defined by ex vivo analyses of human tumors. Cell cycle. 2012;11(14):2756-61.*

43.   *Mohammed H, Russell IA, Stark R, Rueda OM, Hickey TE, Tarulli GA, et al. Progesterone receptor modulates ERalpha action in breast cancer. Nature. 2015;523(7560):313-7.*

44.   *Dai X, Li T, Bai Z, Yang Y, Liu X, Zhan J, et al. Breast cancer intrinsic subtype classification, clinical use and future trends. Am J Cancer Res. 2015;5(10):2929-43.*

45.   *DiRenzo J, Shang Y, Phelan M, Sif S, Myers M, Kingston R, et al. BRG-1 is recruited to estrogen-responsive promoters and cooperates with factors involved in histone acetylation. Molecular and cellular biology. 2000;20(20):7541-9.*

46.   *Perillo B, Ombra MN, Bertoni A, Cuozzo C, Sacchetti S, Sasso A, et al. DNA oxidation as triggered by H3K9me2 demethylation drives estrogen-induced gene expression. Science. 2008;319(5860):202-6.*

47.   *Gong C, Fujino K, Monteiro LJ, Gomes AR, Drost R, Davidson-Smith H, et al. FOXA1 repression is associated with loss of BRCA1 and increased promoter methylation and chromatin silencing in breast cancer. Oncogene. 2015;34(39):5012-24.*

48.   *Stone A, Zotenko E, Locke WJ, Korbie D, Millar EK, Pidsley R, et al. DNA methylation of oestrogen-regulated enhancers defines endocrine sensitivity in breast cancer. Nature communications. 2015;6:7758.*

49.   *Ma J, Wang M. Interplay between DNA supercoiling and transcription elongation. Transcription. 2014;5(3):e28636.*

50.   Santos-Pereira JM, Aguilera A. R loops: new modulators of genome dynamics and function. Nature reviews Genetics. 2015;16(10):583-97.

51.   Stork CT, Bocek M, Crossley MP, Sollier J, Sanz LA, Chedin F, et al. Co-transcriptional R-loops are the main cause of estrogen-induced DNA damage. eLife. 2016;5.

52.   He L, Zhang Y, Sun H, Jiang F, Yang H, Wu H, et al. Targeting DNA Flap Endonuclease 1 to Impede Breast Cancer Progression. EBioMedicine. 2016.

53.   Panda H, Jaiswal AS, Corsino PE, Armas ML, Law BK, Narayan S. Amino acid Asp181 of 5'-flap endonuclease 1 is a useful target for chemotherapeutic development. Biochemistry. 2009;48(42):9952-8.

54.   McManus KJ, Barrett IJ, Nouhi Y, Hieter P. Specific synthetic lethal killing of RAD54B-deficient human colorectal cancer cells by FEN1 silencing. Proc Natl Acad Sci U S A. 2009;106(9):3276-81.

55.   Giresi PG, Lieb JD. Isolation of active regulatory elements from eukaryotic chromatin using FAIRE (Formaldehyde Assisted Isolation of Regulatory Elements). Methods. 2009;48(3):233-9.

56.   Jansen MP, Knijnenburg T, Reijm EA, Simon I, Kerkhoven R, Droog M, et al. Hallmarks of aromatase inhibitor drug resistance revealed by epigenetic profiling in breast cancer. Cancer Res. 2013;73(22):6632-41.

57.   Zhang Y, Liu T, Meyer CA, Eeckhoute J, Johnson DS, Bernstein BE, et al. Model-based analysis of ChIP-Seq (MACS). Genome biology. 2008;9(9):R137.

58.   Kumar V, Muratani M, Rayan NA, Kraus P, Lufkin T, Ng HH, et al. Uniform, optimal signal processing of mapped deep-sequencing data. Nature biotechnology. 2013;31(7):615-22.

59.   Ye T, Krebs AR, Choukrallah MA, Keime C, Plewniak F, Davidson I, et al. seqMINER: an integrated ChIP-seq data interpretation platform. Nucleic acids research. 2011;39(6):e35.

60.   Lopez-Garcia J, Periyasamy M, Thomas RS, Christian M, Leao M, Jat P, et al. ZNF366 is an estrogen receptor corepressor that acts through CtBP and histone deacetylases. Nucleic acids research. 2006;34(21):6126-36.

61.   Kok M, Linn SC, Van Laar RK, Jansen MP, van den Berg TM, Delahaye LJ, et al. Comparison of gene expression profiles predicting progression in breast cancer patients treated with tamoxifen. Breast cancer research and treatment. 2009;113(2):275-83.

62.   Beelen K, Opdam M, Severson TM, Koornstra RH, Vincent AD, Wesseling J, et al. Phosphorylated p-70S6K predicts tamoxifen resistance in postmenopausal breast cancer patients randomized between adjuvant tamoxifen versus no systemic treatment. Breast cancer research : BCR. 2014;16(1):R6.

63. *Michael S, Auld D, Klumpp C, Jadhav A, Zheng W, Thorne N, et al. A robotic platform for quantitative high-throughput screening. Assay and drug development technologies. 2008;6(5):637-57.*

64. *Krueger F, Andrews SR. Bismark: a flexible aligner and methylation caller for Bisulfite-Seq applications. Bioinformatics. 2011;27(11):1571-2.*

65. *Langmead B, Salzberg SL. Fast gapped-read alignment with Bowtie 2. Nature methods. 2012;9(4):357-9.*

66. *Li H, Handsaker B, Wysoker A, Fennell T, Ruan J, Homer N, et al. The Sequence Alignment/Map format and SAMtools. Bioinformatics. 2009;25(16):2078-9.*

67. *Ji X, Li W, Song J, Wei L, Liu XS. CEAS: cis-regulatory element annotation system. Nucleic acids research. 2006;34(Web Server issue):W551-4.*

Supplementary information

Figure S1.

(A) Heatmap showing the correlation of the four individual genes with the disease specific survival of breast cancer patients from METABRIC stratified by ERα status. Discovery (n=827) and validation (n=822) cohorts were analyzed separately. Heatmap values are from an adjusted cox-regression where a color gradient (upper limit log (HR>2), middle limit log (HR=1) and lower limit log (HR=0.4)) was used. Multivariate significant results are in bold with a green border, whereas non-significant results are transparent. (B) Disease specific survival of breast cancer patients over time (days) categorized according to FEN1 expression levels in the METABRIC discovery and validation set. Additionally patients were stratified according to ERα status. The median of FEN1 expression was used as an cut-off to divide patients in a Low expression group (blue) and a High expression group (green). Adjusted cox-regression is shown. (C) As in B, but now ERα-positive patients which received hormonal therapy were included and the validation and discovery cohorts were merged. Log-rank, cox-regression and interaction test between FEN1 levels and hormonal therapy are shown. (D) As in B, but now patients were stratified according to menopausal status and the validation and discovery cohorts were merged. Log-rank and cox-regression are shown.

Figure S2.

(A) Western blot analyses after siRNA targeting or overexpression of FEN1. Protein levels were determined for ERα, endogenous FEN1 and exogenous FLAG-tagged FEN1. Actin was used as loading control. Cells were treated with (+) or without (-) estradiol overnight before lysis. (B) Western blot analyses of cells used for ERα,

p300 and FOXA1 ChIP-seq and ERα ChIP-qPCR after siRNA targeting or overex-pression of FEN1. Protein levels were determined for ERα, p300, FOXA1, endoge-nous FEN1 and exogenous FLAG-tagged FEN1. Actin and RNA Pol II were used as loading control. Blots depicting samples used for Figure 2C,D,E are labelled ERα/ p300 and FOXA1 ChIP-seq, whereas samples used for Figure 2G are labelled ERα-ChIP. (C) ChIP-qPCR validation of FOXA1, ERα and p300 ChIP-seq at enhancer regions proximal to GREB1, XBP1 and RARA. Additionally a RNA Pol II ChIP-qP-CR was performed. Signals for each primer set are normalized over control regions and siControl (blue), which is set as 1. Shown is an example of two biological repli-cates. N=4 with mean ± SD. *=p-value<0.01 Students T-test.

Figure S3.

(A) Deconvolution of pool of siRNA targeting FEN1. (Left) Western blot analyses after siRNA targeting by individual siRNA's or by a pool of 4 (siFEN1 pool). Protein levels were determined for FEN1 and actin, which was used as loading control. Quantified FEN1-protein levels as normalized over loading control actin are shown. (Right) Relative cell growth (Y-axis) of MCF-7 cells treated with estradiol. Cells were transfected with siControl or the individual FEN1 siRNA's. Relative growth was normalized over the plate confluency at timepoint 0. Shown is a representative experiment of two biological replicates. N=6 with mean ± SD. *=p-value<0.05 (B) Relative cell growth (Y-axis) of T47D cells treated with vehicle control, E2, tamox-ifen or fulvestrant. Cells were transfected with control siControl (blue) or siFEN1 (red). Relative growth was normalized over the plate confluency at timepoint 0. Shown is a representative experiment of three biological replicates. N=6 with mean ± SD. *=p-value<0.05 and ***=p-value<0.001 Students T-test.

Figure S4.

(A) Altered FEN1 enzyme activity at the maximum tested concentration of 465,195 screened compounds. The percentage of altered FEN1 enzyme activity (Y-axis) at the maximum tested concentration of all screened compounds (X-axis). Compounds are divided into active inhibitors (green), inconclusive compounds (yellow) and inac-tive compounds (blue). The top hit from our biological validations, MLS002701801 (red), has been highlighted. (B) Relative cell proliferation (Y-axis) over time (X-ax-is) of MCF-7 cells treated with a vehicle or 10 uM of each of the three inhibitors. Shown is an example of two biological replicates. N=6 with mean ± SD. (C) Colony formation assay of ERα-negative cell lines MDA-MB-231 and CAL-120. Cells were treated with the minimum compound concentrations still capable of proficient MCF-7 growth inhibition. Representative experiment is shown of two biological experi-

*ments. (D) ChIP-qPCR validation of PARP1 and XRCC1 ChIP-seq at ERα-bound enhancer regions proximal to TFF1, GREB1, XBP1 and RARA. Two regions negative for ERα binding were used as negative controls (blue). Shown is an example of two biological replicates. Depicted is the percentage of input with N=4 with mean ± SD. ***=p-value<0.001 Students T-test. (E) Bar graph depicting the percentage of γH2AX-foci positive cells (n=500) on immunofluorescence. Hormone-deprived cells where treated with ethanol control or estradiol for 15 minutes, with or without FEN1 inhibitor. Shown is a representative experiment of two biological replicates. (F) ChIP-qPCR validation of ERα, PARP1 and BRG1 ChIP-seq at ERα-bound enhancer regions proximal to TFF1, GREB1 and XBP1. Signals for each primer set are normalized over control regions. Shown is an example of two biological replicates. N=4 (ERα and PARP1) or N=5 (BRG1) with mean ± SD. *=p-value<0.05, **=p-value<0.01 and ***=p-value<0.001 Students T-test. (G) (Left) Western blot depicting ERα, FEN1 and actin protein levels. Hormone-deprived cells were pretreated overnight with or without FEN1 inhibitor and treated three hours with 10uM of MG132 when appropriate before stimulation with estradiol. Shown is an example experiment of two biological replicates with quantified ERα-protein levels as normalized over loading control actin. (Right) ChIP-qPCR of ERα at enhancer regions proximal to TFF1, GREB1 and XBP1. Cells were pretreated overnight with or without FEN1 inhibitor and treated three hours with 10uM of MG132 before 30 minutes of estradiol stimulation. Signals for each primer set are normalized over negative control region. Shown is an example of two biological replicates. N=4 with mean ± SD. *=p-value<0.05 Students T-test.*

Figure S5.
(A) ChIP-qPCR ERα at enhancer regions proximal to TFF1, GREB1 and XBP1. Hormone deprived cells were treated with 0, 15, 30 or 45 minutes of estradiol prior to fixation. Signals for each primer set are normalized over negative control region. Shown is an example of two biological replicates. N=4 with mean ± SD. (B) Left: Western Blot depicting ERα and FEN1 protein levels with actin as a control after pretreatment with the FEN1 inhibitor. In the absence of estradiol stimulation ERα protein levels are unaffected by the FEN1 inhibitor, indicating that the subsequent decrease in ERα-chromatin interactions or ERα-activity are not due to decreased starting amounts of the ERα protein. Representative blot of three biological experiments is shown. Right: Normalized quantification of ERα protein levels of the three biological replicates. N=3 with mean ± SEM. (C) Indication of the percentage of Ki67 positive tumor cells in tumor explants cultured in the presence or absence of FEN1 inhibitor or tamoxifen.

Figure S1.

A

B

Discovery set

All patients **ER- patients** **ER+ patients**

Validation set

All patients **ER- patients** **ER+ patients**

C **FEN1 levels and HT**

D **Premenopausal Postmenopausal**

Figure S2.

A

B

C

Figure S3.

A

B
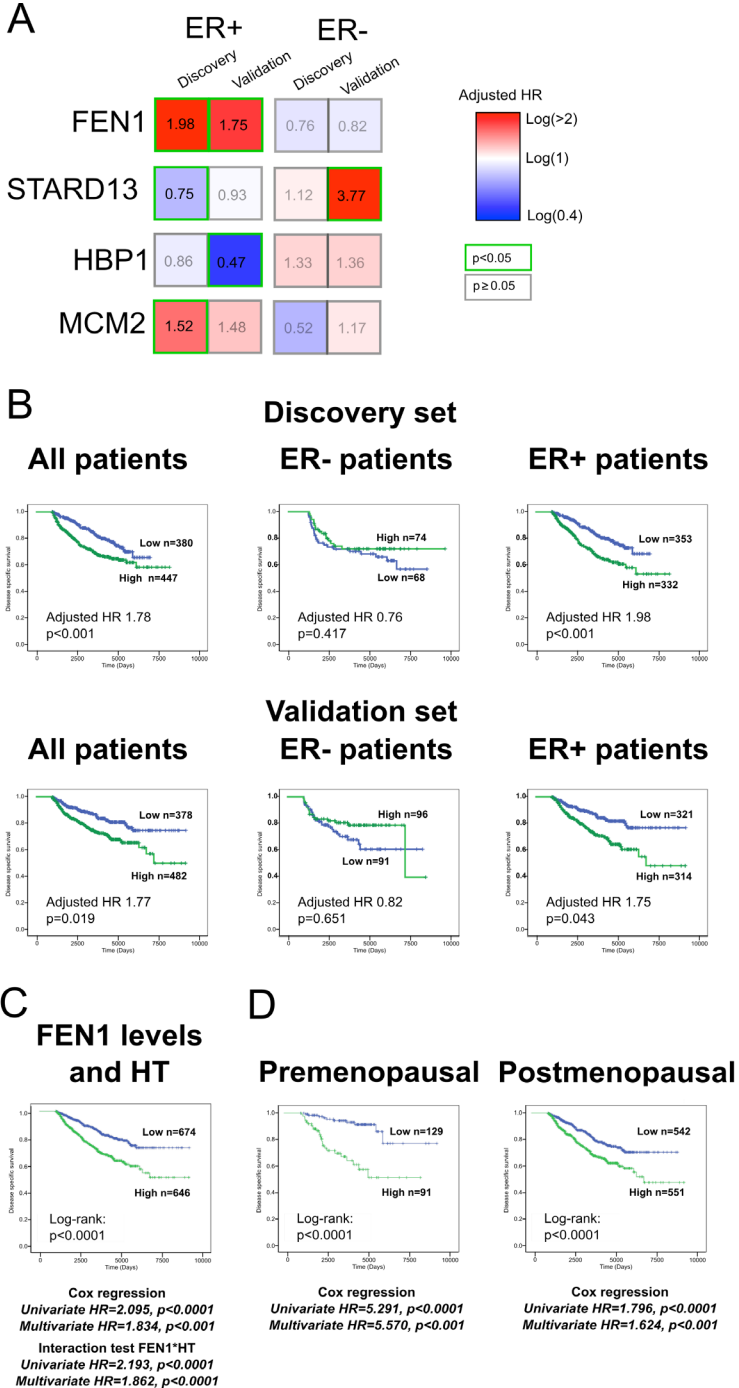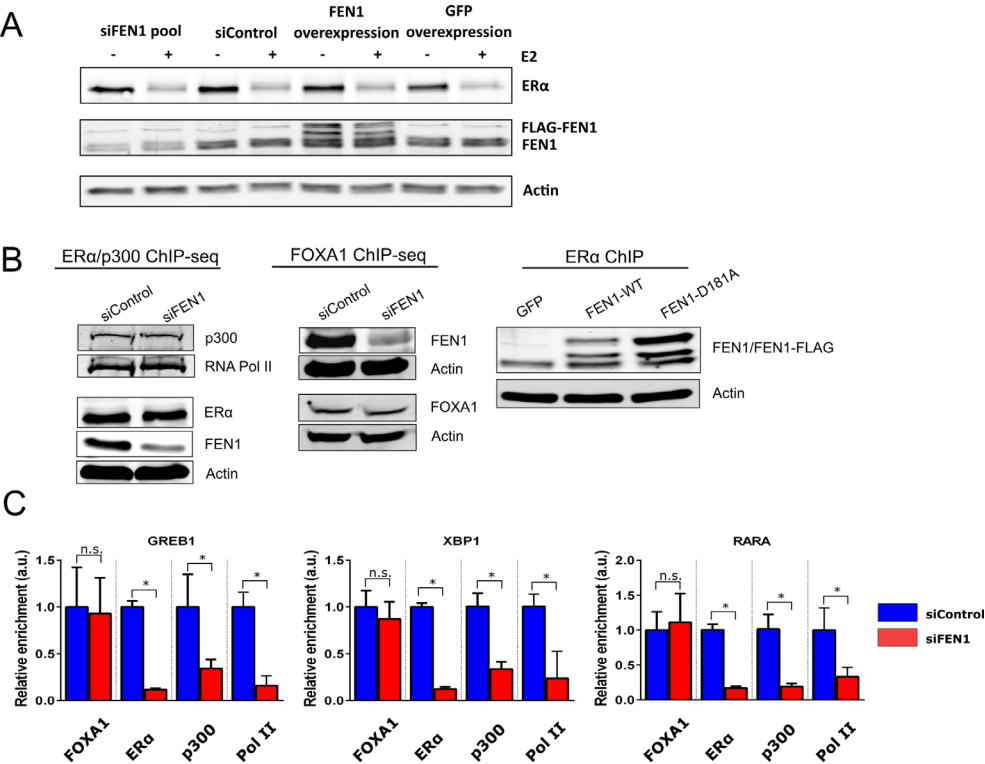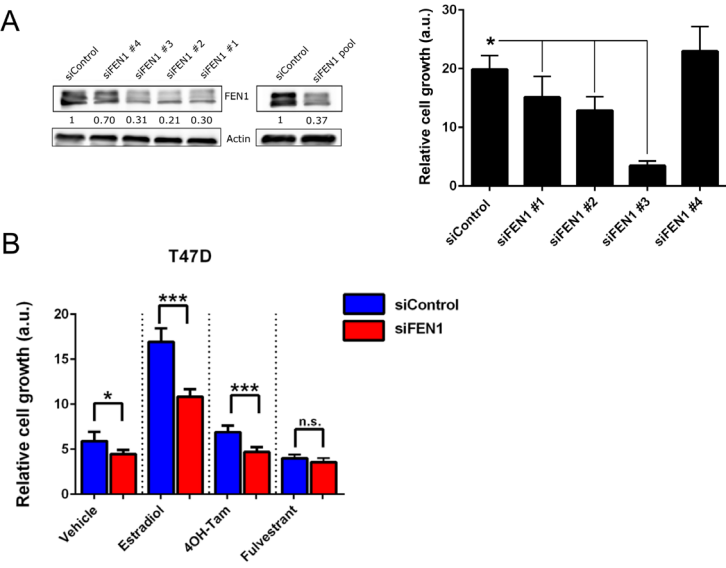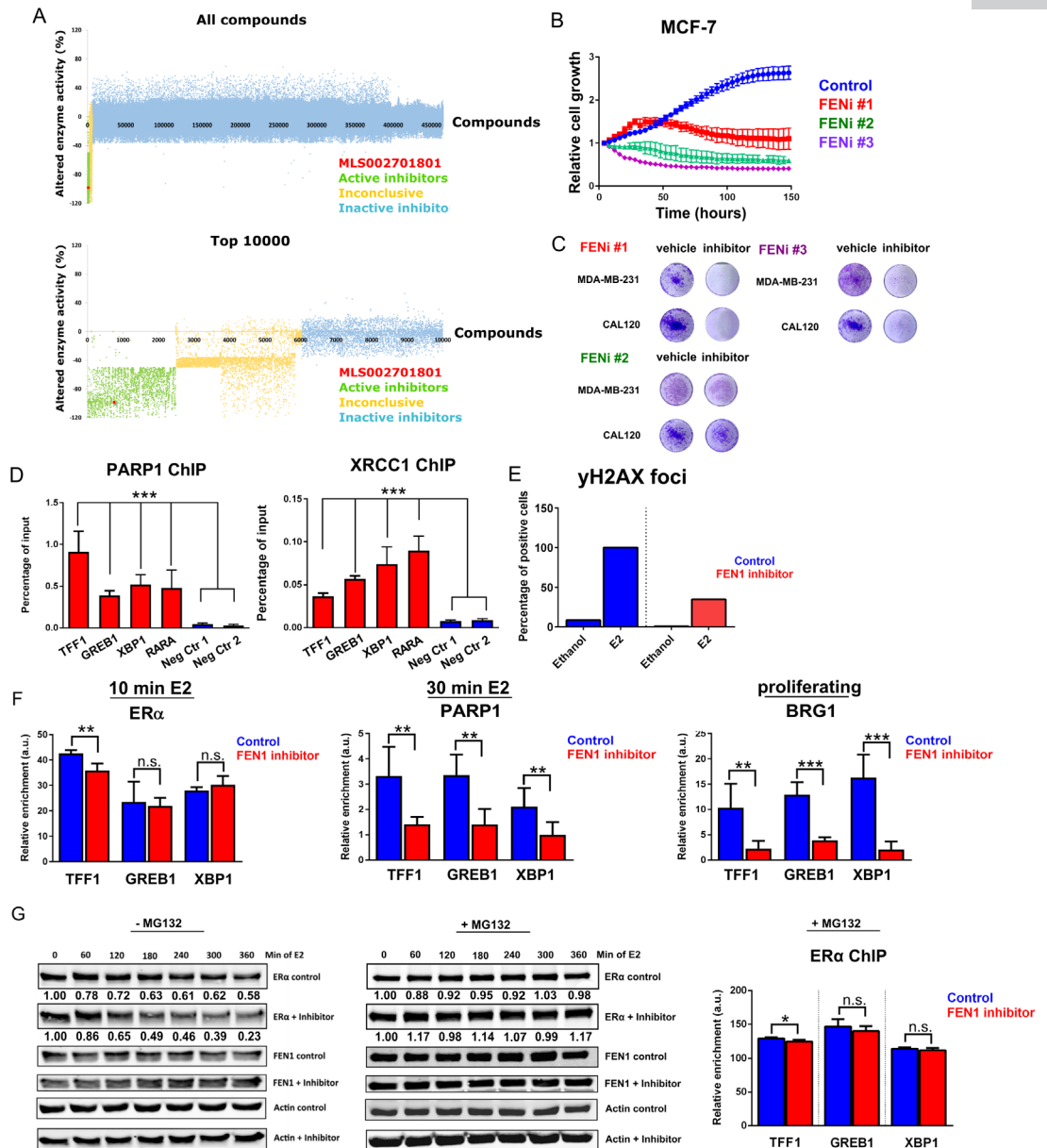
Figure S4.

Figure S5.
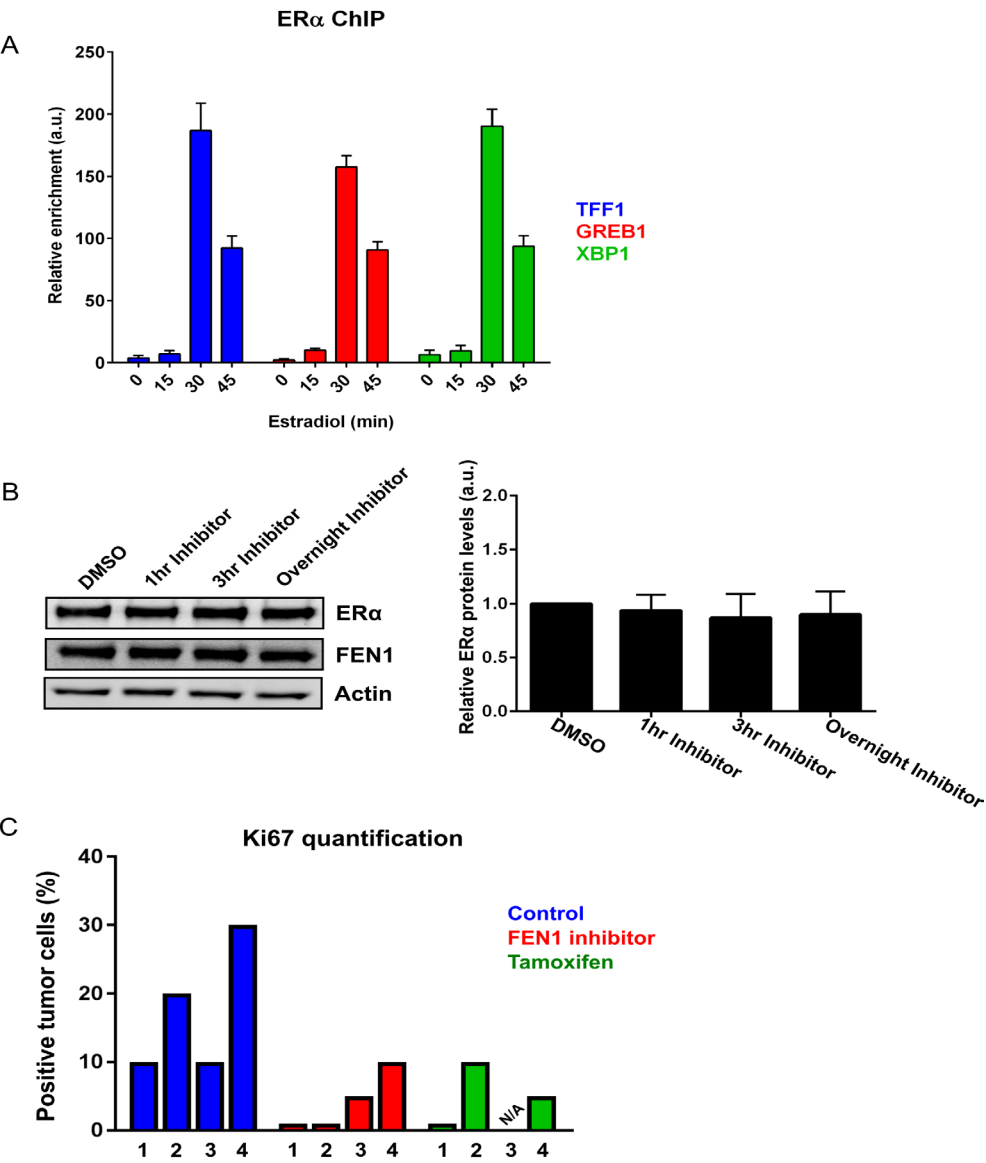
Table S1.

Discovery cohort
Multivariate analyses FEN1 mRNA

Variable	Hazard ratio (95% CI)	p-value
FEN1 mRNA levels	2.02 (0.91-4.49)	0.084
Age *(<60 versus ≥60)*	0.71 (0.35-1.43)	0.333
Affected Lymph nodes *none*		0.015
1-3	1.58 (0.54-4.64)	0.408
≥4	3.94 (1.24-12.50)	0.020
Tumor diameter *≤20 mm*		0.297
20-50 mm	1.71 (0.80-3.68)	0.169
>50 mm	2.59 (0.52-12.83)	0.244
Tumor Grade *Grade 1*		0.827
Grade 2	1.29 (0.57-2.94)	0.539
Grade 3	1.19 (0.40-3.53)	0.749

Multivariate analyses FEN1 IHC

Variable	Hazard ratio (95% CI)	p-value
FEN1 IHC score	1.61 (0.77-3.35)	0.205
Age *(<60 versus ≥60)*	0.69 (0.33-1.45)	0.325
Affected Lymph nodes *none*		0.030
1-3	1.38 (0.46-4.13)	0.565
≥4	3.30 (1.05-10.36)	0.041
Tumor diameter *≤20 mm*		0.057
20-50 mm	2.83 (1.21-6.62)	0.017
>50 mm	2.16 (0.41-11.32)	0.361
Tumor Grade *Grade 1*		0.962
Grade 2	1.12 (0.50-2.51)	0.786
Grade 3	1.05 (0.38-2.94)	0.921

Validation cohort
Multivariate analyses FEN1 in ERα negative patients

Variable	Hazard ratio (95% CI)	p-value
FEN1 IHC score	1.20 (0.69-2.09)	0.514
Age *(<65 versus ≥65)*	0.45 (0.24-0.82)	0.009
Tumor Grade *(grade 1-2 versus grade 3)*	1.12 (0.61-2.04)	0.718
Tumor Stage *(T1-T2 versus T3-T4)*	2.83 (1.41-5.71)	0.004
HER2 status *(Negative versus positive)*	1.54 (0.86-2.77)	0.145
PgR status *(Negative versus positive)*	1.21 (0.36-4.07)	0.761

Multivariate analyses FEN1 in ERα positive patients

Variable	Hazard ratio (95% CI)	p-value
FEN1 IHC score	1.58 (1.01-2.47)	0.047
Age *(<65 versus ≥65)*	1.03 (0.68-1.57)	0.874
Tumor Grade *(grade 1-2 versus grade 3)*	1.87 (1.19-2.94)	0.006
Tumor Stage *(T1-T2 versus T3-T4)*	1.74 (1.04-2.92)	0.035
HER2 status *(Negative versus positive)*	1.12 (0.60-2.08)	0.722
PgR status *(Negative versus positive)*	1.13 (0.74-1.71)	0.579

Multivariate analyses FEN1 in no adjuvant treatment patients

Variable	Hazard ratio (95% CI)	p-value
FEN1 IHC score	1.59 (0.62-4.06)	0.336
Age *(<65 versus ≥65)*	0.87 (0.38-2.00)	0.740

Tumor Grade *(grade 1-2 versus grade 3)*	1.29 (0.47-3.56)	0.623
Tumor Stage *(T1-T2 versus T3-T4)*	3.70 (1.16-11.86)	0.028
HER2 status *(Negative versus positive)*	1.48 (0.26-8.43)	0.656
PgR status *(Negative versus positive)*	0.94 (0.37-2.35)	0.887

Multivariate analyses FEN1 in adjuvant tamoxifen patients

Variable	Hazard ratio (95% CI)	p-value
FEN1 IHC score	1.66 (0.97-2.82)	0.063
Age *(<65 versus ≥65)*	1.13 (0.69-1.84)	0.626
Tumor Grade *(grade 1-2 versus grade 3)*	2.06 (1.22-3.48)	0.007
Tumor Stage *(T1-T2 versus T3-T4)*	1.53 (0.85-2.78)	0.160
HER2 status *(Negative versus positive)*	1.11 (0.56-2.19)	0.764
PgR status *(Negative versus positive)*	1.16 (0.71-1.88)	0.555

Multivariate analyses in FEN1 low patients

Variable	Hazard ratio (95% CI)	p-value
Treatment *(tamoxifen versus no tamoxifen)*	0.39 (0.18-0.83)	0.015
Age *(<65 versus ≥65)*	0.44 (0.23-0.87)	0.017
Tumor Grade *(grade 1-2 versus grade 3)*	1.92 (0.94-3.94)	0.075
Tumor Stage *(T1-T2 versus T3-T4)*	1.41 (0.64-3.15)	0.396
HER2 status *(Negative versus positive)*	3.58 (0.94-13.60)	0.061
PgR status *(Negative versus positive)*	1.13 (0.56-2.30)	0.735

Multivariate analyses in FEN1 High patients

Variable	Hazard ratio (95% CI)	p-value
Treatment *(tamoxifen versus no tamoxifen)*	0.67 (0.35-1.26)	0.213
Age *(<65 versus ≥65)*	1.91 (1.10-3.29)	0.021
Tumor Grade *(grade 1-2 versus grade 3)*	1.85 (1.02-3.38)	0.045
Tumor Stage *(T1-T2 versus T3-T4)*	1.59 (0.79-3.22)	0.197
HER2 status *(Negative versus positive)*	0.95 (0.47-1.93)	0.884
PgR status *(Negative versus positive)*	1.05 (0.60-1.81)	0.872
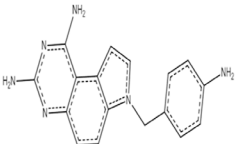
FEN1 levels and tamoxifen interaction test

Variable	Hazard ratio (95% CI)	p-value
Tamoxifen treatment x FEN1 levels	1.48 (0.99-2.21)	0.053

Table S1. *Multivariate cox-regression of FEN1 in the Discovery and Validation cohort.*
Adjusted Cox proportional hazard regression analyses were performed with the following covariates; for the discovery-cohort the covariates age (<60 versus ≥60), diameter of the tumor (≤20 mm versus 20-50 mm versus >50 mm), tumor grade (grade 1 versus grade 2 versus grade 3) and the number of affected lymph nodes (Negative versus 1-3 versus ≥4), and for the validation-cohort the covariates age (< 65 versus ≥ 65), grade (grade 1-2 versus grade 3), tumor stage (T1-T2 versus T3-4), HER2 status (negative versus positive), PgR status (negative versus positive). Adjusted hazard ratio with 95% CI and p-value are shown. Additionally interaction test between the variable tamoxifen treatment and FEN1 levels is shown.

Table S2

Chemical structure	Molecular formula	PubChem CID
	$C_{17}H_{16}N_6$	432465
	Molecular Weight	**registration ID**
	304,35	MLS002701801

Assay Protocol	IC$_{50}$ (uM)	Inhibition at 57 uM
Thiazole orange DNA binding assay	*inactive*	*15.44 %*
DNA Polymerase Beta activity assay	*inactive*	*20.3 %*
DNA Polymerase Iota activity assay	*inactive*	*-15.47 %*
DNA Polymerase Kappa activity assay	*inactive*	*-36.2 %*
BRCA1 activity assay	*inactive*	*-1.7 %*
PCNA activity assay	*inactive*	*23.14 %*
WRN helicase activity assay	*inactive*	*13.09 %*
FEN1 activity assay - initial screen compound source 1	**1,37**	83.68 %
FEN1 activity assay - initial screen compound source 2	**1,22**	79.08 %
FEN1 activity assay - validation screen	**6,75**	74.39 %
FEN1 activity assay - validation screen with purified sample	**1,22**	80.72 %
APE1 activity assay - compound source 1	**25,12**	48.72 %
APE1 activity assay - compound source 2	**28,18**	42.07 %

Table S2. *Characteristics of the small molecule inhibitor of FEN1.*
Chemical structure and characteristics of the FEN1 inhibitor. Additionally the IC50 (μM) and inhibition at the maximum tested concentration (57 μM) in multiple activity assays (NIH Molecular Libraries Program (https://commonfund.nih.gov/molecularlibraries)) is shown.

Table S3

FBS

Cells	IC$_{50}$	Std.Error	CI.Lower	CI.Upper
MCF-7	69	14	39	99
T47D	78	24	28	128
MCF7-T	29	4	21	37
TAMR	29	4	21	38
CAL120	*NA*	*NA*	*NA*	*NA*
BT20	314	298	-286	914

Tamoxifen

Cells	IC$_{50}$	Std.Error	CI.Lower	CI.Upper
MCF-7	*NA*	*NA*	*NA*	*NA*
T47D	*NA*	*NA*	*NA*	*NA*
MCF7-T	22	4	13	31
TAMR	23	5	13	33
CAL120	*NA*	*NA*	*NA*	*NA*
BT20	895	1390	-1904	3694

Table S3. *IC50 of FEN1 inhibitor for individual cell lines under full medium (FBS) or tamoxifen conditions. For cell lines reaching 50% growth inhibition, IC50 was determined and depicted with 95% CI.*

Chapter 6

ERα Cofactor phosphorylation

SRC3 phosphorylation at Serine 543 is a positive independent prognostic factor in ER positive breast cancer

Koen D. Flach[1*], Wilbert Zwart[1*], Bharath Rudraraju[2*], Tarek M.A. Abdel-Fatah[3], Ondrej Gojis[4], Sander Canisius[1], David Moore[5], Ekaterina Nevedomskaya[1], Mark Opdam[1], Marjolein Droog[1], Ingrid Hofland[1], Steve Chan[4], Jacqui Shaw[5], Ian O. Ellis[6], R. Charles Coombes[3], Jason S. Carroll[7], Simak Ali[3], and Carlo Palmieri[2,8,9]

[*]Authors contributed equally
[1]Department of Molecular Pathology, The Netherlands Cancer Institute, Amsterdam, the Netherlands.
[2]Department of Molecular and Clinical Cancer Medicine, Institute of Translational Medicine, The University of Liverpool, Liverpool, UK.
[3]Clinical Oncology Department, Nottingham University City Hospital NHS Trust, Nottingham, UK.
[4]Cancer Research UK Laboratories, Imperial Centre for Translational and Experimental Medicine, Division of Cancer, Imperial College London, London, UK.
[5]Department of Cancer Studies and Molecular Medicine, University of Leicester, Leicester, UK.
[6]Division of Pathology, School of Molecular Medical Sciences, University of Nottingham, Nottingham, UK.
[7]Cancer Research UK Cambridge Institute, Cambridge, UK.
[8]Liverpool and Merseyside Academic Breast Unit, The Linda McCartney Centre, Royal Liverpool University Hospital, Liverpool, UK.
[9]Academic Department of Medical Oncology, Clatterbridge Cancer Centre NHS Foundation Trust, Wirral, UK.

Abstract

Purpose: The steroid receptor coactivator SRC3 is essential for the transcriptional activity of estrogen receptor α (ERα). SRC3 is sufficient to cause mammary tumorigenesis, and has also been implicated in endocrine resistance. SRC3 is posttranslationally modified by phosphorylation, but these events have not been investigated with regard to functionality or disease association. Here, we investigate the spatial selectivity of SRC3-pS543/DNA binding over the human genome and its expression in primary human breast cancer in relation with outcome.

Experimental Design: Chromatin immunoprecipitation, coupled with sequencing, was used to determine the chromatin binding patterns of SRC3-pS543 in the breast cancer cell line MCF7 and two untreated primary breast cancers. IHC was used to assess the expression of SRC3 and SRC3-pS543 in 1,650 primary breast cancers. The relationship between the expression of SRC3 and SRC3-pS543, disease-free survival (DFS), and breast cancer specific survival (BCSS) was assessed.

Results: Although total SRC3 is selectively found at enhancer regions, SRC3-pS543 is recruited to promoters of ERα responsive genes, both in the MCF7 cell line and primary breast tumor specimens. SRC3-pS543 was associated with both improved DFS (P = 0.003) and BCSS (P = 0.001) in tamoxifen untreated high-risk patients, such a correlation was not seen in tamoxifen-treated cases, the interaction was statistically significant (P = 0.001). Multivariate analysis showed SRC3-pS543 to be an independent prognostic factor.

Conclusions: Phosphorylation of SRC3 at S543 affects its genomic interactions on a genome-wide level, where SRC3-pS543 is selectively recruited to promoters of ERα-responsive genes. SRC3-pS543 is a prognostic marker, and a predictive marker of response to endocrine therapy. Clin Cancer Res; 22(2); 479–91. ©2015 AACR.

Translational Relevance: SRC3 is an essential coactivator for the transcriptional activity of ERα and is required for estrogen-dependent cell proliferation. Analogous to ERα, SRC3 is typically found at enhancer regions involved in long-range regulation of hormonal-responsive genes. In this study, we establish the genome-wide chromatin binding preferences for activated SRC3 (SRC3-pS543) in ERα-positive breast cancer, as well as the association

between SRC3-pS543 expression and clinicopathologic features and clinical outcomes in 1,650 primary breast cancers. Our findings reveal that while ERα and total SRC3 are predominately found in distal enhancers and introns, SRC3-pS543 is predominately located at promoters of genes. SRC3-pS543 was associated with favorable clinicopathologic features and was found to be an independent prognostic factor as well as a predictive marker with regard to tamoxifen treatment. These observations illustrate that high expression of SRC3-pS543 can potentially identify a population of early ER-positive breast cancer with a good clinical outcome without receiving adjuvant therapy.

Introduction

Estrogen receptor α (ERα) is a key transcription factor in normal breast development and plays a central role in the pathogenesis of approximately 70% of all breast cancers. Consequently, ERα is recognized as the key therapeutic target in this group of patients (1). The p160 steroid receptor coactivator (SRC) family member, SRC3 (also known as amplified in breast cancer 1; AIB1) is an essential coactivator for the transcriptional activity of ERα, which recruits SRC3 to chromatin (2). SRC3 is required for estrogen-driven proliferation of MCF7 breast cancer cells (3) and is critical for normal mammary development (3). Overexpression of SRC3 can induce mammary tumorigenesis in mice (4), while its absence protects against breast cancer development (5, 6). SRC3 was originally identified as a gene mapping to a region of chromosome 20 (20q12–13), which is frequently amplified in breast cancer and was shown to be amplified in 10% of breast cancers (7). SRC3 mRNA levels are significantly higher in breast cancer as compared with normal mammary tissue (8, 9) and SRC3 protein levels are elevated in 16% to 83% (depending on the study) of human breast tumors (10).

SRC3 expression has been associated with decreased risk of relapse in patients with breast cancer who did not receive adjuvant endocrine therapy (11). Conversely, in tamoxifen-treated patients SRC3 expression was associated with poor outcome and increased risk of relapse (11). Others have found no such association with tamoxifen treatment, although an increased risk was seen with high SRC3 when expressed alongside HER1, HER2, or HER3 (12). In a group of women of whom 82% were postmenopausal, SRC3 expression has been associated with early recurrence on tamoxifen treatment (13), although high SRC3 in premenopausal women was an independent predictive factor of improved response to tamoxifen (14). ERα-associated SRC3 is typically found at enhancer regions, where expression of genes proximal

to shared ERα/SRC3 chromatin binding events correlates with poor outcome of ERα-positive patients with breast cancer treated with tamoxifen (15). This feature was only found for genes where SRC3 was selectively enriched as compared with the other two p160 family members, SRC1 and SRC2.

Phosphorylation of SRC3 is required for it to function as a potent transcriptional activator, and SRC3 possesses multiple phosphorylation sites that may be functionally involved in this process (16, 17). Estradiol treatment increases SRC3 phosphorylation, but the kinase responsible for this remains elusive. However, a number of kinases are known that induce phosphorylation at these residues of SRC3 (16, 17). In addition, dephosphorylation of serine-101 and -102 regulates SRC3 protein stability by preventing proteasome-dependent turnover (18). Of note, the C-terminal domain of SRC3 has weak histone acetyltransferase activity raising the possibility that it may have a role in chromatin remodeling (10).

Previous studies have shown a requirement of SRC3 phosphorylation for SRC3 activity, including phosphorylation of SRC3 at serine residue 543 (SRC3-pS543 (16)). Furthermore, the region around S543 is evolutionarily conserved in mammals, birds, and reptiles, although no sequence homology around S543 is found in SRC1 or SRC2 (19). In addition, thus far no studies explored the genomic consequences and clinical significance of SRC3 phosphorylation. Given all the above, we decided to investigate the chromatin associations of SRC3 in vitro and in vivo when phosphorylated at serine 543 (SRC3-pS543) together with its clinical significance in ERα-positive breast cancer. To separate the prognostic from the predictive potential of SRC3 phosphorylation, tamoxifen-treated patients were compared with patients who did not receive any adjuvant endocrine therapy.

Results

Specificity of SRC3-pS543 antibody
An antibody for SRC3-pS543 was generated, which recognized wild-type phosphorylated SRC3, but not S543-mutated SRC3 (S543A; **Fig. 1A**). The SRC3-pS543 antibody detected SRC3 in immunoprecipitates from MCF7 cell lysates (**Fig. 1A and B**; full size blot Supplementary Figs. S1 and S2), where signal was lost after the phosphatase treatment (**Fig. 1B**). Consistent with a previous report (17), we find estrogen treatment to increase S543 phosphorylation in a dose-dependent manner, further validating our SRC3-pS543 antibody (**Fig. 1C**). To ensure the specificity of the SRC3-pS543 antibody
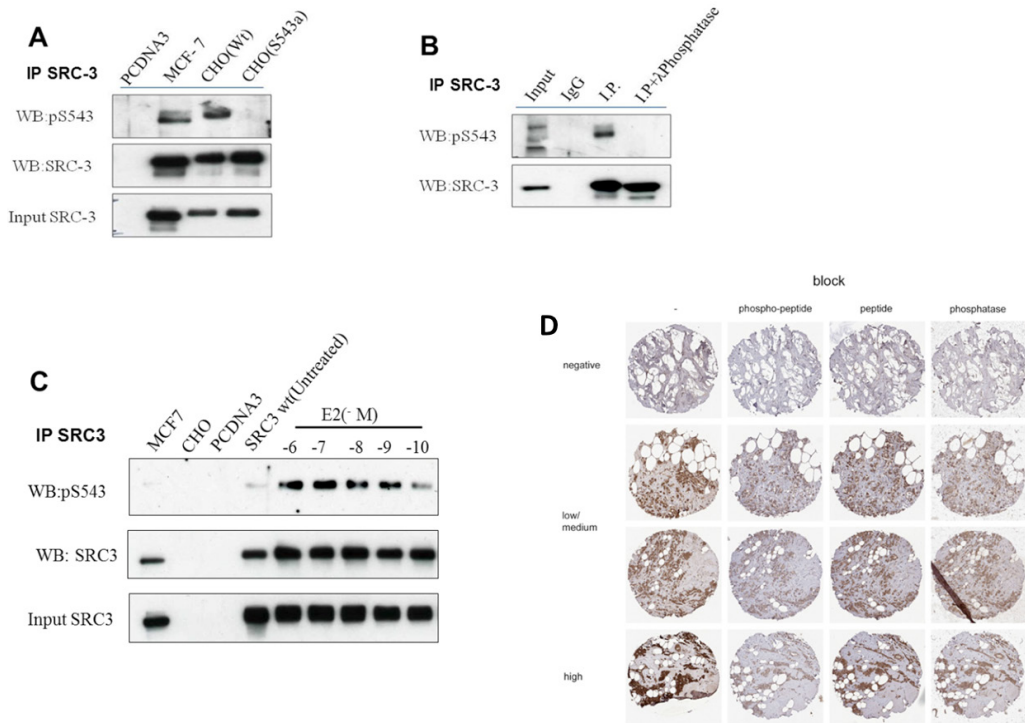
Figure 1: *Validation of phosphostate-specific antibody.*
(A) CHO cells were transfected with pCDNA3, Flag-tagged wild-type (WT) SRC3
or a Flag-tagged SRC3 mutant in which serine at residue 543 has been substituted
by alanine. MCF7 cells were used as control. The lysates were immunoprecipitated
with SRC-3 antibody. Immunoblotting was performed for SRC-3 and phospho-S543.
Note that the Flag-tagged SRC3 migrates slower on Western blot as compared with
endogenous SRC3. (B) MCF7 cell lysate was immunoprecipated with SRC-3 antibo-
dy. The beads were then divided into two halves, one untreated and the other treated
with λ-phosphatase. Immunoblotting was performed for SRC-3 and phosphorylation
state-specific antibody. (C) CHO cells were grown in DMEM with dextran-coated
charcoal stripped FCS for 72 hours and then transfected with vector (pCDNA3) or
SRC-3 for 24 hours. Cells were then treated with vehicle or increasing concentra-
tions of 17ß-estradiol (E2) for 1 hour before making lysates for immunoprecipita-
tion. Western blotting was carried out with the antibodies indicated. MCF7 cells
were used as control. (D) Representative tumor sections following preincubation
with phospho-peptide and nonphospho-peptide and phosphatase treatment prior to
staining with SRC3-pS543 in breast cancers with negative, low/medium, and high
expression of SRC3-pS543.

by IHC, the antibody was incubated with either peptide containing the phospho-moiety or the nonphospho-peptide. Subsequently, the preincubated antibody (bound to nonphospho-peptide and phospho-peptide) was tested on four tumors with different levels of signal for SRC3-pS543 (negative, low/medium, and high; **Fig. 1D**). In addition, phosphatase treatment was applied. Although the phospho-peptide strongly decreased pS543-SRC3 signal, this was not observed with the nonphospho-peptide. In addition, phosphatase treatment strongly diminished pS543-SRC3 signal in all tested specimens (**Fig. 1D**).

ChIP-seq analysis shows a genomic preference of SRC3-pS543 to bind promoter regions

Next, we determined the genome-wide distributions of this SRC3-pS543 phosphorylation as compared with total SRC3 and ERα in asynchronously proliferating luminal breast cancer cells MCF7 as exemplified for well-known ERα binding sites proximal to the XBP-1 locus (**Fig. 2A**). For ERα genomic locations, data from ref. 24 were used, although total SRC3 data were from ref. 15. In total, 47,214 ERα binding sites were detected, of which 15,329 were also bound by SRC3 (ref. 15; **Fig. 2B**). Between ERα, SRC3, and SRC3-pS543, 2,365 peaks were shared (for raw data visualizations, see **Fig. 2C**). Not all SRC3 binding events were phosphorylated and 2,795 peaks for SRC3-pS543 were apparently not shared with total SRC3. However, there was weak total SRC3 signal observed at these positions, which did not reach the detection threshold for peak calling (Supplementary Fig. S3A and S3B). Based on these results, we conclude that differential binding patterns between SRC3-pS543 and total SRC3 should be considered as "enriched" rather than "unique." P160 family members share substantial sequence homology. Even though the sequence surrounding S543 is not conserved in SRC1 and SRC2, the SRC3-pS543 antibody might still detect the other two p160 members. Therefore, we determined potential overlap of SRC3-pS543 enriched sites with SRC1 and SRC2 in MCF7 cells (15). The overlap of SRC3-pS543 enriched sites with SRC1 and SRC2 was limited, rendering it unlikely that the SRC3-pS543 enriched sites can be explained merely by cross-reactivity with one of the other p160s (Supplementary Fig. S4). Differential chromatin binding between SRC3-pS543 and total SRC3 could be validated by qPCR analyses on asynchronous MCF7 cells (Supplementary Fig. S5A), using four primer sets that were designed for each subset of binding sites, that is, SRC3-pS543-enriched, total SRC3-enriched, and shared sites (Supplementary Table S1 for
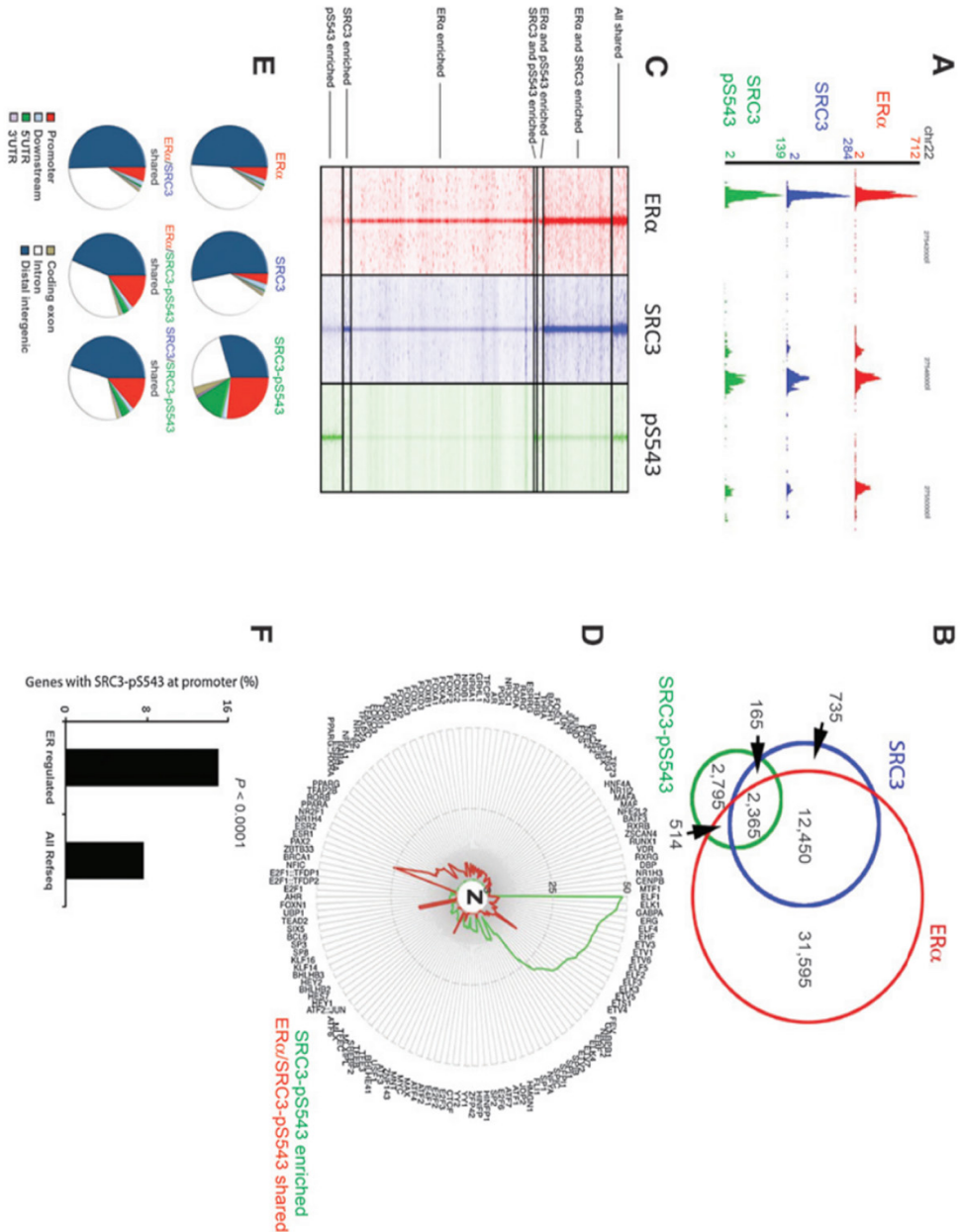
Figure 2: *SRC3-pS543, SRC3, and ERα chromatin binding patterns in MCF7 cells. (A) Genome browser snapshot of ChIP-seq samples for ERα (red), SRC3 (blue), and SRC3-pS543 (green) in proliferating MCF7 cells. Y bar shows tag count. Genomic*

coordinates are indicated. (B) Venn diagram of ERα (red), SRC3 (blue), and SRC3-pS543 (green). Numbers of shared and unique peaks are shown. (C) Heatmap visualization of ERα (red), SRC3 (blue), and SRC3-pS543 (green). (D) Motif analyses of ERα/SRC3-pS543 shared and SRC3-pS543 enriched binding sites. Z-score for each motif is shown in a MRP. Motif enrichment is shown for chromatin binding sites shared between ERα and SRC3-pS543 (red) or selectively enriched for SRC3-pS543 (green). The radial data points represent the absolute value of Z-score. (E) Genomic distributions of ERα, SRC3, and SRC3-pS543 sites. (F) Percentage of ERα-regulated genes with a SRC3-pS543 binding event at the promoter, compared with all refseq genes. χ2 test: P < 0.0001.

primer sequences and Supplementary Fig. S5B for genome browser snapshots of SRC3 and SRC3-pS543 ChIP-seq signal at these sites). To assess hormone dependency of SRC3-pS543 chromatin interactions, SRC3-pS543 ChIP-qPCR was performed on cells that were hormone deprived for 3 days, and subsequently treated for 3 hours with vehicle, E2, or tamoxifen (Supplementary Fig. S6). SRC3-pS543/chromatin interactions at SRC3-pS543-enriched sites (that were not bound by ERα) were hormone independent and not affected by ligand. For SRC3-pS543 sites shared with total SRC3, no chromatin binding was observed in the absence of hormone and in tamoxifen-treated cells, but this interaction was actively induced by E2 treatment. Phosphatase treatment abrogated SRC3-pS543 enrichment at these sites (Supplementary Fig. S6). Genomic distributions of ERα and SRC3 were comparable as reported by others (ref. 29; Supplementary Fig. S7). To further illustrate functional interplay between ERα and SRC3-pS543, ERα was depleted from MCF7 cells using Fulvestrant (Supplementary Fig. S6). SRC3-pS543/SRC3 shared, but not SRC3-pS543-enriched chromatin interactions were dependent on ERα levels, as shown by Fulvestrant-mediated ERα degradation (Supplementary Fig. S8). In order to identify potential selectivity of transcription factor usage, motif analyses were performed on the sites that were either or not shared between SRC3-pS543 and ERα, and visualized in a MRP (**Fig. 2D**). For the shared events, motif enrichment was found for classical luminal breast cancer–selective transcription factors, including ESR1 and forkhead motifs. For SRC3-pS543-enriched binding events, no motifs for ESR1 or FOXA1 were enriched, but a clear enrichment was observed for ELK, ELF, and ETV motifs (see also Supplementary Table S4 for the total list).

Differential motif enrichment could form the basis of differential gene expression programs. Therefore, GO pathway enrichment was assessed

for genes with an SRC3/chromatin binding event proximal (<20 kb) to their transcription start sites. GO terms highly varied for the differential SRC3 subclasses (Supplementary Fig. S9), with 1 out of 80 GO terms for SRC3 enriched sites ("biologic process") shared with the other two subsets. Interestingly, the majority of SRC3-pS543/SRC3 shared peak GO terms, 28 out of 37, were overlapping with those found for the SRC3-pS543-enriched sites, including "metabolic process," "gene expression," and "translation." For a complete list of all GO terms, see Supplementary Table S5.

Because the SRC3-pS543 chromatin binding events only recapitulated a proportion of the total SRC3 binding events, genomic distributions could deviate as well. As described before (15, 30), the majority of ERα and SRC3 binding events are found within enhancers and introns (**Fig. 2E**). In contrast, SRC3-pS543 binding was clearly enriched at promoter regions and 5′UTR, with promoter-bound SRC3-pS543 colocalizing with SRC3, ERα, and histone modifications indicative for active gene transcription (H3K4me2, H3K4me3, and H3K27Ac; Supplementary Fig. S10). As expected, SRC3 and ERα signal was found centered on the SRC3-pS543 signal. Because transcription factors bind accessible chromatin, histone marks indicative for active promoters (H3K4me3 and H3K27Ac) are found around the SRC3-pS543 sites instead of directly centered on them. Interestingly, this was not the case for H3K4me2, which was clearly enriched on the SRC3-pS543 peak. The enhancer-selective histone mark H3K4me1 was not enriched at SRC3-pS543 promoters. Even though less pronounced than the total of SRC3-pS543 peaks, the sites shared between ERα and SRC3-pS543 were also more promoter enriched (13.9%) as compared with the ERα/SRC3 shared regions (4.9%). Furthermore, SRC3-pS543 signal was highly enriched at promoters of E2-regulated genes (31) as compared with all Refseq genes (P < 0.0001; **Fig. 2F**).

SRC3-pS543 and ERα chromatin binding events in primary tumor tissue
Next, we determined phosphorylated SRC3/chromatin interactions in primary tumors (**Fig. 3**). ChIP-seq was performed on two independent ER+/PR+/HER2− breast tumor specimens as described (21, 24), and directly compared with the MCF7 cell line data. Peak intensities between the two tumors and the MCF7 sample were comparable, and peaks are well conserved (**Fig. 3A**). Between the two tumors and MCF7 cells, 2,670 binding events of SRC3-pS543 were shared (**Fig. 3B**, visualized in a raw heatmap in **Fig. 3C**). Furthermore, peaks were also found selectively enriched for only MCF7 (2,523 sites), tumor #1 (1,816 sites), or tumor #2 (4,631 sites). The SRC3-pS543 binding

sites from all samples were annotated for their genomic distributions, and again enrichment for promoters and 5′UTR regions was found (**Fig. 3D**). This was even more strikingly observed for binding events shared by all three samples, with 52% of all sites being localized to promoters and 20% at 5′UTR. For tumor #1, the lysate was divided in two prior to immunoprecipitation, and the second half of the lysate was used for ERα ChIP-seq, enabling a direct comparison of SRC3-pS543 and ERα binding patterns within the same tumor (**Fig. 3E**). Between ERα and SRC3-pS543, 1,727 binding events were shared, although 15,050 binding events were only found for ERα and 5,537 binding sites were only found for SRC3-pS543 (**Fig. 3F**). The shared and enriched binding patterns were not dictated by different thresholds in peak calling algorithms, as shown by heatmap analyses (**Fig. 3G**). The genomic distributions of ERα in the tumor sample closely resemble what was found in the cell line (**Fig. 2E**) and previously reported in breast tumor tissue (21, 24), with approximately 5% of ERα binding events being found at promoters, with the vast majority of sites located at distal enhancers and introns (**Fig. 3H**). The SRC3-pS543 sites (either or not shared with ERα), were highly enriched at promoters and 5′UTR regions.

Motif analyses for the ERα binding events in the tumor specimen revealed enrichment in ERα, FOXA1, and AP-2 motifs, as expected (refs. 30, 32; **Fig. 3I**). Enrichment for these specific motifs was found both for ERα-enriched sites as well as for sites shared between ERα and SRC3-pS543. Furthermore, practically all motifs found at SRC3-pS543–enriched sites were also found at the regions shared by ERα and SRC3-pS543 bounds, including motifs for ELK, ETV, and ETS factors as were observed in the MCF7 cells (see Supplementary Table S6 for the total list).

Association of total SRC3 and SRC3-pS543 with clinicopathologic features

Total SRC3 and SRC3-pS543 expression was evaluated in 1,650 breast carcinomas, with protein expression predominately nuclear (Supplementary Fig. S11). The total SRC3 mean histoscore was 157 (interquartile range, 0–300) and for SRC3-pS543 mean histoscore was 31 (interquartile range, 0–300). For subsequent analysis, total SRC3 expression was categorized as high (above mean, H-score > 157) or low (below mean, H-score < 157) and for SRC3-pS543 high (above mean, H-score > 31) or low (below mean, H-score ≤ 30; Supplementary Table S3). A scatterplot analysis of total SRC3 versus SRC3-pS543 in these tumors shows that the relative levels between total SRC3 ver-
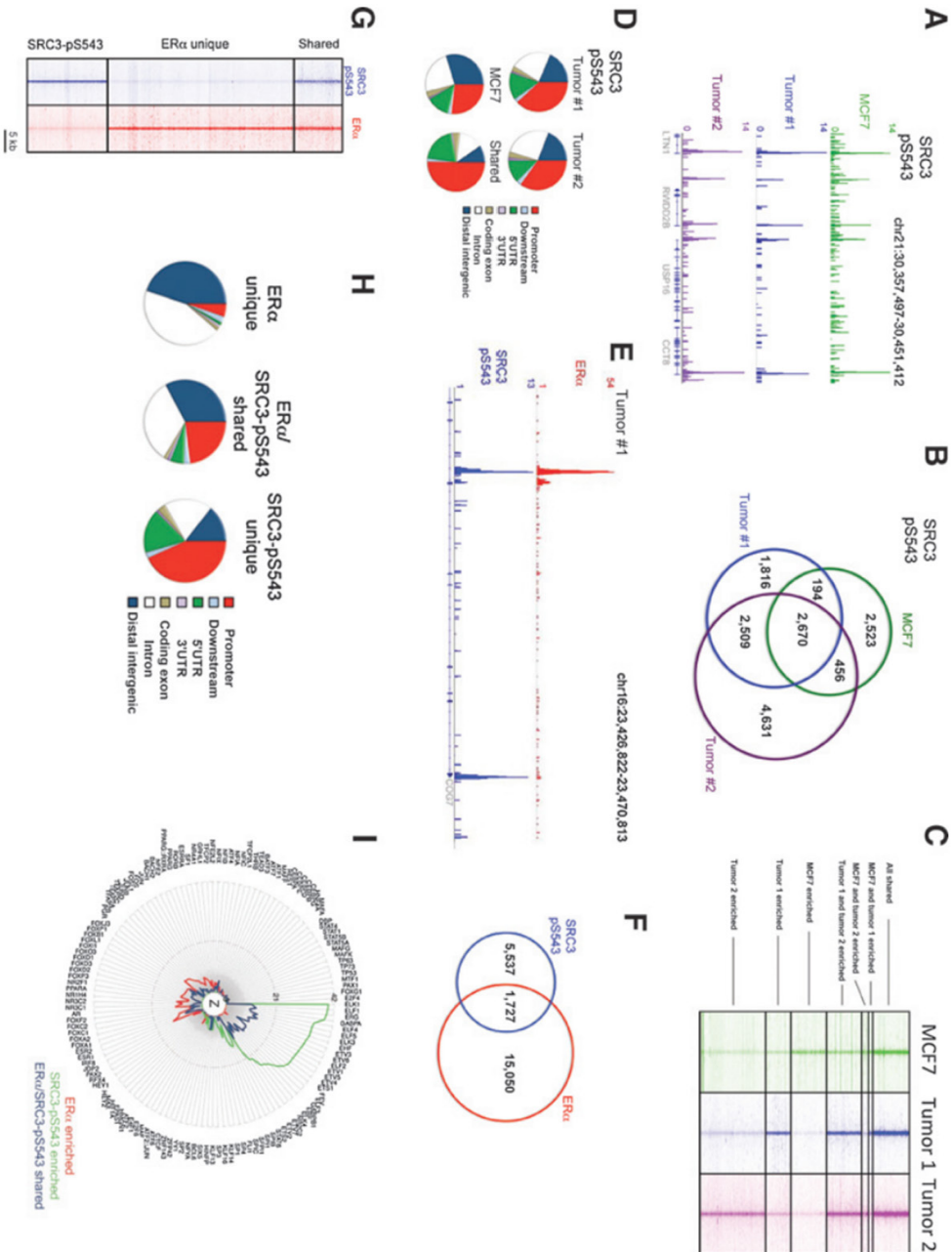
Figure 3: *SRC3-pS543 binding events in MCF7 cells and breast tumors.*
(A) Genome browser snapshot, ChIP-seq for SRC3-pS543 on MCF7 cells (green),

tumor sample #1 (blue), and tumor sample #2 (purple). Y bar shows tag count. Genomic coordinates are indicated. (B) Venn diagram of SRC3-S543P ChIp-seq for MCF7 cells (green), tumor sample #1 (blue), and tumor sample #2 (purple). Number of shared and unique sites is illustrated. (C) Heatmap visualization of SRC3-S543P ChIP-seq for MCF7 cells (green), tumor sample #1 (blue), and tumor sample #2 (purple). Number of shared and enriched sites is illustrated. (D) Genomic distributions of shared and unique SRC3-pS543 binding events for MCF7 cells, tumor sample #1, and tumor sample #2. (E) Genome browser snapshot, ChIP-seq on a primary breast tumor for ERα (red) and SRC3-pS543 (blue). (F) Venn diagram of ERα (red) and SRC3-pS543 (blue) binding events. (G) Heatmap analysis, depicting all shared and enriched binding events for ERα (red) and SRC3-pS543 (blue). Shown are all binding events with a window of 5 kb around the binding site. (H) Genomic distributions of the shared and enriched binding events of ERα and SRC3-pS543. (I) Motif analyses of the shared and enriched binding events of ERα and SRC3-pS543. Z-score for each motif is shown in a MRP. Motif enrichment is shown for chromatin binding sites enriched for ERα (red), SRC3-pS543 (green), or shared between ERα and SRC3-pS543 (blue). The radial data points represent the absolute value of Z-score.

sus SRC3-pS543 were strongly variable between tumors. Most importantly, a large proportion of tumors were identified that were positive for total SRC3, but negative for SRC3-pS543. Furthermore, no tumors could be identified that were positive for the phospho-SRC3 but negative for total SRC3, again highlighting specificity of the antibody (Supplementary Fig. S12).

Although no association on IHC between total SRC3 and ERα was found, there was a strong association for SRC3-pS543 with ERα (P = < 0.0001) and high expression of ERα-associated proteins (progesterone receptor; P = < 0.0001 and Bcl2; P = < 0.0001). Total SRC3 expression was significantly associated with HER2 (P = < 0.0001) and HER3 (P = 0.023), and correlated the absence of basal-like (P = 0.021) and triple negative phenotypes (P = 0.005; Table 1). SRC3-pS543 was significantly associated with well-differentiated (P ≤ 0.0001), low proliferative (P ≤ 0.0001) tumors, as well as androgen receptor (P ≤ 0.0001) expression. In addition, it was associated with the presence of p53 (P = 0.025) and the absence of MDM4 (P < 0.001) and MDM2 (P < 0.001), as well as the absence of both basal-like and triple negative phenotypes (P < 0.0001). The absence of SRC3-pS543 was significantly associated with the overexpression of HER4 (P < 0.0001), the presence of lympho-vascular invasion (P ≤ 0.0001), and loss of expression of the key DNA repair proteins, including BRCA1 (P < 0.0001), ATM (P <

0.0001), and TOP2A (P < 0.0001; Table 1). Apart from being phosphorylated by estrogen treatment, SRC3-S543 is also phosphorylated by JNK and p38 MAPK (16). In line with these previous observations, we find a significant correlation between the phosphorylated JNK and p38 MAPK with SRC3-pS543 (P < 0.0001; Table 1). Additional tumor biomarkers and their correlation with SRC3 and SRC3-pS543 are shown in Supplementary Table S7.

Association of total SRC3 and SRC3-pS543 expression with outcome

With regard to outcome, no association of total SRC3 with outcome was observed in the whole cohort (Supplementary Fig. S11A), the ERα-positive group in total (Supplementary Fig. S11B), or on the basis of tamoxifen treatment (Supplementary Fig. S11D–S11F). Furthermore, no association of total SRC3 with outcome was observed in the ERα-negative cohort (Supplementary Fig. S11C). However, expression of SRC3-pS543 in the whole cohort was associated with significantly longer disease-free survival (DFS) (P < 0.00001) and breast cancer specific survival (BCSS) (P = 0.0001; **Fig. 4A**). SRC3-pS543 expression in the ERα-positive cohort correlated with a longer DFS (P = 0.003) and BCSS (P = 0.001; **Fig. 4B**), although SRC3-pS543 did not associate with survival in ERα-negative breast cancers (**Fig. 4C**). Furthermore, in low-risk ERα-positive cancers, no correlation of SRC3-pS543 with outcome was found (**Fig. 4D**).

Importantly, SRC3-pS543 was associated with a longer DFS (P = 0.035) and BCSS (P = 0.005) in ER-positive high-risk breast cancer not treated with tamoxifen (**Fig. 4E**). In high-risk patients who did receive tamoxifen, SRC3-pS543 did not associate with a longer DFS (P = 0.57) or BCSS (P = 0.21; **Fig. 4F**). For ER-positive high-risk patients with low SRC3-pS543, exposure to tamoxifen reduced the risk of death from breast cancer [HR (95% CI) = 0.68 (0.49–0.94), P = 0.019] by 32% (**Fig. 4G**), whereas for those with high pS543, there was no effect (**Fig. 4H**), the interaction was statistically significant (P = 0.001). Similarly, exposure to tamoxifen reduced risk of recurrence by 42% [HR (95% CI) = 0.58 (0.44–0.77), P = 0.0001] in ER+ high-risk patients with low pS543, whereas no effect on those with high pS543 patients, the interaction was statistically significant (P = 0.000.1). Tamoxifen-treated patients with HER2-positive tumors that expressed high levels of SRC3 had a significantly shorter disease-free and BCSS. This was not observed for the patients who did not receive endocrine treatment (Supplementary Fig. S14). SRC3-pS543 was confirmed as an independent prognostic factor in breast cancers after adjustment for endocrine therapy and other validated prognostic
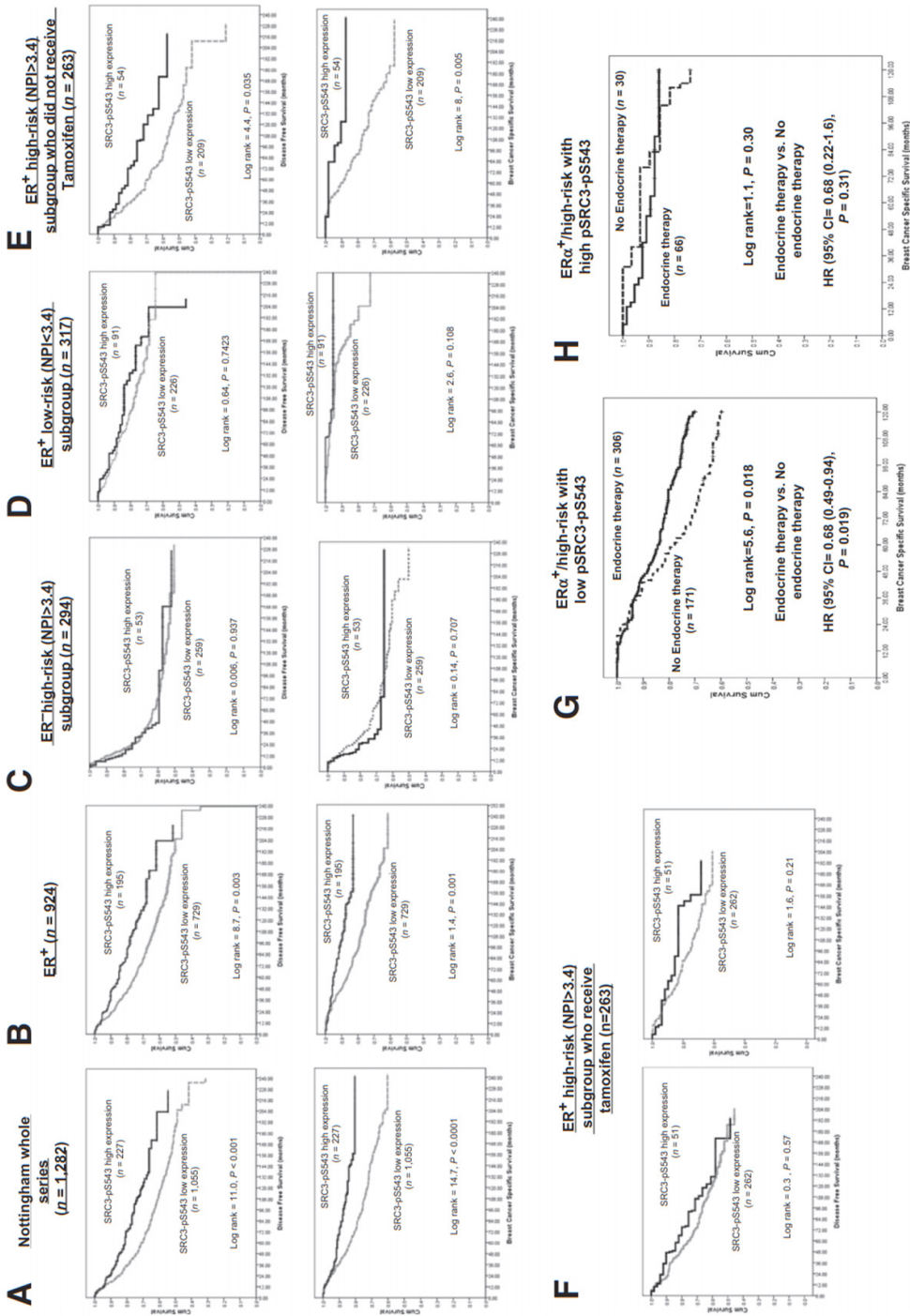
Figure 4: *DFS and BCSS in patients with breast cancer based on SRC3-pS543 protein expression.*
(A) Entire Nottingham cohort. (B) ERα-positive cohort. (C) ERα-negative cohort NPI > 3.4. (D) ERα-positive patients NPI < 3.4 who did not receive tamoxifen. (E) ERα-positive patients NPI ≥ 3.4 who did not receive tamoxifen. (F) ERα-positive patients NPI ≥ 3.4 who received tamoxifen. (G) BCSS based on SRC3-pS543 protein expression and tamoxifen treatment in the ERα-positive high-risk group with low pSRC3-pS543. (H) BCSS based on SRC3-pS543 protein expression and tamoxifen treatment in the ERα-positive high-risk group with high pSRC3-pS543.

factors; and absence of SRC3-pS543 signal correlated with recurrence (HR = 1.4, CI 95%, 1.1–2.5) and death from breast cancer (HR = 1.6, CI 95%, 1.1–2.5; Table 2).

Discussion

Coactivators for ERα have been the focus of many clinical and cell biologic studies. SRC3 is of particular interest, because the SRC3 gene is frequently amplified in breast cancer (7), and its expression was found to correlate with HER2 expression levels and poor outcome (11). SRC3 is a member of the p160 coregulator protein family (along with SRC1 and SRC2), which all have shared and preferred genome-wide chromatin binding patterns, which are strongly induced by ERα activation (15).

Here, we focus on one distinct phosphorylation event on SRC3, Serine 543 phosphorylation. This phosphorylation has spatial selectivity on a genomic scale, where chromatin binding was selectively enriched at active promoter regions. This genomic preference at promoters is on contrast to total SRC3, which is mainly found at enhancers. It is likely that SRC3 and SRC3-pS543 antibodies have different sensitivities, and the level of overlap detected between these two signals is possibly an underestimate of the actual proportion of SRC3 that is phosphorylated. Relative expression levels and antibody sensitivity are likely to alter the threshold of detection in ChIP-seq experiments, forming a major source for false-negative signal. Because the strongest total SRC3 sites are enhancer-selective, whereas the strongest SRC-pS543 were mostly enriched at promoters, this genomic selectivity of phosphorylated SRC3 to promoter regions cannot be merely explained by relative expression levels or antibody sensitivity.

Because ERα typically binds enhancers (30), the determination of which ERα binding events are functionally orchestrating what genes has re-

mained a challenge in the field. Because most ERα binding events are observed within a 20-kb window from the transcription start sites of responsive genes (33), this spacing around the promoter is typically applied to provide an indication of functionality. All p160 coactivators, including SRC3, show comparable genomic features as compared with ERα and are typically found at enhancers as well (15). Because the SRC3-pS543 phosphorylation is promoter-enriched, commonly shared with ERα and induced by estradiol, this phosphorylation event could be considered as a novel ERα functionality probe, highlighting ERα complexes that are actively involved in transcriptional events at gene promoters.

Smaller previous studies on SRC3 expression and its correlations with ERα and members of the EGFR/HER family have reported varying results (11–13). We find no correlation of SRC3 with ERα but do find a correlation with HER2 and HER3. However, SRC3-pS543 does significantly correlate with ERα, potentially reflecting the role of E2/ERα in phosphorylation of SRC3. Consistent with these results was the observed correlation of SRC3-pS543 with known estrogen-regulated genes, including PR. Although previous studies have explored the influence of SRC3 expression on patient outcome as well how it may influence endocrine therapy (11–13, 34–39), the current study is the largest and most well-characterized series to date, with a long median follow-up. We find no statistically significant association between SRC3 levels and DFS and BCSS in patients with ERα-positive breast cancer treated with tamoxifen, consistent with other reports (12, 13). Of note, in those women with ERα-positive tumors not treated with tamoxifen, there is a trend to an improved outcome and survival for SRC3-positive tumors, analogous to the first report relating SRC3 and response to endocrine therapy (11). The poor outcome seen in HER2-positive/SRC3-high tumors for patients treated with tamoxifen is consistent with previously published data (11, 12). One previous study on ERα-negative tumors, which utilized automated quantitative analysis in a subgroup of 133 patients, found SRC3 associated with a poorer overall survival (38). However, in the current study of 377 ERα-negative tumors no correlations with recurrence or outcome were found for SRC3. Of note, we show a significant correlation of p-JNK and p-p38 with SRC3-pS543. These kinases have previously been described to phosphorylate SRC3-S543 (16), and activated (phosphorylated) JNK has previously be linked to endocrine therapy resistance (37) (40), as well as poor outcome in breast cancer (41). The current study linking pJNK with high SRC3-pS543 and a good prognosis group is not comparable with these previous studies for

technical and methodological reasons. In the previous study, which investigated the expression of pJNK in human breast cancer (39), differing reagents, scoring system, as well as a smaller number of cases (n = 68) was used. Furthermore, 40% of the cases were ERα negative, and in those that were ERα positive no clinicopathologic correlation was presented (39). Although the other studies either investigated the activity of JNK and not its expression in the context of breast cancers exposed to tamoxifen (37) or where levels of pJNK were assessed via immunoblotting in the context of a MCF7 breast cancer xenograft model (38).

Our study is the first to explore the clinical significance of a phosphorylated form of SRC3. SRC3-pS543 correlates with an improved DFS and BCSS for the whole cohort and is a predictor of outcome in ERα-positive breast cancer. Furthermore, in high-risk ER-positive disease it is demonstrated that SRC3-pS543 is predictive of benefit with adjuvant tamoxifen. With no benefit being seen with adjuvant tamoxifen in the presence of high SRC3-pS543, although those tumors with low SRC3-pS543 had improved outcomes with tamoxifen treatment. The lack of benefit observed in high SRC3-pS543 tumors treated with tamoxifen indicates that the transcriptional events driven by SRC3-pS543 at gene promoters of ERα responsive result in a phenotype with an excellent clinical outcome, this would be consistent with the clinicopathologic features associated with SRC3-pS543. Although insufficiency or inability to enrich at these promoters as a result of low or absent SRC3-pS543 results in a more aggressive phenotype, which can be abrogated by tamoxifen.

The patient group studied here is a well-characterized historical cohort treated with or without tamoxifen. However, estrogen withdrawal therapy using aromatase inhibitors (AI) is now a standard clinical practice in the adjuvant setting for postmenopausal breast cancer, and correlations of response to AIs with (phosphorylated) SRC3 levels need to be assessed within this setting, particularly because the oncogenicity of SRC3 appears modulated by the hormonal milieu in mouse models (42). Currently, the translational arm of the Intergroup Exemestane Study (so-called Path-IES) is exploring the potential role of SRC3 and pS543 in this context (43).

In summary, we have found a novel biomarker for ERα-positive breast cancer and provide mechanistic insights in its functional involvement in the ERα transcription complex. SRC3-pS543 phospho-specific antibodies could aid in identifying patients with a functional ERα signaling pathway, which predicts for a favorable outcome in the absence of adjuvant therapy

and where tamoxifen might better be withheld.

Material and Methods

Cell lines, plasmids and antibodies.
MCF-7 and CHO cells were from the American Type Culture Collection (ATCC), which utilises short tandem repeat profiling with no authentication being performed by authors. All experiments were performed within 10 passages from the original stock. Cell lines were grown in DMEM with 10% FCS and standard antibiotics. Wild type SRC3 and mutant S543A plasmids kindly provided by BW O'Malley (Baylor College of Medicine). The antibodies used were SRC3 (Immunohistochemistry, BD Transduction Laboratories; 611105), SRC3 (ChIP-seq experiments, SC-9119; Santa Cruz), ERα (SC-543; Santa Cruz). A rabbit polyclonal antiserum for SRC3-pS543 was generated by immunising animals with the peptide 537-LLSTLSSPGPKLDN-550, where the residue in bold is phospho-serine (Moravian Biotechnologies, Czech Republic).

(Chromatin) Immunoprecipitations
Chromatin immunoprecipitations were performed according to standard protocols (Schmidt et al., 2009). Primary breast cancer specimens and proliferation MCF-7 breast cancer cells were used. Tissue was cryosectioned in 30 slices of 30 μm, and subsequently defrosted in solution A (50 mM Hepes, 100 mM NaCl, 1mM EDTA, 0.5 mM EGTA) supplemented with 1% formaldehyde. For MCF-7 cells, formaldehyde as added to the culture medium at a final concentration of 1%. After 10 minutes of fixation, 100 mM Glycine as added, after which cells were washed in PBS in presence of Protease Inhibitor (Roche Diagnostics 11836145001) and Phosphatase Inhibitors (Roche Diagnostics: 04906837001). Tissue was homogenized, and nuclei were isolated, washed and sonicated using a Diagenode Bioruptor as described before (Zwart et al., 2013, Jansen et al., 2013). After sonication, the lysate was cleared by centrifugation. For each ChIP 100μl of Dynabeads (Invitrogen) was used, precoupled overnight with 10μg of SRC3 or SRC-pS543 antibody. Immunoprecipitation was performed overnight while rotating at 4 degrees. Subsequently, beads were washed 10 times using RIPA buffer and reverse crosslinked at 65 degrees for 6 hours. Supernatant was removed, cleaned using a phenol/chloroform column and precipitated as described before (Schmidt et al., 2009). For standard Immunoprecipitations, beads were resuspended in sample buff-

er, boiled at 95˚C for 5mins and the samples run onto 8% Polyacrylamide gel for protein analysis for S543P, Input SRC3 and Immunoprecipitated (IP) SRC3. Immunoprecipitations were performed in presence of Protease Inhibitor (Roche Diagnostics 11836145001) and Phosphatase Inhibitors (Roche Diagnostics: 04906837001). When indicated, samples were incubated with Lambda Protein Phosphatase (Millipore; cat # 14-405) for 30 min prior to ChIP. Primer sequences for QPCR analysis are in Supplementary Table S1.

For MCF-7 experiments, ~6x107 asynchronous proliferating cells were used, and two independent replicates were performed for each ChIP-seq, where only consensus peaks that were found in both experiments were considered. For tumour specimen ChIP-seq, fresh snap-frozen primary ERα-positive, HER2-negative untreated breast cancers were obtained from the Imperial College Healthcare NHS Trust Tissue Bank which has the requisite ethical approval..

Solexa sequencing and enrichment analysis

ChIP DNA was amplified as described (Schmidt et al., 2009). Sequences were generated by the Illumina Hiseq 2000 genome analyser (using 50 bp reads), and aligned to the Human Reference Genome (assembly hg19, February 2009). Enriched regions of the genome were identified by comparing the ChIP samples to mixed input using the MACS peak caller (Zhang et al., 2008) version 1.3.7.1. Total read count, percentage of aligned reads and number of peaks for each ChIP-seq is shown in Supplementary Table S2. For histone modification data, publically available MCF-7 ChIP-seq data for H3K4me1 (GEO: GSM588568), H3K4me2 (GEO: GSM822392), H3K4me3 (GEO: GSM945269) and H3K27Ac (GEO: GSM945854) was used. For ERα ChIP-seq data, peaks from (Ross-Innes et al., 2012) were used. ChIP-seq data for SRC1, SRC2 and total SRC3 were from (Zwart et al., 2011b). For heatmap visualizations, Seqminer software was used.

Motif analysis, heatmaps and genomic distributions of binding events

ChIP-seq data snapshots were generated using the Integrative Genome Viewer IGV 2.1 (www.broadinstitute.org/igv/). Motif analyses were performed through the Cistrome (cistrome.org), applying the SeqPos motif tool (He et al., 2010). The genomic distributions of binding sites were analysed using the cis-regulatory element annotation system (CEAS) (Ji et al., 2006). The genes closest to the binding site on both strands were analysed. If the binding region is within a gene, CEAS software indicates whether it is in a 5′UTR, 3′UTR,

coding exon, or an intron. Promoter is defined as 3 kb upstream from RefSeq 5′ start. If a binding site is >3 kb away from the RefSeq transcription start site, it is considered distal intergenic.

Nottingham Tenovus Primary breast cancer Series

Primary operable breast cancer cases (n = 1,650) from the Nottingham Tenovus Primary Breast Carcinoma Series was utilised as described before (Elston and Ellis, 1991, Ellis et al., 1992), supplementary table S3. Patients were under the age of 71 years (median, 55 years), diagnosed between 1986 and 1999, and treated uniformly in a single institution. Patients within the good prognosis group (Nottingham Prognostic Index (NPI) <3.4) did not receive adjuvant therapy. Pre-menopausal patients within the moderate (NPI >3.4 to <5.4) and poor (NPI >5.4) prognosis groups were candidates for chemotherapy. Conversely, postmenopausal patients with ERα positive breast cancer with moderate or poor NPI were offered hormonal therapy, while ERα-negative patients received chemotherapy. Clinical data were maintained on a prospective basis with a median follow-up of 130 months (Range 2-311 months).

Immunohistochemistry

Breast cancer tissue microarrays (TMAs) from 1,650 cases were immuno-stained with SRC3 (Dilution 1:20) and SRC3-pS543 (Dilution: 1:2000) antibodies overnight at room temperature, after antigen retrieval (citrate buffer (pH 6.0) and microwave (20 minutes at 750Watts). Negative controls were performed by omission of the primary antibody. Nuclear staining was scored based on H-score. Determination of the optimal cut-offs was performed using X-tile bioinformatics software (Yale University, USA) and according to histogram distribution of H-score. For immunohistochemistry blocking experiments, peptides were used which contained the phospho-moiety (CLLSTLS-phosphoS-PGPKLDN) or the non-phospho peptide CLLSTLSSPGPKLDN). The peptides were pre-incubated overnight at 100 fold excess over antibody prior to staining as described previously.

Statistical analysis

Data analysis was performed using SPSS (SPSS, version 17 Chicago, IL). Where appropriate, Pearson's Chi-square, Fisher's exact, Student's t and ANOVAs one-way tests were used. Cumulative survival probabilities were estimated using the Kaplan–Meier method and differences between survival rates were tested using the log-rank test. Multivariate analysis for survival

was performed using the Cox hazard model. The proportional hazards assumption was tested using standard log-log plots. Hazard ratios (HR) and 95% confidence intervals (95% CI) were estimated for each variable, with $p<0.05$ as significant. For multiple comparisons, a stringent p value (<0.001) was considered significant.

Authors' Contributions
Conception and design: W. Zwart, S. Chan, R.C. Coombes, J.S. Carroll, S. Ali, C. Palmieri; Development of methodology: W. Zwart, B. Rudraraju, T.M.A. Abdel-Fatah, O. Gojis, S. Chan, J. Shaw, R.C. Coombes, J.S. Carroll, S. Ali, C. Palmieri; Acquisition of data (provided animals, acquired and managed patients, provided facilities, etc.): W. Zwart, K.D. Flach, B. Rudraraju, T.M.A. Abdel-Fatah, D. Moore, M. Opdam, I. Hofland, S. Chan, I.O. Ellis, R.C. Coombes, C. Palmieri; Analysis and interpretation of data (e.g., statistical analysis, biostatistics, computational analysis): W. Zwart, K.D. Flach, B. Rudraraju, T.M.A. Abdel-Fatah, S. Canisius, E. Nevedomskaya, M. Opdam, M. Droog, S. Chan, J. Shaw, I.O. Ellis, R.C. Coombes, J.S. Carroll; Writing, review, and/or revision of the manuscript: W. Zwart, K.D. Flach, T.M.A. Abdel-Fatah, S. Chan, I.O. Ellis, R.C. Coombes, S. Ali, C. Palmieri; Administrative, technical, or material support (i.e., reporting or organizing data, constructing databases): B. Rudraraju, T.M.A. Abdel-Fatah, M. Opdam, S. Chan, C. Palmieri; Study supervision: W. Zwart, S. Chan, R.C. Coombes
The authors declare no conflict of interest.

References

1. Ali S, Coombes RC. Endocrine-responsive breast cancer and strategies for combating resistance. Nature Rev Cancer 2002;2:101–12.

2. York B, O'Malley BW. Steroid receptor coactivator (SRC) family: masters of systems biology. J Biol Chem 2010;285:38743–50.

3. List HJ, Lauritsen KJ, Reiter R, Powers C, Wellstein A, Riegel AT. Ribozyme targeting demonstrates that the nuclear receptor coactivator AIB1 is a ratelimiting factor for estrogen-dependent growth of human MCF-7 breast cancer cells. J Biol Chem 2001;276:23763–8.

4. Torres-Arzayus MI, Font de Mora J, Yuan J, Vazquez F, Bronson R, Rue M, et al. High tumor incidence and activation of the PI3K/AKT pathway in transgenic mice define AIB1 as an oncogene. Cancer Cell 2004;6: 263–74.

5. Kuang SQ, Liao L, Wang S, Medina D, O'Malley BW, Xu J. Mice lacking the amplified in breast cancer 1/steroid receptor coactivator-3 are resistant to chemical carcinogen-induced mammary tumorigenesis. Cancer Res 2005; 65:7993–8002.

6. Fereshteh MP, Tilli MT, Kim SE, Xu J, O'Malley BW, Wellstein A, et al. The nuclear receptor coactivator amplified in breast cancer-1 is required for Neu (ErbB2/HER2) activation, signaling, and mammary tumorigenesis in mice. Cancer Res 2008;68:3697–706.

7. Anzick SL, Kononen J, Walker RL, Azorsa DO, Tanner MM, Guan XY, et al. AIB1, a steroid receptor coactivator amplified in breast and ovarian cancer. Science 1997;277:965–8.

8. Murphy LC, Simon SL, Parkes A, Leygue E, Dotzlaw H, Snell L, et al. Altered expression of estrogen receptor coregulators during human breast tumorigenesis. Cancer Res 2000;60:6266–71.

9. Bouras T, Southey MC, Venter DJ. Overexpression of the steroid receptor coactivator AIB1 in breast cancer correlates with the absence of estrogen and progesterone receptors and positivity for p53 and HER2/neu. Cancer Res 2001;61:903–7.

10. Gojis O, Rudraraju B, Gudi M, Hogben K, Sousha S, Coombes RC, et al. The role of SRC-3 in human breast cancer. Nature Rev Clin Oncol 2010;7:83–9.

11. Osborne CK, Bardou V, Hopp TA, Chamness GC, Hilsenbeck SG, Fuqua SA, et al. Role of the estrogen receptor coactivator AIB1 (SRC-3) and HER-2/neu in tamoxifen resistance in breast cancer. J Natl Cancer Inst 2003;95: 353–61.

12. Kirkegaard T, McGlynn LM, Campbell FM, Muller S, Tovey SM, Dunne B, et al. Amplified in breast cancer 1 in human epidermal growth factor receptor–positive tumors of tamoxifen-treated breast cancer patients. Clin Cancer Res 2007;13:1405–11.

13. Dihge L, Bendahl PO, Grabau D, Isola J, Lovgren K, Ryden L, et al. Epidermal

growth factor receptor (EGFR) and the estrogen receptor modulator amplified in breast cancer (AIB1) for predicting clinical outcome after adjuvant tamoxifen in breast cancer. Breast Cancer Res Treat 2008; 109:255–62.

14. Alkner S, Bendahl PO, Grabau D, Lovgren K, Stal O, Ryden L, et al. AIB1 is a predictive factor for tamoxifen response in premenopausal women. Ann Oncol 2010;21:238–44.

15. Zwart W, Theodorou V, Kok M, Canisius S, Linn S, Carroll JS. Oestrogen receptor-co-factor-chromatin specificity in the transcriptional regulation of breast cancer. EMBO J 2011;30:4764–76.

16. Wu RC, Qin J, Yi P, Wong J, Tsai SY, Tsai MJ, et al. Selective phosphorylations of the SRC-3/AIB1 coactivator integrate genomic reponses to multiple cellular signaling pathways. Mol Cell 2004;15:937–49.

17. Oh AS, Lahusen JT, Chien CD, Fereshteh MP, Zhang X, Dakshanamurthy S, et al. Tyrosine phosphorylation of the nuclear receptor coactivator AIB1/SRC-3 is enhanced by Abl kinase and is required for its activity in cancer cells. Mol Cell Biol 2008;28:6580–93.

18. Li C, Liang YY, Feng XH, Tsai SY, Tsai MJ, O'Malley BW. Essential phosphatases and a phospho-degron are critical for regulation of SRC-3/AIB1 coactivator function and turnover. Mol Cell 2008;31:835–49.

19. Xu J, Li Q. Review of the in vivo functions of the p160 steroid receptor coactivator family. Mol Endocrinol 2003;17:1681–92.

20. Schmidt D, Wilson MD, Spyrou C, Brown GD, Hadfield J, Odom DT. ChIPseq: using high-throughput sequencing to discover protein-DNA interactions. Methods 2009;48:240–8.

21. Zwart W, Koornstra R, Wesseling J, Rutgers E, Linn S, Carroll JS. A carrierassisted ChIP-seq method for estrogen receptor-chromatin interactions from breast cancer core needle biopsy samples. BMC Genomics 2013; 14:232.

22. Jansen MP, Knijnenburg T, Reijm EA, Simon I, Kerkhoven R, Droog M, et al. Hallmarks of aromatase inhibitor drug resistance revealed by epigenetic profiling in breast cancer. Cancer Res 2013;73:6632–41.

23. Zhang Y, Liu T, Meyer CA, Eeckhoute J, Johnson DS, Bernstein BE, et al. Model-based analysis of ChIP-Seq (MACS). Genome Biol 2008;9: R137.

24. Ross-Innes CS, Stark R, Teschendorff AE, Holmes KA, Ali HR, Dunning MJ, et al. Differential oestrogen receptor binding is associated with clinical outcome in breast cancer. Nature 2012;481:389–93.

25. He HH, Meyer CA, Shin H, Bailey ST, Wei G, Wang Q, et al. Nucleosome dynamics define transcriptional enhancers. Nature Genetics 2010;42: 343–7.

26. Ji X, Li W, Song J, Wei L, Liu XS. CEAS: cis-regulatory element annotation sys-

tem. Nucleic Acids Res 2006;34(Web Server issue):W551–4.

27. Elston CW, Ellis IO. Pathological prognostic factors in breast cancer. I. The value of histological grade in breast cancer: experience from a large study with long-term follow-up. Histopathology 1991;19:403–10.

28. Ellis IO, Galea M, Broughton N, Locker A, Blamey RW, Elston CW. Pathological prognostic factors in breast cancer. II. Histological type. Relationship with survival in a large study with long-term follow-up.
Histopathology 1992;20:479–89.

29. Madak-Erdogan Z, Charn TH, Jiang Y, Liu ET, Katzenellenbogen JA, Katzenellenbogen BS. Integrative genomics of gene and metabolic regulation by estrogen receptors alpha and beta, and their coregulators. Mol Syst Biol 2013;9:676.

30. Carroll JS, Liu XS, Brodsky AS, Li W, Meyer CA, Szary AJ, et al. Chromosome-wide mapping of estrogen receptor binding reveals long-range regulation requiring the forkhead protein FoxA1. Cell 2005;
122:33–43.

31. Zwart W, Theodorou V, Carroll JS. Estrogen receptor-positive breast cancer: a multidisciplinary challenge. Wiley Interdiscip Rev Syst Biol Med 2011;3: 216–30.

32. Tan SK, Lin ZH, Chang CW, Varang V, Chng KR, Pan YF, et al. AP-2gamma regulates oestrogen receptor-mediated long-range chromatin interaction and gene transcription. EMBO J 2011;30:2569–81.

33. Fullwood MJ, Liu MH, Pan YF, Liu J, Xu H, Mohamed YB, et al. An oestrogen-receptor-alpha-bound human chromatin interactome. Nature 2009;462:58–64.

34. Bautista S, Valles H, Walker RL, Anzick S, Zeillinger R, Meltzer P, et al. In breast cancer, amplification of the steroid receptor coactivator gene AIB1 is correlated with estrogen and progesterone receptor positivity. Clin Cancer Res 1998;4:2925–9.

35. List HJ, Reiter R, Singh B, Wellstein A, Riegel AT. Expression of the nuclear coactivator AIB1 in normal and malignant breast tissue. Breast Cancer Res Treat 2001;68:21–8.

36. Hudelist G, Czerwenka K, Kubista E, Marton E, Pischinger K, Singer CF. Expression of sex steroid receptors and their co-factors in normal and malignant breast tissue: AIB1 is a carcinoma-specific co-activator. Breast Cancer Res Treat 2003;78:193–204.

37. Thorat MA, Turbin D, Morimiya A, Leung S, Zhang Q, Jeng MH, et al. Amplified in breast cancer 1 expression in breast cancer. Histopathology 2008;53:634–41.

38. Harigopal M, Heymann J, Ghosh S, Anagnostou V, Camp RL, Rimm DL. Estrogen receptor co-activator (AIB1) protein expression by automated quantitative analysis (AQUA) in a breast cancer tissue microarray and association with patient outcome. Breast Cancer Res Treat 2009;115:77–85.

39. Iwase H, Omoto Y, Toyama T, Yamashita H, Hara Y, Sugiura H, et al. Clinical significance of AIB1 expression in human breast cancer. Breast Cancer Res Treat 2003;80:339–45.

40. Schiff R, Reddy P, Ahotupa M, Coronado-Heinsohn E, Grim M, Hilsenbeck SG, et al. Oxidative stress and AP-1 activity in tamoxifen-resistant breast tumors in vivo. J Natl Cancer Inst 2000;92:1926–34.

41. Yeh YT, Hou MF, Chung YF, Chen YJ, Yang SF, Chen DC, et al. Decreased expression of phosphorylated JNK in breast infiltrating ductal carcinoma is associated with a better overall survival. Int J Cancer 2006;118:2678–84.

42. Torres-Arzayus MI, Zhao J, Bronson R, Brown M. Estrogen-dependent and estrogen-independent mechanisms contribute to AIB1-mediated tumor formation. Cancer Res 2010;70:4102–11.

43. Viale G, Speirs V, Bartlett JM, Mousa K, Kalaitzaki E, Palmieri C , et al. Prognostic and predictive value of IHC4 and ER in the Intergroup Exemestane Study (IES). Ann Oncol 2013;24(Suppl 3):iii37.

Table 1*: Patient characteristics and tumor biomarkers and correlation SRC3 and SRC3-pS543*
See online supplemental information

Supplementary information

Supplementary Figure 1-14 and table 1-6
See online supplemental information

Table 2: *Multivariate analysis using Cox regression analysis confirms that SRC3-pS543 protein expression is an independent prognostic factor for both DFS and BCSS*

Variable	BCSS at 10 years		DFS at 10 years	
	HR (CI 95%)	P	HR (CI 95%)	P
S543 (low expression)	1.6 (1.1–2.5)	0.024[*]	1.4 (1.0–1.9)	0.038[*]
Tumor size	1.1 (1.0–1.3)	0.056	1.1 (1.0–1.2)	0.017^{-7a}
Grade		0.018[*]		0.933
G1	1.0		1.0	
G2	1.4 (1.3–3.1)		0.98 (0.7–1.4)	
G3	2.1 (2.6–5.7)		1.03 (1.2–2.0)	
Lymph node stage		$9.6 \times 10^{-11*}$		$1.6 \times 10^{-10*}$
Negative	1		1	
Positive (1–3 nodes)	1.7 (1.3–2.3)		1.4 (1.1–1.8)	
Positive (>3 nodes)	3.6 (2.5–5.3)		3.2 (2.3–4.4)	
Endocrine therapy (no)	1.1 (0.8–1.4)	0.661	0.9 (0.7–1.2)	0.565
Chemotherapy (no)	1.2 (0.9–1.7)	0.259	1.3 (1.0–1.7)	0.03
Bcl2 expression (positive)	0.4 (0.3–0.6)	$6.8 \times 10^{-8*}$	0.5 (0.4–0.7)	$9.2 \times 10^{-7*}$
Ki67 expression (high)	1.5 (1.1–2.2)	0.022[*]	1.3 (1.0–1.7)	0.093[*]
ER expression (negative)	1.5 (1.1–2.1)	0.016[*]	1.4 (1.0–1.8)	0.036[*]
HER2 (overexpression)	1.7 (1.2–2.4)	0.002[*]	0.7 (0.5–1.0)	0.03[*]

Statistically significant

Chapter 7

Discussion

ERα-positive breast cancer and endocrine resistance prediction

Breast cancer remains the most prevalent form of cancer in women, with approximately 1.7 million annual new diagnoses, while despite the improvement of breast cancer treatment over the years, still over half a million women die of this disease every year (1). The majority of these tumors (70-80%) express estrogen receptor α (ERα) and tumor cell proliferation is thought to be dependent on the activity of this hormone-mediated transcription factor (2, 3). Endocrine treatments options of ERα-positive breast cancer mainly consist of receptor-inhibition by anti-estrogens (e.g. tamoxifen) (4-6) or by inhibition of the estrogen biosynthesis (e.g. aromatase inhibitors) (7). Despite the fact that these treatment modalities have greatly aided in the improvement of patients survival, a large proportion of the patients do not respond, which can ultimately leading to a relapse with limited additional treatment options left due to the development of endocrine resistance (8, 9). As there are multiple ways tumors can become resistant to therapy, a better understanding of the mode of action of ERα and the development of resistance, coupled with the use of biomarkers that can predict the treatment response of a patients on an individual bases could further increase patient survival.

An example of how the discovery of a mechanism behind tamoxifen-resistance can lead to the discovery of a predictive biomarker, is the activation of the protein kinase A (PKA) pathway and the resulting phosphorylation of ERα at Serine residue 305 (ERαS305-P) (10) (**Chapter 2**). Whereas tamoxifen normally inhibits the recruitment of essential coregulators, S305-P induces a conformational change still enabling the composition of an ERα transcriptional complex even when bound by tamoxifen (Michalides et al., 2004, Zwart et al., 2007), affecting the ERα cistrome and transcriptome (Carascossa et al., 2010, Lupien et al., 2009). In **Chapter 2** we demonstrated that although a large proportion of ERαS305-P chromatin interactions overlapped with the cistrome of total ERα, a surprising significant increase in promoter deposition was be observed, resulting in differential gene expression and tamoxifen resistance. The recent finding that besides PKA-activation, pro-inflammatory cytokines are also capable of inducing tamoxifen resistance in MCF-7 cells by the induction of S305-P (11), further strengthens the role of ERαS305-P in tamoxifen resistance. Stender et al. demonstrated that cytokine activation of ERα is dependent on the S305-phosphorylation and is mediated by IKKβ and, similar to PKA-activation, leads to increased levels of MYC. Additionally they show that also this mode of S305-phosphorylation results in a cistrome that substantially overlaps with the conventional estradi-

ol induced ERα cistrome, although the resulting differential gene expression profile differs from the one we found. This difference might be best explained by the difference in stimulation (three hours of estradiol versus four hours of tamoxifen) and the additional exposure of MCF-7 cells to 10 ng/ml TNFα or 10 ng/ml IL1β. Nevertheless, the above findings further strengthen the key role S305-phosphorylation can play in tamoxifen resistance, induced not only by PKA-activation, but possibly also by the tumor microenvironment (11).

The altered gene expression profile as a result of PKA-activation we found in **Chapter 2** could be translated into a gene signature capable of predicting patients response to tamoxifen treatment, potentially allowing the selection of patients that would not benefit from adjuvant tamoxifen and directly providing an alternative treatment modality. This ERαS305-P derived classifier has been tested in a cohort of patients treated with tamoxifen in the adjuvant setting, but unfortunately this cohort lacks a randomized control arm of patients not having received tamoxifen. As this set-up does not allow one to distinguish whether a biomarker is prognostic (natural course of the disease) or predictive (tamoxifen treatment specific), it is crucial to make use of a cohort containing a non-tamoxifen treated group, thus providing an extra level of evidence in predictive biomarker discovery (12).

Compared to the ERαS305-P derived classifier, our findings on the potential of SRC3-pS543 prognostication (**Chapter 6**) provide an additional level of evidence that SRC3-pS543 could be a predictive biomarker with regards to tamoxifen treatment outcome. We demonstrated that SRC3-pS543 phospho-specific antibodies could identify patients with a functional ERα pathway, which is indicative of a favourable outcome in the absence of adjuvant therapy and where tamoxifen is likely not to induce any survival benefit. This additional level of evidence was derived from the Nottingham Tenovus Primary Breast Carcinoma Series we used, which in contrast to the ERαS305-P cohort, besides patients that did received adjuvant tamoxifen, also contains patients which did not receive any adjuvant therapy (13). Herein patients with a poor prognosis (based on tumor grade) received adjuvant tamoxifen and patients with a good prognosis did not. However, this discrepancy between the survival prognosis of the two patients arms isn't ideal as it now remains unclear whether SRC3-pS543 phospho-specific antibodies are genuinely predictive of tamoxifen treatment, or whether they are only associated with survival in patients with a poor prognosis. In order to rule out this type of bias and to achieve even more confidence that a certain biomarker or gene signature is truly predictive of any treatment effect, one could

make use of a cohort containing a matched non-tamoxifen treated group, as was used to assess the predictive capacity of FEN1 (**Chapter 5**). Herein a cohort was used containing tissue blocks from postmenopausal breast cancer patients randomized between tamoxifen and no adjuvant therapy (14), allowing us to directly assess FEN1's tamoxifen specific predictive potential. However it must be noted that during patient accrual in this cohort, it became clear that lymph node positive patients show a great survival benefit from tamoxifen, so after 1989, these patients skipped the first randomization and all received 1 year of tamoxifen, meaning all analyses had to be stratified for nodal status (negative versus positive). Previous research had already shown that FEN1 levels could be indicative of patient outcome but limited its investigation merely to the total population of breast cancer patients, thus analysing both ERα-negative and ERα-positive patients together (15). By analysing the different hormone receptor status of breast cancer patients separately, we were able to demonstrate that FEN1 levels are not indicative of outcome in ERα-negative breast cancers but are in ERα-positive patients, suggesting an ERα-specific biomarker in breast cancer. More importantly, we demonstrated that only in ERα-positive patients receiving adjuvant tamoxifen FEN1 levels were associated with outcome, allowing the use of FEN1 as a predictive marker for tamoxifen treatment response. In line with these findings, we provided evidence that in breast cancer cell lines FEN1 levels are able to dictate ERα-driven cell proliferation in the presence of tamoxifen. By combining successful biomarker-driven patient stratification with matching cell line experiments and biological insights, one can increase the body of evidence that a certain biomarker is truly predictive by incorporating causal cell line data.

The final step to determine with the highest level of confidence whether FEN1 is a predictive marker of tamoxifen efficacy would be to step away from the use of retrospective patients cohorts and move to a prospective trial where patients are randomized between adjuvant tamoxifen or no tamoxifen on the basis of their FEN1 levels. Recently the results from such a trial were reported for a 70-gene signature (MammaPrint) (16, 17), demonstrating the clinical utility of this signature. When drawing the parallel between our FEN1 biomarker and this 70-gene signature, which was first reported in 2002, it becomes clear that still a lot of work has to be done in order to fully demonstrate the clinical functionality of FEN1 as a predictive marker for tamoxifen resistance. In order for this type of prospective trial to be worthwhile for FEN1, it will first be important to validate our findings in additional cohorts, preferably in patient cohorts containing more contemporary hormonal thera-

pies (e.g. five years of an aromatase inhibitor (AI) alone, two-three years of tamoxifen followed by five years of an AI, or less common 5 years of TAM). Although these types of cohorts would be extremely valuable, they are unfortunately extremely rare. In the patient cohort that was utilized for FEN1 explorations, patients were treated with adjuvant tamoxifen only, while currently most postmenopausal breast cancer patients receive an aromatase inhibitor alone, or preceding/following tamoxifen treatment. In part we addressed this difference by investigating FEN1 levels in the non-randomized METABRIC (18), in which FEN1 levels were predictive of treatment outcome in patients treated with more contemporary hormonal therapy strategies. Additionally our cell proliferation data show that in the absence of estradiol FEN1 was able to stimulate cell proliferation, a setting close to the aromatase inhibitor setting.

ERα-cistromics and posttranslational modifications

As described above, in **Chapter 2** we demonstrated that the PKA-induced post-translational modification of ERα (S305-P) can have a major impact on its cistrome, transcriptome and cellular phenotypic behaviour. Besides this well-known and characterized ERα-phosphorylation, other phosphorylation sites are also know to alter ERα-activity and/or correlate with patient outcome (e.g. serine residues 104/106 (19), 118 (20) and 167 (21)). In **Chapter 3**, we provided experimental evidence for a previously unknown ERα-phosphorylation (T594P) and demonstrate that 14-3-3 proteins can interact directly with ERα, which is the basis of the regulatory role of T594P in ERα-regulation. We were able to increase the levels of T594P in cell lines by shielding the phosphorylation site with fusicoccin (FC) (22), the most-likely mechanism of action being a blocked access of phosphatases to the phosphorylated Threonine (23, 24). Induction of T594P greatly decreased ER-chromatin interactions, E2-driven gene transcription and ultimately blocked cell growth. What makes T594P different from most other ERα-phosphorylations is that it is a relatively short-lived intermediate and it regulates ERα-activity in such a different way than other well characterized phosphorylation; our data indicates a model wherein T594P at the ERα C-terminal tip negatively affects receptor dimerization and transactivation through its interaction with 14-3-3 proteins, which could be enhanced by stabilizing the T594P with FC. Perhaps this role of T594P could be part of a regulatory mechanism to keep the levels of ERα-activity within normal physiological boundaries. A first step to determine how prominent this role is would be to compare T594P levels between

normal breast tissue and breast cancer tissue by IHC. Higher levels of T594P levels could indicate that during breast cancer development, the inhibitory mechanism of T594P gets down-regulated.

Besides ERα itself, the phosphorylation of ERα-coactivators can also redirect the cistromic repertoire of ERα, as exemplified by the activating S543-phosphorylation of SRC3 (**Chapter 6**). SRC3 upregulation is, in combination with increased ERBB2 expression, known to correlate with a poor tamoxifen response (25-28). SRC3 is normally predominately found together with ERα at distal enhancers and introns. SRC3-pS543 however, showed a striking increase in promoter deposition, both in cell lines and tumor material, although for now it remains unclear which event is first; the S543-phosphorylation or the deposition of an SRC3/ERα complex near a gene promoter triggering subsequent SRC3-phosphorylation. The use of SRC3 knock-out/down cells with a reconstituted dominant active S543-pointmutant in combination with SRC3 ChIP-seq could, by investigating the potential enrichment of binding events at the SRC3-pS543 enriched promoters, aid in the understanding of this order of events. The altered cistromic profile, together with our findings that SRC3-pS543 expression was associated with a poor response to tamoxifen treatment, makes it very likely that pS543 alters the gene expression profile of breast cancer and thus ultimately its phenotype. A possible explanation for this could come from differential cofactor recruitment by ERα when bound by SRC3-pS543 when compared to an un-phosphorylated SRC3. Investigating the composition of the ERα-transcriptional complex by making use of RIME (rapid immunoprecipitation mass spectrometry of endogenous proteins) (29) in SRC3 knock-out/down cells with an inactive S543-pointmutant (thus disabling phosphorylation) could shed a light on any altered cofactor recruitment. Recent publications have not only shown promising results in SRC3-targeted therapies (30-32), but also demonstrated that ERα-bound SRC3 results in the recruitment of CARM1 which enables methyltransferase activity of the ERα-complex and induces a conformational change of p300 which increases its HAT-activity and ultimately enhanced transcriptional activity of the ERα-complex (33). Additionally, the posttranslational modifications of ERα-coactivators such as SRC2-S736-phosphorylation (facilitating SRC2 recruitment to the ERα complex) (34) and sumolation of the CREB-binding protein (CBP) at lys 999, 1034, and 1057 (repressing its transcriptional activity) (35), further demonstrate the impact of coactivators and their posttranslational modifications can have on the functionality and behaviour of the ERα-complex. It is likely that the ERα-transcriptional com-

plex functions within a fine balance of activating and inhibiting modifications which together determine ERα's cistromic profile and functionality.

Novel drug targets in ERα-biology

Minimization of predictive gene-profiles, as found in **Chapter 2**, can make a classifier more easily implementable in clinical practice. Especially when only protein levels of one or a few proteins are sufficient this can be added with relative ease to existing pathological (IHC) assessment. Besides their use in patient prognostication, predictive gene-profiles can also be useful for identification of novel drug targets or biological insights in ERα biology. An example of this is the identification of FEN1 as a crucial ERα-regulator by the computational refinement of a previously reported predictive gene profile consisting of 111-genes (36) (**Chapter 5**). We were able to minimize the number of genes needed from this classifier towards a minimum of 4 genes (FEN1, HBP1, MCM2 and STARD13). Individual assessment of these genes as predictive biomarkers in both ERα-positive and negative patients demonstrated the exclusive ERα-positive predictive potential of FEN1. Where FEN1 previously has been reported to be a prognostic biomarker in breast cancer patients (containing both ERα-positive and negative patients) (15), we demonstrated that this is most likely due to the ERα-positive patient population. We found that FEN1 is an ERα-cofactor and modifying its activity by knockdown or overexpression altered ERα-activity, implying FEN1 might be a promising drug target in ERα-positive breast cancer. The small compound screen we performed for FEN1 inhibition, ultimately led to the discovery of a FEN1-specific and potent inhibitor, active in the nanomolar range. To demonstrate its potential as novel drug target we assessed its efficacy in cancer cell lines, where the inhibitor showed a clear sensitivity of ERα-positive breast cancer cell lines when compared to ERα-negative cell lines. Additionally, tamoxifen resistant derivatives of ERα-positive cell lines showed an increased sensitivity for the FEN1 inhibitor, suggesting FEN1 inhibition might be useful in tamoxifen resistant breast cancer patients as an alternative therapy. Although tamoxifen-resistant cell lines (37) and tumors (38) still require ERα function and are thereby targetable by FEN1 inhibition, the exact reason behind this increased sensitivity remains unknown. A possible explanation could be the role FEN1 plays in ERα-mediated DNA-demethylation as in the tamoxifen resistant cell line MCF-T, activation of growth-promoting genes by promotor hypomethylation was observed more frequently than in sensitive cells (39). It's possible FEN1 plays a crucial role in this promoter demethyla-

tion, but further research is needed to validate this hypothesis.

As we tested our inhibitor in cell lines that have been around for a long time and were cultured in the artificial setting of a petridish and might therefor not resemble the primary tumor situation anymore, we next turned to the use of clinical specimens. Primary tumor explants of ERα-positive breast cancer patients were cultured in the presence or absence of our FEN1 inhibitor, demonstrating a clear decrease in tumor proliferation (as assessed by Ki76 staining) upon FEN1 inhibition, performing equally well as tamoxifen in this setting. FEN1 inhibitors have previously been described to be effective as chemo-sensitizers (40, 41) or as a part of synthetic lethal interactions (42, 43), but were not considered to be an effective therapy strategy on their own (44). We however demonstrate that by specifically targeting ERα-positive breast cancer, FEN1 inhibition might be an effective single-agent application. Although promising, it is still far too early to state whether FEN1 inhibition is a realistic therapeutic option on its own.

Multiple rounds of validation, drug optimization and cytotoxicity assessments would have to be performed, before a phase 1 clinical trial could be considered. We did already perform some exploratory cytotoxicity experiments in mice, demonstrating mice were coping well with levels of up to 10mg/kg of FEN1 inhibitor, administered bi-daily. Measurements of FEN1 inhibitor levels in the blood of these mice, showed that there was on average 400-500 nM of compound left four hours after injection. Unfortunately a rapid decrease in inhibitor levels (estimated half-time 2 hours) was observed, which could possibly limit drug efficacy on tumor growth. We have tested the compound in 20 mice, but our screen hit was not sufficiently effective to block ERα-driven tumor cells in these animals. An explanation for the lack of efficacy could be found in the fact that due to the high half-time of 2 hours, there might not have been high enough inhibitor levels to achieve a (relative) continues blockage of FEN1 function, enabling recovery of ERα-function during times of FEN1 inhibitor absence. This explanation is substantiated by cell lines experiments where a continuous exposure of FEN1 inhibitor yielded the best results with regards to inhibition, and bi-daily drug treatment with extensive washing after four hours was inferior to the continues exposure with regards to the degree of inhibition of cell proliferation (data not shown). As the inhibitor we have now used has not gone through a medicinal chemistry compound optimization pipeline, and thus is not expected to have optimal AdMe/Tox properties, it would be advisable to see whether drug optimization can increase the bioavailability and stability of the compound. Additionally,

investigating previously reported compounds might provide better in vivo bioavailability/stability and thereby greater drug efficacy, although tumor cell growth inhibition by the previously reported FEN1 inhibitor PTPD (45) was inferior to our novel FEN1 inhibitor (data not shown). At the moment the therapeutic option of FEN1 inhibition in ERα-positive breast cancer is far from clinically applicable, nevertheless our findings do show the potential minimization of predictive gene-profiles can have in identifying the causal genes in prognostication and the discovery of novel drug targets.

An additional novel therapeutic option may lay in the use of compounds hindering ERα dimerization such as fusicoccin (FC) (22). We demonstrated that the endogenous interaction between 14-3-3 proteins and ERα, can be stabilized by administration of FC, resulting in an inhibition of ERα chromatin interactions, diminished transactivation and subsequent block of cell proliferation (**Chapter 3**). An additional benefit of FC might be that its specificity for ERα still enables the anti-proliferative role of ERβ in breast cancer (46-48), although the occurrence of ERβ in breast cancer has recently been questioned (49). Despite the fact that we have demonstrated FC is small molecule ligand that has potential as a drug target in ERα-positive breast cancer, the relatively low affinity of the compound might pose as a problem for further pre-clinical development. As FC is a member of the group of fusicoccanes (50), investigation of these members and their specific potential to stabilize the ERα and 14-3-3 interaction might yield more potent hits which could possibly be chemically modified to increase their efficacy in stabilizing this interaction and subsequent T594-Phosphorylation even further. Additionally the recent discovery of secondary sites on 14-3-3 proteins bound by small molecule ligands by applying fragment-based screening methods (51) might further facilitate the discovery of compounds with a higher affinity (52).

Novel mechanistic insights in ERα action

As described above, there are multiple ways tumors can become resistant to therapy, making it clear that a better understanding of the mode of action of ERα is required. As discussed in **Chapter 1**, ERα-function is not only influenced by its coregulators, but also by other nuclear receptors. An example of this is liver receptor homolog-1 (LRH-1) (**Chapter 4**), which canonically has a role in the regulation of bile acid and cholesterol homeostasis (53) as well as dictating inflammatory responses in the liver and gut (54). In the ERα-positive setting however, LRH-1 but has been found to be an ERα-regulated gene

capable of directly regulating cell proliferation (55), although the exact mechanism behind this regulation remained unclear. However, we identified a subset of 222 genes that were differentially expressed when LRH-1 levels were knocked down in breast cancer cells. As these genes were known for their response to estrogen, this suggested that LRH-1 can regulate ERα-responsive genes. We tested this hypothesis by mapping LRH-1 chromatin binding events using ChIP-seq, where we found a large proportion of LRH-1 sites shared with ERα. At these shared regions both nuclear receptors promoted each other's recruitment, resulting in increased recruitment of ERα co-regulators such as p300, CBP and SRC3 and subsequently altered ERα-responsive gene expression. As the above findings are suggestive for direct nuclear receptor interactions, as previously described for Retinoic acid receptor-alpha (RAR alpha) (56), and the Progesterone Receptor (PR) (57) and Glucocorticoid Receptor (GR) (58, 59), it is seems plausible the same holds true for ERα and LRH-1. However, our efforts to demonstrate such direct physical interactions between ERα and LRH-1 failed as we were unable to detect binding between them, using either ChIP-reChIP or co-immunoprecipitation. An alternative explanation for the shared binding sites between ERα and LRH-1 could be found in the possibility of "assisted loading" (60); A mode of action wherein one nuclear receptor is able to induce binding of a second receptor by promoting e.g. chromatin accessibility, resulting in increased co-occupancy at the same region in a population of cells. This hypothesis would be consistent with our findings that knockdown of LRH-1 altered chromatin remodelling at ERα binding sites and that E2 promotes LRH-1 recruitment, but not in the presence of ERα-degrading agent fulvestrant. Besides the previously mentioned interactions between ERα and PR/GR, the Androgen Receptor (AR) is also able to bind shared regions in ERα-positive breast cancer cells resulting in inhibition of ERα-activity, most likely by direct competition between ERα and AR binding the same genomic regions (61), although inhibition by cross-interference, or "squelching", might also play a role (**Chapter 1**) (62, 63). To add even more complexity to this interaction, preclinical studies have demonstrated AR may have both proliferative (64) as well as anti-proliferative properties (61, 65, 66). Altogether it becomes clear that a complex interplay exists between not only different steroid hormone receptor family members, but also nuclear receptors as LRH-1, where it is likely that multiple receptors together can influence the direction of ERα-activation.

Another way breast cancer can become tamoxifen resistant is by the overexpression of FEN1 (**Chapter 5**). Besides the previously discussed link

between high levels of the FEN1 protein and the correlation with poor patient outcome and decreased sensitivity of cell lines for tamoxifen, we also revealed that FEN1 is an ERα-coregulator that is capable of dictating the transcriptional activity of ERα by regulating the formation and base excision repair of hormone-induced DNA damage. Others have previously proposed that the reason for this link between ERα-action and DNA-damage is the fact that nicking of the DNA could relieve the torsional stress resulting from DNA supercoiling at ERα-bound promotors and enhancers (67), although it remains unclear what the exact role of DNA supercoiling is as it has also been reported to aid enhancer-promotor looping and induce DNA conformational changes that can regulate transcription (68-70). We however propose an additional reason for this damage induction, as we identified FEN1 plays a key role during the excision of APOBEC3B mediated methylated-Cytosine-to-Uracil modifications (71) which, after inducing DNA-damage, can be replaced by an un-methylated Cytosine, alleviating some local epigenetic repression. Besides regions of hypomethylation, we also find E2 stimulation yielded regions of hypermethylation. A possible explanation for this might be that DNA methyltransferases have been reported to co-occupy ERα-interacting regions near the TFF1 and FOXA1 promoter (72, 73). It's possible that the balance between methylating (e.g. DNMT's) and demethylating (e.g. FEN1's role in BER) proteins at ERα-binding sites drives the directionality of DNA methylation alterations at these sites.

Additionally the FEN1-regulated ERα-mediated DNA-damage results in increased levels of yH2AX, which is known to promote chromatin remodelling by recruitment of the catalytic subunit of the SWI/SNF chromatin remodelling complex BRG1 (74). This link between chromatin remodelling and ERα-induced yH2AX was recently further illustrated by the impairment of APOBEC3B mediated C-to-U modifications (and thereby the need for BER), which resulted in decreased induction of activating histone marks H3K9ac and H3K4me3 (71). This reduction in APOBEC3B activity also led to reduced BRG1 recruitment, similar to the reduced BRG1 chromatin interactions at ERα-bindings sites we find upon FEN1 inhibition. Altogether, this is suggestive of a mode-of-action where FEN1 can, at least partly, decrease ERα-activity by altering its epigenetic landscape.

Besides these roles in epigenetic regulation, FEN1 can also modulate ERα-activity by stabilizing its chromatin interactions after activation. As we found that pre-treatment with proteasome inhibitor MG132 prevented the FEN1 inhibition-induced reduction of ERα-chromatin interactions

and ERα-chromatin interactions were not affected by FEN1 inhibition until the point of damage induction, we hypothesise that FEN1 can also dictate ERα-activity by regulating the stability of its chromatin binding after activation by E2 by altering its proteasome degradation. It seems plausible that FEN1 is being part of a fail-safe mechanism, only allowing the induction of relevant damage intermediates when FEN1 is part of the ERα complex. A similar mode-of-action has been reported for DNA-dependent protein kinase (DNA-PK), where DNA-PK inhibition by NU7441 resulted in the absence of γH2AX formation upon ERα-activation (71). Consequently, this favours a model wherein FEN1 blockade reduces ERα-responsive gene expression and ERα-driven cell proliferation by deregulating ERα-chromatin interactions after activation by E2, most likely due to improper induction/processing of DNA damage, which result in proteasome-mediated degradation of ERα.

References

1.   Ferlay J, Soerjomataram I, Dikshit R, Eser S, Mathers C, Rebelo M, et al. *Cancer incidence and mortality worldwide: sources, methods and major patterns in GLOBOCAN 2012. Int J Cancer. 2015;136(5):E359-86.*

2.   Hayashi SI, Eguchi H, Tanimoto K, Yoshida T, Omoto Y, Inoue A, et al. *The expression and function of estrogen receptor alpha and beta in human breast cancer and its clinical application. Endocr Relat Cancer. 2003;10(2):193-202.*

3.   Dahlman-Wright K, Cavailles V, Fuqua SA, Jordan VC, Katzenellenbogen JA, Korach KS, et al. *International Union of Pharmacology. LXIV. Estrogen receptors. Pharmacol Rev. 2006;58(4):773-81.*

4.   Jordan VC, Murphy CS. *Endocrine pharmacology of antiestrogens as antitumor agents. Endocrine reviews. 1990;11(4):578-610.*

5.   Katzenellenbogen BS, Miller MA, Mullick A, Sheen YY. *Antiestrogen action in breast cancer cells: modulation of proliferation and protein synthesis, and interaction with estrogen receptors and additional antiestrogen binding sites. Breast cancer research and treatment. 1985;5(3):231-43.*

6.   Arpino G, De Angelis C, Giuliano M, Giordano A, Falato C, De Laurentiis M, et al. *Molecular mechanism and clinical implications of endocrine therapy resistance in breast cancer. Oncology. 2009;77 Suppl 1:23-37.*

7.   Fabian CJ. *The what, why and how of aromatase inhibitors: hormonal agents for treatment and prevention of breast cancer. International journal of clinical practice. 2007;61(12):2051-63.*

8.   Ali S, Coombes RC. *Endocrine-responsive breast cancer and strategies for combating resistance. Nat Rev Cancer. 2002;2(2):101-12.*

Discussion

9.   Osborne CK, Schiff R. Mechanisms of endocrine resistance in breast cancer. Annu Rev Med. 2011;62:233-47.

10.   Michalides R, Griekspoor A, Balkenende A, Verwoerd D, Janssen L, Jalink K, et al. Tamoxifen resistance by a conformational arrest of the estrogen receptor alpha after PKA activation in breast cancer. Cancer Cell. 2004;5(6):597-605.

11.   Stender JD, Nwachukwu JC, Kastrati I, Kim Y, Strid T, Yakir M, et al. Structural and Molecular Mechanisms of Cytokine-Mediated Endocrine Resistance in Human Breast Cancer Cells. Mol Cell. 2017;65(6):1122-35 e5.

12.   Beelen K, Zwart W, Linn SC. Can predictive biomarkers in breast cancer guide adjuvant endocrine therapy? Nat Rev Clin Oncol. 2012;9(9):529-41.

13.   Elston CW, Ellis IO. Pathological prognostic factors in breast cancer. I. The value of histological grade in breast cancer: experience from a large study with long-term follow-up. Histopathology. 1991;19(5):403-10.

14.   Michalides R, van Tinteren H, Balkenende A, Vermorken JB, Benraadt J, Huldij J, et al. Cyclin A is a prognostic indicator in early stage breast cancer with and without tamoxifen treatment. Br J Cancer. 2002;86(3):402-8.

15.   Abdel-Fatah TM, Russell R, Albarakati N, Maloney DJ, Dorjsuren D, Rueda OM, et al. Genomic and protein expression analysis reveals flap endonuclease 1 (FEN1) as a key biomarker in breast and ovarian cancer. Mol Oncol. 2014.

16.   van 't Veer LJ, Dai H, van de Vijver MJ, He YD, Hart AA, Mao M, et al. Gene expression profiling predicts clinical outcome of breast cancer. Nature. 2002;415(6871):530-6.

17.   Cardoso F, van't Veer LJ, Bogaerts J, Slaets L, Viale G, Delaloge S, et al. 70-Gene Signature as an Aid to Treatment Decisions in Early-Stage Breast Cancer. N Engl J Med. 2016;375(8):717-29.

18.   Curtis C, Shah SP, Chin SF, Turashvili G, Rueda OM, Dunning MJ, et al. The genomic and transcriptomic architecture of 2,000 breast tumours reveals novel subgroups. Nature. 2012;486(7403):346-52.

19.   Thomas RS, Sarwar N, Phoenix F, Coombes RC, Ali S. Phosphorylation at serines 104 and 106 by Erk1/2 MAPK is important for estrogen receptor-alpha activity. J Mol Endocrinol. 2008;40(4):173-84.

20.   Kok M, Holm-Wigerup C, Hauptmann M, Michalides R, Stal O, Linn S, et al. Estrogen receptor-alpha phosphorylation at serine-118 and tamoxifen response in breast cancer. J Natl Cancer Inst. 2009;101(24):1725-9.

21.   Yamashita H, Nishio M, Kobayashi S, Ando Y, Sugiura H, Zhang Z, et al. Phosphorylation of estrogen receptor alpha serine 167 is predictive of response to endocrine therapy and increases postrelapse survival in metastatic breast cancer. Breast Cancer Res. 2005;7(5):R753-64.

22.   *Ballio A, Chain EB, De Leo P, Erlanger BF, Mauri M, Tonolo A. Fusicoccin: a New Wilting Toxin produced by Fusicoccum amygdali Del. 1964;203:297.*

23.   *Olsson A, Svennelid F, Ek B, Sommarin M, Larsson C. A phosphothreonine residue at the C-terminal end of the plasma membrane H+-ATPase is protected by fusicoccin-induced 14-3-3 binding. Plant Physiol. 1998;118(2):551-5.*

24.   *Kinoshita T, Shimazaki K. Analysis of the phosphorylation level in guard-cell plasma membrane H+-ATPase in response to fusicoccin. Plant Cell Physiol. 2001;42(4):424-32.*

25.   *Osborne CK, Schiff R. Growth factor receptor cross-talk with estro-gen receptor as a mechanism for tamoxifen resistance in breast cancer. Breast. 2003;12(6):362-7.*

26.   *Hurtado A, Holmes KA, Geistlinger TR, Hutcheson IR, Nicholson RI, Brown M, et al. Regulation of ERBB2 by oestrogen receptor-PAX2 determines response to tamoxifen. Nature. 2008;456(7222):663-6.*

27.   *Shou J, Massarweh S, Osborne CK, Wakeling AE, Ali S, Weiss H, et al. Mechanisms of tamoxifen resistance: increased estrogen receptor-HER2/neu cross-talk in ER/HER2-positive breast cancer. J Natl Cancer Inst. 2004;96(12):926-35.*

28.   *Zhao W, Zhang Q, Kang X, Jin S, Lou C. AIB1 is required for the acquisition of epithelial growth factor receptor-mediated tamoxifen resistance in breast cancer cells. Biochem Biophys Res Commun. 2009;380(3):699-704.*

29.   *Mohammed H, D'Santos C, Serandour AA, Ali HR, Brown GD, Atkins A, et al. Endogenous purification reveals GREB1 as a key estrogen receptor regulatory factor. Cell Rep. 2013;3(2):342-9.*

30.   *Wang L, Yu Y, Chow DC, Yan F, Hsu CC, Stossi F, et al. Characterization of a Steroid Receptor Coactivator Small Molecule Stimulator that Overstimulates Cancer Cells and Leads to Cell Stress and Death. Cancer Cell. 2015;28(2):240-52.*

31.   *Wang Y, Lonard DM, Yu Y, Chow DC, Palzkill TG, O'Malley BW. Small molecule inhibition of the steroid receptor coactivators, SRC-3 and SRC-1. Mol En-docrinol. 2011;25(12):2041-53.*

32.   *Yan F, Yu Y, Chow DC, Palzkill T, Madoux F, Hodder P, et al. Identification of verrucarin a as a potent and selective steroid receptor coactivator-3 small mole-cule inhibitor. PLoS One. 2014;9(4):e95243.*

33.   *Yi P, Wang Z, Feng Q, Chou CK, Pintilie GD, Shen H, et al. Structural and Functional Impacts of ER Coactivator Sequential Recruitment. Mol Cell. 2017;67(5):733-43 e4.*

34.   *Lopez GN, Turck CW, Schaufele F, Stallcup MR, Kushner PJ. Growth factors signal to steroid receptors through mitogen-activated protein kinase regulation of p160 coactivator activity. The Journal of biological chemistry. 2001;276(25):22177-*

82.

35.   Kuo HY, Chang CC, Jeng JC, Hu HM, Lin DY, Maul GG, et al. SUMO modification negatively modulates the transcriptional activity of CREB-binding protein via the recruitment of Daxx. Proc Natl Acad Sci U S A. 2005;102(47):16973-8.

36.   Zwart W, Theodorou V, Kok M, Canisius S, Linn S, Carroll JS. Oestrogen receptor-co-factor-chromatin specificity in the transcriptional regulation of breast cancer. EMBO J. 2011;30(23):4764-76.

37.   Hurtado A, Holmes KA, Ross-Innes CS, Schmidt D, Carroll JS. FOXA1 is a key determinant of estrogen receptor function and endocrine response. Nature genetics. 2011;43(1):27-33.

38.   Robinson DR, Wu YM, Vats P, Su F, Lonigro RJ, Cao X, et al. Activating ESR1 mutations in hormone-resistant metastatic breast cancer. Nature genetics. 2013;45(12):1446-51.

39.   Fan M, Yan PS, Hartman-Frey C, Chen L, Paik H, Oyer SL, et al. Diverse gene expression and DNA methylation profiles correlate with differential adaptation of breast cancer cells to the antiestrogens tamoxifen and fulvestrant. Cancer Res. 2006;66(24):11954-66.

40.   He L, Zhang Y, Sun H, Jiang F, Yang H, Wu H, et al. Targeting DNA Flap Endonuclease 1 to Impede Breast Cancer Progression. EBioMedicine. 2016.

41.   Panda H, Jaiswal AS, Corsino PE, Armas ML, Law BK, Narayan S. Amino acid Asp181 of 5'-flap endonuclease 1 is a useful target for chemotherapeutic development. Biochemistry. 2009;48(42):9952-8.

42.   van Pel DM, Barrett IJ, Shimizu Y, Sajesh BV, Guppy BJ, Pfeifer T, et al. An evolutionarily conserved synthetic lethal interaction network identifies FEN1 as a broad-spectrum target for anticancer therapeutic development. PLoS genetics. 2013;9(1):e1003254.

43.   McManus KJ, Barrett IJ, Nouhi Y, Hieter P. Specific synthetic lethal killing of RAD54B-deficient human colorectal cancer cells by FEN1 silencing. Proc Natl Acad Sci U S A. 2009;106(9):3276-81.

44.   Exell JC, Thompson MJ, Finger LD, Shaw SJ, Debreczeni J, Ward TA, et al. Cellularly active N-hydroxyurea FEN1 inhibitors block substrate entry to the active site. Nature chemical biology. 2016;12(10):815-21.

45.   Dorjsuren D, Kim D, Maloney DJ, Wilson DM, 3rd, Simeonov A. Complementary non-radioactive assays for investigation of human flap endonuclease 1 activity. Nucleic acids research. 2011;39(2):e11.

46.   Bartella V, Rizza P, Barone I, Zito D, Giordano F, Giordano C, et al. Estrogen receptor beta binds Sp1 and recruits a corepressor complex to the estrogen receptor alpha gene promoter. Breast cancer research and treatment. 2012;134(2):569-81.

47.   Fox EM, Davis RJ, Shupnik MA. ERbeta in breast cancer--onlooker, passive player, or active protector? Steroids. 2008;73(11):1039-51.

48.   Palmieri C, Cheng GJ, Saji S, Zelada-Hedman M, Warri A, Weihua Z, et al. Estrogen receptor beta in breast cancer. Endocr Relat Cancer. 2002;9(1):1-13.

49.   Andersson S, Sundberg M, Pristovsek N, Ibrahim A, Jonsson P, Katona B, et al. Insufficient antibody validation challenges oestrogen receptor beta research. Nature communications. 2017;8:15840.

50.   de Boer AH, de Vries-van Leeuwen IJ. Fusicoccanes: diterpenes with surprising biological functions. Trends Plant Sci. 2012;17(6):360-8.

51.   Sijbesma E, Skora L, Leysen S, Brunsveld L, Koch U, Nussbaumer P, et al. Identification of Two Secondary Ligand Binding Sites in 14-3-3 Proteins Using Fragment Screening. Biochemistry. 2017;56(30):3972-82.

52.   Stevers LM, Sijbesma E, Botta M, MacKintosh C, Obsil T, Landrieu I, et al. Modulators of 14-3-3 Protein-Protein Interactions. Journal of medicinal chemistry. 2017.

53.   Fayard E, Auwerx J, Schoonjans K. LRH-1: an orphan nuclear receptor involved in development, metabolism and steroidogenesis. Trends Cell Biol. 2004;14(5):250-60.

54.   Venteclef N, Jakobsson T, Ehrlund A, Damdimopoulos A, Mikkonen L, Ellis E, et al. GPS2-dependent corepressor/SUMO pathways govern anti-inflammatory actions of LRH-1 and LXRbeta in the hepatic acute phase response. Genes Dev. 2010;24(4):381-95.

55.   Annicotte JS, Chavey C, Servant N, Teyssier J, Bardin A, Licznar A, et al. The nuclear receptor liver receptor homolog-1 is an estrogen receptor target gene. Oncogene. 2005;24(55):8167-75.

56.   Ross-Innes CS, Stark R, Holmes KA, Schmidt D, Spyrou C, Russell R, et al. Cooperative interaction between retinoic acid receptor-alpha and estrogen receptor in breast cancer. Genes Dev. 2010;24(2):171-82.

57.   Mohammed H, Russell IA, Stark R, Rueda OM, Hickey TE, Tarulli GA, et al. Progesterone receptor modulates ERalpha action in breast cancer. Nature. 2015;523(7560):313-7.

58.   Karmakar S, Jin Y, Nagaich AK. Interaction of glucocorticoid receptor (GR) with estrogen receptor (ER) alpha and activator protein 1 (AP1) in dexamethasone-mediated interference of ERalpha activity. The Journal of biological chemistry. 2013;288(33):24020-34.

59.   Yang F, Ma Q, Liu Z, Li W, Tan Y, Jin C, et al. Glucocorticoid Receptor:MegaTrans Switching Mediates the Repression of an ERalpha-Regulated Transcriptional Program. Mol Cell. 2017;66(3):321-31 e6.

60.   Voss TC, Schiltz RL, Sung MH, Yen PM, Stamatoyannopoulos JA, Biddie SC, et al. Dynamic exchange at regulatory elements during chromatin remodeling underlies assisted loading mechanism. Cell. 2011;146(4):544-54.

61.   Peters AA, Buchanan G, Ricciardelli C, Bianco-Miotto T, Centenera MM, Harris JM, et al. Androgen receptor inhibits estrogen receptor-alpha activity and is prognostic in breast cancer. Cancer Res. 2009;69(15):6131-40.

62.   Cahill MA, Ernst WH, Janknecht R, Nordheim A. Regulatory squelching. FEBS letters. 1994;344(2-3):105-8.

63.   Lopez GN, Webb P, Shinsako JH, Baxter JD, Greene GL, Kushner PJ. Titration by estrogen receptor activation function-2 of targets that are downstream from coactivators. Mol Endocrinol. 1999;13(6):897-909.

64.   De Amicis F, Thirugnansampanthan J, Cui Y, Selever J, Beyer A, Parra I, et al. Androgen receptor overexpression induces tamoxifen resistance in human breast cancer cells. Breast cancer research and treatment. 2010;121(1):1-11.

65.   Szelei J, Jimenez J, Soto AM, Luizzi MF, Sonnenschein C. Androgen-induced inhibition of proliferation in human breast cancer MCF7 cells transfected with androgen receptor. Endocrinology. 1997;138(4):1406-12.

66.   Cops EJ, Bianco-Miotto T, Moore NL, Clarke CL, Birrell SN, Butler LM, et al. Antiproliferative actions of the synthetic androgen, mibolerone, in breast cancer cells are mediated by both androgen and progesterone receptors. The Journal of steroid biochemistry and molecular biology. 2008;110(3-5):236-43.

67.   Puc J, Aggarwal AK, Rosenfeld MG. Physiological functions of programmed DNA breaks in signal-induced transcription. Nat Rev Mol Cell Biol. 2017;18(8):471-6.

68.   Luchnik AN. DNA conformational transitions induced by supercoiling control transcription in chromatin. Gene Regul Syst Bio. 2014;8:89-96.

69.   Gilbert N, Allan J. Supercoiling in DNA and chromatin. Curr Opin Genet Dev. 2014;25:15-21.

70.   Corless S, Gilbert N. Effects of DNA supercoiling on chromatin architecture. Biophys Rev. 2016;8(Suppl 1):51-64.

71.   Periyasamy M, Patel H, Lai CF, Nguyen VT, Nevedomskaya E, Harrod A, et al. APOBEC3B-Mediated Cytidine Deamination Is Required for Estrogen Receptor Action in Breast Cancer. Cell Rep. 2015;13(1):108-21.

72.   Kangaspeska S, Stride B, Metivier R, Polycarpou-Schwarz M, Ibberson D, Carmouche RP, et al. Transient cyclical methylation of promoter DNA. Nature. 2008;452(7183):112-5.

73.   Gong C, Fujino K, Monteiro LJ, Gomes AR, Drost R, Davidson-Smith H, et al. FOXA1 repression is associated with loss of BRCA1 and increased promoter

methylation and chromatin silencing in breast cancer. Oncogene. 2015;34(39):5012-24.

74.　　*Lee HS, Park JH, Kim SJ, Kwon SJ, Kwon J. A cooperative activation loop among SWI/SNF, gamma-H2AX and H3 acetylation for DNA double-strand break repair. EMBO J. 2010;29(8):1434-45.*

Addendum

Nederlandse samenvatting
English summary
Nederlands Curriculum Vitae
English Curriculum Vitae
List of publications
Dankwoord

Nederlandse samenvatting

Waar gaat dit proefschrift over?

In dit proefschrift gaan we in op de effecten die differentiële DNA-binding van estrogen receptor α (ERα) kan hebben op het gedrag van borstkanker en welke factoren daartoe kunnen bijdragen. ERα is een transcriptiefactor die tumorcelproliferatie kan veroorzaken en ongeveer 70% van alle borsttumoren wordt verondersteld afhankelijk te zijn van de activiteit van deze door hormonen geactiveerde transcriptiefactor. Na activatie van ERα wordt een groot aantal cofactoren gerekruteerd, wat leidt tot de vorming van een transcriptiecomplex. Hoewel er meerdere manieren zijn om de werking van ERα te ontregelen en daardoor tumorgroei te remmen, komt toch bij een aanzienlijk deel van de patiënten de tumor terug. Kruisresistentie tussen verschillende endocriene behandelingen kan optreden, maar een deel van de patiënten waarbij de tumor terugkeert na één type therapie kan nog steeds baat hebben bij een andere behandelingsmethode, wat het bestaan van meerdere resistentiemechanismen illustreert welke behandeling specifiek kunnen zijn. Een beter begrip omtrent de werking van ERα en zijn resistentiemechanismen, kan de weg wijzen naar de ontdekking van nieuwe biomarkers en potentieel nieuwe behandelmethodes, die de overleving van de patiënt verder vergroten.

Voorspelling van resistentie

In **Hoofdstuk 2** hebben we aangetoond dat tamoxifen-resistentie door PKA-geïnduceerde fosforylering van ERα op Serine-residu 305 (ERαS305-P), ERα herpositioneert op andere plaatsen van het genoom, resulterend in differentiële genexpressie. Dit veranderde genexpressieprofiel hebben we gebruikt als gen-signatuur en waren instaat hiermee de "survival-outcome" van tamoxifen behandelde patiënten te voorspellen. Naast dit genexpressieprofiel beschrijven we ook de ontdekking van twee enkelvoudige gen-signaturen; FEN1 en SRC3-pS543. Zoals beschreven in **Hoofdstuk 5**, vonden we dat ERα-coregulator FEN1 correleerde met de survival-outcome van patiënten met ERα-positieve borstkanker, maar niet bij ERα-negatieve patiënten. Interessant genoeg vonden we tevens dat FEN1- eiwithoeveelheden voorspellend waren voor de uitkomst bij ERα-positieve patiënten die adjuvant tamoxifen kregen. Daarnaast beschrijft **Hoofdstuk 6** onze bevindingen over een SRC3-pS543 fosfo-specifiek antilichaam dat in staat was om patiënten met een actieve ERα-pathway te identificeren, wat indicatief is voor een gunstig resultaat in de afwezigheid van adjuvante therapie en daarbij een gebrek aan ta-

moxifen-werkzaamheid. Alles tezamen gaan we in op onze bevindingen over drie verschillende biomarkers met het potentieel om de behandelingsrespons van een patiënt op individuele basis te voorspellen. Deze biomarkers kunnen helpen bij het proces van besluitvorming over endocriene behandelingstherapieën wanneer de eerstelijnsbehandeling tamoxifen waarschijnlijk niet zal leiden tot een voordeel voor de patiënt en daarom direct met een alternatieve behandeling gestart kan worden.

Differentiële DNA-binding van ERα
Zoals hierboven kort beschreven, kunnen post-translationele modificaties van ERα, zoals fosforylaties, diens activiteit veranderen en ERα naar andere plaatsen op het DNA sturen, waardoor het DNA-bindingsrepertoire (ook wel bekend als cistrome) wordt veranderd. Dit differentiële cistrome kan een grote invloed hebben op de genen die worden afgeschreven en het resulterende fenotype van een cel. Naast de eerder genoemde ERαS305-P, leveren we in **Hoofdstuk 3** experimenteel bewijs voor een tot nu toe onbekende ERα-fosforylatie (T594P) en laten we zien dat door directe interactie van 14-3-3-eiwitten met ERα, de DNA-bindingscapaciteit sterk verminderd wordt. Door deze fosforyleringsplaats te beschermen met fusicoccin (FC) waren we in staat om deze T594P te stabiliseren en te induceren, wat uiteindelijk resulteerde in verminderde gentranscriptie en geremde celgroei. Naast ERα zelf, kan de fosforylatie van essentiële ERα-cofactoren ook het cistromische repertoire beïnvloeden, zoals beschreven in **Hoofdstuk 6**. Hierin laten we zien dat S543-fosforylatie van SRC3 resulteerde in een verhoogde binding op promotorregio's, terwijl normaal gesproken SRC3 voornamelijk samen met ERα nabij distale enhancers en intronen bindt. Dit veranderde cistromische profiel, samen met de hierboven genoemde bevindingen dat SRC3-pS543-expressie geassocieerd was met een slechte respons bij een tamoxifen behandeling, maakt het zeer waarschijnlijk dat pS543 ook de genexpressie van borstkanker kan veranderen en daardoor uiteindelijk haar fenotype.

Nieuwe drug targets
Minimalisatie van het aantal genen in een voorspellend genexpressieprofiel kan niet alleen een profiel makkelijker implementeerbaar maken in de kliniek, maar kan ook worden gebruikt om nieuwe drug targets te identificeren door de causale genen uit een voorspellend profiel te destilleren. In **Hoofdstuk 5** demonstreren we hier een voorbeeld van met de ontdekking van FEN1 als cruciale ERα-coregulator door minimalisatie van een 111-genenprofiel.

We toonden aan dat het wijzigen van FEN1- eiwithoeveelheden door knock-down of over expressie resulteert in differentiële ERα-activiteit, wat impliceert dat FEN1 een veelbelovend doelwit kan zijn bij ERα-positieve borstkanker. We testen een groot aantal kleine chemische verbindingen voor hun effect op FEN1-remming, wat uiteindelijk leidde tot de ontdekking van een FEN1-specifieke en krachtige remmer. We onderzochten het potentieel hiervan als een nieuwe therapeutische optie door de werkzaamheid ervan in borstkankercellijnen te onderzoeken, waarbij een duidelijke gevoeligheid van ERα-positieve borstkankercellijnen voor deze remmer werd aangetoond in vergelijking met ERα-negatieve cellijnen. De nog grotere gevoeligheid van tamoxifen-resistente varianten van de ERα-positieve cellijnen, suggereert dat FEN1-remming nuttig kan zijn bij tamoxifen-resistente borstkankerpatiënten als een alternatieve therapie. Hoewel veelbelovend, op dit moment is het nog te vroeg om definitief te weten of FEN1-remming op zichzelf een realistische therapeutische optie zou zijn.

Bovendien kan de stabilisatie van ERα-T594P door FC die we in **Hoofdstuk 3** beschrijven, ook een nieuwe therapeutische optie opleveren. We hebben aangetoond dat FC-toediening leidt tot verminderde transactivatie van ERα en vervolgens resulteerde in remming van cel proliferatie. Op dit moment kan de relatief lage bindingsaffiniteit van FC echter een belemmering vormen voor verdere preklinische ontwikkeling. Verder onderzoek naar het identificeren van fusicoccanen met een hogere bindingsaffiniteit zal nodig zijn om eventuele therapeutische opties verder te onderzoeken.

Nieuwe mechanistische inzichten

Zoals besproken in **Hoofdstuk 1**, wordt de activiteit van ERα niet alleen beïnvloed door zijn coregulatoren, maar ook door andere nucleaire receptoren. In **Hoofdstuk 4** laten we een voorbeeld hiervan zien met liver receptor homolog-1 (LRH-1). Knockdown van LRH-1-eiwithoeveelheden leidde tot een subset van 222 differentieel tot expressie gebrachte genen, welke bekend zijn als ERα geïnduceerde genen. We laten zien dat er een grote overlapping is tussen de chromatine-interacties van LRH-1 en ERα. In deze gedeelde regio's stimuleerden beide receptoren elkaars binding, wat leidde tot een verhoogde rekrutering van ERα-coregulatoren en veranderde genexpressie. Tot op heden is het exacte mechanisme achter deze synergetische stimulatie nog onbekend. Een ander aanvullend nieuw inzicht in ERα-biologie wordt beschreven in **Hoofdstuk 5**, waar we bewijs leveren dat FEN1 een ERα-coregulator is die in staat is om ERα-activiteit op meerdere manieren te reguleren. 1) Het in kaart

brengen van het methylome (de delen van het DNA die gemethyleerde base bevatten) na ERα-stimulatie met en zonder FEN1-remmer onthulde dat FEN1 een sleutelrol speelt bij actieve DNA-demethylatie, waardoor een deel van de lokale epigenetische repressie wordt verlicht. 2) Remming van FEN1 resulteerde in verminderde rekrutering van chromatine her-modelleringsfactor BRG1 op plaatsen van ERα chromatine-interacties, waardoor de activerende aard van ERα-geïnduceerde chromatine her-modellering afnam. 3) Remming van het proteasoom verhinderde de door FEN1-remming geïnduceerde reductie van ERα chromatine-interacties. Dit suggereert dat FEN1 ERα chromatine-interacties kan stabiliseren door de proteasoom-gemedieerde afbraak van ERα te voorkomen.

English summary

What is this Thesis about?

In this thesis we reflect on the effects differential DNA binding of the estrogen receptor α (ERα) can have on the behavior of breast cancer and which factors can contribute to this. ERα is a transcription factor than can drive tumor cell proliferation and approximately 70% off all breast tumors is thought to be dependent on the activity of this hormone-mediated transcription factor. After stimulation of ERα a wild variety of co-factors are recruited, leading to the assembly of a transcriptional complex. Although there are multiple ways of targeting the action of ERα and thereby inhibiting tumor growth, still a significant proportion of patients develop a recurrence. Cross-resistance between the different endocrine therapy options can occur, but a proportion of patients that relapse on one type of therapy can still benefit from a different treatment modality, illustrating the existence of multiple resistance mechanisms which can be treatment selective. A better understanding of ERα-biology and the development of endocrine therapy resistance, can lead the way to the discovery of novel biomarkers and potential drug targets, that can further increase patient survival.

Endocrine resistance prediction

In **Chapter 2** we demonstrated that tamoxifen-resistance by PKA-induced phosphorylation of ERα at Serine residue 305 (ERαS305-P), positions ERα at different sites of the genome, resulting in differential gene expression. We were able to translate this altered gene expression profile into a gene signature that was able to predict the outcome of patients treated with tamoxifen. Besides this gene profile, we also describe the discovery of two single gene classifiers; FEN1 and SRC3-pS543. As described in **Chapter 5**, we found that ERα-coregulator FEN1 correlated with patient outcome in ERα-positive, but not ERα-negative patients. More importantly, FEN1 levels were predictive of outcome in ERα-positive patients receiving adjuvant tamoxifen. Additionally **Chapter 6** describes our findings on a SRC3-pS543 phospho-specific antibody which was able to identify patients with a functional ERα pathway, which is indicative of a favorable outcome in the absence of adjuvant therapy and therefore a lack of tamoxifen efficacy. All together we elaborate on our findings of three types of biomarkers with the potential to predict the treatment response of a patients on an individual bases. These biomarkers could aid in the process of decision-making on endocrine treatment regimens when

first-in-line treatment tamoxifen is not likely to result in a benefit for the patient, by directly administrating an alternative treatment.

Differential ERα-chromatin interactions

As briefly described above, post-translational modifications of ERα, such as phosphorylations, can modify its activity and can redirect ERα to different places on the DNA, thereby altering its binding repertoire (also known as cistrome). This differential cistrome can have a major impact on the genes that are transcribed and the resulting phenotypic behavior of a cell. Besides the above mentioned ERαS305-P, we provided experimental evidence in **Chapter 3** for a previously unknown ERα-phosphorylation (T594P) and demonstrate that by direct interaction of 14-3-3 proteins with ERα, its DNA binding capacity is greatly diminished. By shielding the T594 phosphorylation site with fusicoccin (FC) we were able to stabilize and induce this T594P, ultimately resulting in decreased gene transcription and inhibited cell growth.

Besides ERα itself, the phosphorylation of essential ERα-cofactors can also redirect the cistromic repertoire, as described in **Chapter 6**. Herein we demonstrated that S543-phosphorylation of SRC3 resulted in an increased deposition at promoter regions, while normally SRC3 is predominately found together with ERα at distal enhancers and introns. This changed cistromic profile, together with the above described findings that SRC3-pS543 expression was associated with a poor response to tamoxifen treatment, makes it very likely that pS543 can also alter the gene expression of breast cancer and thereby ultimately its phenotype.

Novel drug targets

Minimization of predictive gene-profiles can not only make a classifier more easily implementable in the clinic, but can also be used to identify novel drug targets by eluting the driving genes in a predictive profile. In **Chapter 5** we demonstrated an example of this in the discovery of FEN1 as a crucial ERα-coregulator by minimization of a 111-genes profile. We showed that altering FEN1 protein levels by knockdown or overexpression results in differential ERα-activity, implying FEN1 might be a promising drug target in ERα-positive breast cancer. We performed a small-compound screen for FEN1 inhibition, which ultimately led to the discovery of a FEN1-specific and potent inhibitor. We investigated its potential as novel therapeutic option by assessing its efficacy in breast cancer cell lines, demonstrating clear sensitivity of ERα-positive breast cancer cell lines to this inhibitor when compared to ERα-negative cell lines. The even greater sensitivity of tamoxifen-resistant

derivatives of the ERα-positive cell lines, suggests FEN1 inhibition might be useful in tamoxifen resistant breast cancer patients as an alternative therapy. Although promising, at the moment it is still too early to state definitively whether FEN1 inhibition would be a realistic therapeutic option on its own.

Additionally the stabilization of ERα-T594P by FC we describe in **Chapter 3**, might also yield a novel therapeutic option. We demonstrated that FC administration leads to diminished transactivation of ERα and subsequently resulted in inhibition of cell proliferation. At the moment however, the relatively low binding affinity of FC might hinder further pre-clinical development, making further research into identifying fusicoccanes with an higher binding affinity necessary in order to further pursue its therapeutic options.

Novel mechanistic insights

As discussed in **Chapter 1**, ERα-function is not only influenced by its coregulators, but also by other nuclear receptors. In **Chapter 4** we demonstrate an example of this in the case of liver receptor homolog-1 (LRH-1). Knockdown of LRH-1 levels led to a subset of 222 differentially expressed genes, known for their estrogen responsiveness. We revealed that there is a large overlap between the chromatin interactions of LRH-1 and ERα. At these shared regions both receptors stimulated each other's recruitment, leading to increased recruitment of ERα co-regulators and altered gene expression. To date, the exact mechanism behind this synergistic stimulation remains unknown.

An additional novel insight in ERα-biology is described in **Chapter 5**, where we provide evidence that FEN1 is an ERα co-regulator capable of modulating ERα-activity in multiple ways. 1) Mapping the methylome (the parts of the DNA that contain methylation modifications) after ERα-stimulation with and without FEN1-inhibitor was suggestive of a key role for FEN1 in active DNA demethylation, thereby alleviating some local epigenetic repression. 2) Inhibition of FEN1 resulted in reduced recruitment of chromatin remodeling factor BRG1 to sites of ERα-chromatin interactions, thereby decreasing the activating nature of ERα-induced chromatin remodeling. 3) Inhibition of the proteasome prevented the FEN1 inhibition-induced reduction of ERα-chromatin interactions. This suggests that FEN1 can stabilize ERα-chromatin interactions by preventing the proteasome-mediated degradation of ERα.

Addendum

Nederlands Curriculum Vitae

Koen Flach is geboren op 16 september 1987 te Amsterdam. In 2005 behaalde hij zijn VWO diploma op het Hermann Wesselink College te Amstelveen. Na een jaar de bachelor Scheikunde te hebben gevolgd aan de Vrije Universiteit te Amsterdam, stapte hij in 2006 over op de bachelor Biomedische Wetenschappen. Na deze in 2010 te hebben afgerond is hij ditzelfde jaar doorgegaan met de master Oncology, tevens aan de Vrije Universiteit te Amsterdam. Tijdens deze master deed Koen zijn eerste stage op het Cancer Center Amsterdam in de groep van Prof. Dr. G.J. Peters onder begeleiding van Drs. K. Azijli. Tijdens deze stage deed hij onderzoek naar de rol van MAPK p38 en JNK in TRAIL-gemedieerde apoptosis in niet-kleincellig longkanker. Als onderdeel van zijn master Oncology schreef Koen, tevens onder begeleiding van Prof. Dr. G.J. Peters, zijn literatuurscriptie over de huidige status en vooruitzichten betreffende het gebruik van medicijnen specifiek gericht tegen het veranderde metabolisme in kankercellen. Zijn tweede master deed hij in de groep van Dr. W. Zwart op het Nederlands Kanker Instituut (NKI) te Amsterdam. Hier werkte hij aan het verfijnen en verder ontwikkelen van een genexpressieprofiel voor het voorspellen van tamoxifen resistentie bij borstkankerpatiënten. Na afronding van deze stage ontving Koen in 2012 zijn master Oncology en begon als PhD-student in de groep van Dr. W. Zwart, alwaar het in dit proefschrift beschreven onderzoek gedurende de periode van Juni 2012 tot en met December 2017 is uitgevoerd.

English Curriculum Vitae

Koen Flach was born on September 16, 1987 in Amsterdam. In 2005 he received his pre-university high school degree (VWO) at the Hermann Wesselink College in Amstelveen. After one year of taking courses of the Chemistry bachelor at the Vrije Universiteit in Amsterdam for a year, in 2006 he switched to the Biomedical Sciences bachelor. After completing this in 2010, he continued the same year with the master Oncology, also at the VU University in Amsterdam. During this master, Koen performed his first internship at the Cancer Center Amsterdam in the group of Prof. Dr. G.J. Peters under supervision of Drs. K. Azijli. During this internship he investigated the role of MAPK p38 and JNK in TRAIL-mediated apoptosis in non-small-cell lung cancer. As part of his master Oncology, Koen wrote, also under supervision of Prof. Dr. G.J. Peters, his literature thesis on the current status and prospects concerning the therapeutic options of drugs specifically aimed at the altered metabolism in tumor cells. He then performed his second internship in the lab of Dr. W. Zwart at the Netherlands Cancer Institute (NKI) in Amsterdam. Here he worked on refining and further developing a gene-expression profile for predicting tamoxifen resistance in breast cancer patients. After completing this internship, Koen received his master's degree in Oncology in 2012 and started as a PhD student in the group of Dr. W. Zwart, where the research described in this thesis was conducted during the period of June 2012 - December 2017.

Addendum

List of publications

Flach KD, Periyasamy M, Prekovic S, Jadhav A, Hickey TE, Opdam M, Patel H, Canisius S, Wilson III DM, Dorjsuren D, Nieuwland M, Kluin R, Zakharov AV, Wesseling J, Wessels LFA, Linn SC, Tilley WD, Simeonov A, Ali S, Zwart W.
Estrogen Receptor DNA-damage/methylation cycle as drug interface in tamoxifen resistant breast cancer by FEN1 blockade.
Manuscript in submission

Flach KD *, Szijgyarto Z*, Opdam M, Palmieri C, Linn SC, Wesseling J, Ali S, Bliss JM, Cheang MCU, Zwart W, Coombes RC. *these authors contributed equally.
Dissecting the MAPK/AKT/Estrogen Receptor phosphorylation axis in primary breast cancer revealed to treatment response for tamoxifen over exemestane: a Translational Report of The Intergroup Exemestane Study (IES)-PathIES.
Manuscript in submission

Droog M, Nevedomskaya E, Kim Y, Severson T, **Flach KD**, Opdam M, Schuurman K, Gradowska P, Hauptmann M, Dackus G, Hollema H, Mourits M, Nederlof P, van Boven H, Linn SC, Wessels L, van Leeuwen FE, Zwart W.
Comparative Cistromics Reveals Genomic Cross-talk between FOXA1 and ERα in Tamoxifen-Associated Endometrial Carcinomas.
Cancer Research, 76(13); 3773-84, 2016.

Flach KD, Zwart W.
The first decade of estrogen receptor cistromics in breast cancer.
Journal of endocrinology, 229(2):R43-56, 2016.

Flach KD*, Wilbert Zwart*, Bharath Rudraraju*, Tarek Abdel-Fatah, Ondrej Gojis, Sander Canisius, David Moore, Ekaterina Nevedomskaya, Mark Opdam, Marjolein Droog, Ingrid Hofland, Steve Chan, Jacqui Shad, Ian O ellis, R. Charles Coombes, Jason S Carroll, Simak Ali, Carlo Palmieri. *these authors contributed equally
SRC3 phosphorylation at Serine 543 is a positive independent prognostic factor in ER positive breast cancer.
Clinical Cancer Research, 15;22(2):479-91, 2016.

Chun-Fui Lai, **Flach KD**, Xanthippi Alexi, Stephen Fox, Silvia Ottaviani, Paul T. R. Thiruchelvam, Fiona J. Kyle, Ross S. Thomas, Rosalind Launchbury, Hui Hua, Holly Callaghan, Jason S. Carroll, R. Charles Coombes, Wilbert Zwart, Laki Buluwela, Simak Ali.
Co-regulated gene expression by estrogen receptor-α and liver receptor homolog-1 is a feature of the estrogen response in breast cancer cells.
Nucleic Acids Research, 41(22):10228-40, 2013.

De Vries-van Leeuwen IJ, da Costa Pereira D, **Flach KD**, Piersma SR, Haase C, Bier D, Yalcin Z, Michalides R, Feenstra KA, Jiménez CR, de Greef TF, Brunsveld L, Ottmann C, Zwart W, de Boer AH.
Interaction of 14-3-3 proteins with the Estrogen Receptor Alpha F domain provides a drug target interface.
Proceedings of the National Academy of Sciences, 110(22):8894-9, 2013.

Azijli K, Yuvaraj S, van Roosmalen I, **Flach KD**, Giovannetti E, Peters GJ, de Jong S, Kruyt FA.
MAPK p38 and JNK have opposing activities on TRAIL-induced apoptosis activation in NSCLC H460 cells that involves RIP1 and caspase-8 and is mediated by Mcl-1.
Apoptosis, 18(7):851-60, 2013

de Leeuw R, **Flach KD**, Bentin Toaldo C, Alexi X, Canisius S, Neefjes J, Michalides R, Zwart W.
PKA phosphorylation redirects ERα to promoters of a unique gene set to induce tamoxifen resistance.
Oncogene, 32(30):3543-51, 2013.

Addendum

Dankwoord

Terugkijkend op mijn periode als PhD-student wil ik hen bedanken die mij in de afgelopen periode tot steun zijn geweest en hebben bijgedragen aan mijn wetenschappelijk onderzoek. Bedankt Sjaak voor de mogelijkheid om te promoveren aan de Leidse Universiteit en je waardevolle feedback tijdens mijn jaarlijkse OIO-commissie sessies. Ook bedankt Andre, Jos en Bas voor jullie begeleiding als deel van mijn commissie.

Bedankt Wilbert, mijn copromoter en groepsleider. Het was een genoegen om vanaf het begin onderdeel van je onderzoeksgroep te zijn geweest. Eerst als masterstudent, om vervolgens als PhD-student in hetzelfde project door te stromen. In de loop der tijd heb je jezelf als groepsleider steeds verder ontwikkelt en dit uiteindelijk ook bekroont zien worden met een aanstelling als senior group leader. Bedankt voor je steun en je niet aflatende optimisme en enthousiasme.

Of course thanks to all members of the Zwart Lab, including its former members. Xanthippi, thank you for showing me how everything worked in the lab and it was a pleasure having spent so much time with you discussing all sorts of topics. Marjolein, mijn mede startende PhD-kameraad, het was me een genoegen met je gewerkt te hebben en grotendeels samen het PhD-pad te hebben bewandeld. Je droge humor, no pun intended, was precies wat nodig was als dingen even tegen zaten. Suzan, bedankt voor je humor en fijn dat er toch iemand van mijn muzikale keuzes kon genieten! Katja and Yongsoo, thanks for taking the time to help me understand how to analyze sequencing data myself. Karianne, het was fijn om met een ervaren analist op het lab te hebben gewerkt, waarnaast je zelfgebakken brownies voor smakelijke koffie-breaks zorgden. Stacey, het was bijzonder om je van master-student tot PhD-student te zien transformeren. Bedankt voor de vele directe gesprekken op het lab, tijdens de borrels en op retreats. Succes de komende PhD-jaren en we blijven elkaar nog genoeg zien op het NKI. Laurel, je open geest en gezelligheid heb ik altijd erg gewaardeerd en succes met de aankomende afronding van je PhD. Furthermore thanks Yanyun, Isabel, Jeroen, Simon, Abishek, Anniek, Bianca and Stefan for the fun times during the end of my period as a PhD-student.

From C2 thank you Sjors, Julian, Lisette, Koen S, Ciara, Micha, Stefano, Marcello, Bart, Didier, Robin, Vincent, Marco, Ewa, Anne Paulien, Lindy,

Emilie, Linda, Dick, Heleen, Alexandra, Arne, Sjoerd, Tanya and Sanne for all the small talk during our working days and all the feedback you provided. Bedankt Ellen, Peter, Mirjam, Ingrid, Hanneke, Linde, Sten, Annegien en Esther voor jullie optimistische peptalks en altijd klaar staan voor vragen. Met veel plezier denk ik ook terug aan deze periode op C2 omdat daar altijd de bulderende lach van mijn Poolse makker Arthur was. We blijven elkaar de komende tijd nog vaak zien voor een bakje koffie. Jelle en Mark bedankt voor jullie hulp bij het scoren (en het leren van) mijn FEN1-kleuringen en Sabine, Marleen, Karin, Tesa, Izhar, Philip, Gwen, Annelot, Dinja en Sonja voor jullie feedback tijdens onze gezamenlijke meetings.

Thanks all the people from the new H5 department of Oncogenomics for making me (as part of Wilbert's group) feel so welcome.

Thanks all (former) members of B4 for our shared work discussions.

Tijdens mijn PhD heb ik veel hulp gehad van de NKI-faciliteiten. Bedankt voor jullie hulp; Maarten en Onno bij de mass spec; Lenny en Lauran bij de confocale microscopie; Klaas and Kathy with the Incucyte; Ron, Roel en Marja bij de deep secuencing en de RRBS; Marieke, Bas, Renske, Nathalie en de muis-interventie unit bij het opzetten en uitvoeren van de interventie; Olaf voor het analyseren en verkrijgen van de benodigde hoeveelheden FEN1 inhibitor; Mirna, Patty en Pauline (LUMC) bij het inplannen van mijn vele afspraken en het vergaren van het benodigde papierwerk voor mijn promotie.

During my time at the NKI I met a lot of kind and interesting people with whom I've shared both scientific and non-scientific thoughts; Thank you Judith, Ahmed, Chelsea, Hellen, Bente, Tim, Thomas, Eva, Tess, Inge, Vera, Santiago, Lisanne, Feline, Jeffrey, Gözde, Joppe, Rui, Bram, Stéphanie and Nils. And with so many kind people at the NKI, I hope I am not forgetting anyone.

Uiteraard wil ik hen die me het dierbaarst zijn als laatste bedanken. Bedankt Joost, Marloes, Pa en Ma voor jullie steun, vertrouwen en gezelligheid. Mam, ontzettend bedankt voor je onvoorwaardelijke steun en hulp in de afgelopen tijd. Het was bijzonder om te zien hoe je altijd voor ons klaarstaat. Dankjewel.

Maar tot slot mijn grote liefde en steun en toeverlaat Judith. Je bent er de

Addendum

afgelopen periode altijd voor me geweest, hoe moeilijk en zwaar de situatie soms ook was. Hoe heerlijk is het om er samen met jou in het weekend op uit te trekken en dat nu samen met ons kleine zoontje te doen. Ook de komende jaren kunnen we samen alles aan. En Luka, mijn lieve zoon, bedankt voor de glimlach die je altijd weer op je moeders en mijn gezicht tovert als een van ons thuiskomt en jij vrolijk lachend aan komt rennen.

Addendum